Hybrid Life Cycle Assessment and Modelling Approaches. The Case of Desalination in Australia

vorgelegt von

Michael Heihsel, M.Sc.
ORCID: 0000-0001-9886-0006

an der Fakultät III - Prozesswissenschaften
der Technischen Universität Berlin
zur Erlangung des akademischen Grades

Doktor der Ingenieurwissenschaften
- Dr.-Ing. -

genehmigte Dissertation

Promotionsausschuss

Vorsitzender:	Prof. Dr. Matthias Finkbeiner
Gutachter:	Prof. Dr. Frank Behrendt
Gutachter:	Prof. Dr. Thomas Wiedmann

Tag der wissenschaftlichen Aussprache: 02.12.2020

Berlin 2021

Danksagung

Zuerst möchte ich meinen persönlichen Dank an Prof. Dr. Frank Behrendt richten, der mich die Jahre meiner Dissertation stets konstruktiv begleitet, mir viele Anregungen gegeben und mir gleichzeitig durch die große eingeräumte Freiheit die Möglichkeiten für diese Dissertation erst geschaffen hat. Ein weiterer Dank richtet sich an Prof. Dr. Manfred Lenzen. Durch die Ermöglichung meiner Forschungsaufenthalte in Sydney und die gemeinsame Arbeit in seiner Forschungsgruppe ISA konnte ich in kurzer Zeit wissenschaftlich wachsen. Das tiefe Wissen in der Welt der Input-Output-Analyse, das ich in dieser Zeit aufgesogen habe, ist unbezahlbar. In all dieser Zeit habe ich stets die unkomplizierte, effiziente und aber auch freundschaftliche Arbeitsweise geschätzt. Ich danke weiter Prof. Dr. Thomas Wiedmann, mit dem ich viele inspirierende Gespräche führen durfte. Nicht zuletzt danke ich ihm für seine Arbeit als Zweitgutachter und seine Unterstützung bei der Datenbeschaffung. Prof. Dr. Finkbeiner danke ich für den Vorsitz des Prüfungsausschusses. Ich danke den Co-Autoren meiner veröffentlichten Studien; die Zusammenarbeit habe ich sehr geschätzt: Arunima Malik, Arne Geschke, Syed Muhammad Hassan, Julian Kirchherr, Ana María Rodríguez-Alloza, Jacob Fry, Juan Gallego und Richard Wood. Nicht unerwähnt bleiben soll die Unterstützung von Prof. Dr. Dennis A. Ostwald, der mir insbesondere in der Anfangszeit dieser Arbeit durch sein Vertrauen und die Unterstützung von WifOR vieles ermöglicht hat. Nicht zuletzt geht der Dank an meine Freunde und Familie. Meine Eltern Bettina und Bernd, die stets an mich geglaubt haben und mich zu dem gemacht haben, was ich heute bin. Ich wäre hier nicht ohne Euch! Und zuletzt an den liebsten Menschen: Meine Ehefrau und beste Freundin. Danke Marlene für all das, was du mir gibst!

Die Dissertation wurde im Rahmen eines Promotionsstipendiums der Friedrich-Naumann-Stiftung für die Freiheit mit Mitteln des Bundesministeriums für Bildung und Forschung gefördert. Ich danke der Friedrich-Naumann-Stiftung für die Freiheit, den Mitarbeiterinnen und Mitarbeitern für die Förderung und die besonders spannende Zeit.

FRIEDRICH NAUMANN STIFTUNG Für die Freiheit.

Bundesministerium für Bildung und Forschung

Zusammenfassung

Ein immer größer werdender Teil der Weltbevölkerung ist mit Wassermangel und Trockenheit konfrontiert. Das Bevölkerungswachstum, die ökonomische Entwicklung und der Klimawandel sind die Treiber dieser Entwicklung. Australien ist von dieser Entwicklung seit Anfang des Jahrtausends immer wieder stark betroffen, weshalb das Land nach Wegen sucht, um unabhängiger von Niederschlag zu werden.

Meerwasserentsalzung ist insbesondere für küstennahe Regionen vielversprechend, da das Verfahren im Grunde eine unerschöpfliche Quelle für die Frischwasserbereitstellung erschließt. Die Technologie ermöglicht eine auf die Nachfrage ausgerichtete Produktion von Wasser, bietet somit Versorgungssicherheit und gewährleistet dadurch den Wohlstand einer Gesellschaft. Dennoch ist sie die letzte Wahl im Kampf gegen Wasserknappheit. Der beträchtliche Energieverbrauch, die damit verbundenen hohen Kosten und CO_2-Emissionen sowie die Auswirkungen auf die Meeresbiologie sind die größten Hürden. Die Nutzung erneuerbarer Energien könnte der Meerwasserentsalzung deutliche Vorteile bieten, jedoch steht die Integration beider Technologien noch am Anfang. Die vorliegende Arbeit hat die Kopplungspotenziale von Meerwasserentsalzung und erneuerbaren Energien quantifiziert und hierfür einen methodischen Rahmen erarbeitet. Hierfür wurden *input-output*-basierte hybride *life cycle assessment*-Modelle entwickelt und ein *load-shifting*-Modell modifiziert. Die dabei verfassten Studien sind in den Kapiteln 2 bis 4 dargestellt.

In Kapitel 2 steht der CO_2-Fußabdruck der in Australien zu Beginn der 2000er Jahre errichteten Meerwasserentsalzungsanlagen im Fokus. Hierbei wurden sowohl der Bau als auch der Betrieb und die Wartung der Anlagen berücksichtigt. Die Studie untersucht die 20 größten Umkehrosmose-Anlagen vor dem Hintergrund der Nutzung des regional vorherrschenden konventionellen Strommixes. Die Anlagen entsprechen 95% der australischen Meerwasserentsalzungskapazität. Wir beziffern die Gesamtemissionen für 2015 auf 1193 kt CO_2e. Kapitel 3 zeigt mit Hilfe eines *load-shifting*-Modells die Synergieeffekte von Meerwasserentsalzungsanlagen und einem 100% erneuerbaren Energienetz auf. Es wurde die Stromnachfrage fiktiver Meerwasserentsalzungsanlagen modelliert, die das fehlende Wasser im *Murray-Darling basin* deckt. In Kapitel 4 wurden schließlich die Ergebnisse dieser Studie genutzt, um die soziale, ökologische und ökonomische Nachhaltigkeit der Meerwasserentsalzungsanlagen im fiktiven Netz aus 100% erneuerbarer Energien mit der Nachhaltigkeit bei der Nutzung konventioneller Elektrizität zu vergleichen. Durch erneuerbare Energien würden 90% weniger Treibhausgase emittiert und 20% weniger Wasser verbraucht. Allerdings würde auch die Bruttowertschöpfung um 10% reduziert.

Abstract

A steadily growing part of the world population is confronted with water shortages and drought. Population growth, economic development and climate change are the drivers of this development. Australia has been severely affected by this trend since the beginning of the millennium, which is why the country is looking for paths to become less dependent on precipitation.

Seawater desalination is particularly promising for coastal regions, as the process basically provides an inexhaustible source of freshwater. The technology enables water production in response to demand, thus providing security of supply and ensuring the prosperity of a society. Nevertheless, it is the last resort in the battle against water scarcity. The considerable energy consumption, the associated high costs and carbon emissions, and the impact on marine biology are the main obstacles. The use of renewable energy could offer significant benefits to seawater desalination, but the integration of both technologies is still evolving. This thesis has quantified the coupling potentials of seawater desalination and renewable energies and developed a methodological framework to this end. For this purpose, input-output-based hybrid life cycle assessment models were developed, and a load-shifting model was modified. The studies carried out in the process are presented in chapters 2 to 4.

Chapter 2 focuses on the carbon footprint of seawater desalination plants constructed in Australia at the beginning of the 2000s. Both the construction and the operation and maintenance of the plants were considered. The study examines the 20 largest reverse osmosis plants against the background of using the regionally predominant conventional electricity mix. The plants represent 95% of Australia's seawater desalination capacity. We estimate the total emissions for 2015 at 1193 kt CO_2e. Chapter 3 shows the synergy effects of seawater desalination plants and a 100% renewable electricity grid using a load-shifting model. The electricity demand of fictitious desalination plants was modelled to cover the missing water in the Murray-Darling basin. Finally, in chapter 4 the results of this study were used to compare the social, environmental and economic sustainability of the desalination plants in the fictitious 100% renewable energy grid with the sustainability in the use of conventional electricity. Using renewable energies would result in 90% less greenhouse gas emissions and 20% less water consumption. However, gross value added would be reduced by 10%.

Rechtliche Erklärung

Ich erkläre hiermit, dass ich die vorliegende Arbeit selbständig verfasst und keine anderen als die angegebenen Quellen und Hilfsmittel verwendet habe.

Michael Heihsel
Berlin, den 17. Januar 2021

Contributions to the articles

Chapter	Study	Co-Author	Contribution
2	The carbon footprint of desalination: An input-output analysis of seawater reverse osmosis desalination in Australia for 2005-2015 [73].	Michael Heihsel	* Data preparation of desalination data * Defining sectoral and regional resolution * Designing the study * Mathematical formulation and calculation * Analysing results * Writing the paper
		Manfred Lenzen	* Designing the study * Coordinating tasks * Preparing IO data
		Arunima Malik	* Preparing IO data * Mathematical formulation
		Arne Geschke	* Preparing IO data
3	Renewable-powered desalination as an optimisation pathway for renewable energy systems: The case of Australia's Murray-Darling Basin [71].	Michael Heihsel	* Data preparation of desalination and pipeline data * Mathematical formulation and calculation of desalination and pipelines * Designing the study * Analysing results * Writing the paper
		Syed Muhammad Hassan Ali	* Mathematical formulation and calculation of the load-shifting process * Analysing results
		Julian Kirchherr	* Revising the paper
		Manfred Lenzen	* Mathematical formulation and calculation of the clean-grid * Designing the study * Coordinating tasks
4	Desalination and sustainability: A triple bottom line study of Australia [72].	Michael Heihsel	* Data preparation of desalination data * Defining sectoral and regional resolution * Preparing IO data * Designing the study * Mathematical formulation and calculation * Analysing results * Writing the paper
		Manfred Lenzen	* Designing the study * Coordinating tasks * Preparing IO data
		Frank Behrendt	* Revising the paper

Contents

List of Figures

List of Tables

Acronyms

ACT	Australian Capital Territory
CAPEX	capital expenses
CSP	concentrated solar power
ED	electrodialysis
EPC	Engineering-Procurement-Construction
FTE	full-time equivalent
GIS	geographic information system
GHG	greenhouse gas
GVA	gross value added
hLCA	hybrid life cycle assessment
IELab	Industrial Ecology Virtual Laboratory
IO	input-output
IOA	input-output analysis
IOT	input-output table
IAEA	International Atomic Energy Agency
LCOE	levelised cost of electricity
LCA	life cycle assessment
LCI	life cycle inventory
MVC	mechanical vapour compression
MD	membrane distillation
MENA	Middle East and North Africa
MED	multi-effect distillation
MRIO	multi-regional input-output

MSF	multi-stage flash distillation
MDB	Murray-Darling Basin
MDBA	Murray-Darling Basin Authority
NSW	New South Wales
NT	Northern Territory
OPEX	operational expenses
PV	photovoltaic
PLD	production layer decomposition
Qld	Queensland
RE	renewable energy
RO	reverse osmosis
SWRO	seawater reverse osmosis
SA	South Australia
Tas	Tasmania
TBL	triple bottom line
Vic	Victoria
WA	Western Australia

Symbols

Symbols for chapter 2

Symbol	Unit	Description
$\mathbf{y}_i$	US$ or AU$	Demand vector of processing stage i
r^a	AU$/US$	Exchange rate for year a
n	-	Number of construction years
p_s^a	-	Producer price index of sector s and year a
$\mathbf{C}$	-	Concordance matrix
$\mathbf{q}^a$	%	Import quota vector of year a
$\mathbf{I}_{i,j}$	AU$m	Import intermediate demand matrix
$\mathbf{U}_{i,j}$	AU$m	Total intermediate demand matrix
$\mathbf{T}_{i,j}$	AU$m	Domestic intermediate demand matrix
$\mathbf{O}_p$	AU$m	Opex demand matrix of plant p
$\mathbf{C}_p$	AU$m	Capex demand matrix of plant p
$\mathbf{Y}$	AU$m	Final demand matrix
$\mathbf{x}$	AU$m	Output vector
$\mathbf{A}$	AU$m	Technical coefficient matrix
$\mathbf{L}$	-	Leontief matrix
$\mathbf{I}$	-	Identity matrix
$\mathbf{q}$	kt CO_2e/AU$m	Direct carbon emission equivalent intensities
$\mathbf{m}$	kt CO_2e/AU$m	Total carbon emission equivalent intensities
$\mathbf{E}$	kt CO_2e	Total emissions
$\mathbf{i}$	-	Summation vector
$\mathbf{v}$	kt CO_2e	Total emissions in industy / commodity classification
Q_{dir}^a	kt CO_2e	Total emissions of year a
Q_{dir}^a	kt CO_2e	Direct emissions of year a
c	%	Carbon emission multiplier

Symbols for chapter 3

Symbol	Unit	Description
b	m	Altitude
bc	\$	Annual difference of benefits and costs
$\mathbf{C}$	-	Concordance for supply links between pipelines and areas
$\mathbf{c}$	m^3/d	Capacity of the pipelines
$\mathbf{d}$	GL	Average water demand vector
d	m	Hydraulic diameter
d	mm	Diameter of the pipeline
$\mathbf{D}$	MWh	Electricity demand of desalination available for load shifting
Δb	\$	Difference of costs
Δc	\$	Additional cost for desalination
Δt_s	hours	Load shifting period
$\mathbf{e}$	kWh/m^3	Specific energy consumption of pipeline
$\mathbf{e}_{tot}$	kWh	Total electricity consumption of pipeline
η_{tot}	%	Efficiency factor
$\mathbf{G}$	MWh	Electricity generation
g	m/s^2	Gravitational acceleration
g_i	kWh	Generated electricity
h_f	m	Hydraulic head loss
k	mm	Absolute roughness
l	GL	Total water supply
l	m	Length of pipeline
λ	-	Friction factor
$lcoe$	\$/kWh	Levelised cost of electricity
n	years	Lifetime
$\mathbf{P}$	MWh	Load shifting potential
$\mathbf{p}$	%	Capacity fraction of the pipelines
$\mathbf{q}$	%	Percentage distribution of water to pipelines
q	%	Interest rate
$\mathbf{r}$	%	Percentage demand distribution vector to areas
r	-	Reynolds number
ρ	kg/m^3	Density
$\mathbf{S}$	MWh	Spilt energy
t	hours	Time
tce	\$	Total cost of electricity
v	m/s	Flow velocity
$\mathbf{w}$	GL/y	Water supply vector by pipelines

Symbols for chapter 4

Symbol	Unit	Description
$\mathbf{1}^Q$	-	Summation vector
$\mathbf{A}$	%	Technical coefficient matrix
$\mathbf{C}$	-	Aggregation concordance
$\mathbf{C}_d$	Process unit/AU$	Downstream cut-off matrix
$\mathbf{C}_u$	AU$/MJ	Upstream cut-off matrix
$\mathbf{d}_t$	AU$/AU$	Total intermediate demand
$\mathbf{d}_t^f$	AU$m/MJ	Specific intermediate demand vector
e	MJ	Electricity demand
g_t	MJ	Generated electricity of technology t
$\mathbf{I}$	-	Identity matrix
$i_{k,s,y}$	Indicator value	Indicator value for key figure k, scenario s and year y
λ	%	Renewable electricity penetration ratio
n	-	Number of extracted plants
$n_{k,s}$	-	Normalised index for key figure k and scenario s
o_t	AU$m	Output of technology t
ω	AU$/Physical value	Life cycle inventory price vector
$p_{k,r}$	%	Relative change of the indicator value for keyfigure k and region r
$\mathbf{P}_t$	Physical value/MJ	Physical life cycle inventory of technology t
$\mathbf{p}_t$	Physical value/MJ	Average process coefficient vector of technology t
$\mathbf{Q}$	Indicator value	Matrix of the pyhsical satellite accounts
$\mathbf{Q}_i^d$	Indicator value	Total supply chain impact matrix of indicator i
$\mathbf{q}_t$	Indicator value/AU$m	Satellite intensities of technology t
$\mathbf{q}_i$	Indicator value/AU$m	Indicator intensity
r	%	Intermediate demand ratio
$\mathbf{R}$	kt CO_2e/AU$m	Greenhouse gas emission intensity
$\mathbf{S}$	AU$m	Supply table
$\mathbf{T}$	AU$m	Intermediate consumption matrix
$\mathbf{U}$	AU$m	Use table
$\mathbf{U}_t$	AU$/AU$	Cut-off matrix of technology t
$\mathbf{v}$	AU$m	Gross value added vector
v_t	AU$m	Gross value added of technology t
$\mathbf{x}$	AU$m	Output vector
$\mathbf{y}$	AU$m	Final demand vector
$\mathbf{Y}$	AU$m	Final demand matrix

Chapter 1

Introduction

Water consumption is increasing worldwide, driven by population growth and economic development. The economic progress made by emerging and developing countries will further increase the demand for water in the coming years. In addition, a growing number of countries experience difficulties in securing their water supply, as less reliable precipitation is expected due to climate change [109]. Growing demand and decreasing supply will, therefore, lead to water stress in many countries in the coming decades (fig. 1.1).

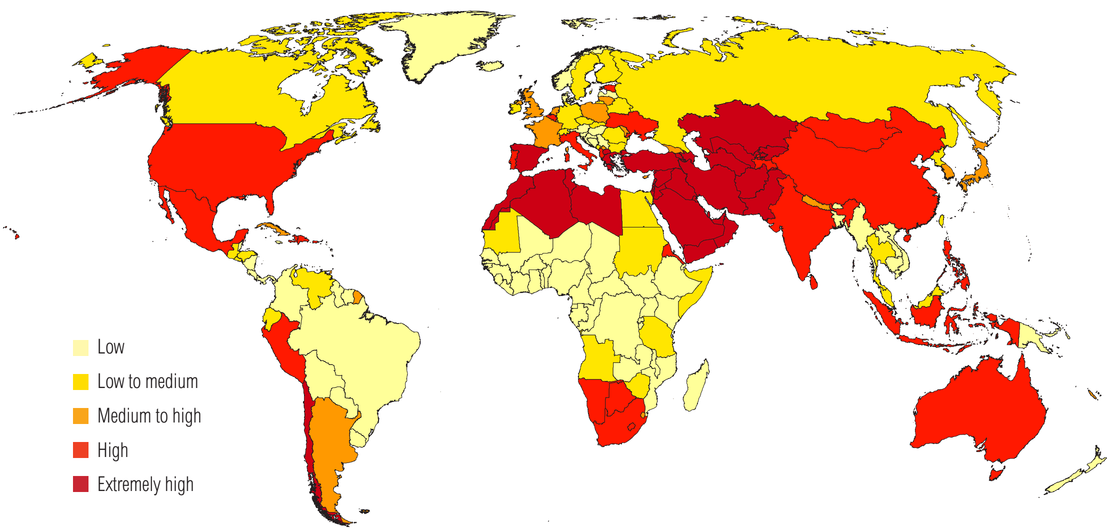

Figure 1.1: *Global water stress in 2040 under business as usual.*

Source: [109].

1.1 Water and desalination challenges

Australia, which is the driest inhabited continent, depends primarily on surface water and thus on precipitation. The increasing variability of precipitation endangers the security of the country's water supply. The consequences of drought and water shortage have a significant impact on the social, economic and health condition of a country and its population [43]. Nevertheless, Australia's strong economy continues to drive the rising water demand. Agricultural activities promote intensive water consumption, especially in south-eastern Australia in the Murray-Darling Basin (MDB). Here, the extent of water shortage has become apparent in recent decades. The environmental consequences, such as the salination of surface water and the resulting considerable fish deaths, bear witness to the ecological dimension.

The last major drought from 1997 to 2010, the Millennium Drought, marked a turning point in Australian water policy. The Murray-Darling Basin Authority (MDBA) was established under the Water Act 2007 [160] to implement sustainable water management and to meet the requirements of the Ramsar Convention on Wetlands. Part of the new policy were water restrictions, the implementation of water use rights and their trade. The authority monitors and enforces compliance with the requirements of the water protection law.

Another response to the prolonged drought was the construction of several large seawater desalination plants to ensure water availability in the major cities and their metropolitan areas. Except for Darwin, Hobart and Canberra, all capitals of the eight Australian States and Territories built large desalination plants. The first plant was built in Perth in 2006, followed by plants on the Gold Coast and in Sydney in 2009 and 2010, with further plants to follow in Perth, Melbourne and Adelaide in 2012. In 2005, the cities of Australia had a seawater desalination capacity of only 1 $^{GL}/_{y}$. By 2014, the capacity increased to 500 $^{GL}/_{y}$, which corresponds to one third of the average demand of the corresponding cities [58]. The construction of new plants led to rising water bills for Australian households. Together with private plants, there are now 89 seawater desalination plants in Australia with a total capacity of about 1.8m $^{m^3}/_{d}$, representing about 2% of the global desalination capacity [66]. However, the bulk of Australia's desalination plants are small. Some of them are private and are used to supply e.g. industrial plants or mines. The 20 largest Australian desalination plants cover 95% of the total Australian seawater desalination capacity.

Throughout the years, the political debate on the necessity of the plants has been highly controversial. In the mid-2000s, the state governments decided with considerable haste to build desalination plants in almost all major cities [58]. However, the millennium drought ended in 2010 with high precipitation due to the ocean-atmosphere phenomenon La Niña. As many of the desalination plants were put into standby mode, the political discourse at that time was dominated by the perception that inappropriate investments had been made. In 2017, however, the drought had returned. In 2019, the Sydney Desalination Plant was ordered to produce water for the first time since its completion due to the rapidly decreasing water level of the reservoirs (until then, the plant had been mothballed). That same year, Australia experienced its driest November since records began. The devastating bushfires in the summer of 2019/20 further reflected the drought across the continent. As a result of the water shortage, the Government of New South Wales (NSW) decided in January 2020 to double the capacity of the seawater desalination plant in Sydney to 500,000 m^3/d.

Like many other countries, Australia needs solutions to tackle water scarcity. When selecting appropriate measures, those with the lowest costs should be implemented first. One of the first measures is to improve demand management. Increasing the efficiency of the existing water infrastructure is a high priority. Since agriculture is a major driver of water demand, improving irrigation management, enhancing technology and integrating intelligent irrigation planning is of great importance. Also, municipal water supply systems generally suffer from high losses due to leaking pipes and inefficient distribution technologies. Australia is already one of the most technologically advanced countries in these areas. Although Australia loses 10% of its total pipeline input, it is, in fact, one of the world leaders in this area [161, 179].

In order to raise efficiency potentials, the supply side should also be analysed. Conventional supply options include improving rainwater harvesting and building dams. While rainwater harvesting is a small, decentralised measure with high unit costs [154], the construction of dams is centralised, the projects are large-scale, and their implementation often faces considerable political and ecological challenges. Australia has already developed many high capacity dams to reduce the variability caused by precipitation. Despite their high storage capacity, concerns have been raised repeatedly in recent years that water supply from surface water is not reliable. Moreover, further potential is rather limited.

Unconventional techniques offer further opportunities to improve water supply. One promising option is the reuse of wastewater, which is used by countries like Singapore on a large scale. Water can be treated to different quality levels. Depending on the purification level, the use of water can be limited to certain uses (e.g. irrigation in agriculture or toilet flushing). Water can also be treated to such an extent that it reaches potable water quality so that it can be fed directly into the drinking water network. However, in order to integrate the technology, high investments in fresh and wastewater infrastructure and treatment technologies are necessary. Social acceptance is probably the biggest challenge if the treated water is to be fed directly into the drinking water network.

If all these measures are not sufficient or cannot be implemented, desalination of seawater or brackish water offers a promising option. Although the desalination of brackish water is possible with substantially less energy input, there is often only limited potential here. In most cases, the available resources are limited, e.g. if water from aquifers or rivers is used. Simultaneously, the disposal of brine is a challenge. In contrast, the desalination of seawater offers an almost inexhaustible resource potential. The process enables water to be provided independently of external influences such as limited resources or climatic conditions. Seawater desalination thus enables a high level of supply security.

For this reason, almost every major city in Australia has now adopted the technology. In the long run, the use of seawater desalination plants may even be cheaper than dams, especially when climatic conditions are characterised by long periods of drought and rain [146]. Due to the decisive advantage that seawater desalination guarantees an almost inexhaustible water supply, the use of the technology is rapidly increasing in Australia and worldwide. In 2018, there were about 20,000 desalination plants worldwide with a production capacity of 97.4m $^{m^3}/_{d}$ [65,144]. The main market with 46.7% of global capacity is in the Middle East and North Africa (MENA) region, followed by East Asia / Pacific and North America with 17.5% and 12.9% respectively [67]. (see fig. 1.2).

1.2 Desalination approaches

Seawater desalination is a process that removes salt from water to make it suitable for drinking or other purposes such as industrial or agricultural use. Desalination technologies can use different water sources such as seawater, brackish water or generally polluted water. Worldwide, 59% of desalination capacity is used for seawater desalination, 22% for the treatment of brackish water, and 9% of capacity uses river water. Wastewater, purification and recovery water systems each account for 5% of the total capacity [65]. A pre- and post-treatment process complements the basic desalination process. Pretreatment includes filtration, disinfection or the addition of chemicals to prevent scaling,

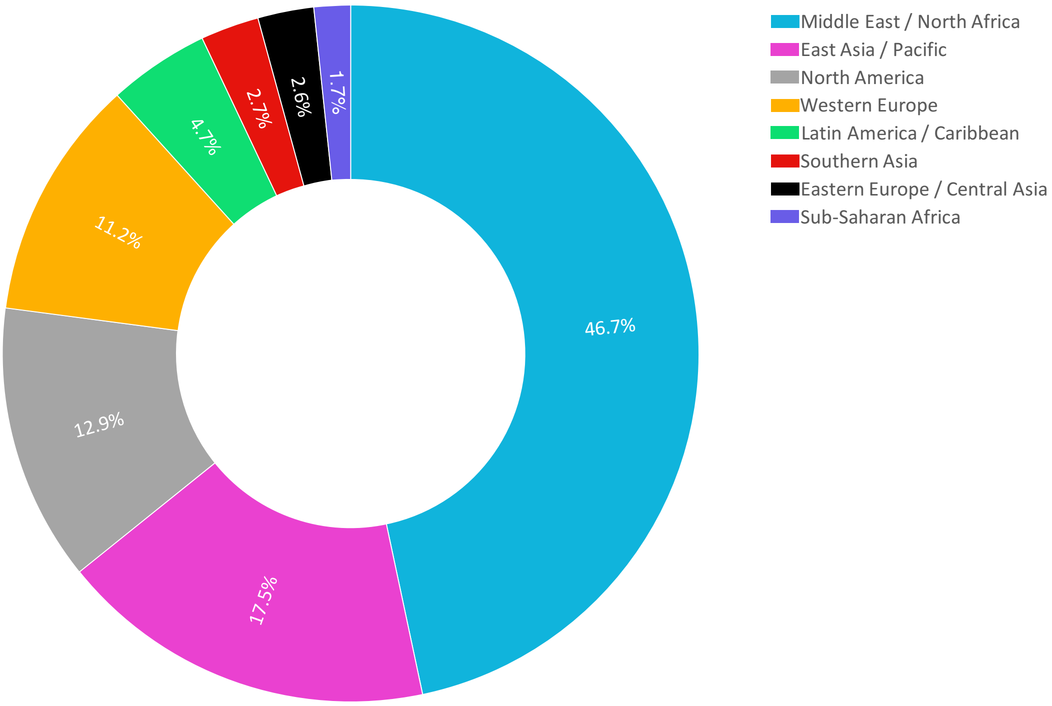

Figure 1.2: *Worldwide distribution of desalination capacity.*

Source: [67], own depiction.

biofouling or corrosion. Post-treatment generally consists of optimising the water properties for transport in the pipelines and consumption. Part of this is the adjustment of the pH-value and water hardness.

The various processes for water desalination can be classified into thermal, mechanical and electrochemical processes. Table 1.1 gives an overview of desalination technologies that are currently being used commercially. Historically, desalination technology was developed on the basis of thermal processes. The original rudimentary process using solar stills is a simple application for the evaporation and condensation of water to achieve desalination. In recent decades, the thermal processes multi-effect distillation (MED) and multi-stage flash distillation (MSF), which are based on the principles of evaporation and subsequent condensation, have gained particular technical relevance. These plants make up the majority of the plants built between the 1960s and 1980s [161]. Today, thermal plants are mainly used where water quality is poor or irregular. High water temperature, high salinity or high algae content may argue in favour of thermal desalination because, unlike membrane-based processes, energy consumption does not increase with poorer water quality. In the MENA region, thermal desalination was favoured because of the high salt content, but also because of the high availability of waste heat from conventional power plants. Many plants in this region are therefore cogeneration plants, i.e. power plants that produce electricity as the main product and water as a by-product.

Another technology for water desalination is electrodialysis (ED). Here, an electric field between two electrodes is used to perform ion separation, which enables the water molecules to be separated from the salt molecules. Furthermore, hybrid processes such as membrane distillation (MD) or reverse osmosis (RO) combined with forward osmosis, MSF or MED should be mentioned. However, since these methods have little relevance in the current commercial application, they are also less relevant for this work and are therefore not considered in detail.

Table 1.1: *Overview of current commercial desalination technologies.*

Desalination technology	Multi-stage flash	Multi-effect distillation (Plain)	Multi-effect distillation + TVC	Reverse osmosis	Ultra-/ micro-/ nanofiltration	Electro-dialysis reversal
Energy source/type	Thermal	Thermal	Thermal	Electricity	Electricity	Electricity
Typical electricity onsumption [kWh/m³]	3–5	1.5–2.5	<1.0	3–5	3–5	3–5
Typical heat onsumption [MJ/m³]	233–258	233–258	233–258	No heat energy needed	No heat	No heat
Capacity range	Current modular capacity up to 90,000 m³/d	Current modular capacity up to 38,000 m³/d	Current modular capacity up to 68,000 m³/d	Current modular capacity up to 10,000 m³/d	Current modular capacity up to 10,000 m³/d	Current modular capacity up to 34,000 m³/d
Advantages	Easy to manage and operate. Can treat very salty water up to 70,000 mg/L.	Can be operated between 0% and 100% capacity while MED unit is kept under vacuum and cold circulation. Suitable to combine with RE sources that supply intermittent energy. Suitable to link with RE.	Helps reduce number of effects Adapts MED design to a broad range of pressures (1–40 bars). Very low electrical consumption compared to MSF and plain MED or RO. Operate at low temp (<70°C) and low concentration (<1.5) to avoid corrosion and scaling.	Easily adapts to local conditions. Plant size can be adjusted to meet short-term increases in demand and expanded incrementally as needed. Significant cost advantage in treating brackish groundwater. Can remove silica. Capital cost approximately 25% less than thermal options.	Usually used in combination with RO plants (for pretreatment). Reduces fouling on RO plants, hence reducing cost and saving energy as well as reducing chemical use in RO. NF in particular could be used as a “softening” step for RO, rejecting multivalent and monovalent ions.	High recovery rate of up to 94%. Longer-life membranes (up to 15 years when operated properly). Can be combined with RO for higher water recovery of up to 98%.
Disadvantages	Cannot operate at below 60% capacity. Not suitable to combine with renewable energy that have intermittent energy supplies. High energy use (3–5 kWh/m³ electricity and 233–258 MJ/m³ heat required).	Antiscalents required to stop scale. Build-up on evaporating surfaces.	Cannot operate at below 60% capacity. Not suitable to combine with RE that has intermittent energy supply.	Requires comprehensive pretreatment to be used for high saline water. Membrane fouling. Complex configuration and requires skilled personnel for O&M.	Membrane fouling. Although much less than RO, still a complex configuration and requires skilled personnel for O&M.	Capital intensive and costly compared to RO.

Source: [161], own depiction.

1.2.1 Thermal desalination processes

In the early period of large-scale application, MSF was the dominant desalination technology. MSF plants operate according to the principle of flash evaporation, in which the pressure is reduced in various stages, thus lowering the boiling point. The individual stages are heat exchangers and condensers to collect the condensed water. Figure 1.3 shows the schematic structure of an MSF plant. The feedwater passes through the various stages for pre-heating, starting with the coldest and last evaporation stage. After passing through all stages, the feedwater passes through the brine heater where it is heated by external thermal energy. The feedwater then flows into the first stage where the pressure is reduced, causing the water to evaporate and finally condense through the cooler feedwater passing through. The desalinated water is drained off, and the remaining concentrate is fed to the next stage. Here the pressure is reduced again, allowing the evaporation to occur at a lower temperature. This procedure is repeated over several stages.

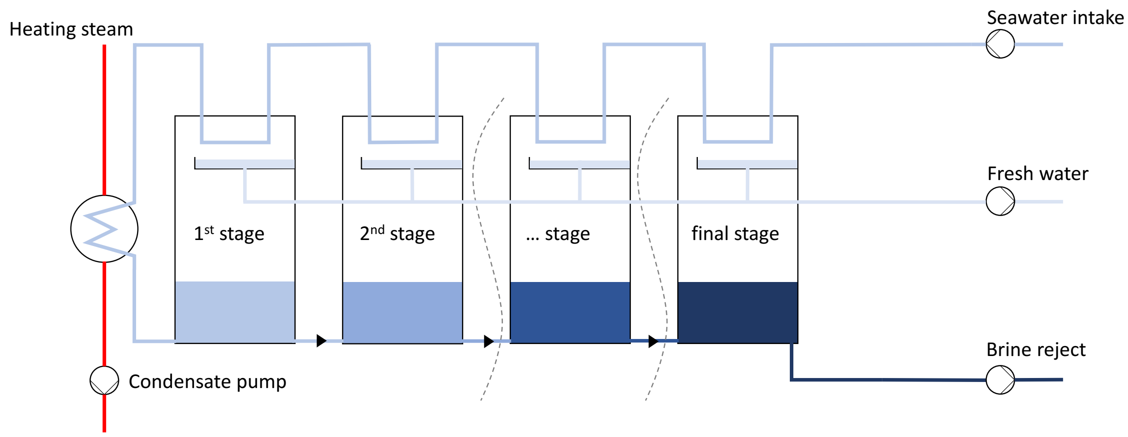

Figure 1.3: *Schematic representation of the MSF process.*

Source: [140], own depiction.

Also, the MED process uses several stages for evaporation and condensation, so-called effects. Figure 1.4 shows the simplified layout of a MED plant. Ahead of the first effect, steam is generated, which is fed through a pipe into the first stage. Here the salty feedwater is sprayed onto the heated pipes, which causes part of the water to evaporate. The hot water in the pipe then flows back into the circuit for reheating. The evaporated water is then fed into pipes where it is used for heating in the subsequent stages. Here again, feedwater is sprayed onto the hot pipe, which in turn leads to evaporation due to the reduced pressure. The energy content in the steam is thus used to evaporate the feedwater, which causes the water in the pipe to condense. These effects are repeated several times, whereby the initial and final temperature limit the number of effects and thus the efficiency of the process.

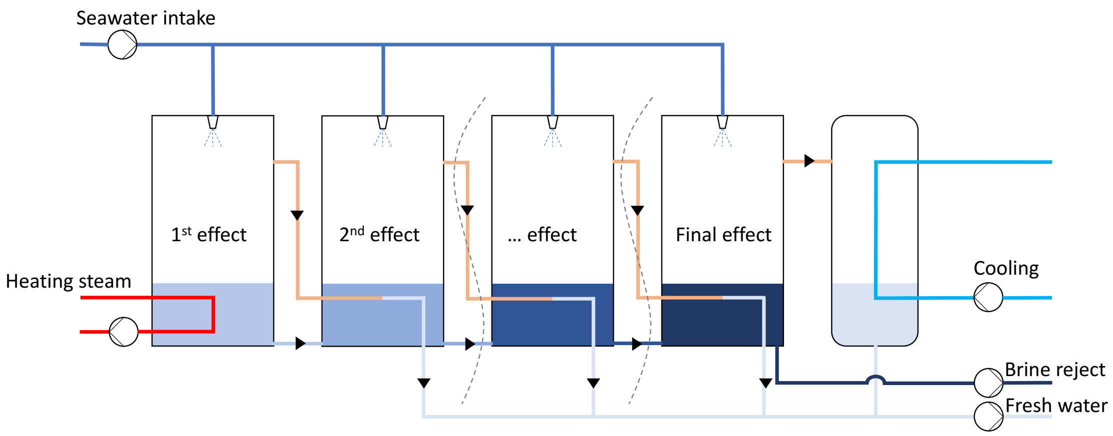

Figure 1.4: *Schematic representation of the MED process.*

Source: [140], own depiction.

Compared to other thermal processes, the specific energy consumption of MED technology is lower, so that it is increasingly replacing MSF technology. Some systems work with an initial temperature of more than 90 °C (high temperature) and others with a temperature of 50-70 °C (low temperature) [65]. The specific thermal energy consumption is in the range of 145-230 $^{MJ}/_{m^3}$ and 190-282 $^{MJ}/_{m^3}$ for MED and MSF respectively [17]. The pumps in MED require 2.0-2.5 $^{kWh}/_{m^3}$. For MSF these are 2.5-5.0 $^{kWh}/_{m^3}$ [17]. Besides, there are other thermal processes such as TVC (Technical vapour compression) and also combinations of individual processes, which are not discussed in detail in this thesis due to their limited relevance in practical application.

1.2.2 Mechanical desalination processes

Today, the most commonly used desalination process is RO, mainly because of its high energy efficiency. Although thermal plants are still of great importance in the MENA region, new plants in the region are also primarily designed as RO plants. Worldwide, most of the large-scale facilities are now RO projects. Also in Australia, all large plants are RO systems. For this reason, the investigations in this dissertation deal exclusively with RO.

The centrepiece of the RO technique is a semi-permeable membrane. The principle is based on the reversal of the osmosis process. The osmosis process describes the phenomenon that water separated by a semi-permeable membrane balances a different chemical potential. Water with higher chemical potential due to fewer dissolved particles flows through the membrane to water with lower chemical potential due to a higher amount of dissolved particles. This phenomenon is of central importance for the water balance of cells of living organisms. The osmotic pressure is the pressure required to stop this natural process mechanically.

The approach of RO reverses this process by applying a higher pressure than the osmotic pressure on the side of the saline water. The membrane is designed to allow the water to flow through the semi-permeable membrane, with the membrane retaining the salt molecules. Due to the properties of the membrane, almost all substances can be filtered out of the water, i.e. especially salts, but also other particles such as chemicals, viruses or bacteria. Figure 1.5 shows the basic principle of RO.

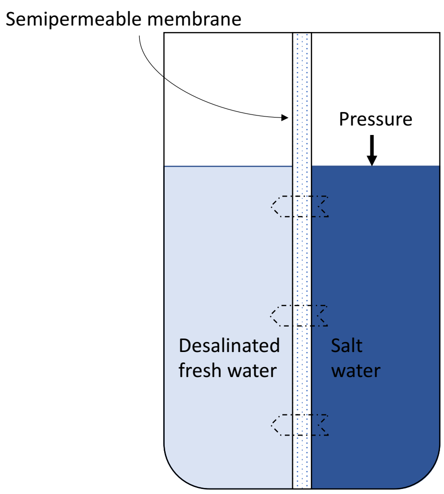

Figure 1.5: *Schematic representation of the RO process.*

Source: [94], own depiction.

Depending on the feedwater quality, different working pressures are required. Brackish water requires a pressure of 17-27 bar, a pressure of 55-82 bar is required for seawater [18]. In contrast to thermal processes, the energy requirement, therefore, increases with poorer water quality (i.e. higher salinity or pollution). In order to clean the membranes from scaling, backwashing must be carried out regularly. Typically, recovery rates of 40-50% are achieved, representing the amount of desalinated water in relation to the feedwater. By further concentration, recovery rates of 80% can be achieved in modern plants.

RO has made significant progress over the last two decades. Meanwhile, the achieved cost reduction has led to considerable competitive advantages, primarily when waste heat from other processes cannot be used. The development of membranes, in particular, has led to high cost reductions. Today's membranes are characterised by high resistance, higher flow rates and a thinner membrane layer. Membranes consist of several layers, generally made of different polymers. Between the layers, spacers in the feed channels provide space for the cross-flowing feedwater. Moreover, the spaces ensure turbulent flow. On the opposite side of the membrane, a permeate spacer ensures room for the output water. In desalination plants, the layers are formed into spiral-wound elements around a central core tube. After passing through the membrane, the water can flow in a spiral direction to the core tube to be collected and transported to the outside. Figure 1.6 shows a spiral-wound element as used in the Sydney Desalination Plant.

Figure 1.6: *A spiral-wound RO element of the Sydney Desalination Plant.*

Source: Own picture.

Several spiral-wound elements are arranged in series in a pressure vessel. The feedwater is fed into the surrounding area of the vessel. The feedwater is not forced straight against the membrane, but the direction of water flow is along the membrane. The pressure applied to the water causes the latter to pass through the membrane layers, producing what is known as permeate. Concentrated saline water (so-called concentrate or retentate) is retained. Several vessels are combined to form a train. Such trains can be arranged parallel or in series. Figure 1.7 shows one train in the foreground and others in the background. Usually, the concentrate of the first train is transferred to another, smaller train where it is further concentrated. Thus the high pressure still acting on the water can be utilised further. Furthermore, it is possible to further reduce the amount of brine, which is crucial if the water is not released back into the sea.

Figure 1.7: *Several RO trains in the Sydney Desalination Plant.*

Source: Own picture.

Further progress has been made in the field of pretreatment procedures. If the feedwater is of good quality, minimal energy input or chemical additives need to be used. Figure 1.8 shows the pretreatment process of the Sydney Desalination Plant. Gravity-based pretreatment uses only sand and coal filtration to remove organic and small particles.

Due to the exclusive operation with electricity, choosing a location for RO plants is in principle more flexible, since no waste heat from other processes is required. The typical electricity consumption of large seawater reverse osmosis (SWRO) plants is 3-4 $^{kWh}/_{m^3}$, including pre- and post-treatment [65]. When using brackish water, the specific energy consumption is reduced to 1.5-2.5 $^{kWh}/_{m^3}$ at a feedwater salt content of 5,000-20,000

Figure 1.8: *The gravity-based pretreatment process of the Sydney Desalination Plant using coal and sand for filtration.*

Source: Own picture.

ppm [70]. The thermodynamic limit of electricity consumption for RO at a separation efficiency of 50% is 1.06 $^{kWh}/_{m^3}$ [77].

1.3 Desalination with renewable energy

Due to the high energy intensity of desalination, renewable energy (RE) are considered a prerequisite for sustainable water desalination. This section will, therefore, briefly outline the current status and challenges of coupling desalination and RE.

A rough distinction can be made between small and large scale in the application of desalination with renewable energy. Small, decentralised off-grid solutions, which are directly coupled with a RE technology, are already commercially offered and operated [61]. Various combinations are possible, which have different advantages and disadvantages depending on size and application area. The smallest application is a simple solar still, which is technically very simple, inexpensive in terms of capital costs, but also inefficient. RE is used with the help of solar collectors. With a capacity of usually less than 100 $^{L}/_{d}$, they are therefore only suitable for small users. The drop in prices for photovoltaic (PV) has made it feasible to couple PV and electrically operated desalination plants such as RO or ED as decentralised systems.

In principle, wind energy can also be directly coupled with desalination plants, for example, with RO or mechanical vapour compression (MVC). The higher capacity factor of wind energy is an advantage here, but the requirement for land is substantial. The scarcity of sites with good wind conditions and sufficient space often leads developers to choose PV. These variants are usually chosen for smaller plants up to 2,000 m^3/d, which are used for small communities or hotel facilities. The high variability due to the dependence on a single RE source leads to relatively low utilisation rates. Utilisation can be increased by RE technologies such as concentrated solar power (CSP) since the collected heat can be stored and used over a more extended period [170]. However, due to the sharp drop in the price of PV in recent years, CSP experiences increasing competition from this side.

Combinations of PV-RO and CSP-MED are most advanced for commercial application to provide larger quantities of water, i.e. more than 1,000 m^3/d [65]. The fluctuation of energy sources is the main challenge for the economic efficiency of integrated desalination and RE systems. However, in order to minimise the total cost of direct operation, it is advisable to increase the generation capacity of RE to achieve high utilisation rates of the desalination plants and thus to utilise the capital employed as much as possible. However, at maximum power generation, the electricity generated by the RE plants cannot be fully used by the desalination plants. Though, the excess electricity can be fed into the grid and thus be monetised. The advantage of CSP in combination with seawater desalination, in contrast, is that the heat generated can be stored to extend electricity generation over a longer period.

However, the approach shows that the direct coupling of RE and desalination is confronted with the challenge of volatility and the associated inefficient utilisation. Using a stand-alone RE technology is associated with higher volatility, as opposed to combining different RE technologies. Integration into larger systems, preferably the integration of desalination and RE technologies into the power grid, thus generally offers the advantage of reducing volatility. This allows both systems to operate more efficiently. Therefore, it is economically advantageous to feed a wind farm into the grid and connect a seawater desalination plant straight to the grid instead of operating both technologies coupled. This strategy is pursued, for example, at the Sydney Desalination Plant. Since the share of RE in the Australian grid is very low, the grid absorbs the volatility of RE. However, if the share of RE increases, new strategies such as demand management should be considered in order to raise further efficiency potentials. That option is examined in chapter 3 of this thesis.

Current and future trends show that renewable energy and desalination can produce water at competitive prices in a growing number of applications. The production costs of water with a high degree of grid integration of RE are currently around 0.5 $/m^3$ [65, 123]. Thermal plants are used in particular through the further development of heat recovery and the increased use of waste heat. The further development of hybrid plants, i.e. the combination of thermal and membrane-based plants, is expected to lead to further developments in terms of energy savings. In addition, membrane technology is expected to gain further importance due to its advantages in terms of overall energy efficiency and associated cost effectiveness. In this area, the further development of membranes is particularly important. Membranes will be further improved in terms of their resistance to fouling, higher flow rates and better retention properties, which will reduce the required pressure. New materials in the research field of nanotechnology, aquaporins or graphene continue to promise high potential [65]. A reduction in specific energy consumption to 1.7-2.5 kWh/m^3 seems to be achievable here [77, 158]. Batch and semi-batch RO process modifications may increase efficiency by over 60% [167].

The focus of this work is on the coupling of large-scale seawater desalination plants with RE of various resources. The investigation focuses on municipal water applications where the desalination plants are not directly coupled to RE but indirectly via grid integration. Due to the predominance of RO in practice, the work focuses on this technology.

1.4 Research motivation

Seawater desalination faces a number of challenges. Despite considerable efficiency improvements in recent decades, seawater desalination is the water supply option with the highest energy intensity. Desalination using conventional energy leads to high greenhouse gas (GHG) emissions. Environmental impacts on marine biology can already occur at the water inlet, where marine animals can be sucked into the inlet. However, this threat can be eliminated by large and distributed inlets, resulting in low flow rates.

The disposal of brine also creates environmental issues and risks for marine life. If the plant is located inland, brine is disposed of by deep well injection or using evaporation ponds. For smaller plants, disposal via the sewerage system is also an option. In the case of seashore installations, brine is usually discharged into the sea, either directly via surface water injection or, in the case of newer installations and generally in Australia, underwater in distributed outlets on the seafloor. Worldwide brine production in 2012 was about 40 km^3, and in 2050 it is estimated to be 240 km^3 [161]. Brine from thermal plants has a salt content of 46,000 to 80,000 ppm, about twice as high as the feedwater [161]. Thermal seawater desalination plants produce three times as much brine as membrane plants, with the brine in the latter being correspondingly more concentrated [161]. For this reason, membrane plants are particularly advantageous for domestic brine disposal.

Another negative impact on marine life can be caused by the increase in local seawater temperature at the outlet, which occurs most commonly in thermal systems. Chemicals contained in brine pose a further threat to marine biology [91, 161, 161]. Chemicals can already be used in the catchment area to combat molluscs. Within the plant, substances such as chlorine are used to prevent biofouling. Flocculants are also used. Antiscalant and antifoaming agents are generally used below the toxic limit, the latter only in thermal plants. Corrosion can lead to the presence of various heavy metals in water, including iron, chromium, nickel, molybdenum and copper. Alkaline or acidic cleaning agents such as complexing agents, oxidants and biocides are also used in seawater desalination plants. When certain substances enter seawater through the brine, the local concentration of these substances and also the heat input is of central importance.

When designing modern plants, however, the attempt is made to keep the quantity of chemicals and other substances in the brine as low as possible. Recent studies have shown that intelligent engineering, i.e. decentralisation of inlet and outlet, low flow velocity at the inlet and high diffusion and distribution at the outlet, has avoided negative impacts on marine life. Positive effects have even been demonstrated for large-scale plants [35]. The effects of inflow and outflow on marine organisms are complex, as they depend on the local conditions of the water body. Water depth, water temperature and water flow play a decisive role [78].

The high costs of seawater desalination are another challenge. Figure 1.9 shows the cost reduction of the last decades for thermal MSF and membrane-based SWRO. The costs of MSF, in particular, could be reduced by a factor of ten, but the costs of SWRO could also be reduced considerably, and it is generally the cheapest technology.

Figure 1.10 shows the allocation of water production costs to different components for MSF (left) and RO (right). Capital costs account for almost 50% for both technologies. For RO, energy and membrane costs follow with 19% and 16% of the total costs, respectively. In recent years, the development of novel, cost-effective membranes with high performance and durability has given RO a competitive advantage, so that the majority of plants built today are RO. However, the main cost driver of desalination plants is energy costs. The development of energy prices in the future may put considerable pressure on the technology. Here, too, significant improvements have been achieved in

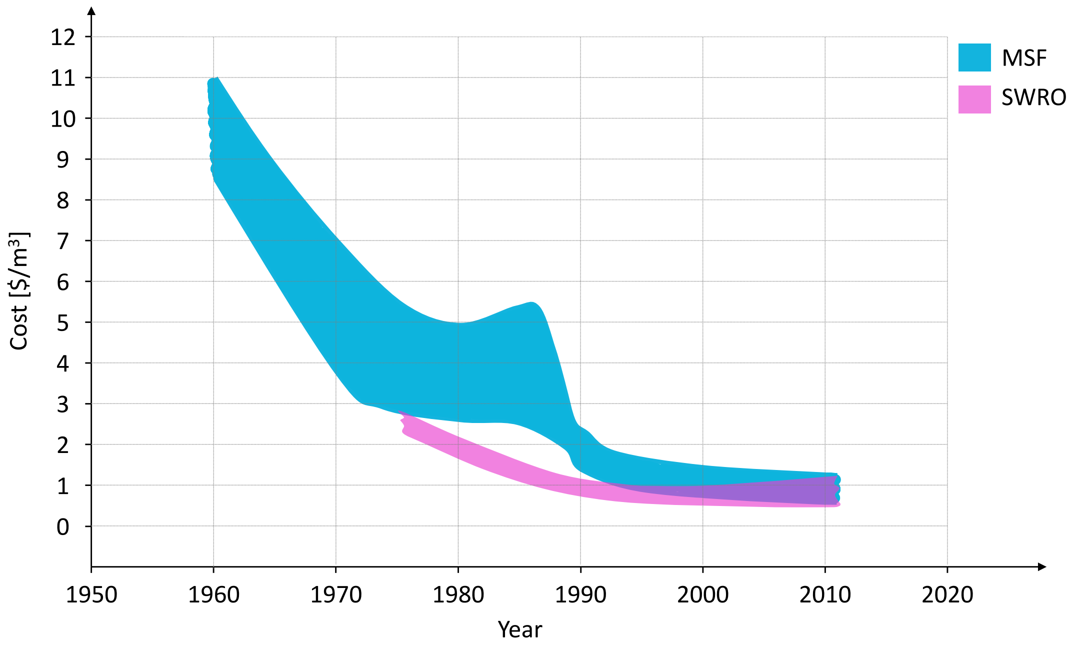

Figure 1.9: *Specific water production cost trends for MSF and SWRO.*

Source: [56], own depiction.

the past. For example, efficiency has been increased by energy recovery devices, and the efficiency of individual processes has been improved. Efficiency improvements are also expected in the coming years. Furthermore, a carbon price would put considerable pressure on the energy cost factor. Operation with renewable energy could, therefore, lead to considerable cost advantages in the long term.

Seawater desalination is generally seen as a last resort to counteract water shortages [147]. High costs but also the environmental impacts give rise to this perception. Therefore, it is generally agreed that water as a scarce resource should be saved first and foremost. Increasing the availability of water significantly could, in turn, increase the demand for water, which could lead to higher costs and further environmental degradation [120]. However, market-based instruments can foster intrinsic incentives to reduce costs and make technical progress. Moreover, environmental regulations can minimise environmental damage. Therefore, increasing water availability should not be rejected per se, even if it increases non-essential consumption. After all, increasing consumption and production opportunities usually lead to positive social impacts, such as the creation of new jobs [54, 80]. However, on the issue of overconsumption, see Wiedmann et al. [173]. Moreover, in countries with unreliable rainy seasons, reduced dependence on volatile water supply systems such as dams leads to lower costs in the long run [132].

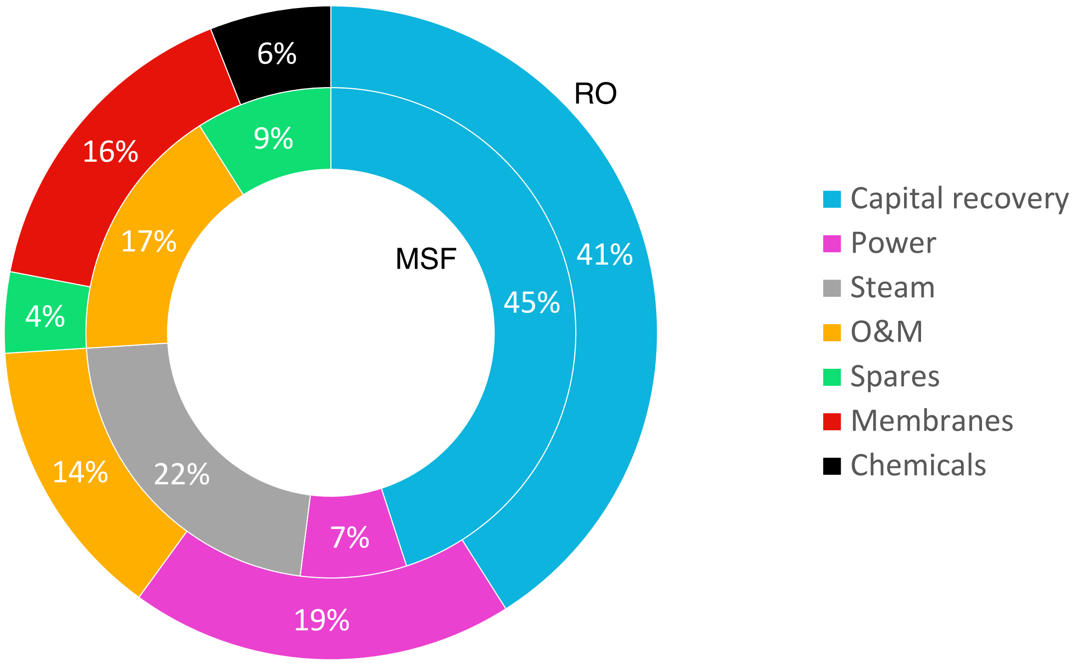

Figure 1.10: *Breakdown of the unit water cost of MSF and RO.*

Source: [56], own depiction.

The construction and operation of desalination plants also bring additional economic benefits [143, 185].

Renewable energy has the potential to increase overall sustainability in the social, economic and environmental dimensions. Since infrastructure facilities are typically in operation for several decades, these effects add up over a long period of time. For this reason, the investment decisions taken are also effective for several decades, so that the decisions define the degree of sustainability over this long period. Consequently, the emission intensity of these plants during operation and maintenance determines the emissions over several decades. Hence, such decisions must be examined in detail before the investments are made. However, too little attention has been paid to this necessity when investing in seawater desalination projects. A better understanding of the social, environmental and economic consequences is therefore urgently needed [64]. In particular, the effects of coupling intermittent renewable energy sources with desalination plants have the potential to make essential contributions to their overall sustainability [68]. This thesis aims to find answers to these questions and to provide a deeper understanding of the holistic impacts of seawater desalination.

1.5 Research questions

Whether coupling desalination with RE is a promising option for increasing water availability in arid and semi-arid regions depends mainly on its socio-economic and environmental sustainability. This thesis aims to show the overall sustainability of seawater desalination depending on the electricity source used. The driving forces of positive and negative influences are to be identified and quantified in detail. In the literature, the coupling of seawater desalination plants with RE is seen as a crucial factor which enhances environmental sustainability in particular. Nevertheless, only a few studies examine the interaction of both technologies for positive synergy effects. A lack of research is particularly evident for large-scale approaches, i.e. for municipal seawater desalination plants with a capacity of more than 100,000 $^{m^3}/_{d}$, which are not directly coupled with RE technologies but integrated into a RE network. Besides, there is a lack of research that considers not only direct effects within narrow system boundaries but includes the entire value chain.

The integrated and holistic approach of this work allows to examine the dimensions mentioned above and to better estimate the overall sustainability potential of coupling desalination and RE. By integrating the economic, social and environmental aspects in macroeconomic models, comprehensive cause-effect chains can be identified. The consideration of the entire value chain shows not only direct but also indirect effects. Last but not least, the sectoral and regional view helps to shape economic policy effectively. To this end, we have carried out several studies which answer the sub-questions arising from this research.

This dissertation comprises three peer-reviewed and published articles, which have been uniformly formatted and slightly adapted editorially for this thesis. Chapter 2 presents the paper "The carbon footprint of desalination: An input-output analysis of seawater reverse osmosis desalination in Australia for 2005-2015" [73]. In this chapter, we examined **research questions 1**: What carbon emissions are generated by the existing desalination plants in Australia? Which industries, goods and regions are the drivers of these emissions? The paper examines the carbon footprint of Australia's 20 largest seawater desalination plants. The plants represent 95% of the total desalination capacity in Australia. When building some of the plants in Australia, the Government decided to build RE plants simultaneously to offset carbon emissions during operation. Such agreements exist, for example, at the Sydney Desalination Plant or the Victorian Desalination Plant. However, the plants are operated using the Australian electricity mix, i.e. the electricity grid. In this first study, we determined the CO_2e emissions caused by operation based on the underlying physical electricity mix. The work aimed to show both direct and indirect carbon emissions across the entire value chain. In particular, we analysed which industries and commodities are accountable for carbon emissions. The regional distribution of emissions was also shown. The chosen period between 2005 and 2015 allowed an illustration of the construction and operation phase of these plants. Also, the carbon emissions per unit of water produced with conventional energy sources were determined.

Chapter 3 contains the paper "Renewable-powered desalination as an optimisation pathway for renewable energy systems: The case of Australia's Murray-Darling Basin" [71]. This chapter explores **research question 2**: What economic synergy effects arise from the coupling of large-scale desalination plants with a 100% RE system? The study investigates the integration of desalination plants into a 100% RE grid. The central question in this work is to what extent seawater desalination as a variable load can minimise the capacity of the RE system by load-shifting. As seawater desalination plants are usually operated at constant load, their capacity for load-shifting has to be increased accordingly. Therefore, the question was investigated whether the savings on the RE side offset the additional costs on the desalination side. The influence of the load-shifting period was also examined. Furthermore, it was examined which synergy effects result from the diversification of the RE technologies used and from the diversification of location and time of electricity generation.

Chapter 4 examines the social, environmental and economic impacts of desalination and the influence of the choice of electricity source on these indicators, based on the previous two chapters. In this chapter, we examine **research question 3**: What are the social, economic and environmental benefits and costs of coupling large-scale desalination plants with a 100% RE system? The chapter comprises the study "Desalination and sustainability: A triple bottom line study of Australia" [72]. Again, we are not investigating the direct coupling of individual plants with RE. Instead, we simulate the embedding in an electricity grid with different penetration of RE. The economic indicator used here is gross value added (GVA), and the social indicator is employment. Water consumption, land use and carbon emissions were examined as environmental indicators. For each indicator, the sectors and regions that are crucial for sustainability and that would have a significant impact on them when switching to RE were identified.

Chapter 2

The carbon footprint of desalination: An input-output analysis of seawater reverse osmosis desalination in Australia for 2005-2015

Michael Heihsel[1], Manfred Lenzen[2], Arunima Malik[2,3], Arne Geschke[2]

[1] Department of Energy Engineering, Technical University of Berlin, Straße des 17. Juni 153, 10623 Berlin Germany

[2] ISA, School of Physics, The University of Sydney, Sydney, New South Wales 2006, Australia

[3] Discipline of Accounting, The University of Sydney Business School, Sydney, New South Wales 2006 Australia

Published in: Desalination vol. 454 (2019), accepted manuscript, https://doi.org/10.1016/j.desal.2018.12.008, [73].

Abstract

This study examines greenhouse gas emissions for 2005-2015 from seawater desalination in Australia, using conventional energies. We developed a tailor-made multi-regional input-output-model. We complemented macroeconomic top-down data with plant-specific desalination data of the largest 20 desalination plants in Australia. The analysed capacity cumulates to 95% of Australia's overall seawater desalination capacity. We considered the construction and the operation of desalination plants. We measure not only direct effects, but also indirect effects throughout the entire value chain. Our results show the following: We identify the state of Victoria with the highest emissions due to capital and operational expenditures (capex and opex). The contribution of the upstream value chain to total greenhouse gas emissions increases for capex and decreases for opex. For capex, the construction of intake and outfall is the driving factor for carbon emissions. For opex, electricity consumption is the decisive input factor. Both in construction and operation, we identify the critical role of the electricity sector for carbon emissions throughout the supply chain effects. The sector contributes 69% during the zenith of the construction phase and 96% during the operating phase to the entire emissions. We estimate the total emissions for 2015 at 1,193 kt CO_2e.

2.1 Introduction

Increasing lack of fresh water is one of the most severe global problems of the future decades. About two thirds of the world's population has no access to fresh drinking water at least once a year [121]. More than 783m people have no access to clean drinking water [171], and half a billion people suffer from water shortages throughout the year [121]. The most affected regions include the west of North America, the east of Spain, the Middle East and North Africa (MENA) region, as well as Australia and northern China. Archipelagos like the Canary Islands face these problems, too [91].

Meanwhile, California experienced a prolonged and unusually severe drought from 2011 to 2017, resulting in daily life restrictions, high water costs, and economic slowdown. Climate change, prosperity, and exponential population growth will further aggravate these problems. Water is increasingly becoming a scarce and therefore valuable commodity. It is becoming more difficult for the regions mentioned to meet the demand for fresh water which inevitably leads to conflicts of use.

Many of these arid regions are close to the seashore and thus close to substantial water resources. Some areas are already using desalination technology, which is the most expensive option to meet water demand. However, it is already indispensable for many regions. For example, Saudi Arabia covers 50% of its water needs from desalination, using 25% of its oil and gas for water and electricity production in combined power-desalination plants [163]. Mitigating water scarcity becomes a self-accelerating problem. Drought is increasing as a result of climate change. In order to solve this problem, the use of desalination is proliferating, which in turn catalyses climate change due to high energy demand. Water production needs energy, but electricity generation also needs water in large quantities, that is why academia speaks of the water-energy-nexus [148].

Numerous studies address technical, economic or ecological issues of conventional and renewable operated desalination. However, the current literature shows some knowledge gaps. Gude states in his study:

> "Although some of the facts and recent developments discussed here show that desalination can be affordable and potentially sustainable, contributions that meaningfully address socio-economic and ecological and environmental issues of desalination processes are urgently required in this critical era." [64]

Haddad also draws attention to the need for holistic studies in the field of desalination research [68]. Only by incorporating effects throughout the entire supply chain (indirect effects), a comprehensive assessment is possible [68]. Whether or not desalination can sustainably solve the problems of water availability in arid and semi-arid regions depends on its holistic socio-economic and ecological sustainability.

Lattemann and Höpner provide an overview of the leading environmental impacts of desalination and possibilities to minimise impact and risks [91]. The World Bank estimates that 99% of carbon dioxide equivalent (CO_2e) involved in a business-as-usual scenario could be avoided by desalination with renewable energys (REs) [161]. This estimation illustrates the enormous carbon reduction potential of combining REs and desalination. Einav et al. show the factors that significantly influence the ecological footprint of desalination [44]. These factors are land use, the groundwater, the marine environment, noise pollution and the use of energy. According to Muñoz and Fernández-Alba, the type and quality of feedwater can reduce the environmental impact (such as energy demand, acidification potential or human toxicity potential) of the reverse osmosis (RO) process up to 50% [124]. Liu et al., Setiawan et al., Vince et al. and Sadhwani et al. offer analyses of the ecological effects [108, 141, 149, 166]. A good overview of current trends and ecological challenges can be found in Goosen et al. [61].

We have found several studies in the field of input-output analysis (IOA) and life cycle assessment (LCA) of desalination. Raluy et al. use a process-based LCA to investigate different desalination technologies [135]. Zou and Liu use IOA on desalination in China to measure the economic impact of investments [185]. Storkes and Horvath use hybrid life cycle assessment (hLCA) to study water supply systems in California [156]. Shahabi et al. use a hybrid approach to investigate a desalination plant in Western Australia (WA) [150].

There is no doubt that desalination plays an essential part in the water supply strategy of regions which are affected by severe drought and have access to seawater. However, desalination must prove its economic, environmental and social sustainability. Our study contributes to quantifying environmental sustainability by measuring the carbon footprint of desalination in Australia. For the study, we assume that operation and construction processes use electricity from conventional energy in line with the Australian energy mix. It is the first study of desalination, where a comprehensive multi-regional model has been created and used for measuring the supply chain impacts. With the aid of our multi-regional model, we can also present regional impacts for the first time. Our approach rates the country's largest 20 plants, which represents 95% of the total capacity – that to over more than ten years.

2.2 Methods and data

A carbon footprint captures the carbon emissions of a product, a technology or a technical process. This approach does not only analyse carbon emissions directly generated by the desalination process itself. It also accounts for indirect effects, defined as all carbon emissions generated by suppliers within the entire supply chain. Our approach captures carbon emissions throughout the entire supply chain (upstream). We consider desalination as final demand and analyse carbon emissions from sectors from which desalination purchases inputs. Our approach does not assume that additional water from desalination induces further carbon emission downstream the supply chain.

Leontief [105] invented IOA and applied it in several studies. For this seminal work, Leontief earned the Nobel Prize in 1973. Researchers have used IOA to analyse economic effects of monetary demand on economic key figures, mainly effects on industrial output. Model extensions use IOA to analyse further economic, social or environmental effects [37, 125]. We apply input-output (IO)-methodology to estimate the carbon footprint of desalination in Australia.

Footprint studies apply input-output tables (IOTs) that show monetary trade flows of economic sectors. In order to produce goods, companies purchase intermediate goods from other companies. These intermediate streams are the core of IOTs. The columns of these tables show which input factors a particular sector purchases to produce their goods. The rows of the table show the production of a sector, which this sector produces for other sectors as intermediate inputs. The intermediate input matrix gives a comprehensive picture of the intermediary inputs and creates a production recipe for the produced goods of each sector. These recipes provide the opportunity to carry out value-added analysis and combine it with satellite accounts (such as the sectors' greenhouse gas (GHG) emissions). The combination allows for comprehensive carbon footprint studies by considering the entire value chain, without truncation errors such as those found in classic process-based LCAs [131].

The benefit of a hLCA approach is to combine bottom-up process data with top-down macroeconomic IO data and hence include the technical process into the macroeconomic system of a whole economy.

To the best of our knowledge, our study is the first comprehensive multi-regional carbon footprint study for a country's desalination application.

2.2.1 Construction of a multi-regional input-output database

IOA applies data from national accounts. IOTs arrange and structure the data. The tables describe the structure of an economy with detailed information about output, intermediate and final demand. IOTs can describe an economy by industry or commodity classification. Furthermore, IO-models can classify an economy in a single-regional or a multi-regional framework.

Compiling tailor-made IOTs is a work-intensive task. Finding data for different regions and sectors is challenging because the data are often incomplete or inconsistent. Lenzen et al. developed a cloud-based virtual laboratory, the Industrial Ecology Virtual Laboratory (IELab), to compile tailor-made IOTs for Australia [98]. A collaborative group of researchers feeds the database in an ongoing process. An algorithm converts the data into a specific structure, the so-called root classification. The root has 1,284 sectors in Input-Output Product Classification (IOPC) [4] and 2,214 regions in Statistical Area Level 2 (SA2) classification [1]. Due to the vast amount of data, IELab offers high-performance-computing for IOT compiling and calculations [97]. We apply a supply-use-framework [102].

For this study, we constructed a multi-regional input-output (MRIO) framework with 123 sectors and eight regions that represent the Australian States and Territories. The desalination input data determine the structure of the sector classification. In contrast to available IOTs, this allows for a detailed and accurate analysis that avoids aggregation errors. For our carbon footprint study, we compiled a satellite account of CO_2e emissions of industrial sectors.

We compiled several concordances for this study [98]. The generation of tailor-made IOTs requires concordances from root to study-specific sector classification and from root to study-specific region classification. To compute demand vectors, we compiled concordances from desalination input data structure to study-specific sector classification. Since supply-use-frameworks are twice the size of usual IO-frameworks, the framework includes 2 x 123 sectors (industry and commodity) in eight regions. The structure results in a transaction matrix in the size of 1,968 x 1,968. We compiled tables for the years 2005-2015, whereas the years refer to Australian financial years.

Compiling IOTs requires the application of mathematic optimisation algorithms. The critical challenge is that the number of variables to be determined significantly exceeds the number of constraints. The IELab implemented advanced optimisation approaches like quadratic programming and Konfliktfreies RAS (KRAS) to solve the optimisation problem [96].

The creation of large MRIO tables represents an underdetermined optimisation problem. Raw data for large economic transactions are much more available than raw data of small transactions. Hence, the number of constraints used for the optimisation is much smaller than the number of elements that we determine in the table. Therefore, large transactions are supported by many raw data points, while small transactions are supported only by a few raw data points. Within the optimisation process, this results in MRIOs representing large transactions with high reliability. However, small transactions are often subject to significant adjustments. Monte Carlo techniques can be used to show that the results of impact analyses remain stable [99].

We show this phenomenon in the calculation of the sectors' outputs from the MRIO. We can calculate outputs in IOTs in two ways. One way is to calculate outputs by row sums, which represents the production of the intermediate demand for other sectors and the production for the final demand. Also, we can determine the output of a sector by the column sum of this sector. The column sum corresponds to the sum of all goods necessary for the production of one sector's goods, and the value added created by this sector.

Both ways should ideally come to the same result. Since the creation of an MRIO is an underdetermined optimisation problem, adjustments are necessary, which results in deviations. Figure 2.1 shows, however, that our MRIO represents large transactions with high reliability and small transactions are subject to greater uncertainty. The impact analysis thus provides reliable results.

2.2.2 Preparation of desalination data

Data on desalination is scarce [60, 184]. Wittholz et al. attempted to estimate the cost structures of desalination plants [175]. The Desalination Economic Evaluation Program (DEEP) model of the International Atomic Energy Agency (IAEA) is also a common model to estimate the cost structure of desalination plants [85]. For our analysis, we deployed data from desaldata, a database with additional functions [66]. Desaldata offers the most detailed database we found. The cost estimator tool for estimating capital expenses (CAPEX) and operational expenses (OPEX) structures as functions of several variables is also a part of the platform.

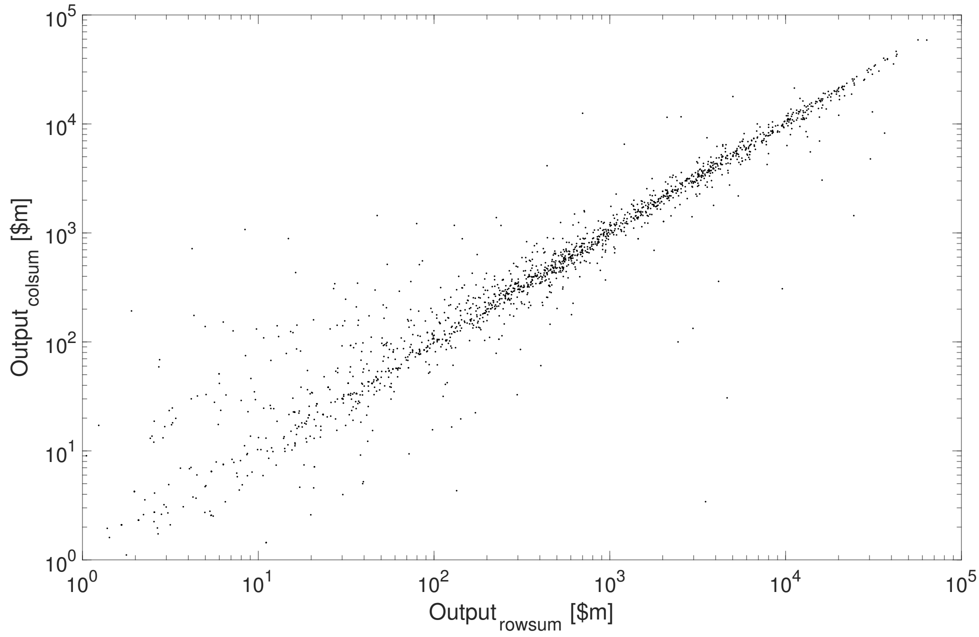

Figure 2.1: *Rocket plot of outputs calculated via row sum and column sum in 2015.*

Desaldata contains data for 349 seawater desalination, brackish water and wastewater plants in Australia with capacities from 30 to 444,000 $^{m^3}/_{d}$. For our study, we used data for of the largest 20 seawater reverse osmosis (SWRO) that cumulate to 95% capacity of all Australian seawater desalination plants with particular plant capacities from 4,000 to 444,000 $^{m^3}/_{d}$ (see appendix 2.5.1). RO is the common desalination technology in Australia, and there is only a small number of other technologies like multi-effect distillation (MED) or multi-stage flash distillation (MSF).

Even though desaldata is the most detailed database we found, it is fragmentary and partially unreliable. Desaldata offers complete data for location, capacity, feedwater type, award date, and online date. Data of Engineering-Procurement-Construction (EPC) price, feedwater conditions, and power consumption were sketchy. We validated years of construction, capacity, CAPEX, OPEX , and specific energy consumption by additional literature and adjusted the data if necessary (see appendix 2.5.2). Thus, we were able to validate data for the largest eight plants with a cumulated capacity of 95.9% of all 20 analysed plants. For the residual plants with 4.1% of cumulated capacity, we used the raw results of desaldata's cost estimator and adjusted CAPEX sums by the database's value if available.

Desaldata's cost estimator tool provides a breakdown for OPEX and CAPEX depending on different attributes such as location, salinity, temperature or energy consumption. If data for EPC prices were available, we used the CAPEX cost estimator only for ratios of the cost structure. If EPC prices were not available, we used the CAPEX cost estimation for the CAPEX sum as well. We estimated seawater temperatures by yearly average temperatures of the nearest city [178]. We estimated electricity prices by the annual volume-weighted spot prices of states and territories in 2009 [13]. We used WA's Short Term Energy Market (STEM) data for both WA and the Northern Territory (NT) since data for the NT is not available [11]. The cost estimator is only capable of calculating costs for plant capacities larger than 8,000 $\mathrm{m^3/d}$. Hence, we used values of this plant to extrapolate cost structures of all smaller plants. The smaller plants account for only about 3.5% of the total investigated capacity. An over- or underestimation will therefore not significantly affect the overall outcome of the study. The cost estimator calculates in US$ currency, so we converted US$ into AU$ using exchange rates from International Monetary Fund [82]. We used 2009 as the base year for the initial cost estimation. We assumed a utilisation rate of 95% for all modelled plants. Even if some plants are currently unused because municipalities are currently not in water shortage (like Sydney or Melbourne), we also modelled these plants with a utilisation rate of 95%. Our research objective is not to focus on the reproduction of the most accurate costs of real operations, but rather quantify the carbon footprint of the plants when they produce their capability.

Finally, we estimated data for 20 plants, each of the plant covers twelve data points for CAPEX and four data points for OPEX demand. The left diagram in fig. 2.2 shows the input data for our analysis.

We calculated the final demand vectors as follows:

1. Construction of preliminary demand vectors $\mathbf{y}_1$ for OPEX and CAPEX.

2. $\mathbf{y}_2 = \mathbf{y}_1 r^a$ converts the demand vector $\mathbf{y}_1$ from US$ into AU$ with the exchange rate r^a for year a. We applied the exchange rate of the online year for all CAPEX vectors. We converted the OPEX vectors by the exchange rate of 2015.

3. We distribute CAPEX and OPEX over the construction period. We prorated CAPEX according to $\mathbf{y}_3^a = \frac{1}{n}\mathbf{y}_2$ for each year a with n as the number of construction years. We assumed only half of the CAPEX investments in the first and the last year of construction works, so we apply $\mathbf{y}_3^a = 0.5\frac{1}{n}\mathbf{y}_2$ for the online and award year respectively. If we assumed a plant that was awarded in 2009 and went online in 2012, then n is 3 as award and online year respectively only gets a half year value. The vector $\mathbf{y}_2$ is distributed among $n+1$ vectors $\mathbf{y}_3^a$. For OPEX

distribution, we applied $\mathbf{y}_3^a = \mathbf{y}_2$ for each year after the online year. We assumed $\mathbf{y}_3^o = \frac{1}{2}\mathbf{y}_2$ for the online year o.

4. We inflated the demand vectors by $\mathbf{y}_4 = \mathbf{y}_3 \frac{p_s^a}{p_s^b}$, where p_s^a is the producer price index for sector s of year a [10]. p_s^b is the producer price index of the base year. The base year of CAPEX vectors is the online year. For OPEX , we assumed 2015 as the base year.

5. We applied $\mathbf{y}_5^a = \mathbf{C}\mathbf{y}_4^a$ to expand the demand vectors of each year from a 1 x 15 to a 1 x 123 demand vector. $\mathbf{C}$ is a 123 x 15 concordance matrix.

6. Since we use an Australian MRIO, we separated the domestic vectors from (rest of the world) import vectors. We aggregated the compiled MRIO tables to the national level to compute the import quota vectors $\mathbf{q}^a$ for each year a. The vector consists of q_i^a for each sector i , defined by $q_i^a = \frac{\sum_{j=1}^{N} \mathbf{I}_{i,j}^a}{\sum_{j=1}^{N} \mathbf{U}_{i,j}^a}$. $\mathbf{I}_{i,j}$ is the import intermediate demand matrix and $\mathbf{U}_{i,j}$ the total intermediate demand matrix, composed as $\mathbf{U}_{i,j} = \mathbf{T}_{i,j} + \mathbf{I}_{i,j}$. $\mathbf{T}_{i,j}$ is the domestic intermediate demand aggregated to the national level. We calculated the domestic desalination demand vectors by $\mathbf{y}_6^a = \mathbf{y}_5^a \# (\mathbf{1}\text{-}\mathbf{q}^a)$, where # denotes element-wise multiplication. The import quota in our model was about twenty per cent in average respective the different years and sectors.

7. As the last point, we expanded the demand vectors $\mathbf{y}_6^a$ to the size of the MRIO framework. For the regional allocation, we converted the geographical coordinates of the location of the desalination plants into SA2 classification. We placed the vector $\mathbf{y}_6^a$ into the rows of the respective region and the columns of the respective year. The constructed OPEX and CAPEX demand matrices $\mathbf{O}_p$ and $\mathbf{C}_p$ of each plant p have 1,968 rows (MRIO size) and 11 columns (one column for each year). We aggregated all matrices to one final demand matrix $\mathbf{Y} = \sum_{p=1}^{66} \mathbf{O}_p + \sum_{p=1}^{66} \mathbf{C}_p$.

2.2.3 Calculation of the carbon footprint

Researchers widely use environmentally extended IOA for carbon footprints of individual products, processes, economic agents like companies or final consumers [172]. Pomponi and Lenzen demonstrate the superiority of using IOTs in a hLCA approach over of using only bottom-up process-based data for LCA [131].

IOTs catch the industrial intermediate dependencies by linear functions. The linear approach causes basic assumptions: Industries have fixed input structures (linear production function), constant economies of scale and commodity prices are constant. Hence, we can interpret the cost structure as average variable costs rather than marginal costs. Furthermore, IOA is an ex-post analysis. Miller and Blair provide a well-detailed overview on IOA [122].

In IOA, we use Leontief's inverse to calculate the total impact of a demand on the output of an economy. We derive the inverse from the basic relationship between supply and demand. Suppose $\mathbf{x}$ as the M x 1 total output vector, $\mathbf{T}$ as the M x M intermediate demand matrix and $\mathbf{Y}$ as the M x N final demand matrix, then

$$\mathbf{x} = \sum_{j=1}^{M} \mathbf{T}_{i,j} + \sum_{j=1}^{N} \mathbf{Y}_{i,j}. \tag{2.1}$$

As the production recipe of the sectors, we can express the technical coefficient matrix $\mathbf{A}$ as

$$\mathbf{A} = \mathbf{T}\hat{\mathbf{x}}^{-1} \tag{2.2}$$

It follows from the preceding that

$$\mathbf{T} = \mathbf{A}\hat{\mathbf{x}}. \tag{2.3}$$

We can insert the preceding equation in eq. (2.1) and rearrange to

$$\mathbf{x} = (\mathbf{I} - \mathbf{A})^{-1}\mathbf{Y} \tag{2.4}$$

as the basic formulation of Leontief, while

$$\mathbf{L} = (\mathbf{I} - \mathbf{A})^{-1} \tag{2.5}$$

is the Leontief inverse that captures all direct and indirect effects of demand $\mathbf{Y}$ on the output $\mathbf{x}$. The matrix $\mathbf{I}$ is the identity matrix. We extend the economic Leontief model by a satellite account of industrial carbon dioxide equivalent emissions $\mathbf{e}$ and calculate the direct emission intensities

$$\mathbf{q} = \mathbf{e}\hat{\mathbf{x}}^{-1}. \tag{2.6}$$

Furthermore, we obtain the direct and indirect effects captured in a matrix representing the multipliers for each sector-to-sector relationship from

$$\mathbf{m} = \hat{\mathbf{q}}\mathbf{L}. \tag{2.7}$$

The total carbon emissions of desalination throughout the entire value chain are finally captured by

$$\mathbf{E} = \hat{\mathbf{q}}\mathbf{L}\hat{\mathbf{y}}. \tag{2.8}$$

Row sums $\mathbf{r}$ of the matrix $\mathbf{E}$ result in carbon emissions referring to sectors and regions where they physically occur. Hence, row sums reflect the emitting sectors or regions, depending if we aggregate to sectors or regions. Column sums $\mathbf{c}$ will refer to desalination inputs and regions where emissions are accounted regarding consumption responsibility of the analysed desalination plant. We calculate row sums or the column sums by multiplying the Matrix $\mathbf{E}$ by sum vector $\mathbf{i}$, which is a column vector with the number of rows according to matrix $\mathbf{E}$ with every element equal to 1 by

$$\mathbf{r} = \mathbf{E}\mathbf{i}, \tag{2.9}$$

or

$$\mathbf{c} = \mathbf{i}'\mathbf{E}. \tag{2.10}$$

We aggregate the vectors by multiplying them with aggregators, so-called concordances $\mathbf{C}$.[1] The concordances are tailored to each aggregation and sum up the 1,968 sectors to sectors or regions of research interest (e.g. classification of Australian States or desalination input commodities). For example, if the desalination plants emit 100 kt CO_2e, row sums of matrix $\mathbf{E}$ assign emissions to the region where the desalination plant is located respectively the input products, which the desalination plant directly demanded. Column sums assign the same 100 kt CO_2e emissions to the regions where the emissions effectively occur respectively to the sectors which physically emitted GHG.

We get the final vectors as

$$\mathbf{v} = \mathbf{C}\mathbf{r}, \tag{2.11}$$

respectively

$$\mathbf{v} = \mathbf{c}\mathbf{C}. \tag{2.12}$$

For the production layer decomposition (PLD), we formulate the Leontief inverse as

$$\mathbf{L} = \mathbf{I} + \mathbf{A} + \mathbf{A}^2 + \mathbf{A}^3 + ... + \mathbf{A}^n. \tag{2.13}$$

We disaggregate the total carbon emission into several layers. $\mathbf{E}_1 = \hat{\mathbf{q}}\mathbf{A}\hat{\mathbf{y}}$ results in emission for the first layer, defined as direct effects. $\mathbf{E}_2 = \hat{\mathbf{q}}\mathbf{A}^3\hat{\mathbf{y}}$ gives emission for the second layer and so on. Each layer represents one supplier-stage of production. The first layer consists of carbon emissions from direct suppliers. The second layer shows carbon emissions of the supplier-suppliers.

2.3 Results and discussion

Desalination is an energy- and thus carbon-intensive technology for gaining fresh water. IOA methodology enables to uncover not only direct carbon emissions of desalination

[1] For more information on using concordances, see supporting information in Lenzen et al. [98].

but also indirect effects along the entire value chain. The following section will present detailed insights into the carbon footprint of desalination in Australia over the years 2005-2015.

2.3.1 Cost and CO_2e emissions overview

Within the last 15 years, Australia has faced an extreme drought, mainly from 2003 to 2012. One consequence of this drought has been a political discussion about Australian's freshwater strategy. Desalination was used already before in a much smaller scale. However, facing this severe drought, several Australian cities, states, and firms have started huge investments in desalination plants.

The left axis curve of the left diagram in fig. 2.2 shows domestic CAPEX and OPEX expenditures from 2005 to 2015 in current year prices. The total expenditures reach their maximum in 2010 by AU$2.3bn. CAPEX was the predominantly driver of the expenditures.

Average OPEX per produced water (right axis) increased within the 11 years from about 0.2 $^{AU\$}/_{m^3}$ to 0.5 $^{AU\$}/_{m^3}$. Increasing energy costs mainly determine the growth of OPEX. The construction of different sized desalination plants within the analysed period also affect the growth of OPEX.

The bar graph (left axis) in the right figure shows the total carbon emissions (direct and indirect effects) due to OPEX and CAPEX. We can see that CO_2e due to CAPEX is predominant until 2011. After the main investment period, OPEX becomes predominant. In 2013, desalination emitted 1,269 kt CO_2e mainly driven by OPEX. The right axis figure shows the total carbon emission per cubic meter of produced water, only determined by OPEX. We observed increasing OPEX emissions per cubic meter up to 2,000 $^{g}/_{m^3}$ at the end of the investigated period.

Table 2.1 shows the direct, indirect and total carbon emissions for the years 2005-2015 due to OPEX and CAPEX. Construction activities determine CAPEX while the operation of existing plants results in OPEX. In 2005, only CAPEX was responsible for CO_2e emissions. As of 2012, OPEX was the driving force. During the construction phase, CO_2e emissions due to CAPEX played a significant role with a peak of 820 kt CO_2e. These high carbon emissions focus on just a few years. The annual CO_2e emissions due to OPEX exceed the emissions of CAPEX already in 2012 with 759 kt CO_2e. Due to the runtime of the plants over several decades, OPEX makes a significant contribution to the carbon footprint over its life cycle. The last column shows the carbon multiplier

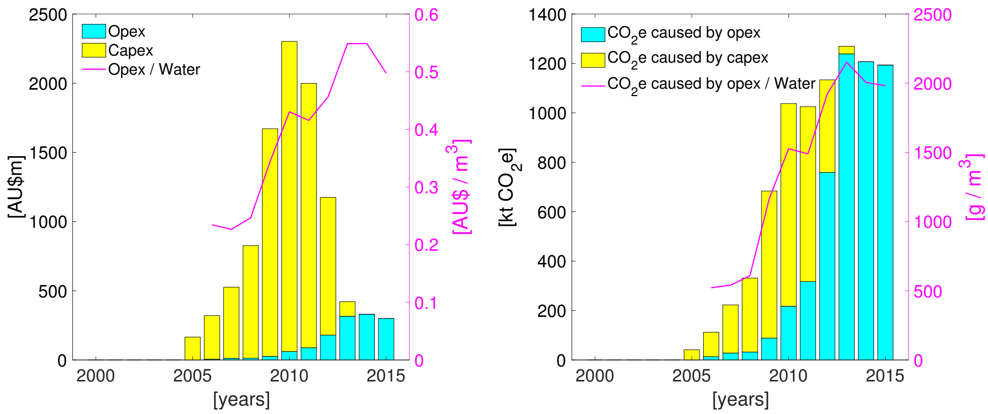

Figure 2.2: *Overview of costs and CO_2e emissions.*

c, that is defined by $c = \frac{Q^a_{\mathrm{tot}}}{Q^a_{\mathrm{dir}}}$, with the total carbon emission Q^a_{tot} and the direct carbon emission Q^a_{dir} for the year a. Due to the larger multiplier of CAPEX, we see that its supply chain has a more significant impact on CO_2e emissions than the supply chain of OPEX. Over the years, the multiplier of CAPEX increases (except in 2013), while the multiplier of OPEX decreases. The higher the multiplier, the higher is the contribution of the upstream value chain to the overall effects. In conclusion, the value chain of the construction of desalination plants becomes more unsustainable over time, while the value chain of operations becomes more sustainable.

Table 2.1: *Carbon emissions due to opex and capex of desalination in Australia.*

Year	CO_2e effects caused by capex Direct effect [kt CO_2e]	Indirect effect [kt CO_2e]	Total effect [kt CO_2e]	Multiplier [kt CO_2e/kt CO_2e]	CO_2e effects caused by opex Direct effect [kt CO_2e]	Indirect effect [kt CO_2e]	Total effect [kt CO_2e]	Multiplier [kt CO_2e/kt CO_2e]
2005	21	20	41	2	0	0	0	-
2006	50	48	99	2	8	5	13	1.7
2007	100	95	195	1.9	17	12	28	1.7
2008	158	141	299	1.9	19	13	32	1.7
2009	286	309	595	2.1	58	30	89	1.5
2010	375	445	820	2.2	155	62	217	1.4
2011	311	397	708	2.3	229	88	317	1.4
2012	159	216	375	2.4	544	215	759	1.4
2013	16	15	31	1.9	882	356	1239	1.4
2014	0	0	0	-	854	353	1207	1.4
2015	0	0	0	-	845	349	1193	1.4

IOA with MRIOs is well suitable to uncover the spatial distribution of observed effects. In our study, we show the spatial distribution of carbon emissions. We can assign carbon emissions either to desalination inputs and locations of the plants or to emitting industries and emitting locations. Figure 2.3 shows carbon emissions in 2012 due to

CAPEX and OPEX assigned to locations of the desalination plants. We created tables with eight regions representing the eight States and Territories in Australia. In 2012, we can still observe a high level of construction activities, but also high expenses for operations. Australian Capital Territory (ACT) and Tasmania (Tas) do not operate desalination plants, so there is no carbon emission assigned. NT's desalination activity induces negligible emissions due to OPEX in 2012. In Queensland (Qld) and New South Wales (NSW), we only find emissions due to OPEX. WA and South Australia (SA) have emissions due to OPEX and CAPEX on a medium scale. Victoria (Vic) built the Victorian Desalination Plant from 2009 to 2012. Hence, the state is the leader in emission due to OPEX and CAPEX in 2012.

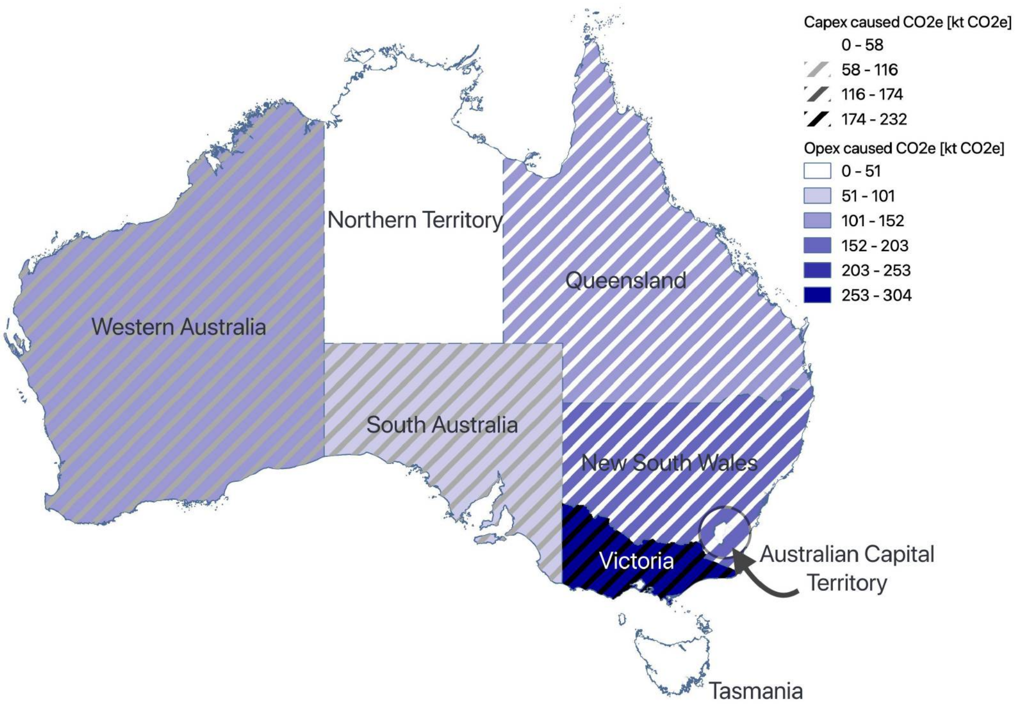

Figure 2.3: *CO_2e emissions by states and territories caused by capex and opex in 2012.*

Figure 2.4 shows the total carbon emissions for 2005-2015. The four individual diagrams break down the emissions according to different systematics. We see that the emissions increase over time, dominated by CAPEX in 2010. As of 2012, OPEX contributes significantly to carbon emissions.

In the left-hand diagrams, we assigned carbon emissions to emission-causing desalination inputs and locations of the plants. The diagrams on the right side show emitting

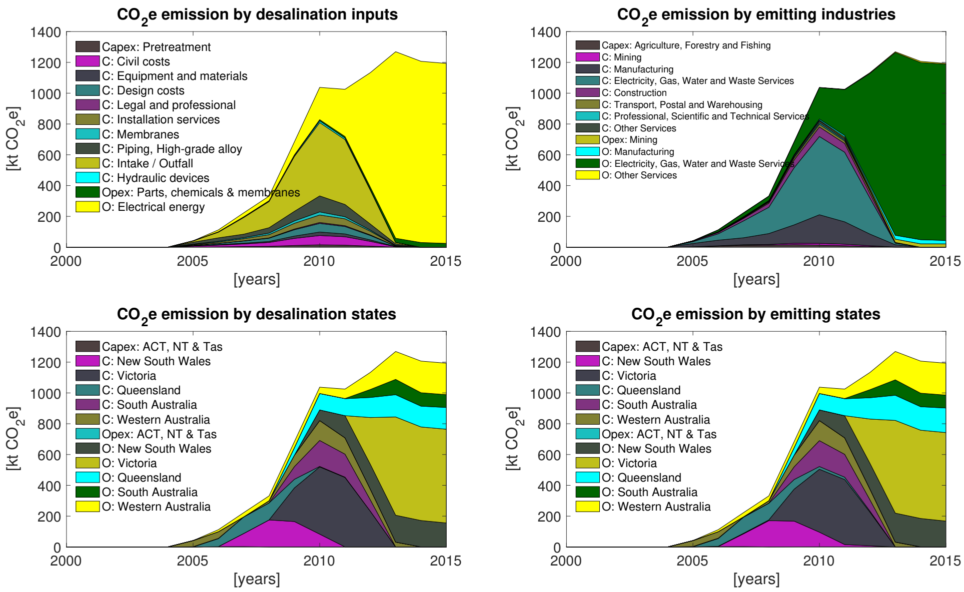

Figure 2.4: *CO_2e emission by desalination inputs and emitting industries.*

industries and emitting locations. We compiled individual demand vectors for CAPEX and OPEX so that we can illustrate the effects of OPEX and CAPEX separately.

The diagram on the top left shows the carbon emissions assigned according to desalination inputs, each for CAPEX and OPEX. The peak of CAPEX caused emissions marks the boom in construction activities around 2010. Construction of inlets and outlets cause the main emissions. The second most considerable emission-causing input is the construction process of pipes. Both mainly require steel, which explains the high-level emissions. OPEX-caused emissions mainly occur due to the demand for electricity as a direct input. At the end of the period, electricity causes almost all carbon dioxide. We aggregated all other inputs such as parts, chemicals and membranes for the sake of convenience. Since desalination plants usually operate for several decades up to 20-40 years, OPEX especially the energy source is the crucial point regarding environmental sustainability of desalination in the long run.

In the upper right chart, we can see which industry sectors emitted CO_2e due to the production of inputs, also divided into emissions caused by CAPEX and OPEX. It is noticeable that even for CAPEX demand the electricity sector emits a significant amount of CO_2e. The manufacturing sector is another key sector for carbon emissions during the construction phase, followed by the construction sector as the third largest emitter. As we have already discovered that the primary input of OPEX is electricity, it is not surprising that the electricity sector has the highest emissions. It indicates that the value chain of conventional energy plays a minor role in carbon emissions.

The graph at the bottom left shows the carbon emissions assigned to the desalination plant's locations, separated by CAPEX and OPEX. Around the year 2010 Vic caused the most substantial emissions due to CAPEX, followed by SA. In the years around 2008, construction activities in NSW were a significant driver. In the following years after 2011, when the construction activities decline, OPEX becomes dominant for carbon emissions. Vic has by far the most significant emissions of CO_2e, followed by WA and NSW.

The diagram to the right shows in which states and territories CO_2e was emitted. At high trading volume, the graphs differ because consumption and production happen on different locations. Here we see that the diagrams are almost identical. Already in the diagrams above, we found for CAPEX and OPEX that the electricity, gas, water and waste service sector dominates the carbon emissions. Even if Australia has a national electricity market, electricity trade between different states is at a low level. WA and the NT are not even connected to the National Electricity Market [14].

Finally, we compiled a PLD analysis for 2012. This approach determines the emissions for each production layer individually. Production layers are the several tiers within a value chain. We define the first layer as the direct effect. The direct effect accounts for carbon dioxide emitted by the direct supplier. Thus, the direct effect is the emission directly assigned to the desalination industry itself. The second layer is the supplier of the first supplier and so on. The Leontief inverse captures the whole supply chain with an infinite number of suppliers. Figure 2.5 illustrates the results of the PLD Analysis for 2012 for desalination inputs (left diagrams) and emitting industries (right diagrams). We see that a higher proportion of CAPEX's emissions (compared to OPEX) occur in upstream stages of the value chain (lower diagrams). For OPEX, this means that the direct supplier already contributes a higher share to the total CO_2e emissions. The value chain is less critical for total emissions at OPEX than at CAPEX. Generally, carbon emission mainly occurs within the first three to five layers. The following layers contribute with decreasing significance.

On the upper left diagram, we see that about two thirds of CAPEX carbon emission occurs due to the construction of intake and outfall. For intake and outfall, we note that the supply chain makes a higher contribution to total emissions than we can note e.g. for piping and high-grade alloy. On the upper right chart, we see how the supply chains of emitting sectors contribute to total emissions. The electricity sector mainly contributes

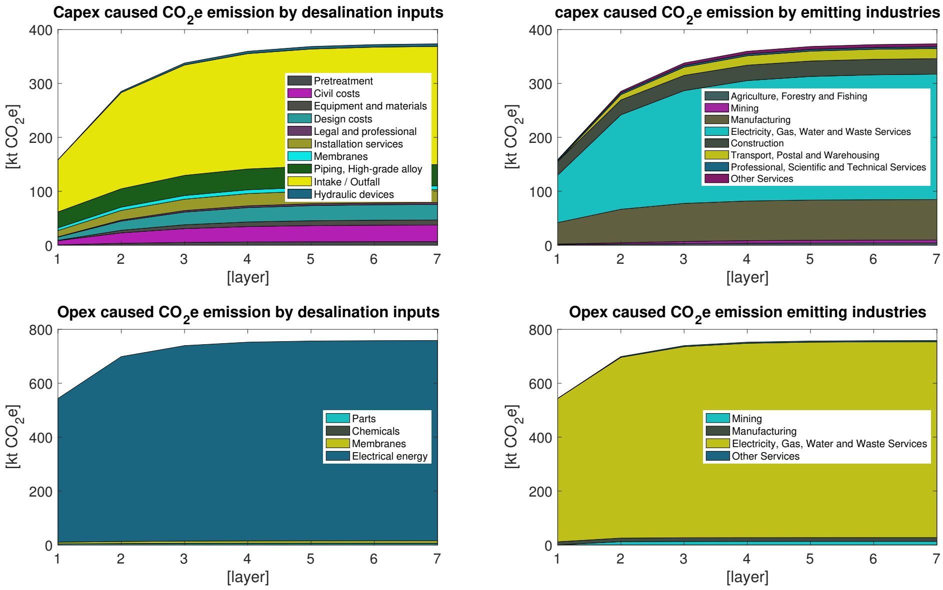

Figure 2.5: *Production layer decomposition for desalination inputs and emitting industries in 2012.*

in later layers, because the manufacturing industry sectors mainly use electricity as an input.

The situation is different at OPEX in the lower diagrams. In the left diagram, we can see the inputs of operating desalination plants. Electricity is the input factor, that is responsible for a significant share of total emissions. As a result, the electricity sector contributes a high proportion of its total emissions already in earlier stages, as we see on the right chart. The share that the sector emits as a supplier is higher than at CAPEX.

2.4 Conclusion

Desalination is an energy-intensive technology. When powered by fossil fuel, high carbon emissions ensue. For our study, we have assumed that all seawater desalination plants are operated by conventional energy, even if Australia operates some plants with RE. Economic requirements and population growth are the drivers of desalination and carbon emission in the first place. Carbon emissions from desalination occur first notably at the economic hot spots, especially in Vic as the location of Australia's largest desalination plant. We want to point out that the results relate to CO_2e emissions in Australia. Our model does not cover the value chains of imports. According to the estimated domestic quotas of about 80% on average[2], we estimate that CAPEX has covered about 80% of the emissions. Supplying countries emit additional GHGs.

We show that policy must consider the entire supply chains to make desalination environmentally sustainable. Construction of intake and outfall is highly carbon-intensive within the construction period. In the construction phase, the electricity industry is the economic sector with the highest carbon emissions. The electricity sector becomes even more crucial for carbon emissions within the operation phase. The sector is not only the crucial point for carbon emissions due to direct demand, but the sector is also a key factor regarding intermediate demands throughout the entire value chain. This is made clear once again, as Australia's energy sector accounts for 35% of GHG emissions in 2012-2013 [177].

The electricity sector significantly outperforms its contribution to carbon emissions within the life cycle of desalination, compared to its national contribution of 35%. During the construction phase in 2010 (with simultaneous operation), the electricity sector accounts for 69% of all GHG emissions attributable to seawater desalination. In the pure operating phase in 2015, the share of carbon emissions of the electricity sector even accounts for 96% of the total emissions.

Substitution of fossil energies by REs can thus be the game changer for the sustainability of desalination. Especially dry regions are affected by climate change. These regions are strongly dependent on seawater desalination. The use of desalination is only sustainable if it does not substantially emit more GHGs. Policy must act and focus on the energy sector. The key is the transformation of the electricity sector and the change in the current energy mix with a drastic increase in the share of REs.

In our following studies, we will analyse carbon effects if we substitute electrical energies by renewable sources. We will further study the social and economic effects of desalination.

Acknowledgements

This research was supported by Integrated Sustainability Analysis in the School of Physics at the University of Sydney. The Authors acknowledge financial support by the Department of Energy Engineering at Technical University of Berlin, the National eResearch

[2]In the published version of this study, an import quota of 80% was accidentally mentioned. We have corrected this here.

Collaboration Tools and Resources project (NeCTAR) through its Industrial Ecology Virtual Laboratory. NeCTAR is an Australian Government project conducted as part of the Super Science initiative and financed by the Education Investment Fund. We finally acknowledge the Friedrich Naumann Foundation for Freedom. The authors appreciate the anonymous reviewers for their helpful comments and suggestions on the paper.

2.5 Appendices

2.5.1 Overview of the analysed seawater desalination plants in Australia

Table 2.2: *Analysed desalination plants.*

Desalination plant	Capacity [m^3/d]	Location	Award year	Online year
Victorian Desalination Plant	444000	Victoria	2009	2012
Port Stanvac	274000	South Australia	2009	2012
Sydney Desalination Plant (Kurnell)	250000	New South Wales	2007	2010
Kwinana	143700	Western Australia	2005	2006
Southern Seawater desalination plant	140000	Western Australia	2009	2011
Sino Iron Ore Project, Cape Preston	140000	Western Australia	2008	2012
Southern Seawater Desalination Plant (expansion)	140000	Western Australia	2011	2013
Tugun (Gold Coast)	133000	Queensland	2006	2009
Browse downstream engineering processes	10560	Western Australia	2011	2012
Agnes Water Integrated Water Project	7500	Queensland	2008	2011
Bechtel Wheatstone construction	7500	Western Australia	2012	2012
Onslow	7500	Western Australia	2013	2013
Gorgon	7000	Western Australia	2010	2012
Curtis LNG Project	5000	Queensland	2010	2011
Jabiru	5000	Northern Territory	2006	2007
Bechtel Wheatstone compaction 2	4500	Western Australia	2011	2012
Onslow2	4500	Western Australia	2013	2013
Onesteel Whyalla Plant	4100	South Australia	2010	2011
Penrice	4050	South Australia	2005	2006
Fortescue Metals Group Port Headland	4000	Western Australia	2011	2012

2.5.2 Adjustment of the costs of seawater desalination plants

Table 2.3: *Adjusted desalination data.*

#	Plant	Adjustment	Used Sources
1	Victoria Desalination Plant (Melbourne)	Capacity and construction years not adjusted	Capacity: https://www.aquasure.com.au/uploads/files/DesalinationProcessFactSheet-1482449673.pdf
		· not adjusted	Capex:
		Capex:	https://www.copyschool.com/wp-content/uploads/2014/09/Olex-Cables-Case-Studies.pdf
		· $1.8bn (desaldata)	https://www.dtf.vic.gov.au/sites/default/files/2018-01/Project-Summary-for-Victorian-Desalination-Project.pdf
		· A$3.5bn (2009)	https://en.wikipedia.org/wiki/Victorian_Desalination_Plant#Cost
		· adjusted to US$3.908bn (2012)	https://www.water.vic.gov.au/__data/assets/pdf_file/0013/54202/Fact-sheet-project-costs-March-2015.pdf
		Opex:	https://www.water.vic.gov.au/__data/assets/pdf_file/0013/54202/Fact-sheet-project-costs-March-2015.pdf

Table continued from previous page

#	Plant	Adjustment	Used sources
		· net present value $2.602bn, 27 years, intern 7.3%, assumption progression factor 3%,	
		result: A$167m (2009), US$162m (2015), subtracted labour cost according to share of cost estimator, final result: US$128m (2015)	Opex:
		Electricity: · 4.8 $^{kWh}/_{m^3}$	https://en.wikipedia.org/wiki/ Victorian_Desalination_Plant https://www.dtf.vic.gov.au/sites/default/ files/2018-01/Project-Summary-for- Victorian-Desalination-Project.pdf Electricity: email from operator watersure

Table continued from previous page

#	Plant	Adjustment	Used sources
2	Port Stanvac (Adelaide)	Capacity and construction years not adjusted Capex: · US$1.374bn (desaldata) · Source AU$1.824bn · adjusted to AU$1.883bn (2012) Opex: · Source AU$130m (2010) · adjusted to US$123m (2015)	Capex: https://www.water-technology.net/projects/adelaide-plant/ http://www.acciona.com.au/projects/water/desalination-plants/adelaide-desalination-plant/ https://www.mcconnelldowell.com/markets/water-waste-water/42-adelaide-desalination-plant-project https://www.environment.sa.gov.au/topics/water/resources/desalination https://en.wikipedia.org/wiki/Adelaide_Desalination_Plant Opex: http://www.abc.net.au/news/2017-10-28/adelaide-desal-plant-too-big-and-too-expensive/9096046

Table continued from previous page

#	Plant	Adjustment	Used sources
		Electricity: · 3.6 kWh/m^3	http://www.abc.net.au/news/2010-12-01/130m-annual-cost-to-run-desal-plant/2358158 Electricity: http://www.awa.asn.au/AWA_MBRR/Publications/Water_e-Journal/SEAWATER_DESALINATION__A_SUSTAINABLE_SOLUTION_TO_WORLD_WATER_SHORTAGE_.aspx
3	Sydney Desalination Plant	Capacity and construction years not adjusted Capex: · US$865m (desaldata)	Official reports: https://www.ipart.nsw.gov.au/Home/Publications Capex:

Table continued from previous page

#	Plant	Adjustment	Used sources
		· source AU$1.803m (2010)	https://ac.els-cdn.com/S0011916409004822/1-s2.0-S0011916409004822-main.pdf?_tid=772d2a54-cf01-4a98-a874-d046d29407f1&acdnat=1537779245_70eb5b6abda146143e7804e2640c58cb
		· US$1.591m (2010)	http://www.awa.asn.au/AWA_MBRR/Publications/Fact_Sheets/Desalination_Fact_Sheet.aspx
		Opex:	https://link.springer.com/content/pdf/10.1007%2Fs11269-014-0901-y.pdf
		· own calculations of average from 2012-2017 cost at full production: AU$85.5m (2012)	http://www.onlineopinion.com.au/view.asp?article=19874
		· US$76m (2015)	Opex:

Table continued from previous page

#	Plant	Adjustment	Used sources
		Electricity:	https://www.ipart.nsw.gov.au/files/sharedassets/website/shared-files/pricing-reviews-water-services-metro-water-legislative-requirements-investigation-into-pricing-for-sydney-desalination-plant-pty-ltd-from-1-july-2017/final-report-sydney-desalination-plant-pty-ltd-review-of-prices-from-1-july-2017-to-30-june-2022.pdf
		· own calculations 3.6 $^{kWh}/_{m^3}$	https://www.ipart.nsw.gov.au/files/sharedassets/website/trimholdingbay/consultant_report_-_review_of_operating_and_capital_expenditure_by_sydney_desalination_plant_pty_ltd_-_halcrow_-_october_2011-_website_document.pdf
			Electricity:

Table continued from previous page

#	Plant	Adjustment	Used sources
			https://www.ipart.nsw.gov.au/files/sharedassets/website/shared-files/pricing-reviews-water-services-metro-water-legislative-requirements-investigation-into-pricing-for-sydney-desalination-plant-pty-ltd-from-1-july-2017/consultant-report-by-atkins-sydney-desalination-plant-expenditure-review-february-2017.pdf
4	Perth Seawater Desalination Plant	Capacity and construction years not adjusted	Capex:
		Capex:	https://www.water-technology.net/projects/perth/

Table continued from previous page

#	Plant	Adjustment	Used sources
		· AU$347m (desaldata)	https://ac.els-cdn.com/S0011916409004822/1-s2.0-S0011916409004822-main.pdf?_tid=7f58ad1e-7572-4dbb-8969-98a20db72204&acdnat=1537799019_c48bd7caca98a56c8fb033b96743b013
		· source AU$387m (2007)	https://www.watercorporation.com.au/about-us/news/media-statements/media-release/desalination-plant-per-kilolitre-cost-based-on-comprehensive-analysis
		· US$304m (2006)	Opex:
		Opex	https://www.water-technology.net/projects/perth/
		· source AU$22.5m (2006)	https://www.watercorporation.com.au/about-us/news/media-statements/media-release/desalination-plant-per-kilolitre-cost-based-on-comprehensive-analysis
		· adjusted to US$24m (2015)	http://pacinst.org/wp-content/uploads/2013/02/financing_final_report3.pdf

Table continued from previous page

#	Plant	Adjustment	Used sources
		Electricity: · 4.2 $^{kWh}/_{m^3}$	http://www.ecosmagazine.com/?act=view_file&file_id=EC124p23.pdf Electricity: https://www.water-technology.net/projects/perth/ http://www.degremont.com.au/media/general/Perth_Seawater_Desalination_Plant_1.pdf https://ac.els-cdn.com/S0011916409004822/1-s2.0-S0011916409004822-main.pdf?_tid=7f58ad1e-7572-4dbb-8969-98a20db72204&acdnat=1537799019_c48bd7caca98a56c8fb033b96743b013 https://www.researchgate.net/publication/228491362_Low_energy_consumption_in_the_Perth_seawater_desalination_plant

Table continued from previous page

#	Plant	Adjustment	Used sources
			Construction: http://www.degremont.com.au/projects/perth-seawater-desalination-plant/ Electricity: https://en.wikipedia.org/wiki/Perth_Seawater_Desalination_Plant
5 & 7	Southern Seawater Desalination Plant (Perth)	Capacity not adjusted Online year of expansion adjusted to 2014	Capex: https://www.water-technology.net/projects/southern-seawater-desalination-plant/

Table continued from previous page

#	Plant	Adjustment	Used sources
		Capex:	http://www.abc.net.au/news/2009-06-24/final-approval-for-sw-desalination-plant/1330958?site=news
		· desaldata: US$592m first stage and US$471 m expansion	https://www.bunburymail.com.au/story/1253516/first-seawater-flows-into-binningup-desalination-plant/
		· AU$955m (first stage in 2011)	https://www.water-technology.net/projects/southern-seawater-desalination-plant/
		· US$944m (2011)	http://www.ancr.com.au/southern_seawater_desalination.pdf
		· AU$450m (expansion in 2013)	Construction:
		· US$463m (2013)	https://www.bunburymail.com.au/story/1253516/first-seawater-flows-into-binningup-desalination-plant/

Table continued from previous page

#	Plant	Adjustment	Used sources
		Opex: · no data, we used cost estimator sum	https://www.water-technology.net/projects/southern-seawater-desalination-plant/ https://www.watercorporation.com.au/about-us/news/media-statements/media-release/southern-seawater-desalination-plant—expansion-project-update
		Electricity: · 4.0 $^{\text{kWh}}/_{m^3}$	Electricity: http://www.epa.wa.gov.au/sites/default/files/EPA_Report/2797_Rep1302Desal_61008.pdf http://www.epa.wa.gov.au/sites/default/files/EPA_Report/2797_Rep1302Desal_61008.pdf

Table continued from previous page

#	Plant	Adjustment	Used sources
6	Sino Iron Project	Capacity and construction years not adjusted no further data found, we used data from desaldata without adjustments	Capacity: https://www.ide-tech.com/en/our-projects/cape-preston-desalination-plant/?data=item_1 Construction: https://www.ide-tech.com/en/our-projects/cape-preston-desalination-plant/?data=item_1
7	Gold Coast Desalination Plant	Capacity and construction years not adjusted Capex: · Desaldata: US$838m (2009) · AU$1.12bn (2009)	Capex: https://www.advisian.com/en-gb/global-perspectives/the-cost-of-desalination https://en.wikipedia.org/wiki/Gold_Coast_Desalination_Plant https://www.water-technology.net/projects/gold-coast-plant/

Table continued from previous page

#	Plant	Adjustment	Used sources
		· Desaldata is correct, no adjustment needed	Opex:
		·	https://www.advisian.com/en-gb/global-perspectives/the-cost-of-desalination
		Opex:	http://www.qca.org.au/getattachment/8da7c759-06cf-462c-96df-de7bcbe29514/Seqwater-submission-Appendix-C.aspx
		· Desaldata:	http://www.parliament.qld.gov.au/Documents/TableOffice/TabledPapers/2015/5515T1824.pdf
		· 1,021 AU$/ML (2012) at full capacity	Electricity:
		· own calculations: AU$47m (2012), US$42m (2015)	https://www.water-technology.net/projects/gold-coast-plant/
		Electricity:	https://www.water-technology.net/projects/gold-coast-plant/

Table continued from previous page

#	Plant	Adjustment	Used sources
		$\cdot\ 3.6\ ^{kWh}/_{m^3}$	

Chapter 3

Renewable-powered desalination as an optimisation pathway for renewable energy systems: The case of Australia's Murray–Darling Basin

Michael Heihsel[1], Syed Muhammad Hassan Ali[2], Julian Kirchherr[3], Manfred Lenzen[2]

[1] Department of Energy Engineering, Technical University of Berlin, Straße des 17. Juni 153, 10623 Berlin Germany

[2] ISA, School of Physics, The University of Sydney, Sydney, New South Wales 2006, Australia

[3] Copernicus Institute of Sustainable Development, Utrecht University, Utrecht, The Netherlands

Published in: Environmental Research Letters, vol. 14 (2019), accepted manuscript, https://doi.org/10.1088/1748-9326/ab57ab, [71].

Abstract

The ecology in the Murray-Darling Basin in Australia is threatened by water scarcity due to climate change and the over-extraction and over-use of natural water resources. Ensuring environmental flows and sustainable water resources management is urgently needed. Seawater desalination offers high potential to deliver water in virtually unlimited quantity. However, this technology is energy-intensive. In order to prevent desalination becoming a driver of greenhouse gases, the operation of seawater desalination with renewables is increasingly being considered. Our study examines the optimisation of the operation of a 100% renewable energy grid by integrating seawater desalination plants and pipelines as a variable load. We use a GIS-based renewable energy load-shifting model and show how both technologies create synergy effects. First, we analyse what quantity of water is missing in the basin in the long run. We determine locations for seawater desalination plants and pipelines to distribute the water into existing storages in the Murray-Darling Basin. Second, we design a pipeline system and calculate the electricity needed to pump the water from the plants to the storages. Third, we use the combined renewable energy load-shifting model. We minimise the total cost of the energy

system by shifting energy demand for water production to periods of high renewable energy availability. Our calculations show that in such a system, the unused spilt electricity can be reduced by at least 27 TWh. The electricity system's installed capacity and levelised cost of electricity can be reduced by up to 29%, and 43% respectively. This approach can provide an annual net economic benefit of $22.5bn. The results illustrate that the expansion of seawater desalination capacity for load-shifting is economically beneficial.

3.1 Introduction

The Murray-Darling Basin (MDB) is Australia's largest river catchment. The MDB includes about 30,000 wetlands and the multinational Ramsar Convention on Wetlands protects 16 of these wetlands [51]. Between 1997 and 2009, Australia and especially the MDB suffered heavily from drought [92]. The MDB supplies about 20 million people with food [51], and Agricultural production in the MDB amounts to $24bn [118]. The natural habitat of many animal and plant species, and the agricultural economy are in danger [39, 87, 88, 176]. Extreme and changeable climate conditions have intensified recently. Following the hottest December since records began, January 2019 marked the hottest month ever measured [31].

To fight the drought in the MDB, the Australian Government passed the Water Act 2007 [160]. Based on this, the Murray-Darling Basin Authority (MDBA) published the Guide to the Proposed Basin Plan in 2010 [115]. In it, the MDBA stated that it plans to shorten the existing water allocation rights and thereby to increase natural flows [36]. In a recently published study, Williams and Grafton have shown that the government's actions worth $3.5bn to increase water flows in the MDB are failing [174].

Desalination has a high technical potential to provide large amounts of additional water. Since the millennium drought, every major city in Australia operates a seawater desalination plant [45]. Porter et al. have shown that desalination can be a strategy for the economic development of arid coastal regions [132]. Reverse osmosis (RO) is the leading desalination technology worldwide. With 3-5 $^{kWh}/_{m^3}$, RO is more energy-efficient than other thermal desalination technologies, which results in lower specific costs of less than 0.75 $^{\$}/_{m^3}$ [19, 28]. Nevertheless, RO is an energy-, and therefore carbon-intensive technology when operated with conventional energy. When operated within the Australian grid, electricity causes over 90% of carbon emissions during operation [73]. Renewable energy (RE) thus solves a fundamental issue with desalination, rendering the process sustainable [26, 55, 161]. Despite its high ecological potential, only 1% of desalination water worldwide is produced using RE [151]. Market barriers for widespread use are high capital costs and system integration strategies [20]. A high proportion of RE in the electricity grid requires a completely different operational management [127]. Australia has a high potential for generating electricity from renewable resources. However, without corresponding operational management, the generation capacity is about three times larger than the current capacity in an almost exclusively conventional energy system [101]. Seawater desalination can buffer the volatility in RE production, which in turn is followed by economic benefits due to the reduction in generation capacity.

Some researchers and operators believe that RO should be operated in a steady state. However, membrane technology has evolved significantly in recent years. As a result, more flexible operation in a partial load range is possible without damaging membranes [57]. Although the durability of the membranes will be reduced by intermittent operation, operating with antiscalant and rinsing reduces this effect significantly [52]. Anyway, with 32%, eletricity contributes significantly to the total cost of water production, while membranes account for just 4% of the total costs and they are becoming continually cheaper (the other cost components are 38% capital costs, 13% labour costs, 9% chemicals, and 4% other parts) [183]. To realise a flexible operation, desalination plants can be provided by a positive displacement pump with a variable frequency drive [57]. Numerous studies show the feasibility of RO's direct operation with intermittent energies such as wind and sun [30, 106, 129, 130, 136, 137]. Besides, practical examples show the feasibility of direct coupling of RO and RE and the associated variability of electricity [24, 168].

For the first time, our study examines the economic benefits of coupling a large seawater desalination and pipeline system with a 100% RE grid within a geographic information system (GIS) based load-shifting model. At the same time, we introduce an entirely new approach to the water management of a large basin like the MDB. In doing so, we address a crucial problem of arid regions in the critical area of the water-energy-food nexus [63, 93, 145]. This study is particularly relevant for water management and energy practitioners, such as government agencies and engineers. Furthermore, our study shows the potential for additional benefit from the coupling of both technologies. Policymakers can benefit from this knowledge regarding the implementation of regulatory frameworks.

3.2 Methods and data

3.2.1 A 100% renewable energy model[1]

We used a GIS-based electricity dispatch model with a geographic resolution of 90 x 110 grid boxes by Lenzen et al. [101]. Within this model, we simulated a sequential competitive bidding process that proceeds hourly over one year. In our dispatch optimisation model of the RE system, we simulated a spot market with competitive bidding. We optimised the cost of power generation sequentially and iteratively for every hour and every location. The algorithm proceeds by the following steps:

[1]Please see appendix section 3.5.1 for more details.

1. The generators supply the demand for every hour and every location grid box of the optimisation period. We rank all generators according to the lowest total cost for each hour and location separately. The total cost results from variable cost and fixed cost per MWh. Variable costs and fuel costs are data-based. We estimate fixed capital, maintenance and transmission costs for the first run.

2. After a run, the model recalculates the pre-run estimated fixed costs with the endogenously determined capacity factor. Based on these post-run costs, the algorithm calculates the total cost for each generator.

3. The algorithm adjusts the transmission network according to the new generator capacity and location.

4. We rank all generators based on cost efficiency over the entire optimisation period. We subsequently exclude inefficient generators.

5. The algorithm repeats the exclusion of inefficient generators while the reliability standard of 0.002% of the total demand complies.

Lenzen et al. have provided a more detailed formal description of the optimisation approach [101].

3.2.2 The load-shifting algorithm

Our load-shifting algorithm is based on the work of Ali et al. and Keck et al. [21, 22, 86]. Our concept of using the demand of seawater desalination for load-shifting has the following additional key benefits:

- Seawater reverse osmosis (SWRO) plants have a high electricity consumption which is available for load-shifting.
- The plants are utility-scale; in other words, they are centrally and simply controllable. They do not depend directly on a specific user behaviour. Thus, network operators can directly control them.
- Unlike electricity, water can easily and economically be stored in large reservoirs.

We integrated the load-shifting algorithm into the clean grid optimisation model from Lenzen et al. [101]. We considered the electricity load of Australia as a non-shiftable load.

We used the additional load of desalination and pipelines for the load-shifting procedure. The algorithm applies the locally and hourly optimised electricity system from Lenzen's clean grid as a starting point. The algorithm shifts demand from expensive generators to cheaper ones to utilise spilt energy. Spilt energy is the generated electricity which cannot be utilised due to missing demand at a specific time. It runs according to the following procedure:

1. We set a load-shifting period that determines a time range that the algorithm considers for the shifting. For our study, we considered shifting periods of 10 days, 30 days, and 90 days, respectively. The length of the periods is derived from the ability to store water in more extended periods. The computational requirement increases exponentially with the extension of the shifting period.

2. The variables of generated and spilt electricity are ranked separately.

3. The programme consequently shifts the demand within the load shifting period from the generators with the highest cost to those with the lowest cost that produce spilt electricity. We determine the load shifting potential $\mathbf{P}$ by

   $$\mathbf{P} = \min\left[\mathbf{G}_{\text{inefficient}}\left(\mathbf{t}+\Delta t_{\text{s}}\right),\ \mathbf{S}_{\text{efficient}}\left(\mathbf{t}\right),\ \mathbf{D}\left(\mathbf{t}+\Delta t_{\text{s}}\right)\right], \tag{3.1}$$

   where $\mathbf{G}_{\text{inefficient}}$ is the generation of the expensive generator, which we reduce. $\mathbf{S}_{\text{efficient}}$ is the spilt energy of the cost-efficient generator. $\mathbf{D}$ is the electricity demand of the SWROs that is available for shifting. The variable $\mathbf{t}$ determines each hour of the optimisation period. The period Δt_{s} is the shifting period. The algorithm considers every single hour within the shifting period.

4. The next step is to update the variables of the power generation to

   $$\mathbf{G}^{\text{update}}_{\text{efficient}}\left(\mathbf{t}\right) = \mathbf{G}_{\text{efficient}}\left(\mathbf{t}\right) + \mathbf{P} \tag{3.2}$$

   and

   $$\mathbf{G}^{\text{update}}_{\text{inefficient}}\left(\mathbf{t}+\Delta t_{\text{s}}\right) = \mathbf{G}_{\text{inefficient}}\left(\mathbf{t}+\Delta t_{\text{s}}\right) - \mathbf{P}. \tag{3.3}$$

   $\mathbf{G}_{\text{efficient}}$ is the electricity produced by the cost-efficient generators. $\mathbf{G}_{\text{inefficient}}$ is the electricity produced by reduced inefficient generators. The index update marks the adjusted variables.

5. As with the variables of electricity generation, we update the spilt energy variables resulting in

$$\mathbf{S}^{\text{update}}_{\text{efficient}}(\mathbf{t}) = \mathbf{S}_{\text{efficient}}(\mathbf{t}) - \mathbf{P} \tag{3.4}$$

and

$$\mathbf{S}^{\text{update}}_{\text{inefficient}}(\mathbf{t} + \Delta t_{\text{s}}) = \mathbf{S}_{\text{inefficient}}(\mathbf{t} + \Delta t_{\text{s}}) + \mathbf{P}. \tag{3.5}$$

Here, $\mathbf{S}_{\text{efficient}}$ is the spilt energy of the efficient generator, which is utilised by the shifted demand. $\mathbf{S}_{\text{inefficient}}$ is the spilt energy of the inefficient generator, which is increased by the shifting. The algorithm aims to supply the demand throughout the optimisation period by efficient generators alone. Consequently, we eliminate inefficient generators from the system.

6. Finally, we update the electricity demand $\mathbf{D}$ by the shifted reduction potential. We reduce electricity production by the reduction potential at time $(\mathbf{t} + \Delta t_{\text{s}})$ and shift it to $\mathbf{t}$, which is represented by

$$\mathbf{D}^{\text{update}}(\mathbf{t} + \Delta t_{\text{s}}) = \mathbf{D}(\mathbf{t} + \Delta t_{\text{s}}) - \mathbf{P} \tag{3.6}$$

and

$$\mathbf{D}^{\text{update}}(\mathbf{t}) = \mathbf{D}(\mathbf{t}) + \mathbf{P}. \tag{3.7}$$

We repeat from step 3 onwards for every hour and every demand location. The shifting ends when either the available demand $\mathbf{D}$ is completely shifted or when no more spilt energy is available. After the load-shifting programme has optimised all hours and locations, all inefficient generators that are no longer needed are removed from the system. Subsequently, we adjust the transmission system and the total demand.

3.2.3 Modelling the desalination energy demand

Total desalination water demand

The government's Guide to the Proposed Basin Plan [115] demanded a total of between 3,000 and 7,600 GL per year of recovered water in order to achieve the objectives of the Water Act 2007 [160]. For economic reasons, the MDBA recommended that no more than 4,000 GL should be recovered. In the end, the government agreed on only 2,750 GL [116].

Hoekstra et al. [76] have calculated the total runoff and the blue water footprint for the MDB, including the resulting available water according to the presumptive environmental standard (see fig. 3.1) [75, 76, 138]. During the months where demand exceeds supply, water should be added from outside the system. The water shortage is the difference between blue water availability and the blue water footprint. We calculated the difference for each month and added up all negative water budgets, which results in 6,200 GL. However, it is conceivable that from May to September when the budget is positive, water is stored to compensate for negative budgets in other months. In this way, the water shortage would amount to 5,100 GL. We calculated a weighted average of both values, with a slightly higher weighting of the lower limit (60%) which results in 5,500 GL.

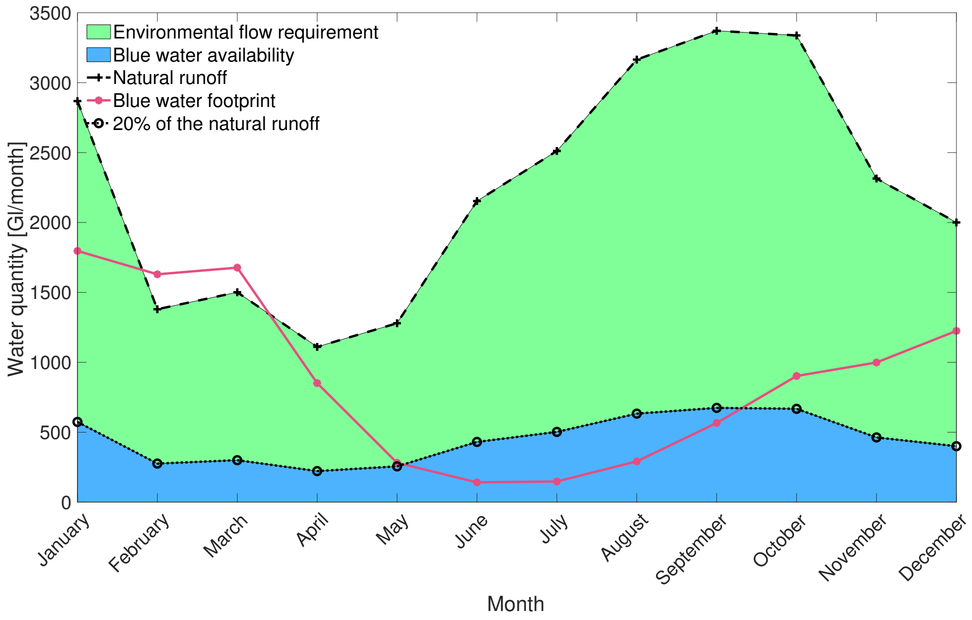

Figure 3.1: *The water availability in the MDB.*

Source: According to [76], own depiction.

Local water distribution

We estimated locations and capacities of desalination plants that pump the produced water into existing storages via a modelled pipeline system. Therefore, we used 31 MDBA government storages and data concerning their capacity and extended this with coordinates, altitudes and direct distances to the sea [119]. We locally distributed the 5,500 GL of water in the MDB according to the relative demand of the areas. For this purpose, we followed the area delineation according to the MDBA [117] and used the water demand data for the 29 areas. Pipelines supplied the desalinated water to storages in or near the area. Each storage was supplied by one or more pipelines. Each pipeline, in turn, supplied one or more storages. We have planned 29 sites for pipelines and desalination plants. We considered 35 pipelines, which were determined endogenously. The number of desalination plants has not been determined because only location and capacity are critical for the modelling.

Distributing the water to the pipeline locations required the following steps:

1. In a GIS analysis, we linked all storages to the areas in which they are located. If there was no storage in an area, we allocated the closest storage.

2. The pipelines temporarily supplied the storages with water. From the storages, the water was distributed to the areas. We created an i x j concordance $\mathbf{C}$, which describes the supply links between the pipelines and the areas. The rows represent area i; the columns represent pipeline j. The concordance consists of ones and zeros. If pipeline j supplies water to area i, then $c_{i,j} = 1$, otherwise $c_{i,j} = 0$.

3. We determined the distribution of the water among the areas. For this, we used the data from the surface water diversion limit (SDL) Trial Water Take Account [117]. We calculated the average demand $\mathbf{d}$ of area i of the annual Take Account for the years 2012-13 to 2016-17. With these data, we calculated the percentage distribution $\mathbf{r}$ of the demand in area i by

$$\mathbf{r} = \frac{\mathbf{d}}{\sum_{i=1}^{29} \mathbf{d}} \; , \tag{3.8}$$

4. We calculated the capacity fraction $\mathbf{p}$ of the pipelines j,

$$\mathbf{p} = \frac{\mathbf{c}}{\sum_{j=1}^{29} \mathbf{c}} \; , \tag{3.9}$$

   where the vector $\mathbf{c}$ is the capacity of the pipelines j resulting from the capacity of the supplied storages.

   Each area i is supplied by one or more pipelines. The sum $\mathbf{s}$ of the capacity fractions for each area i results in

$$\mathbf{s} = \mathbf{C} * \mathbf{p}, \tag{3.10}$$

   where the column vector $\mathbf{s}$ is the sum of the capacity fractions of the pipelines supplying each area i. In the next step, we modified the concordance $\mathbf{C}$ by placing the capacity fraction $\mathbf{p}$ of the pipeline j where $c_{i,j} = 1$. Therefore,

$$\widetilde{\mathbf{C}} = \mathbf{C} * \hat{\mathbf{p}}, \tag{3.11}$$

where $\widetilde{\mathbf{C}}$ is the modified concordance, and $\hat{}$ denotes the diagonalisation. For each $\widetilde{c}_{i,j}$, the capacity fraction of pipeline j that supplies area i was divided by the sum of the capacity fractions of all pipelines supplying area i, resulting in

$$\dot{\mathbf{C}} = \hat{\mathbf{s}}^{-1} * \widetilde{\mathbf{C}}. \tag{3.12}$$

For each i, $\sum_{j=1}^{29} \dot{\mathbf{c}}_{i,j} = 1$ applies. So far, the concordance $\mathbf{C}$ merely indicated that an area receives water from a given pipeline. The normalised concordance $\dot{\mathbf{C}}$ indicates the percentage of water for each area i delivered by pipeline j.

5. We calculated the amount of water $\mathbf{w}$ supplied by pipeline j by multiplying the transposed normalised concordance $\dot{\mathbf{C}}'$ by the vector $\mathbf{r}$, resulting in

$$\mathbf{q} = \dot{\mathbf{C}}' * \mathbf{r}. \tag{3.13}$$

The vector $\mathbf{q}$ indicates the percentage distribution of the water on the pipelines j. To distribute the total amount of water l to the pipelines, we calculated

$$\mathbf{w} = l * \mathbf{q}, \tag{3.14}$$

where $\mathbf{w}$ is the vector for the amount of water that each pipeline j supplies, and l is the total quantity of 5,500 GL of water. Figure 3.2 shows the MDB with the locations of the storages, the pipelines, the desalination plants, and the areas overlaid.

The electricity demand of the pipeline and desalination locations

We have iteratively optimised the pipelines' diameters based on their hydraulic head loss h_f. The iteration procedure is explained in more detail in the appendix section 3.5.2. We limited the maximum diameter to 3.1m.[2] If the diameter exceeded this limit, we added another pipeline to this location and split up the flow. The specific energy consumption e for each pipeline results in

$$e = \frac{\rho g \left(b + h_f\right)}{\eta_{tot} * 3.6 * 10^6}, \tag{3.15}$$

where ρ represents the density of water, g the gravitational acceleration b the altitude and η_{tot} the total efficiency of the motor and pump, with an assumed $\eta_{tot} = 0.873$.

[2] For comparison: The diameter of the Victorian Desalination Plant pipeline is 1.93m [23].

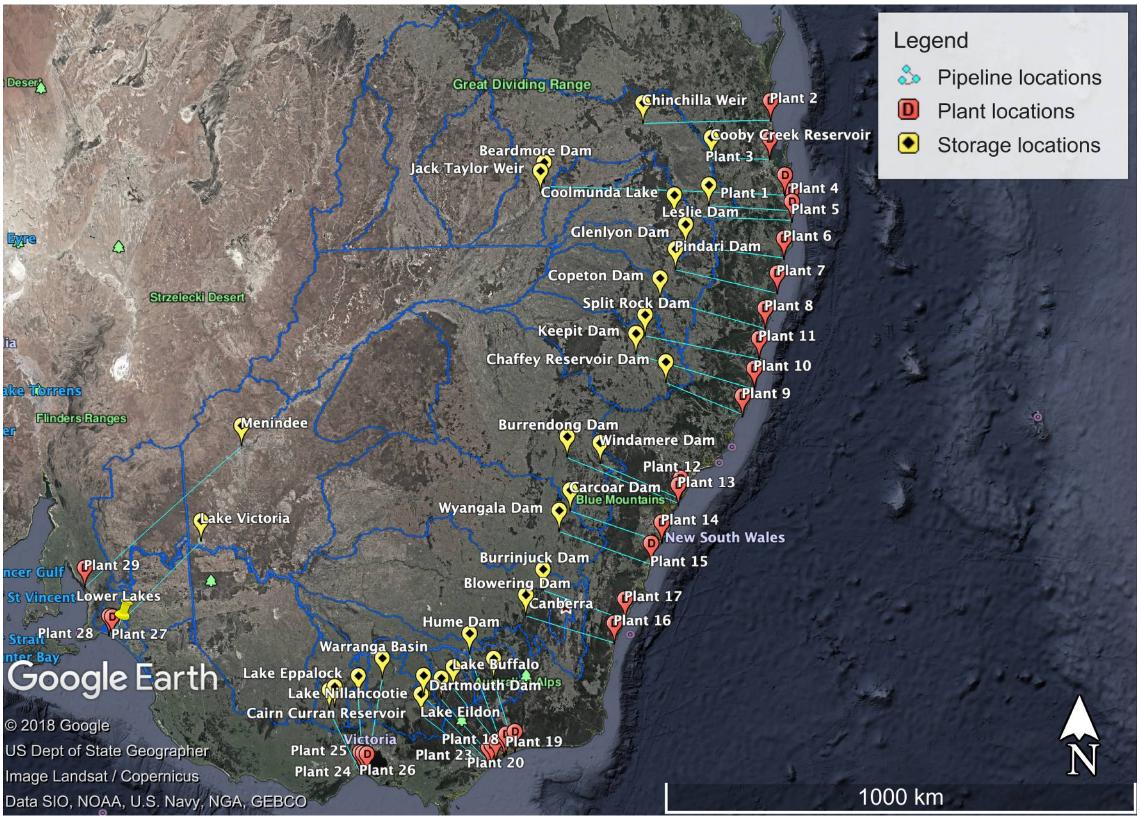

Figure 3.2: *Locations of the storages, the desalination plants, the pipelines and the MDB areas.*

Electricity demand profiles

For the desalination plants, we assumed a specific electricity consumption of $\mathrm{e}_{\mathrm{desal}} = 3.5\,{}^{\mathrm{kWh}}/_{\mathrm{m}^3}$, which corresponds to the average value for large SWROs [73]. Thus, we used the vector $\mathbf{e}$ with the specific electricity consumption for all pipelines to calculate the specific electricity demand $\mathbf{e}_{\mathrm{spec}}$ for each desalination/pipeline location by

$$\mathbf{e}_{\mathrm{spec}} = \mathrm{e}_{\mathrm{desal}} + \mathbf{e}. \tag{3.16}$$

We get the vector with the total electricity demand $\mathbf{e}_{\mathrm{tot}}$ for all locations by

$$\mathbf{e}_{\mathrm{tot}} = \mathbf{e}_{\mathrm{spec}} \# \mathbf{w} * 10^{-3}, \tag{3.17}$$

where $\mathbf{w}$ is the vector with the water demand of all pipelines from eq. (3.14), and $\#$ denotes the elementwise multiplication. From monthly profiles of missing water in the MDB [76], we derived a monthly percentage distribution profile. In order to avoid huge production differences between individual months, we equally distributed a share of the total electricity demand over the year. We distributed 50% of the electricity demand (from eq. (3.17)) as a constant baseload throughout the year, and the remaining 50% was distributed using the monthly percentage distribution profiles. Figure 3.3 shows the compiled and curve fitted load profiles. Finally, we used the 29 hourly resolved electricity demand profiles for the load-shifting analysis.

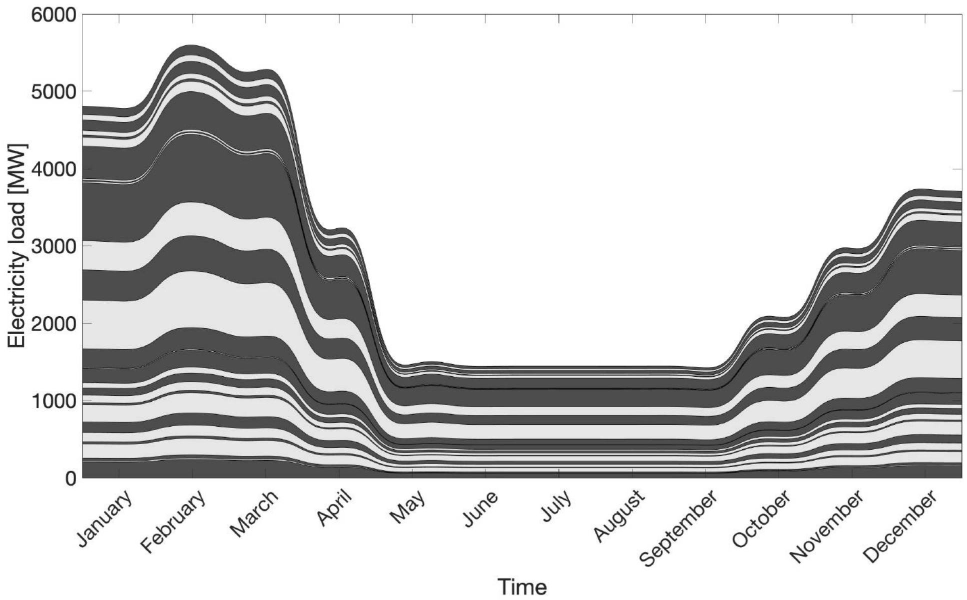

Figure 3.3: *Monthly distributed electricity demand of the 29 combined pipeline and desalination locations.*

3.3 Results and discussion

3.3.1 Electricity demand-side implications

Subplot a) of fig. 3.4 shows the electricity demand of the ten-day load-shifting period scenario.[3] In the load-shifting program, we set demand caps (according to the oversize factor of 1.5) that specify the largest possible electricity demand for the desalination and pipeline spots (blue line). We note that the load-shifting algorithm exploits the maximum values especially in the Australian summer months (October–April). At the same time, the demand available for shifting is exploited to zero more extensively in the winter months.

[3]Please see appendix section 3.5.3 for the results of the 30 days and 90 days load-shifting periods.

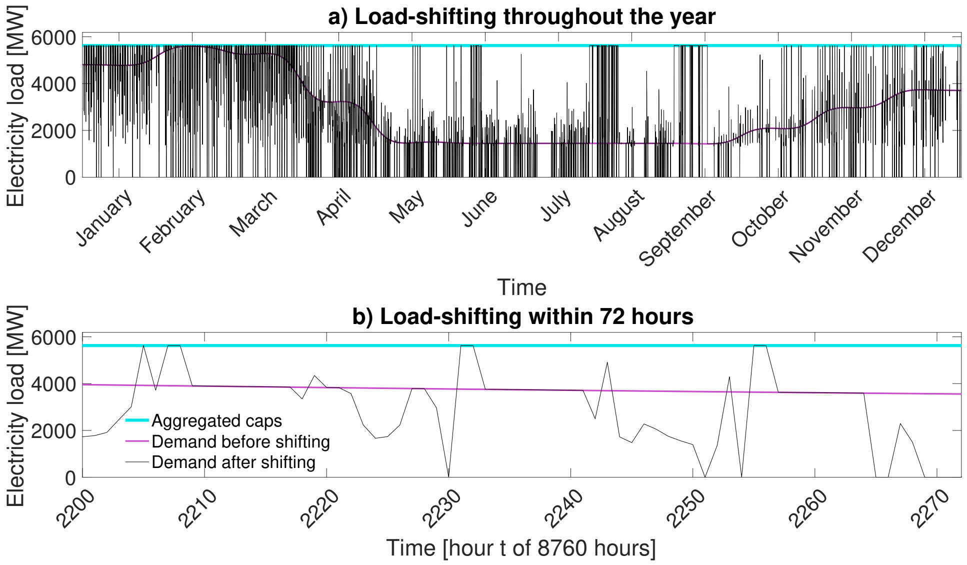

Figure 3.4: *Aggregated electricity demand before and after the load-shifting process for the 10 days load-shifting period. Subplot a) shows the entire observation period of one year. Subplot b) shows a period of 72 hours.*

We also recognise that the months around the Australian summer from October to April ('high-season months') dominate in demand before shifting. As a result of the load-shifting, the 'low-season months' from May to September were used more intensively for desalination. The considerable shifting period is possible in particular due to the large storage capacities in the MDB. The shift in water production from summer to winter thus allows more cost-effective production of water, as we can reduce the capacity of the power generation system.

Subplot b) shows a typical load variation within 72 hours for the 10 days load-shifting period. In our calculation, we did not limit the variability of ramp-ups and shut-downs. We analysed the variability of demand for load-shifting on a daily basis. For the load-shifting with a shifting period of 10 days, the median of the coefficient of variation of all days is 0.33. The largest value is 1.53, the smallest 1e-16. Although this shows a significant variability in the resulting demand, the variability is realistic for the real operation of the seawater desalination plants [52, 130, 136].

In fig. 3.5, we see the monthly average shift by time of day. Positive values show the amount of electricity that was shifted to the specific hour of a month so that desalination plants utilise additional electricity at these points. A negative value shows that demand was reduced in this hour of the month. We recognise the shift in demand from summer to winter, which has already been discussed above, causing a seasonal balance of demand. The axis of hours shows a significant shift to the morning hours until early noon. This effect is strong around April and at the end of the year. Around 5 a.m. and 7 p.m., a systematic reduction of the resulting demand can be observed throughout the year. We explain this effect by the combination of high residual demand and low electricity supply, in particular from solar power. The negative peaks of the shifting are higher than the positive peaks. This effect stems from the limitation of maximum demand by caps. At the same time, this shows that the use of higher permissible demand could have a positive effect on the electricity system. In conclusion, we find that the ability to move demand both seasonally and across the hours of the day is useful for optimising the energy system.

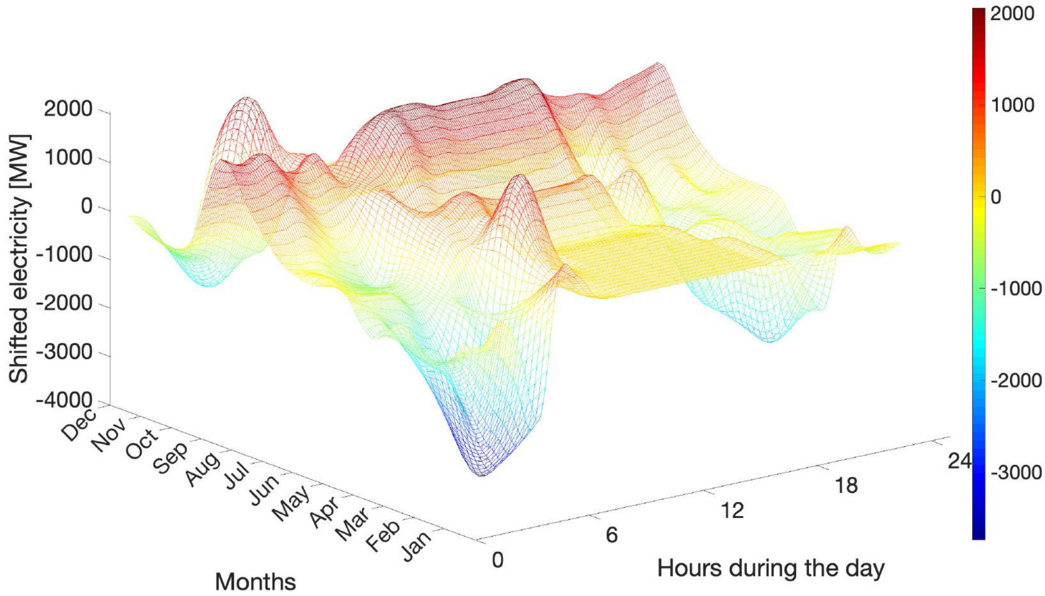

Figure 3.5: *Average shifted load by month and daytime for the 10 days load-shifting period.*

3.3.2 Electricity supply-side and cost-implications

Table 3.1 provides an overview of the electricity supply resulting from load-shifting with a period of 10 days. Here, the total electricity generation capacity is 135 GW. We see that utility photovoltaic (PV) holds the highest share with 70.1 GW of generation capacity, which equates to 52% of the total capacity. The energy generated by utility PV (and utilised by the demand i.e. which is not spilt) is 119.1 TWh, which is only 36.9%. Wind energy has the largest share here, with 135.0 TWh and a share of 41.8% – the higher

Table 3.1: *Optimised electricity supply system after load-shifting with a 10-day period.*

Fuel type	Capacity [GW]	Capacity share	Generation [TWh]	Generation share	Spillage [TWh]	Capacity factor
Hydro	3.7	2.7%	23.0	7.1%	0	71.1%
Biofuels	1.6	1.2%	5.0	1.5%	0	35.4%
Wind	42.7	31.7%	135.0	41.8%	13.4	39.7%
Utility PV	70.1	52.0%	119.1	36.9%	49.5	27.5%
CSP	12.3	9.1%	26.9	8.3%	9.5	33.8%
Ocean	0.2	0.2%	1.5	0.5%	0	83.6%
Geothermal	0.1	0.1%	0.7	0.2%	0	80.3%
Rooftop PV	4.0	3.0%	11.7	3.6%	0	33.5%
Total	135.0	100%	322.9	100%	72.3	33.5%

value for generated energy results from the fact that wind energy is the most continuous, compared to other volatile energy carriers. Therefore, wind energy can also achieve the relatively high capacity factor of 39.7%. Although energy sources with continuous availability such as ocean power have a very high capacity factor of up to 83.6%, they have minimal expansion potential.

Furthermore, wind energy, which contributes the largest share to the amount of electricity generated, has a relatively small amount of spilt energy itself. Only 13.4 TWh of the produced wind energy is lost. By way of comparison, utility PV generates 49.5 TWh of spilt energy. Thus, not even 9% of electricity produced by wind is spilt energy, whereas utility PV reaches 29%; The high value of the spilt PV energy, which is still prevalent even after the load-shifting, illustrates the range of PV electricity availability. High electricity supply with low demand prevails in many periods. Wind energy, on the other hand, is much more congruent with demand. If a load-shifting is performed, the spilt energy can thus be reduced by at least 27 TWh. If we increase the load-shifting period to 30 days and 90 days, the necessary generation capacity decreases to 122.5 GW and 114.5 GW respectively. Overall, desalination load-shifting can reduce the installed capacity and levelised cost of electricity (LCOE) by up to 29%, and 43%, respectively (see appendix sections 3.5.3 and 3.5.4 for further details).

Figure 3.6 presents the change in the electricity supply after load-shifting for a range of 1,000 hours. Subfigure a) shows the structure of electricity generation. Utility PV is dominant among the generators. During the nights, wind power produces electricity, whereas during the days, utility PV dominates electricity production. Subfigure b) shows the shifted generation. Positive values mean that electricity demand is shifted to the respective hour. Negative values indicate hours where electricity is no longer utilised. We can see that the load-shifting program has systematically replaced concentrated solar power (CSP) and partially replaced wind with cheaper utility PV.

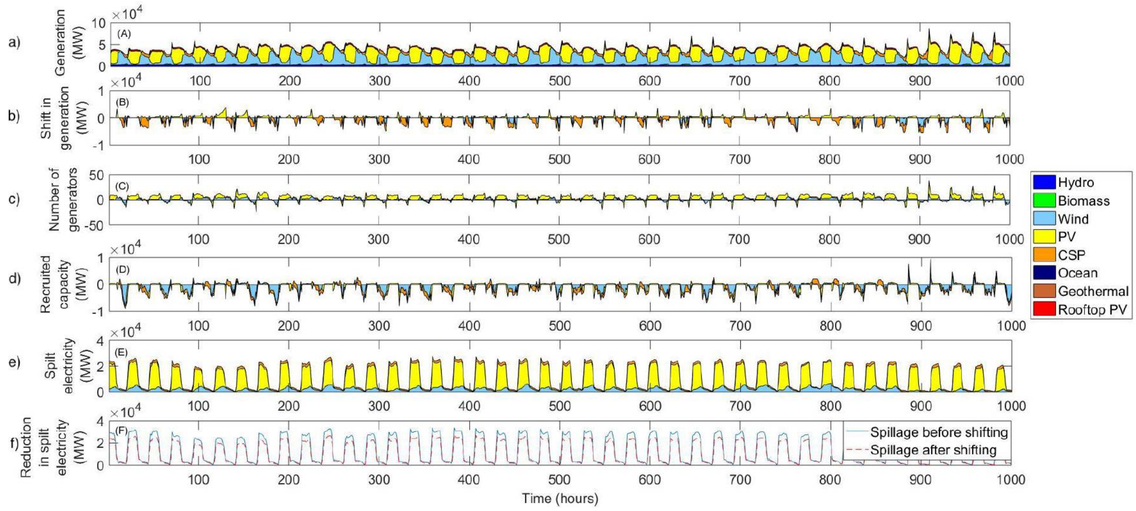

Figure 3.6: *Electricity supply after the load-shifting process for a 10 days load-shifting period. With a) generation, b) shifted electricity, c) number of shifted generators, d) change in recruited capacity, e) spilt electricity, f) reduction in spilt electricity.*

Subfigure c) shows the change in the number of generators dispatched for electricity production after the load-shifting process. Subfigure d) illustrates the recruited capacity of these generators. A negative recruited capacity means that the capacity utilised before the load-shifting is no longer needed at this hour. The program shifted the respective loads from more expensive to less expensive generators. At the end of an optimisation run, unused expensive generators are removed from the network.

Subfigures e) and f) visualise the spilt electricity. Figure e) shows that a significant proportion of the spilt electricity comes from utility PV. Wind power, on the other hand, has a much smaller amount of spilt electricity. Now it becomes clear that on the one hand, the load-shifting program replaces wind power with PV; on the other hand, it shifts the demand so as to utilise more PV to reduce the total cost of the system. Figure f) shows how the load-shifting optimises the generation structure. Hence, the peaks of spilt energy were reduced significantly. The results show that wind and solar complement each other under Australian conditions. The peaks of PV occur during the day, while the peaks of wind occur mostly at night. The use of CSP can further flatten the supply by the use of heat storages. Therefore, we recommend a mixed application of these technologies when combining with desalination.

3.3.3 Estimation of additional costs and benefits[4]

In the following, we estimated the benefits and costs directly related to the load-shifting. When load-shifting is applied, less power generation capacity is needed compared to the situation where no load-shifting would be applied. Hence, we define the additional benefit as saving in the total cost of electricity generation. We define the direct costs related to the load-shifting by the necessary increase in the desalination capacity. Our approach is a simple static analysis. Hence, we do not consider dynamic price changes or indirect effects, such as social effects. We provide further details on the assumptions and the calculation in the appendix section 3.5.5. With applied load-shifting, the LCOE of power generation was 11.3-13.5 ct/kWh. Without load-shifting, LCOE was 20 ct/kWh. With the LCOEs and the respective total electricity quantities, we calculated the total costs of electricity generation for both the load-shifting scenarios and the basic scenario without load-shifting. The difference between the total costs of electricity results in an average gross economic benefit of $24.6bn per year. This cost saving is made possible by not operating desalination plants continuously but providing their demand flexibly for load-shifting purposes. In our study, we applied an oversize factor of 1.5; in other words, the desalination and pipeline capacity were 50% higher than in a baseload scenario for continuous operation throughout the year. To calculate the additional costs of the desalination plants and the pipelines, we used specific capital costs from International Atomic Energy Agency (IAEA) and Bluefield Research [29,79], respectively. Oversizing desalination plants results in an additional annuity of $1.27bn. The expansion of pipeline capacity leads to an additional annuity of $809m. In conclusion, considering desalination demand for load-shifting under the given assumptions promises high net economic benefits of $22.5bn, which is 35% of the total cost of electricity in the no-shifting scenario.

3.3.4 Challenges and global prospects

Recently, we see a growing awareness of climate change worldwide. Movements, such as the protests movement of 'Fridays for Future', are pushing governments to take more determined action. The electricity sector plays a key role for a climate-neutral economy [177], but a high proportion of RE in the electricity sector requires a fundamentally different network operation [127]. The slow implementation of RE technologies in Australia, although with very high meteorological potential, is a major obstacle to

[4]Explanations of the methodology and assumptions can be found in the appendix section 3.5.5.

implementing these strategies. The slow adaptation, as well as the historically high dependence on coal, currently lead to a carbon lock-in of the Australian economy [164].

When implementing seawater desalination on this scale, other environmental effects must be considered. The impacts of brine discharge on the marine environment continue to be the subject of controversial research discussions [41, 114, 142, 182]. However, in a recent large-scale ecological impact study, Clark et al. have demonstrated that the effects of brine in seawater desalination are significantly smaller than previously thought [35]. Furthermore, Seawater desalination is still costly, but the cost of technology has decreased significantly in recent decades. New research in the field of graphene for desalination shows that the energy efficiency of seawater desalination could once again decrease by a factor of more than ten [16]. Through international agreements such as the Paris Agreement, countries worldwide will increasingly implement climate policy measures, whereby RE will become competitive by pricing CO_2.

In our study, we demonstrated the advantages of the combination of desalination plants, pipelines and RE. The calculated 35 pipelines with an average diameter of 2.1 m are an enormous challenge to build. Twenty-four locations can be supplied with just one pipeline each, two locations require two pipelines each, and one location requires three pipelines. An adaptation of the operational management, e.g. by pursuing a more continuous operation, would provide opportunities to reduce the number of pipelines at individual sites. We are aware of the magnitude of the idea of building seawater desalination plants with a capacity of 5,500 GL per year for the MDB. Cutting edge practice and research worldwide show that projects on this scale are a realistic option in the battle against drought: The Israeli Government plans to save the drought-threatened Sea of Galilee with seawater desalination [159]. To do this, they want to increase their desalination capacity and pump water from the Mediterranean Sea to the Sea of Galilee. At the World Water Conference 2019, the idea of a 'climate correction project' was presented [155]. The idea applies seawater desalination with RE to keep the rising sea level constant in the context of climate change. At the same time, according to this idea, water should be pumped into dry regions to increase vegetation and simultaneously to counteract climate change.

3.4 Conclusion

Our study focuses on two global challenges: First, global areas of arid regions are growing due to climate change. Second, the majority of the world community has agreed on ambitious CO_2 reductions for the coming decades, which should limit global temperature increases to 1.5 °C. This study proposes a combined solution of seawater desalination with RE. For this, we modelled a desalination and pipeline system to provide water for the MDB. RE contribute to making desalination plants sustainable. At the same time, desalination serves as a variable load, which reduces the generation capacity of RE plants and therefore, the cost of the system. With our approach, the generation capacity of the electricity system can be reduced by more than 29%. We achieve net annual cost savings of more than $22.5bn, which equates to 35% of the total cost of electricity in the no-shifting scenario. Desalination is particularly suitable for load-shifting, because storing water for a longer period is affordable and technically feasible.

Our study showed how available flexible loads in a 100% RE system can significantly reduce the installed capacity. We demonstrated how sun and wind energy complement each other when coupling with desalination. Instead of operating with only one energy source, a mix of both is preferable. Furthermore, loads are advantageous, which can be shifted both, within a day and between seasons. However, the policy needs to create regulatory frameworks that price the external costs of carbon emissions and water extraction and distribute the benefits of load-shifting to the shiftable loads, i.e. desalination and pipeline operators, creating incentives to provide the necessary variable loads. Given the continuing aridity, the MDBA should limit the water extraction in the short term (in the 5,500 GL range) to increase environmental flows. In the medium term, water prices for extracted water should be increased (e.g. through taxes) in order to ensure sustainable water use. In the long term, the collected taxes can be used to expand RE, desalination plants and pipelines.

Nonetheless, our study is limited to investigating the immediate interaction of RE and desalination plants. Our study does not analyse environmental, economic and social factors or compile a comprehensive cost-benefit analysis. We also do not compare with alternative water supply options, such as wastewater reuse or reducing water consumption. Even though these options are essential for the entire Australian water supply, we show a solution that is able to provide large volumes of water in dry coastal regions. We will investigate social, environmental and economic factors in detail in further research.

Acknowledgements

We thank Prof. Dr. Frank Behrendt from the Department of Energy Engineering of the Technical University of Berlin for his continuous support. This work was financially supported the Friedrich Naumann Foundation for Freedom. Finally, we also thank the anonymous reviewers for the valuable comments, which have improved this study.

3.5 Appendices

3.5.1 Modelling the clean grid: a 100% renewable energy system

Numerous studies have investigated the feasibility of a 100% RE system. RE systems have lower capacity utilisation than conventional energy systems. Prior work (for example AEMO and Elliston et al. [12, 47]) has shown that the importance of minimising the installed capacity of renewable power generation plants in order to minimise the LCOE.

We used a GIS-based electricity dispatch model with a geographic resolution of 90 x 110 grid boxes by Lenzen et al. [101]. Within this model, we simulated a sequential competitive bidding process that proceeds hourly over one year. We considered only RE generators. Our electricity market model consisted of biomass, hydropower, wind, utility PV, rooftop PV, CSP, geothermal, and ocean power (wave & tidal). We considered the current reliability standard of 0.002% of demand according to the Australian Energy Market Commission's Reliability Panel [12].

Furthermore, we limited rooftop PV, geothermal, hydro and ocean to today's capacity, because of potential limitations, infancy or integration issues. Due to the conflicts of use for biomass, we restricted the expansion of biomass to 15 times today's capacity [12, 38, 48]. We did not limit wind or solar; we exhausted their potential as much as possible. We assumed a copper plate for electricity transmission [12, 47]. Moreover, we modelled transmission losses and thus transmission costs, but we did not apply further restrictions.

Table 3.2 shows the initial estimate and the data-based variable costs. The pre-run estimate is necessary as these costs are directly dependent on the amount of electricity produced. However, we can calculate the fixed cost per MWh only when we know the utilisation (capacity factor) of the generator. The model determines the utilisation endogenously. Hence, the fixed costs per MWh are only known post-run ('pre-run fixed cost problem') [101].

3.5.2 The electricity demand of the pipeline and desalination locations

For each pipeline, we iteratively applied the Darcy-Weisbach equation for the friction loss h_f expressed as a hydraulic head loss by:

$$h_\mathrm{f} = \lambda * \frac{l}{d} * \frac{v^2}{2\mathrm{g}} \ , \tag{3.18}$$

Table 3.2: *Initial estimated cost assumptions for various generation technologies.*

Fuel Type	Capital cost [$/kW]	Fixed O&M cost [$/kW y]	Variable cost [$/MWh]	Fuel cost [$/MWh]	Total cost [$/MWh]	Capacity factor	Liftime [yr]
Biomass	5,350	109	7.0	1.5	38.8	0.85	45
Hydropower	5,114	48	6.7	0	26.2	0.85	55
Utility PV	1,342	33	0.0	0	45.5	0.20	30
Wind	2,693	35	10.5	0	52.5	0.40	25
CSP (15-h storage)	6,256	68	13.1	0	67.2	0.60	30
Rooftop PV	1,075	22	0.0	0	37.6	0.18	30
Ocean	2,738	166	15.0	0	46.4	0.95	30
Geothermal	5,457	175	15.0	0	63.3	0.95	25

Source: [12, 101, 153, 162]

where λ is the friction factor, l is the length of the pipeline, *d* is the hydraulic diameter, *v* is the flow velocity, and g is the gravitational acceleration. The length of the pipeline results from the direct distance from the storage to the sea and the altitude. The direct distance was multiplied by a pipeline extension factor of 1.2, because the pipeline cannot be built in a straight line. The extension factor follows that of the Victorian Desalination Plant [23]. Since we wanted to operate the plants and the pipelines variably, we designed them with an oversize factor of 1.5. This oversize factor corresponds to an average utilisation rate of 66%.

The friction factor λ for eq. (3.18) was also determined iteratively. For this, we used the formula according to Colebrook and White for the transition area to turbulent flows:

$$\lambda = \left(-2 * log_{10}\left(\frac{2.51}{r\sqrt{\lambda}}\right) + \frac{k}{3.71d}\right)^{-2}. \tag{3.19}$$

Here, *r* is the Reynolds number, *k* is the absolute roughness, and *d* is the diameter of the pipeline.

The head loss in the first iteration loop, which we determined by eq. (3.18), usually shows an inefficient pipeline design. Either an excessively large (small pressure loss) or an excessively small diameter (large pressure loss) is responsible for the inefficient design. We recognised this through the derivation of eq. (3.18):

$$\frac{\partial h_{\mathrm{f}}}{\partial d} = \frac{-\lambda * l}{d^2} * \frac{v^2}{2g}. \tag{3.20}$$

We optimised the head loss by setting limits between -24 and -25 for the derived head loss function. We obtained these limits from the Victorian Desalination Plant pipeline at 66% partial load. For each pipeline, we adjusted the diameter until the derived head loss was between -24 and -25.

3.5.3 Optimised electricity supply system after load-shifting with 30- and 90-days period and the results without load-shifting

Table 3.3: *Optimised electricity supply system after load-shifting with a 30-day period.*

Fuel Type	Capacity [GW]	Capacity share	Generation [TWh]	Generation share	Spillage [TWh]	Capacity factor
Hydro Power	3.4	2.8%	23.0	7.1%	0	77.2%
Biofuels	2.9	2.4%	4.3	1.3%	0	16.8%
Wind	36.4	29.7%	117.7	36.5%	12.2	40.8%
Utility PV	52.4	42.8%	109.3	33.9%	47.3	34.2%
CSP	21	17.1%	54.9	17.0%	7.9	34.2%
Ocean	0.21	0.2%	1.5	0.5%	0	83.4%
Geothermal	0.1	0.1%	0.5	0.1%	0	54.9%
Rooftop PV	6.1	5.0%	11.7	3.6%	0	21.9%
Total	122.5	100%	322.9	100%	67.3	36.4%

Table 3.4: *Optimised electricity supply system after load-shifting with a 90-day period.*

Fuel Type	Capacity [GW]	Capacity share	Generation [TWh]	Generation share	Spillage [TWh]	Capacity factor
Hydro Power	3.4	3.0%	23.0	7.1%	0	77.2%
Biofuels	1.9	1.7%	4.4	1.4%	0	26.4%
Wind	43.1	37.6%	146.7	45.5%	12.6	42.2%
Utility PV	50.3	43.9%	108.7	33.7%	42.6	34.4%
CSP	10.3	9.0%	25.9	8.0%	8.6	38.3%
Ocean	0.21	0.2%	1.5	0.5%	0	83.5%
Geothermal	0.1	0.1%	0.7	0.2%	0	77.3%
Rooftop PV	5.2	4.5%	11.7	3.6%	0	25.8%
Total	114.5	100%	322.6	100%	63.7	38.6%

Table 3.5: *Electricity supply system without load-shifting.*

Fuel Type	Capacity [GW]	Capacity share	Generation [TWh]	Generation share	Spillage [TWh]	Capacity factor
Hydro Power	3.4	2.1%	10.6	3.3%	0	36%
Biofuels	15.6	9.6%	40.6	12.6%	0	30%
Wind	71.6	44.3%	124.7	38.8%	48.9	28%
Utility PV	27.9	17.3%	31.6	9.8%	20.2	21%
CSP	42.1	26.0%	110.7	34.5%	30.6	38%
Ocean	0.2	0.1%	0.4	0.1%	0	29%
Geothermal	0.1	0.0%	0.1	0.0%	0	9%
Rooftop PV	0.8	0.5%	2.6	0.8%	0	35%
Total	161.7	100%	321.3	100%	99.7	30%

3.5.4 Load-shifting potential

Here, we compare our results from the 90-day load-shifting period with results from Ali et al. and Keck et al. [21, 22, 86] who used the same load-shifting algorithm. In their studies, Ali et al. have investigated load-shifting with the demand of air conditioners and residential water heaters [21, 22]. Keck et al., on the other hand, have integrated battery storage into the power grid to enable load-shifting [86].

Table 3.6 shows the potential for the reduction of the required capacity and LCOE, for the increase of the capacity factor, and for the reduction of spilt electricity. Due to the high demand for load-shifting and the very long shift-period, we were able to show the reduction potential of the necessary capacity. We were able to reduce the capacity by more than 47 GW, which corresponds to a reduction of 29%, illustrating the benefits of load-shifting. This saving had an influence on the LCOE, which was significantly reduced by 43.3% to 11.34 ct/kWh. The capacity factor was increased by 28.7%, a similar result to that obtained by Keck et al. [86]. In their study, however, Keck et al. reduced the spilt electricity by 76% [86]. We were not able to achieve this value, yet we reduced spilt electricity by more than one third. Our results are far from the business-as-usual scenario in Ali et al. [22] – which is typical of the other studies. However, we have to consider that CO_2 currently has no price, making this comparison only partially appropriate.

Table 3.6: *Load-shifting potential in other case studies.*

	Desalination this study	Air conditioners [21]	Water heaters [22]	Battery storage [86]
Installed capacity	-29.20%	-14.50%	-4.70%	up to -22.0%
LCOE	-43.30%	-30.60%	-15.60%	up to -22.0%
Capacity factor	28.70%	18.50%	7.10%	28.00%
Spilt electricity	-36.10%	-9.10%	-9.10%	up to -76%

3.5.5 Estimation of costs and benefits

Calculation of the benefits of load-shifting

We calculated the benefits that result from the optimisation of the power grid. Load-shifting reduces the installed capacity of the power plants. This capacity reduction results in a reduction of the LCOE compared to the LCOE without load-shifting. A summary of the input data is provided in table 3.7.

Table 3.7: *Inputdata for the cost-benefit estimation.*

Input	Description	Value	Comment
$LCOE_1$	Levelised cost of electricity (10-day shifting period)	13.5 ct/kWh	
$LCOE_2$	Levelised cost of electricity (30-day shifting period)	12 ct/kWh	
$LCOE_3$	Levelised cost of electricity (90-day shifting period)	11.34 ct/kWh	
$LCOE_0$	Levelised cost of electricity (without load-shifting)	20 ct/kWh	
q	Interest rate	1.08	[79]
n	Lifetime	20 y	[79]
capexdesal	Specific capital cost desalination plants	1,490 $/(m³ d)	[79]
capexpipeline	Specific capital cost pipeline	1,737 $/(diameter[m] * length[m])	extrapolated, according to Bluefield Research [29]

We calculated the total generation cost of the electricity that results without load-shifting by

$$tce^{\text{noshift}} = LCOE_0 * g_0, \tag{3.21}$$

with *tce* as the total cost of electricity, *LCOE* as the levelised cost of electricity and g_i as the amount of generated electricity. Similarly, when a load-shifting is performed, we calculate the total cost of electricity as the average of all scenarios.

$$tce^{\text{shift}} = \frac{\sum_{i=1}^{3} LCOE_i * g_i}{3}. \tag{3.22}$$

The benefit of load-shifting Δb is the difference between the total cost of both scenarios, where,

$$\Delta b = tce^{\text{noshift}} - tce^{\text{shift}}. \tag{3.23}$$

Calculation of the costs of load-shifting

In order to enable a load-shifting, the capacity of the desalination plants and the pipelines have to be increased compared to the no-shift scenario. The increased capacity results in increased capital costs which is

$$\Delta c = capex^{\text{desal}} \left(cap^{\text{desal,shift}} - cap^{\text{desal,const}} \right) + capex^{\text{pipe}} \left(cap^{\text{pipe,shift}} - cap^{\text{pipe,const}} \right). \tag{3.24}$$

The value Δc is the additional cost of capital for desalination plants and pipelines due to the load-shifting. The values for capital expenses (CAPEX) represent the specific capital cost for the desalination plants and pipelines, respectively. The variable cap^{shift} is the capacity that is required in the load-shifting scenario and cap^{const} is the capacity that is required for constant operation throughout the year (at 90% utilisation).

The cost of capital was converted into an annuity by

$$\Delta c^a = \frac{q^n\,(q-1)}{q^n - 1} * \Delta c. \tag{3.25}$$

We got the annual difference of additional benefits and costs *bc* that result from the load-shifting by

$$bc = \Delta b - \Delta c^a. \tag{3.26}$$

Chapter 4

Desalination and sustainability: A triple bottom line study of Australia

Michael Heihsel[1],Manfred Lenzen[2], Frank Behrendt[1]

[1] EVUR, Department of Energy Engineering, Technical University of Berlin, Straße des 17. Juni 153, 10623 Berlin Germany

[2] ISA, School of Physics, The University of Sydney, Sydney, New South Wales 2006, Australia

Published in: Environmental Research Letters, vol. 15 (2020), accepted manuscript, https://doi.org/10.1088/1748-9326/abbd63, [72].

Abstract

For many arid countries, desalination is considered as the final possible option to ensure water availability. Although seawater desalination offers the utilisation of almost infinite water resources, the technology is associated with high costs, high energy consumption and thus high carbon emissions when using electricity from fossil sources. In our study, we compare different electricity mixes for seawater desalination in terms of some economic, social and environmental attributes. For this purpose, we developed a comprehensive multi-regional input-output model that we apply in a hybrid life cycle assessment (LCA) spanning a period of 29 years. In our case study, we model desalination plants destined to close the water gap in the Murray-Darling Basin, Australia's major agricultural area. We find that under a 100%-renewable electricity system, desalination consumes 20% less water, emits 90% less greenhouse gases, and generates 14% more employment. However, the positive impacts go hand in hand with 17% higher land use, and a 10% decrease in gross value added, excluding external effects.

4.1 Introduction

Water scarcity affects an increasing proportion of the world's population [62]. In Australia, water shortages have intensified over the past two decades [165]. In the 'granary of Australia', the Murray-Darling Basin (MDB), little precipitation and water over-use has led to environmental issues like high salinity of rivers and fish death [133, 169]. Over the past few years, Australia faced heat records and intense bushfires [32]. The latter put the country in a state of emergency for weeks in early 2020 [89].

If using natural resources, improving water management, and measures like wastewater reuse are not sufficient to meet water demand, desalination offers great potential, especially for regions with access to the sea [27, 40]. However, the technology has some severe drawbacks. The production cost of desalinated water is about twice or three times higher than water from conventional sources [183]. Furthermore, effects on the marine ecosystem, high energy consumption and the associated greenhouse gas (GHG) emissions are the primary ecological challenges [35, 65, 91, 108, 141, 150, 152, 156, 181]. The use of renewable energy (RE) could make a major contribution to environmental sustainability in particular [19,26,34,83]. However, studies that assess total sustainability by measuring environmental, social and economic indicators are missing [64, 68].

The motivation of this study is to quantify the three dimensions of sustainability of desalination depending on the used electricity source. Therefore, we apply a hybrid life cycle assessment (hLCA) approach [69, 111] to measure supply chain effects. We applied an input-output (IO)-based hLCA for this study [84]. The IO analysis goes back to the research work of Wassily Leontief, who received the Nobel Prize for this in 1973 [105]. We applied the Australian Industrial Ecology Virtual Laboratory (IELab) to compile tailor-made multi-regional input-output (MRIO) tables [98].

In this study, we simulated fictive desalination plants at 29 sites around the MDB in southeast Australia. The desalination plants were designed to provide the missing water supply in the MDB of 5,500 GL in total. The plants were not designed for continuous operation, but take into account an oversize factor of 1.5, allowing load-shifting of the electricity demand. Like all large plants in Australia, the plants are designed as reverse osmosis (RO) systems. For the power supply, we considered five scenarios, with 0, 25, 50, 75 and 100% RE. In the 0% RE scenario, the electricity sector corresponds to the generation mix of the corresponding year in Australia, as shown in the IO data. The electricity mix, as well as the locations of the generators in the 100% RE scenario, were the results of a geographic information system (GIS)-based dispatch optimisation model of a previous study [71]. The transitional scenarios apply pro-rata combinations of both electricity mixes. The capacities of the technologies wind, biomass, hydro and photovoltaic (PV) are shown in the table in the appendix section 4.5.1.

To the best of our knowledge, this study is the first comprehensive MRIO triple bottom line (TBL) study comparing desalination plants in RE and fossil-fuelled electricity scenarios. Thus, we contribute to the research gap in the area of holistic studies on socio-economic and environmental impacts of desalination. The study is structured as follows: In the next section, we describe the methodology and the data used. After that, we present our results and end with a conclusion. Further technical details on the methods used can be found in the appendix.

4.2 Methods and data

Two methods are applicable for carrying out LCAs: the bottom-up approach (a process-based LCA) and the top-down approach (based on input-output tables (IOTs)) [49]. The bottom-up approach employs physical process data, allowing very accurate modelling of immediate upstream stages of the value chain. Since the processes are explicitly modelled, the value chain is only reflected to a limited extent due to data availability, and subordinate levels are not considered. Therefore, a truncation error occurs. The top-down approach, on the other hand, uses statistical data on economic sectors, which allows infinite value chains to be modelled. A truncation error, therefore, does not occur, but an aggregation error arises from the aggregation of different processes in industrial sectors. The combination of top-down and bottom-up data in a hybrid approach minimises both errors, which is the advantage of this method [131].

Hybrid LCAs are used for carbon footprint studies of products, companies or sectors by extending IOTs with physical environmental satellites [73, 107, 126, 139]. Numerous sustainability studies expand the focus on further economic and social indicators, the so-called TBL [46, 50, 69, 111, 128]. The present framework builds on previous research from Heihsel et al. [73].

We extended an existing IO model as follows: In addition to the GHG satellite, we implemented additional indicators, namely water use, land use, employment, and gross value added (GVA). Furthermore, we extended the regional resolution up to 46 regions. The highly detailed regional resolution enables to aggregate the results according to different regional classifications (Australian States and Territories, water catchment and rainfall areas). We increased the time series to the years 1990-2018. Since the existing

IO data do not contain RE sectors, we augmented the tables with additional process data. By using hybridised process-data from Yu and Wiedmann [180], we modelled RE sectors for wind, solar, hydro and biomass technologies. Hereby, we analysed the TBL impacts of the construction and operation period of desalination plants. In this study, we followed the IO-based hLCA approach by Malik et al. and Suh and Huppes [110, 157]. A projection of the IO data and the process data into the future would be possible in principle but would be subject to considerable uncertainty when analysing investments spanning decades.

4.2.1 Input-output and renewable electricity data

To complement the IO data with RE specific data, we used process data from AusLCI and Ecoinvent [25, 42], which Yu and Wiedmann have hybridised [180]. Yu uses an integrated hLCA framework that includes monetary and physical data. Yu's hLCA framework contains 4,463 processes (physical data) and 1,284 monetary IO sectors, both in matrix form. For our study, we extracted data from the process-coefficient matrix (the primary life cycle inventory (LCI) of the processes). Moreover, we utilised the cut-off matrix, which supplements the pure process-based data with IO data. Both matrices describe the production recipe of the technology. While the process-coefficient matrix shows upstream physical pre-processes as inputs to produce a functional unit of the process, the cut-off matrix primarily contains upstream services. Each process is represented by an individual column in the matrices. Section 4.5.2 in the appendix shows the structure of the integrated hLCA framework by Yu. The processes extracted for this study are shown in section 4.5.3. In our hLCA framework, we augmented four RE technologies, namely wind, biomass, hydro and PV.

Furthermore, adding new sectors to the IO-framework requires physical data for the satellite accounts. Therefore, we collected data for the environmental indicators GHG, water use and land use as well as for the social indicator employment. The electricity generation processes in Yu's LCI have a functional unit of 1 MJ. Hence, we normalised the satellite intensities accordingly. Table 4.1 summarises the direct intensities of the considered RE technologies. The RE vectors represent the intermediate consumption of the electricity generated and thus take into account both operation and maintenance as well as construction, the latter weighted according to expected lifetime. The construction of RE plants is thus reflected in the indirect effects on an annual basis. The direct intensities of RE thus only refer to direct electricity generation. In the appendix section 4.5.1, we show the LCI data preparation process before augmenting the IOTs.

Table 4.1: *Direct intensities of renewable electricity generation.*

		Wind	Biomass	Hydro	Photovoltaic
Water use	[L/MJ]	0	1.41	7.22	1.05E-03
Land use	[sqm/MJ]	3.28E-04	1.75E-05	2.16E-03	1.08E-04
Greenhouse gases	[g CO_2e/MJ]	0	2.1	1.6	0
Employment	[FTE/MJ]	4.53E-08	3.15E-07	2.92E-08	3.85E-07

4.2.2 Input-output data

We used the Australian IELab to compile tailor-made IO-tables for our study [98]. The IELab offers a unique disaggregation level of 1,284 IOPC sectors and 2,214 SA2 regions. For our study, we created a framework of 64 IO-sectors, including the four augmented RE sectors. Our framework consists of 46 Australian regions. The framework contains both industries and commodities, which means that the intermediate demand framework has a size of 2 x 64 x 46 = 5,888 rows and columns. The IELab uses statistical data from [3–7] for the IO data and [2, 8, 9, 15] for the social and environmental data, respectively. We created time series IOTs for the years 1990-2018.

4.2.3 Sector augmentation and re-balancing

Australian IOTs do not include separate RE sectors. Therefore, we post-augmented the IOTs with process data. Columns in IOTs show the input of the production of a particular industry; in other words, it is the recipe of the manufactured commodities. The rows describe the intermediate sales structure of commodities to other industries. While we supplemented columns with the LCI data, we adopted the rows (i.e. sales structure) from the structure of the existing electricity sectors. The location of the generators resulted from Heihsel et al. [71].

We compiled separate IOTs for each of the five scenarios with 0, 25, 50, 75 and 100% RE generation. The RE sectors were scaled accordingly. The conventional electricity sectors were scaled according to the complementary value. A schematic diagram of the augmented IOT framework can be found in the appendix section 4.5.4.

Due to the augmentation of the IOTs, they were no longer balanced, which means that input and output were no longer equal. We used a RAS-type biproportional numerical algorithm to post-balance the IOTs [90, 110].

4.2.4 Desalination process-data

Heihsel et al. analysed Australia's largest 20 desalination plants, which correspond to 95% of the Australian seawater desalination capacity [73]. For their study, they used process-data from the desaldata database [66]. We used these data as a weighted-average proxy for the 29 desalination plants. We applied results from Heihsel et al. [71] to specify the capacity and the locations of the plants. We assumed the construction period between 1990–1992. We allocated 25% of the capital expenses (CAPEX) each to the first and the last year. Thus 50% of the capital costs were taken into account for the second year. The operation and maintenance period runs continuously from 1993. Since the desalination plants were used for load shifting scenario in this study, we considered an oversize factor of 1.5.

4.2.5 Calculation of the triple bottom line impacts

The TBL framework describes an accounting concept in which all three fields of sustainability are examined. The term was first introduced by Elkington [46]. In our analysis, we assessed water use, land use and GHG emissions as environmental indicators. The social indicator is employment and the economic indicator GVA. To measure the supply chain impacts of the choice of electricity source on the sustainability of seawater desalination, we used the standard IO methodology, which goes back to Leontief [105]. In the following section, we present the basic principles of the methodology.

Let $\mathbf{Q}$ be the matrix of the physical satellite accounts containing the social and environmental indicators. The same calculations were applied accordingly to GVA as an economic indicator. Each row within the matrix represents another indicator. For each indicator row i, we got the vector of the intensities by dividing by outputs with

$$\mathbf{q}_i = \mathbf{Q}_i \hat{\mathbf{x}}^{-1}, \tag{4.1}$$

where $\hat{\mathbf{x}}$ represents the diagonal matrix of the output.

The standard Leontief equation estimates the output $\mathbf{x}$ of the sectors depending on the final demand $\mathbf{y}$ by

$$\mathbf{x} = (\mathbf{I} - \mathbf{A})^{-1}\,\mathbf{y}, \tag{4.2}$$

where $\mathbf{I}$ is the identity matrix and $\mathbf{A}$ represents the technical coefficient matrix. The matrix of technical coefficients representing the production recipe of the sectors is defined by $\mathbf{A} = \mathbf{T}\hat{\mathbf{x}}^{-1}$. The Leontief inverse $\mathbf{L} = (\mathbf{I} - \mathbf{A})^{-1}$ contains the supply chain multipliers. We obtained the supply chain impacts $\mathbf{Q}^{\mathrm{d}}{}_i$ (k x l) from eq. (4.1) and eq. (4.2) by

$$\mathbf{Q}_i^d = \hat{\mathbf{q}}_i (\mathbf{I} - \mathbf{A})^{-1} \hat{\mathbf{y}}. \tag{4.3}$$

Each value in row k and column l in $\mathbf{Q}^{\mathrm{d}}{}_i$ shows the contribution of industry k or the product l to the total magnitude of indicator i.

The GVA impacts were determined accordingly to eq. (4.3), using the GVA intensities $\mathbf{v}$ instead of $\mathbf{q}$. The results can be aggregated into two different representations. The formula $\mathbf{1}^{\mathrm{Q}'}\mathbf{Q}_i^{\mathrm{d}}$ shows the impacts caused by the production of commodities. Summing the rows by $\mathbf{Q}_i^{\mathrm{d}}\mathbf{1}^{\mathrm{Q}}$ aggregates the impacts by emitting industries. The operator ' transposes the summation vector $\mathbf{1}^{\mathrm{Q}}$. Electricity is distributed to the conventional electricity sector and to the RE sectors by the electricity penetration ratio $\lambda = 0$, 25, 50, 75 100%. We allocated the total electricity demand e with $e_c = (1 - \lambda)\, e$ to the conventional electricity sector and with $e_t = \lambda e \frac{g_t}{\sum_{t=1}^{4} g_t}$ to the RE sector in the demand vector $\mathbf{y}$. Here, g is the generation of the RE technology t.

4.2.6 Uncertainties

Prior LCAs similar to ours (e.g. Malik et al. [112]) have shown that measurement uncertainty contained in information on the satellite account $\mathbf{Q}$ and the supply-use data $\mathbf{T}$ represent the main origins for uncertainties in aggregate results, such as the TBL scores calculated in this work [113]. Because of nonlinearities in Leontief's eq. (4.2), the latter are usually determined using Monte-Carlo simulation [33, 81, 104]. Because of particular features in the propagation of errors in the Leontief system [74], high errors of individual matrix elements cancel each other out because of their stochastic nature [95,134], and the uncertainties of aggregate results are usually much smaller than matrix errors. Whilst the latter occupy a wide range between typically a few and a few hundred percent [33, 81, 104], the former hover between about 5% and 20% (see e.g. Lenzen et al. [100, 103]). Given the high similarity of data sources and mathematical procedures, these uncertainty magnitudes also apply to this study.

4.3 Results and discussion

4.3.1 Holistic triple bottom line impacts

In our study, we investigated the TBL impacts of seawater desalination depending on the electrical energy supply on the environmental indicators water use, land use and GHG. We used GVA as an economic indicator and employment as a social indicator.

Table 4.2 shows the overall results of the TBL footprints from 1990 to 2018, for the scenarios with only conventional electricity and 100% RE. The first three years represent the construction period of all plants, the years from 1993 onwards represent the operating and maintenance period over 26 years, which is in the average range of the concession periods of large Australian plants [66]. The spider plots in fig. 4.1 and fig. 4.2 show the relative performance of the different scenarios in relation to the 0% RE scenario. The values of the charts are calculated by summing the indicator values of each scenario and relating them to the sum of the indicator values of the 0% RE scenario. The values of the 0% RE scenario are thus always 1, i.e. they set the benchmark. In order to show better performance consistently greater than 1, the reciprocal value is formed for indicators for which less is better (for example, GHG, land use, water use). Hence, the normalised index $n_{k,s}$ for key figure k and scenario s (where scenario 0 is the base scenario with 0% RE) in the spider plots result from $n_{k,s} = \frac{\sum_{y=1}^{29} i_{k,s,y}}{\sum_{y=1}^{29} i_{k,0,y}}$ for the key figure employment and GVA (where more is better) and from $n_{k,s} = \frac{\sum_{y=1}^{29} i_{k,0,y}}{\sum_{y=1}^{29} i_{k,s,y}}$ for water use, land use and GHG emissions (where less is better) with y as year of investigation and i as the indicator values. Hence, the spider plots indicate better performances compared to the base scenario outside and weaker performances inside the blue base scenario circle.

We see that RE have a positive impact on water consumption during the entire life cycle. In both scenarios, the construction phase accounts for around half of the total water consumption. The use of 100% RE would reduce water consumption by 31% in the operating phase and by 7% in the construction phase of desalination plants. Thermal power plants require vast quantities of water due to their technical concept. In particular, the cooling required for the thermodynamic process is highly water-intensive. In coal-fired power plants, the amount of water required to generate electricity can, therefore, account for up to ten times the weight of the coal required [59]. Further water is required for the post-treatment of ash and waste disposal. Indirectly, coal mining and recultivation of the landscape are water-intensive. In contrast, the direct water consumption of PV and wind is negligible. Although the water consumption of hydro and geothermal electricity by

Table 4.2: *Overall results of the TBL footprints of desalination with 0% RE and 100% RE.*

		Water use		Land use		Greenhouse gas emission		Employment		Gross value added	
	RE-ratio	0%	100%	0%	100%	0%	100%	0%	100%	0%	100%
	Year	[GL]	[GL]	[kha]	[kha]	[Mt CO_2e]	[Mt CO_2e]	[10^3 FTE]	[10^3 FTE]	[AU$bn]	[AU$bn]
Construction	1990	443	414	5,747	5,643	50	15	273	272	13	13
	1991	912	852	11,668	11,470	105	31	533	531	26	26
	1992	439	411	5,613	5,511	51	15	255	253	13	13
	Total	1,794	1,677	23,029	22,623	206	60	1,061	1,056	52	52
	Contribution	43%	51%	77%	65%	23%	70%	72%	63%	42%	47%
Operation and maintenance	1993	114	73	582	842	32	1	24	29	2.1	1.7
	1994	109	70	534	785	31	1.4	23	29	2.1	1.6
	1995	105	69	493	752	30	1.3	22	29	2	1.6
	1996	103	68	461	723	30	1.3	20	28	2.1	1.7
	1997	101	66	434	663	30	1.2	20	28	2.1	1.7
	1998	97	65	370	625	29	1.2	18	26	2	1.7
	1999	88	64	327	592	27	1.1	16	25	1.9	1.6
	2000	89	63	299	552	27	1.1	16	25	2	1.6
	2001	85	63	273	563	26	1.1	15	25	1.9	1.7
	2002	94	66	276	620	29	1.1	15	25	2	1.7
	2003	87	62	272	576	27	1	12	22	2.1	1.8
	2004	85	56	156	378	29	1	12	22	2.1	1.8
	2005	64	57	174	377	19	1.1	14	24	2.2	2.1
	2006	63	58	171	339	20	1.1	14	23	2.3	2.2
	2007	59	43	190	237	18	0.9	13	20	2.4	2.2
	2008	60	42	187	234	19	0.9	12	20	2.6	2.4
	2009	62	44	191	237	20	0.9	13	20	2.8	2.6
	2010	56	41	199	246	20	0.8	15	21	3	2.6
	2011	67	54	94	241	24	0.9	11	18	3.2	2.7
	2012	103	61	94	273	27	0.8	12	20	3.3	2.8
	2013	115	70	129	269	31	0.7	15	22	4	3
	2014	113	66	136	280	29	0.7	16	22	4.1	3.1
	2015	96	65	133	287	28	0.7	13	22	4	3.1
	2016	90	70	190	473	25	0.7	14	21	3.6	2.9
	2017	108	73	219	499	31	0.7	16	23	3.8	3
	2018	121	71	239	494	35	0.8	18	23	4.2	3.2
	Total	2,335	1,604	6,821	12,156	692	26	409	613	70	58
	Contribution	57%	49%	23%	35%	77%	30%	28%	37%	58%	53%

evaporation and cooling is also substantial, PV and wind dominate the 100% RE system in this case study, which is why water consumption would be significantly reduced.

For the construction, operation and maintenance of the 29 seawater desalination plants, approx. 3,300 GL of water would be needed over the entire period of 29 years when using RE. In contrast, the plants would produce 5,500 GL of water per year, i.e. over the estimated life cycle of 29 years, water consumption would amount to 2.3% of the total amount of water produced. With conventional energies, the water consumption share is 2.9%. Over the total period, 21% of water use could be saved by using RE.

Within the construction phase, the land use of desalination would average around 7.5 Mha per year. Moreover, the construction phase is the driver in land use with 77% contribution when using conventional electricity. The use of RE during the construction

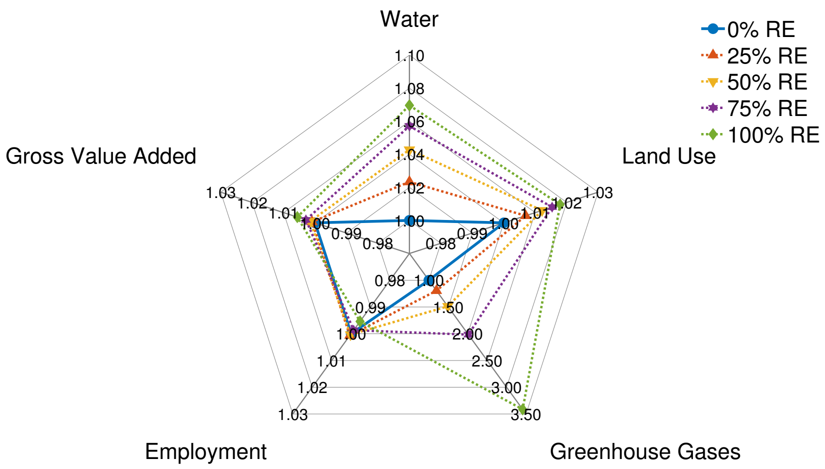

Figure 4.1: *Construction period TBL performances of desalination utilising different electricity mixes.*

phase, which would reduce land consumption by 2%, has only a marginal impact. If RE is used in the operational phase, land use would increase significantly by 78%.

RE would have the most significant positive impact on carbon emissions from desalination plants, both during construction and operation. In detail, 206 Mt CO_2e would be generated by the construction using the Australian electricity mix. Only 60 Mt CO_2e would be emitted if Australia had a 100% RE grid. The savings correspond to a reduction of 71%. An even more significant reduction in emissions could be achieved in the operating phase. While 692 Mt CO_2e is emitted in the 0% RE scenario, we see a reduction to 26 Mt with 100% RE. Consequently, carbon emission could be reduced by 96% in the operational period. In the base scenario, the operating phase contributes 77% to carbon emissions. In the RE scenario, the construction phase is the main contributor, with 70% of the total emissions. The results thus show that further measures are needed in other sectors to further reduce emissions during the construction phase.

Regardless of the power source, the average employment during the construction period would be over 350,000 full-time equivalent (FTE) per year. The construction period therefore contributes significantly to total employment, accounting for around 72% of total jobs. While employment in the 100% RE scenario would decrease slightly during the construction phase, employment during the operation phase would increase significantly

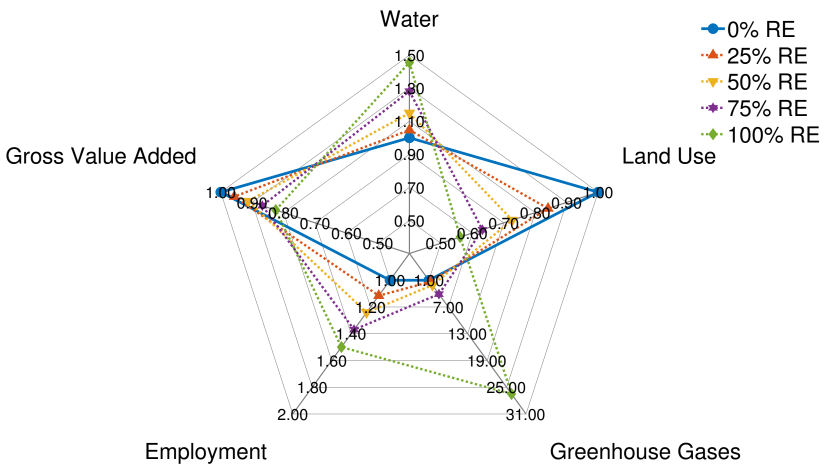

Figure 4.2: *Operation and maintenance period TBL performances of desalination utilising different electricity mixes.*

to 50%. Hence, jobs would increase by 50% from an average of around 16,000 FTE to around 24,000 FTE per year when using 100% RE.

The construction and operating periods have a similarly high contribution to GVA. In both scenarios, the construction of the 29 plants generates GVA of around AU$52bn (current prices). If 100% RE were used, GVA would be significantly reduced by 17.5% during the operation and maintenance period. Only AU$58bn instead of AU$70bn would be generated. Overall, this leads to a reduction of around 10% of GVA over the entire life cycle of 29 years. This decline can be explained by the fact that Australia is mining a large proportion of its conventional fuels domestically. However, this calculation does not take the external costs of using conventional energy into account.

4.3.2 Sectoral implications

In the following section, we identified the sectors that have a significant impact on the indicators. Figure 4.3 shows the percentage contribution of the different sectors to the overall impact. The upper diagram shows the contribution of each industry where the impacts occur. The lower diagram shows the commodities that trigger the impacts through their demand. The bars compare the 0% RE with the 100% RE scenario. The electricity industry is mainly responsible for water consumption in both scenarios.

Furthermore, the decrease in water consumption in the 100% RE scenario is mainly caused by the electricity industry and to a lesser extent by the mining industry. In contrast, the water consumption of the agricultural industry increases with the increasing share of RE in the electricity grid, mainly due to the use of biomass. Moreover, electricity is the most relevant commodity determining water consumption. The decrease in water consumption with 100% RE use is also driven by this commodity.

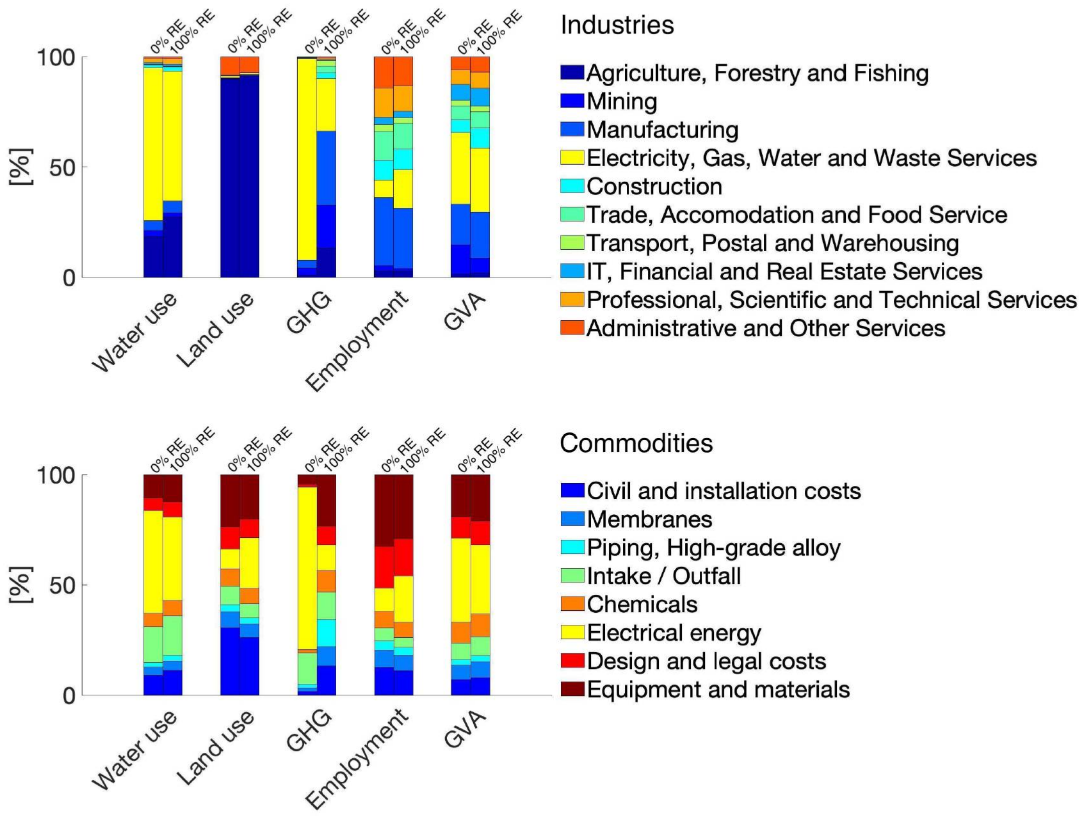

Figure 4.3: *Percentage impact contributions of industries and commodities, comparing the 0% RE and 100% RE scenario.*

Land use in both scenarios is dominated by the agricultural industry. The same industry causes additional land use when increasing RE share. While the contribution of the commodity electricity to land use is still relatively small when fossil-based electricity is used, it would more than double if RE were used. The main contributing commodities for land use are civil engineering services and installations, the construction of intakes and outfalls and the manufacturing of equipment and materials.

The electricity industry is the driving force for GHG emissions when desalination is operated and built by utilising conventional electricity. This picture changes with a higher share of RE so that the manufacturing industry plays the most considerable role. If we examine the commodities, a similar picture emerges. Electricity as a commodity, but also the construction of intake and outlet play a significant role in GHG emissions. Both commodities reduce their contribution in increasing the share of RE.

The manufacturing industry substantially contributes to employment. A transition to 100% RE would not change the contribution. However, the electricity sector becomes more critical in the 100% RE scenario, making it the second most job-relevant industry. When looking to commodities, the production of equipment and materials is primarily responsible for job creation. The contribution of the electricity commodity would also increase significantly due to a higher RE-share.

The electricity industry is the largest contributor to GVA, but the contribution decreases as RE increases. With an increasing share of RE, the mining industry would also reduce its contribution to GVA. On the other hand, the construction industry would increase its GVA contribution by increasing the share of RE. In all scenarios, the second most important industry sector in terms of GVA is the manufacturing industry. In both scenarios, the commodity electricity is the main driver of GVA, although the share is reduced by increasing the RE share.

4.3.3 Regional implications

Figure 4.4 shows the percentage change in the indicator totals for each of the 46 regions over the entire life cycle when switching from conventional electricity to 100% RE. Red indicates a reduction, green an increase of the indicator. The relative change for each region is given by $p_{k,r} = \frac{\sum_{y=1}^{29} i_{k,\ \mathrm{RE100},\ r,\ y}}{\sum_{y=1}^{29} i_{k,\ \mathrm{RE0},\ r,\ y}}$, where *i* is the total amount of the indicator of the key figure *k*, RE100 is the 100% RE scenario and RE0 is the 0% RE scenario. Furthermore, *r* indicates the region and *y* the year. It should be noted that especially regions that previously achieved relatively low values and have now experienced a high relative increase may still show low values in absolute terms. The diagram only shows the relative changes to the values in the 0% RE scenario. The key messages of the chart are the relative change in the indicator values in individual regions and, in particular, the shift in the indicator values, but not the absolute level of these values. The maps on the bottom show the classification of the 46 regions, aggregated to Australian States and Territories, water catchments (with the MDB) and rainfall areas. The map of the states and territories also shows the locations of the desalination plants.

Throughout the Eastern Region, water consumption would increase, particularly in MDB areas, through greater integration of RE. As the desalination plants in our case study were

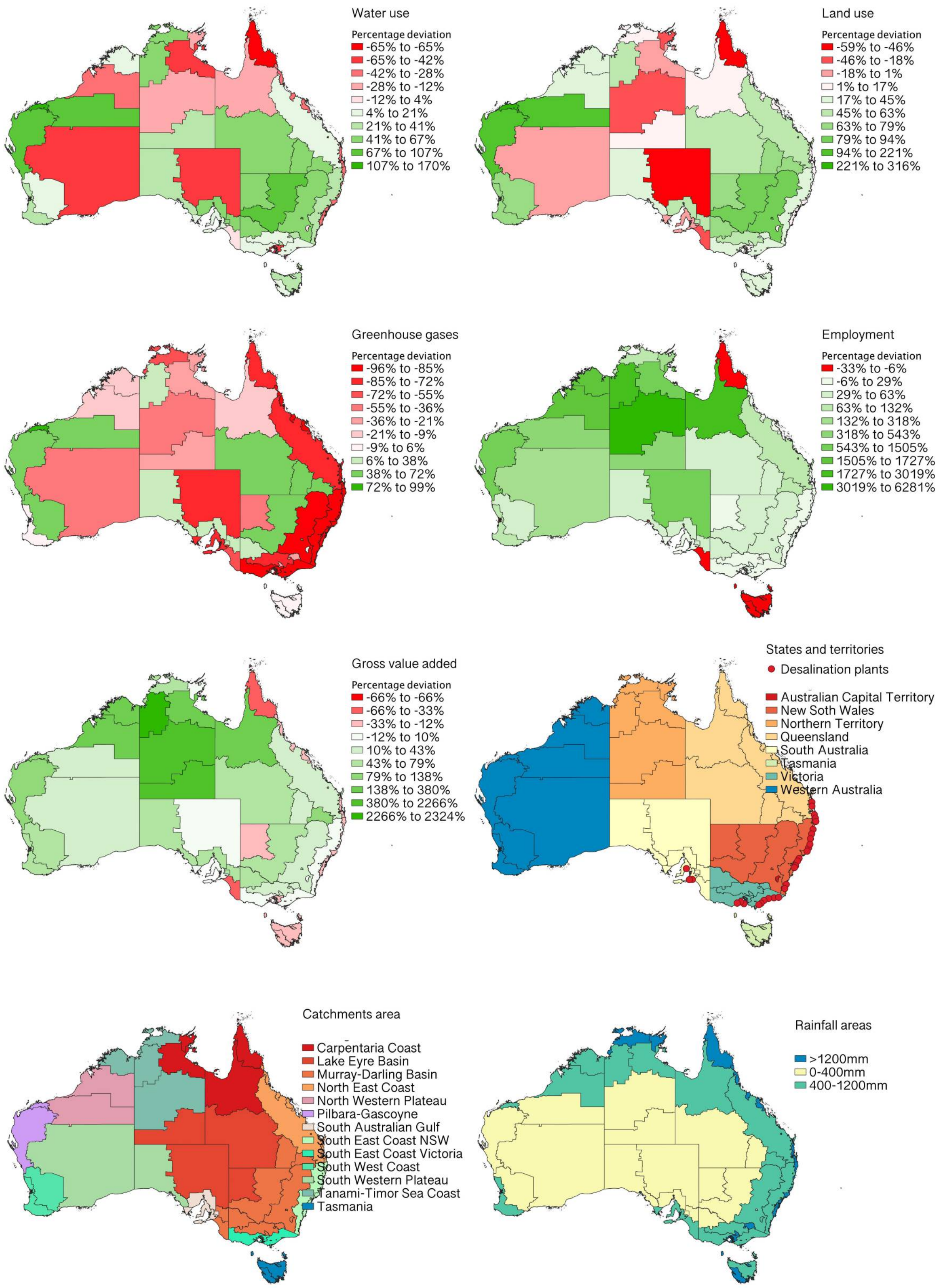

Figure 4.4: *Relative changes of the TBL indicators in the analysed 46 regions.*

built to address water scarcity in this area, this is an unsatisfactory result. However, we have seen in section 4.3.1 that water consumption is only about 2% of total production, so the additional consumption is relatively small. By contrast, water consumption is reduced in the direct coastal areas of the east coast, where most of the economic activity and population is located. Although these regions face higher rainfall than other areas off the coast, these regions are subject to long-term water stress due to high population density and economic activity. Victoria (Vic), in particular, would have to cope with a significant increase in water consumption at 100% RE.

The densely populated areas on the east coast would not face any significant change in land use when shifting to RE. In order to provide water in the MDB, demand is generated at the desalination plant sites shown in the states and territories diagram. Compared to centralised power plants, which are mostly located near the coast, the demand for the construction and operation of decentralised RE plants also generates a decentralised demand. Decentralisation is also reflected in land use, which is why areas in eastern Australia and in the MDB in particular are increasingly used in the 100% RE scenario. In central Australia, on the other hand, land use would tend to decrease, while on the west coast, land use would increase significantly.

On the east coast, where economic activities take place, we see an obvious reduction in carbon emissions at 100% RE. The entire east coast with its high population density and economic activity would significantly reduce carbon emissions from desalination by switching to RE. In areas where decentralised RE increase economic activity, emissions would increase, e.g. inland in eastern Australia or on the west coast.

If desalination is built and operated on the basis of RE instead of conventional electricity, fewer jobs would be created in a few regions in the north and south, including Tasmania (Tas). On the other hand, employment would increase in the inland areas. All areas in central and western Australia would see an increase in employment, as RE is much more decentralised than conventional power stations. Diversification of employment is beneficial for a country like Australia, where population and economic activity are concentrated in a few areas, while there are large unused areas in the hinterland.

Like employment, GVA would be regionally diversified due to the increasing use of RE. However, GVA would decrease in the economic areas of the east coast, especially in the north, but also in Tas. In the Northern Territory (NT), GVA would increase significantly. From an economic point of view, such a development would be beneficial as economic activity diversifies into areas with lower population density and less economic activity.

4.4 Conclusion

In our IO-based hLCA assessment, we showed the comprehensive TBL sustainability impacts of seawater desalination, depending on the utilised electricity source. Using social, economic ecological indicators, we explained in detail which sectors and regions contribute positively or negatively to the sustainability of desalination through a 100% RE grid.

With higher RE penetration, we measured rising employment but also falling GVA. Even if there is a trade-off between employment and GVA, the assessment shows that a higher RE share would contribute to regional diversification of economic activity. In fact, the spatial diversification of GVA is itself a value, as the local concentration of GVA increases the cost of land use. Therefore, decentralised GVA prevents price increases caused by land scarcity. While desalination with conventional electricity generates higher GVA through domestic fuel mining, this economic benefit is not sustainable in the light of the Paris Agreement.

Furthermore, the environmental performance of desalination with RE is highly beneficial. The application of a 100% RE system reduces the carbon emissions of desalination during construction by 71% and during operation by 96%. The benefit becomes even more evident when we monetise the reduced external costs. Let's assume an external cost of 100 $^{AU\$}/_{t\ CO_2}$ and 25 Mt as an average amount of carbon emissions reduced by RE during an operating year. Then the reduction in external costs through avoided emissions would result in savings of AU$3.75bn per year. In contrast, the total loss of GVA over the same period is some hundred million dollars. However, our analysis shows that about 30% of the carbon emissions during the construction period of the desalination plants cannot be reduced by 100% RE. Hence, further measures are still needed.

The results clearly show that RE and desalination benefit from synergy effects. Due to the high energy consumption, this applies in particular to desalination, but similar effects can also be expected for other water supply technologies due to the technical similarities. Due to the consequences of climate change, it is to be predicted that Australia's water problems will increase in the future. Policymakers should, therefore, aim for a common strategy for Australia's water and energy supply. The scope of consideration should be as broad as possible and should also include, for example, other related problems such as the discharge of brine with increased desalination use.

Our holistic assessment approach has several strengths for the analysis of infrastructure projects. Since we examined all three areas of sustainability using an hLCA framework, the results are directly comparable. We used the same system boundaries, the same assumptions and framework conditions, and the same economic linkages. Trade-offs, such as GVA and GHG emissions, can be compared directly. The methodology is particularly useful for practitioners to estimate the impact of infrastructure projects in the early planning phase. The political value of the findings is substantial. Our MRIO approach allows detailed regional and sectoral conclusions. The highly disaggregated analysis enables long-term economic policies, e.g. due to changes in regional water use, employment or economic activities.

The sustainability of seawater desalination plants depends in particular on regional factors such as local energy supply or industrial interconnections. In order to make these influences apparent, regional economic data are indispensable. The hLCA approach with the use of the IELab offers an efficient and effective possibility to break down statistical data to create tailor-made IOTs. The achievable granularity depends in particular on local data availability, whose quality is increasing worldwide. In recent years, IELabs for Australia, China, Indonesia, Taiwan, Japan, and the USA have been created that can be used for these assessments [53].

Further research is needed on the effects of large quantities of brine intake on marine biology. Furthermore, the development of new membranes promises remarkable increases in desalination efficiency. The associated effects on sustainability also require further research.

Acknowledgment

This work was financially supported the Friedrich Naumann Foundation for Freedom. We acknowledge support by the German Research Foundation and the Open Access Publication Fund of TU Berlin. The Authors further acknowledge financial support by the National eResearch Collaboration Tools and Resources project (NeCTAR) through its Industrial Ecology Virtual Laboratory. NeCTAR is an Australian Government project conducted as part of the Super Science initiative and financed by the Education Investment Fund. We thank Man Yu for providing the RE process data. We would also like to thank Ka Leung Lam, Syed Muhammad Hassan Ali and Bonnie McBain for their advice on processing the input data. We would like to acknowledge Arunima Malik for her advice on the post-balance procedure. Finally, we also thank the anonymous reviewers for the valuable comments, which have improved this study.

4.5 Appendices

4.5.1 Renewable electricity data preparation

Process coefficient matrices represent inputs as negative and outputs as positive values. In the first step, we removed outputs and converted inputs into positive values. The matrix $\mathbf{P}_t$ is the physical LCI of technology t extracted from the process coefficient matrix. For each technology we extracted process data for different plants to cover various capacities and regional differences. In a first step, we calculated mean values from the extracted data:

$$\mathbf{p}_t = \frac{\mathbf{P}_t \mathbf{1}^{\mathrm{P}}}{n}, \tag{4.4}$$

where $\mathbf{p}_t$ $(m \times 1)$ is the average process coefficient vector of technology t, $\mathbf{P}_t$ is the $(m \times n)$ process coefficient matrix of all processes for technology t. $\mathbf{1}^{\mathrm{P}}$ is an $(m \times 1)$ summation vector, n is the number of extracted plants for technology t. In order to monetise the data, the vector $\mathbf{p}_t$ was multiplied by the price vector $\boldsymbol{\omega}$ $(m \times 1)$, which has a base-year of 2009 by

$$\mathbf{p}_t^{\$} = \mathbf{p}_t \# \boldsymbol{\omega}, \tag{4.5}$$

where # indicates elementwise multiplication. Moreover, we aggregated the vector to the framework size of the tailored IOT with $i = 64$ sectors by

$$\mathbf{p}_t^{\mathrm{f}} = \mathbf{C}\mathbf{p}_t^{\$}, \tag{4.6}$$

where $\mathbf{C}$ represents an $(i \times m)$ aggregation concordance and $\mathbf{p}_t^{\mathrm{f}}$ is the size-adjusted process coefficient vector. In order to obtain the upstream cut-off vectors $\mathbf{u}_t$ from the cut-off matrix $\mathbf{U}_t$, we followed the procedures from eq. (4.4) and eq. (4.6) accordingly. The Step in eq. (4.5) was unnecessary as the cut-off matrix data were already monetised. The specific intermediate demand vectors $\mathbf{d}_t^{\mathrm{f}}$ for 1 MJ electricity output resulted from aggregating the cut-off and the process coefficient vectors by

$$\mathbf{d}_t^{\mathrm{f}} = \mathbf{p}_t^{\mathrm{f}} + \mathbf{u}_t^{\mathrm{f}}. \tag{4.7}$$

In the next step, we scaled the data relating to the functional unit of 1 MJ to the total electricity produced. The electricity produced by the RE technology t was determined by Heihsel et al. [71]. We used the results of the 90-day load-shifting scenario. Since we only considered the four most significant technologies for our scenario, we distributed the remaining electricity quantities pro rata among these technologies. We assigned the centralised solar power generation quantities to the PV sector. The quantities allocated to each technology, with a total of 322.6 TWh, are shown in table 4.3. The specific intermediate demand was then scaled on the basis of the electricity generated per year by

$$\mathbf{d}_t = \mathbf{d}_t^{\mathrm{f}} g_t, \tag{4.8}$$

where $\mathbf{d}_t$ is the total intermediate demand and g_t is the generated electricity of technology t. The satellite intensities $\mathbf{q}_t^{\mathrm{f}}$ were scaled accordingly by

$$\mathbf{q}_t = \mathbf{q}_t^{\mathrm{f}} g_t, \tag{4.9}$$

where $\mathbf{q}_t$ represents the total value of the environmental or social indicator of technology t. We calculated the economic output o_t using the intermediate demand ratio ($r = 0.62$) of the electricity sector from the IOT from 2009. Following this, the output was scaled by

$$o_t = \frac{\mathbf{1}^{\mathrm{d}} \mathbf{d}_t}{r}, \tag{4.10}$$

where $\mathbf{1}^{\mathrm{d}}$ is an (i x 1) summation vector. Accordingly, we estimated GVA by

$$v_t = o_t \left(1 - r\right), \tag{4.11}$$

where v_t is the GVA of technology t.

Table 4.3: *Yearly generation of the RE technologies.*

		Wind	Biomass	Hydro	Photovoltaic	Total
Generation	[TWh/y]	153.9	4.6	24.1	139.9	322.6

4.5.2 Structure of the integrated hLCA framework

Figure 4.5 shows the integrated hLCA framework by Yu and Wiedmann [180]. In the figure, $\mathbf{T}$ is the process coefficient matrix, $\mathbf{A}$ is the intermediate demand matrix of the IOT, $\mathbf{I}$ is the identity matrix, $\mathbf{C}_{\mathrm{u}}$ is the upstream cut-off matrix, and $\mathbf{C}_{\mathrm{d}}$ is the downstream cut-off matrix. $\mathbf{R}$ and $\tilde{\mathbf{R}}$ are the GHG extensions.

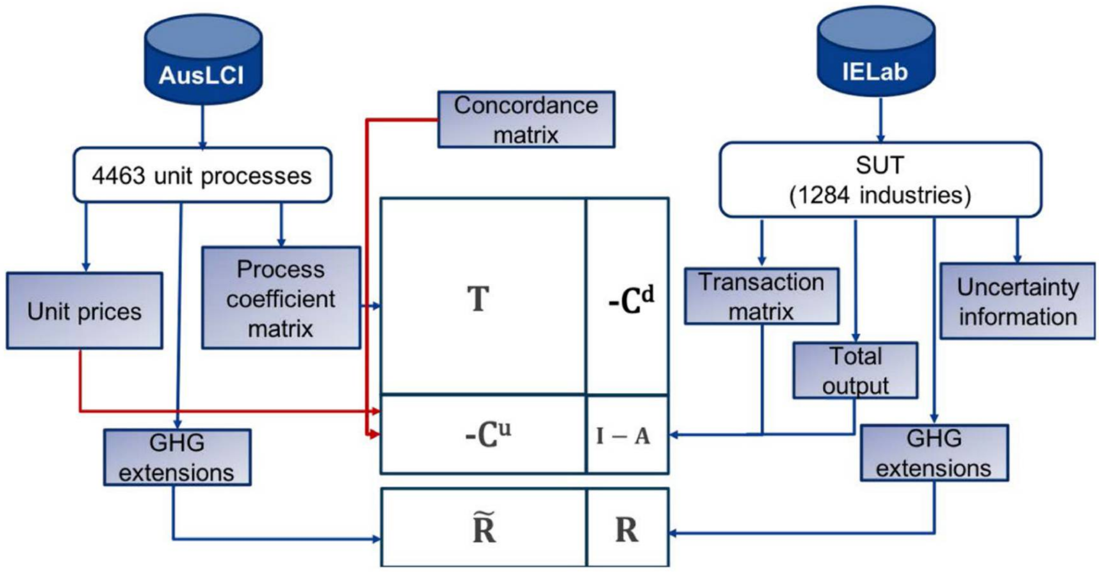

Figure 4.5: *Integrated hybrid life cycle assessment framework.*

Source: [180].

4.5.3 Extracted renewable electricity processes

Table 4.4: *Extracted renewable electricity processes used in the TBL study.*

	ID	Name
Wind	1231	Electricity, at wind power plant 2MW, offshore/OCE U/AusSD U
	1232	Electricity, at wind power plant 600kW/CH U/AusSD U
	1233	Electricity, at wind power plant 800kW/CH U/AusSD U
	1234	Electricity, at wind power plant 800kW/RER U/AusSD U
	1235	Electricity, at wind power plant Grenchenberg 150kW/CH U/AusSD U
	1236	Electricity, at wind power plant Simplon 30kW/CH U/AusSD U
Biomass	1239	Electricity, bagasse, sugarcane, at fermentation plant/BR U/AusSD U
	1240	Electricity, bagasse, sugarcane, at sugar refinery/BR U/AusSD U
	1241	Electricity, bagasse, sweet sorghum, at distillery/CN U/AusSD U
	1242	Electricity, biogas, allocation exergy, at micro gas turbine 100kWe/ CH U/AusSD U
	1243	Electricity, biogas, allocation exergy, at PEM fuel cell 2kWe, future/ CH U/AusSD U
	1244	Electricity, biogas, allocation exergy, at SOFC-GT fuel cell 180kWe, future/CH U/AusSD U

Table 4.4 continued from previous page

	ID	Name
	1245	Electricity, biogas, allocation exergy, at SOFC fuel cell 125kWe, future/CH U/AusSD U
	1246	Electricity, biomass, at power plant/US U
	1541	Electricity, pellets, allocation exergy, at stirling cogen unit 3kWe, future/CH U/AusSD U
	1589	Electricity, wood, at distillery/CH U/AusSD U
Hydro	1331	Electricity, hydropower, at power plant/AT U/AusSD U
	1332	Electricity, hydropower, at power plant/BA U/AusSD U
	1333	Electricity, hydropower, at power plant/BE U/AusSD U
	1334	Electricity, hydropower, at power plant/CH U/AusSD U
	1335	Electricity, hydropower, at power plant/CS U/AusSD U
	1336	Electricity, hydropower, at power plant/DE U/AusSD U
	1337	Electricity, hydropower, at power plant/DK U/AusSD U
	1338	Electricity, hydropower, at power plant/ES U/AusSD U
	1339	Electricity, hydropower, at power plant/FI U/AusSD U
	1340	Electricity, hydropower, at power plant/FR U/AusSD U
	1341	Electricity, hydropower, at power plant/GB U/AusSD U
	1342	Electricity, hydropower, at power plant/GR U/AusSD U
	1343	Electricity, hydropower, at power plant/HR U/AusSD U
	1344	Electricity, hydropower, at power plant/HU U/AusSD U
	1345	Electricity, hydropower, at power plant/IE U/AusSD U
	1346	Electricity, hydropower, at power plant/IT U/AusSD U
	1347	Electricity, hydropower, at power plant/JP U/AusSD U
	1348	Electricity, hydropower, at power plant/LU U/AusSD U
	1349	Electricity, hydropower, at power plant/MK U/AusSD U
	1350	Electricity, hydropower, at power plant/NL U/AusSD U
	1351	Electricity, hydropower, at power plant/NO U/AusSD U
	1352	Electricity, hydropower, at power plant/PL U/AusSD U
	1353	Electricity, hydropower, at power plant/PT U/AusSD U
	1354	Electricity, hydropower, at power plant/SE U/AusSD U
	1355	Electricity, hydropower, at power plant/SI U/AusSD U
	1356	Electricity, hydropower, at power plant/SK U/AusSD U
	1390	Electricity, hydropower, at run-of-river power plant/CH U/AusSD U
	1391	Electricity, hydropower, at run-of-river power plant/RER U/AusSD U

Table 4.4 continued from previous page

	ID	Name
Photovoltaic	1542	Electricity, photovoltaic, at 3kWp slanted-roof , mc-Si, future/CH U/AusSD U
	1543	Electricity, photovoltaic, at 3kWp slanted-roof , pc-Si, future/CH U/AusSD U
	1569	Electricity, production mix photovoltaic, at plant/AT U/AusSD U
	1570	Electricity, production mix photovoltaic, at plant/CH U/AusSD U
	1571	Electricity, production mix photovoltaic, at plant/DE U/AusSD U
	1572	Electricity, production mix photovoltaic, at plant/ES U/AusSD U
	1573	Electricity, production mix photovoltaic, at plant/HU U/AusSD U
	1574	Electricity, production mix photovoltaic, at plant/IT U/AusSD U
	1575	Electricity, production mix photovoltaic, at plant/JP U/AusSD U
	1576	Electricity, production mix photovoltaic, at plant/PT U/AusSD U
	1577	Electricity, production mix photovoltaic, at plant/US U/AusSD U
	1586	Electricity, PV, at 3kWp slanted-roof, CdTe, panel, mounted/CH U/AusSD U
	1587	Electricity, PV, at 3kWp slanted-roof, multi-Si, panel, mounted/CH U/AusSD U

4.5.4 Augmented input-output framework

Figure 4.6 shows the schematic augmented IOT of one region within a MRIO table. **U** is the use-matrix with input and sales structures. **V** is the supply-matrix containing the output values of the sectors. **Y** is the final demand matrix, **x** is the output vector, **v** is the GVA vector, and **Q** is the matrix of the physical satellite accounts.

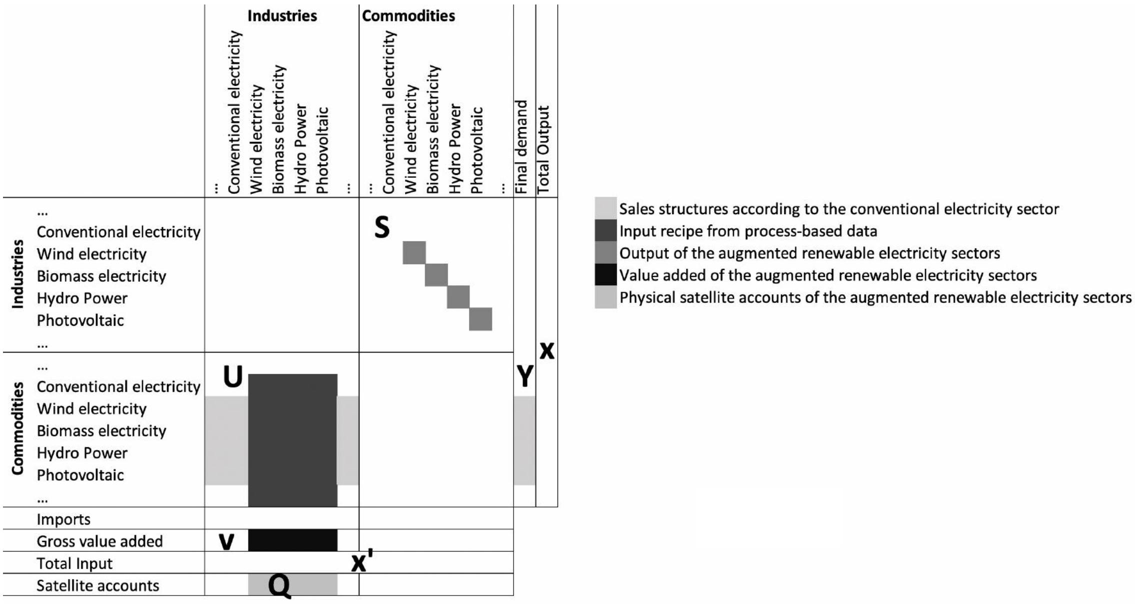

Figure 4.6: *Supply-use input-output-based hybrid LCA framework.*

Chapter 5

Conclusion

In our research work, we comprehensively investigated seawater desalination and the role of the electricity source. Our investigation focused on applications in Australia. Australia is an appropriate choice for several reasons: Firstly, Australia is the driest inhabited continent. Secondly, the use of seawater desalination is gaining importance due to increasing water scarcity. Thirdly, Australia has a prosperous economy and therefore uses state-of-the-art facilities. Due to the dominance of reverse osmosis (RO) plants in Australia and worldwide, we concentrated on this technology. We also focused on utility-scale systems in our analysis, both in terms of plant size and the coupling with power generation plants. We did not look at direct coupling with individual renewable energy (RE) technologies, but at coupling via the power grid.

For this purpose, we chose two different modelling approaches. In order to analyse the sustainability over the entire value chain, we developed a tailor-made input-output (IO) model. For analysing social, economic and environmental sustainability, we extended this model comprehensively. One objective was to show in detail the impacts of the construction and operation of seawater desalination plants over a period of decades. In particular, the influence of the use of different electricity sources in the entire value chain could be analysed.

The development of an own IO model with the use of the Industrial Ecology Virtual Laboratory (IELab) enables a much more comprehensive analysis as it would be possible with available input-output tables (IOTs) or with process-based life cycle assessments (LCAs). The sectoral and regional disaggregation of statistical data allows an analysis tailored to the research object. On the one hand, sectors that play a significant role in seawater desalination can be broken down in great detail. On the other hand, sectors that are less important can be aggregated, which in particular reduces the necessary computing power. Regional influences on the results, such as different electricity mixes in different states, can be directly considered in the analysis. The tailored breakdown of sectors also allows process-based data to be used for the analysis in an hybrid life cycle assessment (hLCA) approach. Thus, especially the first stages of the value chain can be mapped accurately.

Using a load-shifting model, we demonstrated the potential of seawater desalination as a variable load. We developed a scenario in which large-scale desalination could ensure the water supply of an area currently under structural water stress. At the same time, seawater desalination technology is suitable not only to stabilise an electricity grid with high penetration of RE but also to reduce the necessary capacity of RE plants. Thus, the overall system can be made more cost-efficient. In a further study, the results of the calculations from this optimisation of the RE system were incorporated into an IO model, analysing the comprehensive effects on environmental, economic and social sustainability. This study aimed to compare the impact of the use of RE with the impact of the current electricity mix of conventional electricity sources.

Research question 1: What carbon emissions are generated by the existing desalination plants in Australia? Which industries, goods and regions are the drivers of these emissions?

In chapter 2, research question 1 was examined. Therefore, we first examined the cost data of the 349 existing plants in Australia, 89 of which are seawater desalination plants. The analysis showed that the largest 20 plants in Australia cover 95% of total seawater desalination capacity, so we focused on these plants. Desaldata, the most comprehensive database available [66] provides a high level of detail on individual plants, but we have validated and verified the data extensively. We verified the construction time, capacity, total costs at operational expenses (OPEX) and capital expenses (CAPEX) and the specific energy consumption. The cost structure was determined by the desaldata cost estimator tool. The data were not adjusted, since similar tools such as from International Atomic Energy Agency (IAEA) [85] provided comparable results.

Although environmental effects like the carbon emissions of a technology depend significantly on the location due to the industrial linkages and the local electricity mix, the literature review revealed that there has not been a comprehensive multi-regional carbon footprint study on seawater desalination. For this reason, we were motivated to examine the 20 largest plants existing in Australia over more than ten years. The construction as well as the operation of the plants was examined based on the local electricity mix. A multi-regional input-output (MRIO) framework with 123 sectors and eight regions was created.

The investigations revealed a higher multiplier for the construction phase than for the operation phase. Accordingly, in the operating phase, the immediate upstream stage of the value chain contributes relatively more to total emissions than in the construction phase. The electricity sector, in particular, is accountable for this. While electricity is mainly directly demanded in the operation phase, the demand for electricity in the construction phase is found in upstream stages of the value chain. This fact greatly simplifies the reduction of the carbon footprint in the operating phase compared to the construction phase. Although the contribution to total emissions from the operating phase is considerably higher, the construction phase also contributes significantly to total emissions. Thus, the peak of emissions in the construction phase of the plants is 820 $^{kt}/_{y}$, and the peak in the operation phase is 1,239 $^{kt}/_{y}$.

The most relevant commodity for carbon emissions during the operating phase is electricity, while other commodities have comparatively little impact. In the construction phase, the main contributors to emissions are the construction of the inlet and outlet, but also the construction of pipelines. In both phases, the electricity industry is responsible for the bulk of carbon emissions. The manufacturing and construction industries also play an essential role in emissions during the construction of the plant. Victoria (Vic) is the largest emitter of CO_2, but New South Wales (NSW) and Western Australia (WA) also show high emissions. The emissions are mainly generated where the desalination plants are located, as the electricity market in Australia is only moderately characterised by interregional exchanges.

As the electricity sector is a crucial industry for the carbon footprint, emissions in the operating phase occur relatively in the early stages of the value chain. In contrast, in the construction phase emissions occur further upstream. We determined an average carbon footprint of approximately 1.5 $^{kg}/_{m^3}$ from operation alone. Thereby average costs in the range of 0.4 $^{AU\$}/_{m^3}$ are incurred.

The study on the carbon footprint of desalination has shown that it is essential to consider the entire value chain in order to depict the full impact of desalination. This was particularly evident for the construction of the plants, where a large part of the emissions occurs upstream of the value chain. The electricity industry, which accounts for 35% of Australia's total emissions, is a key industry for emissions in this context. The results clearly show that seawater desalination in both construction and operation is strongly dependent on the electricity sector along the value chain: 69% of the emissions in the construction phase are emitted by this industry and as much as 96% in the operation phase. However, the hypothesis of the World Bank [161] that the use of RE could reduce

CO_2 emissions by 99% does not seem tenable. Especially in the construction phase, a considerable part of the emissions is caused by other sectors.

Research question 2: What economic synergy effects arise from the coupling of large-scale desalination plants with a 100% RE system?

Large-scale seawater desalination in Australia is currently carried out for municipal water supply only. However, there are areas, such as the Murray-Darling Basin (MDB), that suffer from structural water stress. The area is environmentally sensitive and is also the most agriculturally productive area in Australia. In chapter 3, we investigated research question 2. Therefore, we examined whether seawater desalination can tackle the structural water shortage in the MDB. To this end, we modelled the electricity demand of desalination plants in a 100% RE system to reduce the necessary power generation capacity by applying load-shifting. The objective was to find out which synergy effects can be achieved with the coupling. Furthermore, we wanted to investigate if the savings by reducing the RE capacity outweigh the additional costs by increasing the desalination capacity.

The simulation has shown that by integrating the desalination plants with an oversize factor of 1.5, the spilt electricity in the RE system can be reduced by at least 27 TWh. The increase in the considered load-shifting period increases the reduction potential. The installed capacity of RE generators can be reduced by up to 29%, the levelised cost of electricity (LCOE) by up to 43%.

Load-shifting of desalination demand allows better coordination of electricity supply and demand, both seasonally and intraday. Thus, water production, i.e. electricity demand, is shifted from the Australian summer months to the winter months. During the day, demand is shifted to the early morning hours until early noon, especially in April and at the end of the year. In our simulation, we capped peak demand by limiting the desalination plants to 1.5 times the capacity required for continuous operation. The analysis indicates that a continued expansion of potential peak demand would bring further benefits in reducing RE capacity.

Among the RE technologies integrated into the simulation, wind has the highest capacity factor and the largest share in total electricity production. Wind energy also has relatively low spilt electricity of about 10%. Wind and solar power complement each other quite effectively for the use of seawater desalination plants. This results in a relatively balanced production curve in the day and night cycle. Although higher capacity factors are possible for ocean and geothermal energy, the potential for expansion is minimal, as is the case with biomass. Load-shifting resulted in the replacement of relatively expensive concentrated solar power (CSP) in particular and, to a limited extent, wind electricity with cheaper photovoltaic (PV) spilt electricity.

By integrating seawater desalination plants with a capacity of 5,500 GL, taking an oversize factor of 1.5 into account, we determined a gross benefit of $24.6bn per year. This benefit results from the total cost savings in reducing the RE capacity. Oversizing the desalination plants and pipelines would cause additional costs of $1.27bn, resulting in an annual net benefit of $22.5bn. The benefit represents about 35% of the total costs of the electricity system in the no-shifting scenario. Nevertheless, our approach to addressing water scarcity in the MDB through the massive construction of seawater desalination plants and pipelines is a huge challenge. Thirty-five pipelines with an average diameter of 2.1 m require high investment volumes, strong political will and considerable courage. However, our analysis clearly shows the advantages of integrating desalination plants into a 100% RE system. The construction of such a RE system is a challenge for the coming decades.

Water supply in the MDB is currently not sustainable. Various studies show that further measures are needed. However, restricting water extraction also has significant economic impacts. In addition, the political headwind is likely to be strong, as a large part of the population living in the region is dependent on agriculture. A strategy that ensures water availability by increasing supply is therefore desirable. The Australian energy sector will also expand RE significantly in the coming decades. This progress is not only driven by international agreements but increasingly by the trend in electricity generation costs. Coupling desalination and RE technologies has the potential for high synergy effects.

Research question 3: What are the social, economic and environmental benefits and costs of coupling large-scale desalination plants with a 100% RE system?

In chapter 4, we answered research question 3. To this end, we investigated the configuration of the desalination plants to supply the MDB in combination with a 100% RE system. We investigated the economic, social and environmental impacts arising from the demand for the construction and operation of the desalination plants. We compared different RE penetration rates from 0%, i.e. the use of conventional electricity, up to 100% RE. The core results for the 100% RE scenario compared to the 0% RE scenario show the following: 20% less water consumption, 90% lower greenhouse gas (GHG) emissions, 14% more jobs, but also 17% higher land use and 10% lower gross value added (GVA), whereby the reduction of negative external effects from the use of fossil-based energy sources has not been taken into account.

In detail, our calculations over a period of 29 years show that the reduction in water consumption when switching to RE takes place mainly in the operating phase. In the 100% RE scenario, the construction and operation phases each contribute approx. 50% to the total water consumption. With 77%, the construction phase is the driver of land consumption. A conversion to 100% RE would have hardly any impact on land use in the construction phase. In the operating phase, however, land use would decrease by 78%. RE have a huge impact on GHG emissions. A reduction of 71% and 96% in the construction and operating phases respectively would be possible. In the base scenario, the operating phase still contributes 77% of total emissions. In the 100% RE scenario, this picture changes and the construction phase is responsible for 70% of the remaining emissions. The results show that further measures than the conversion to RE are necessary to completely decarbonise desalination. Jobs are mainly created in the construction phase, with a contribution of 72%. In the 100% RE scenario, jobs would be lost to a small extent in the construction phase. In the operation and maintenance phase, however, jobs would increase by 50%. GVA is generated to a similar extent in both the construction and the operation phase. The conversion to 100% RE would reduce GVA by about 10%.

Water consumption in all scenarios is mainly due to the electricity industry. The decreasing consumption in the conversion to RE is mainly found in the electricity industry but also the mining industry. The use of biomass increases water consumption of the agricultural industry. The agricultural industry dominates land use in all scenarios. Also, the increasing land use with an increase in the RE share is located in this industry. The electricity industry mainly generates GHG emissions in the 0% RE scenario. A switch to 100% RE changes this, so that the manufacturing industry is now responsible for the majority of the emissions. The manufacturing industry is the driver of jobs. Switching to RE does not change this situation. However, the electricity industry would gain in importance after the RE transformation. The electricity sector is the most significant contributor in terms of GVA, but the contribution decreases when RE is increased. The share of GVA of the mining industry would also decrease if RE were increased.

Although water consumption would increase due to the increase of RE in the regions of the MDB, total water consumption over the entire life cycle is only 2% of annual production. Land use would remain relatively constant in the densely populated areas of the east coast if RE were to be introduced. Inland, however, especially in the MDB, land use would increase significantly. While on the east coast of Australia, GHG emissions would decrease if RE were increased, inland emissions would increase in the east and west. In terms of employment and GVA, RE would cause significant regional diversification.

Although GVA decreases by 10% due to an increase in RE, regional diversification is a clear benefit. While Australia is rich in unused land, land use prices in the densely populated areas are high due to land-use competition. Diversification through RE would counteract this. Against the background of climate change and international agreements such as the Paris Climate Agreement, GVA generation through carbon-intensive technologies is not sustainable. The high external costs associated with the use of fossil fuels also argue against their economic sustainability. In this context, the reduction of GVA is tolerable. The ecological effects of desalination with 100% RE speak for themselves. The reductions of 71% and 96% in the construction and operating phases respectively are significantly higher than the contribution of the electricity sector to Australia's total emissions. While the reduction of GVA by RE amounts to some $100m, the savings of external costs are in the range of $3.75bn per year.

This dissertation has investigated the comprehensive social, environmental and economic sustainability of seawater desalination using renewable and conventional energies. A novel geographic information system (GIS)-based load-shifting model was used to show the synergy effects of both technologies. Furthermore, we showed how state-of-the-art development of IO-based hLCA methods can be used for these purposes. We showed that seawater desalination can be realised in a much more sustainable way by consistently converting the power grid to RE. The research work thus showed that seawater desalination can be a sustainable option for the water supply strategy of arid regions. The potential of this technology is not only underlined by strong growth rates in recent years. The findings of this dissertation indicate that seawater desalination will continue to increase in relevance.

However, other issues must not be ignored. For example, the impact on marine biology requires further research. Seawater desalination projects should also be subject to comprehensive impact analysis before their construction in order to identify major impacts in advance. In particular for the construction phase of plants, the conversion of the electricity system to RE is not sufficient. Further research is needed here to find out in which sectors, and by which processes further GHGs can be saved. The impact of future technologies, such as graphene membranes also requires further research.

Published Articles

Desalination 454 (2019) 71–81

Contents lists available at ScienceDirect

Desalination

journal homepage: www.elsevier.com/locate/desal

The carbon footprint of desalination
An input-output analysis of seawater reverse osmosis desalination in Australia for 2005–2015

Michael Heihsel[a,*], Manfred Lenzen[b], Arunima Malik[b,c], Arne Geschke[b]

[a] Department of Energy Engineering, Technical University of Berlin, Straße des 17. Juni 153, 10623 Berlin, Germany
[b] ISA, School of Physics, The University of Sydney, Sydney, New South Wales 2006, Australia
[c] Discipline of Accounting, The University of Sydney Business School, Sydney, New South Wales 2006, Australia

ARTICLE INFO

Keywords:
Input-output analysis
Life cycle analysis
Multi-regional
Greenhouse gases
Sustainability

ABSTRACT

This study examines greenhouse gas emissions for 2005–2015 from seawater desalination in Australia, using conventional energies. We developed a tailor-made multi-regional input-output-model. We complemented macroeconomic top-down data with plant-specific desalination data of the largest 20 desalination plants in Australia. The analysed capacity cumulates to 95% of Australia's overall seawater desalination capacity. We considered the construction and the operation of desalination plants. We measure not only direct effects, but also indirect effects throughout the entire value chain. Our results show the following: We identify the state of Victoria with the highest emissions due to capital and operational expenditures (capex and opex). The contribution of the upstream value chain to total greenhouse gas emissions increases for capex and decreases for opex. For capex, the construction of intake and outfall is the driving factor for carbon emissions. For opex, electricity consumption is the decisive input factor. Both in construction and operation, we identify the critical role of the electricity sector for carbon emissions throughout the supply chain effects. The sector contributes 69% during the zenith of the construction phase and 96% during the operating phase to the entire emissions. We estimate the total emissions for 2015 at 1193 kt CO_2e.

1. Introduction

Increasing lack of fresh water is one of the most severe global problems of the future decades. About two-thirds of the world's population has no access to fresh drinking water at least once a year [1]. More than 783 million people have no access to clean drinking water [2], and half a billion people suffer from water shortages throughout the year [1]. The most affected regions include the west of North America, the east of Spain, the Middle East and North Africa (MENA) region, as well as Australia and northern China. Archipelagos like the Canary Islands face these problems, too [3].

Meanwhile, California experienced a prolonged and unusually severe drought from 2011 to 2017, resulting in daily life restrictions, high water costs, and economic slowdown. Climate change, prosperity, and exponential population growth will further aggravate these problems. Water is increasingly becoming a scarce and therefore valuable commodity. It is becoming more difficult for the regions mentioned to meet the demand for fresh water which inevitably leads to conflicts of use.

Many of these arid regions are close to the seashore and thus close to substantial water resources. Some areas are already using desalination technology, which is the most expensive option to meet water demand. However, it is already indispensable for many regions. For example, Saudi Arabia covers 50% of its water needs from desalination, using 25% of its oil and gas for water and electricity production in combined power-desalination plants [4]. Mitigating water scarcity becomes a self-accelerating problem. Drought is increasing as a result of climate change. In order to solve this problem, the use of desalination is proliferating, which in turn catalyses climate change due to high energy demand. Water production needs energy, but electricity generation also needs water in large quantities, that is why academia speaks of the water-energy-nexus [5].

Numerous studies address technical, economic or ecological issues of conventional and renewable operated desalination. However, the current literature shows some knowledge gaps. Gude [6] states in his study:

“Although some of the facts and recent developments discussed here

* Corresponding author.
E-mail address: michael.heihsel@campus.tu-berlin.de (M. Heihsel).

https://doi.org/10.1016/j.desal.2018.12.008
Received 4 August 2018; Received in revised form 30 November 2018; Accepted 15 December 2018
Available online 31 December 2018

show that desalination can be affordable and potentially sustainable, contributions that meaningfully address socio-economic and ecological and environmental issues of desalination processes are urgently required in this critical era." [6]

Haddad [7] also draws attention to the need for holistic studies in the field of desalination research. Only by incorporating effects throughout the entire supply chain (indirect effects), a comprehensive assessment is possible [7]. Whether or not desalination can sustainably solve the problems of water availability in arid and semi-arid regions depends on its holistic socio-economic and ecological sustainability.

Lattemann and Höpner provide an overview of the leading environmental impacts of desalination and possibilities to minimise impact and risks [3]. The World Bank estimates that 99% of carbon dioxide equivalent (CO_2e) involved in a business-as-usual scenario could be avoided by desalination with renewable energies [8]. This estimation illustrates the enormous carbon reduction potential of combining renewable energies and desalination. Einav et al. show the factors that significantly influence the ecological footprint of desalination [9]. These factors are land use, the groundwater, the marine environment, noise pollution and the use of energy. According to Muñoz and Fernández-Alba, the type and quality of feedwater can reduce the environmental impact (such as energy demand, acidification potential or human toxicity potential) of the Reverse Osmosis (RO) process up to 50% [10]. Liu et al., Setiawan et al., Vince et al. and Sadhwani et al. offer analyses of the ecological effects [11–14]. A good overview of current trends and ecological challenges can be found in Goosen et al. [15].

We have found several studies in the field of input-output analysis and life cycle assessment of desalination. Raluy et al. use a process-based LCA to investigate different desalination technologies [16]. Zou and Liu use input-output analysis on desalination in China to measure the economic impact of investments [17]. Storkes and Horvath use a hybrid LCA to study water supply systems in California [18]. Shahabi et al. use a hybrid approach to investigate a desalination plant in Western Australia [19].

There is no doubt that desalination plays an essential part in the water supply strategy of regions which are affected by severe drought and have access to seawater. However, desalination must prove its economic, environmental and social sustainability. Our study contributes to quantifying environmental sustainability by measuring the carbon footprint of desalination in Australia. For the study, we assume that operation and construction processes use electricity from conventional energy in line with the Australian energy mix. It is the first study of desalination, where a comprehensive multi-regional model has been created and used for measuring the supply chain impacts. With the aid of our multi-regional model, we can also present regional impacts for the first time. Our approach rates the country's largest 20 plants, which represents 95% of the total capacity – that to over more than ten years.

2. Methods and data

A carbon footprint captures the carbon emissions of a product, a technology or a technical process. This approach does not only analyse carbon emissions directly generated by the desalination process itself. It also accounts for indirect effects, defined as all carbon emissions generated by suppliers within the entire supply chain. Our approach captures carbon emissions throughout the entire supply chain (upstream). We consider desalination as final demand and analyse carbon emissions from sectors from which desalination purchases inputs. Our approach does not assume that additional water from desalination induces further carbon emission downstream the supply chain.

Leontief [20] invented input-output analysis (IOA) and applied it in several studies. For this seminal work, Leontief earned the Nobel Prize in 1973. Researchers have used IOA to analyse economic effects of monetary demand on economic key figures, mainly effects on industrial output. Model extensions use IOA to analyse further economic, social or environmental effects [21] [22]. We apply IO-methodology to estimate the carbon footprint of desalination in Australia.

Footprint studies apply input-output-tables (IOTs) that show monetary trade flows of economic sectors. In order to produce goods, companies purchase intermediate goods from other companies. These intermediate streams are the core of IOTs. The columns of these tables show which input factors a particular sector purchases to produce their goods. The rows of the table show the production of a sector, which this sector produces for other sectors as intermediate inputs. The intermediate input matrix gives a comprehensive picture of the intermediary inputs and creates a production recipe for the produced goods of each sector. These recipes provide the opportunity to carry out value-added analysis and combine it with satellite accounts (such as the sectors' greenhouse gas emissions). The combination allows for comprehensive carbon footprint studies by considering the entire value chain, without truncation errors such as those found in classic process-based LCAs [23].

The benefit of a hybrid LCA approach is to combine bottom-up process data with top-down macroeconomic input-output data and hence include the technical process into the macroeconomic system of a whole economy.

To the best of our knowledge, our study is the first comprehensive multi-regional carbon footprint study for a country's desalination application.

2.1. Construction of a multi-regional input-output database

IOA applies data from national accounts. IOTs arrange and structure the data. The tables describe the structure of an economy with detailed information about output, intermediate and final demand. IOTs can describe an economy by industry or commodity classification. Furthermore, IO-models can classify an economy in a single-regional or a multi-regional framework.

Compiling tailor-made IOTs is a work-intensive task. Finding data for different regions and sectors is challenging because the data are often incomplete or inconsistent. Lenzen et al. developed a cloud-based virtual laboratory, the Industrial Ecology Laboratory (IELab), to compile tailor-made IOTs for Australia [24]. A collaborative group of researchers feeds the database in an ongoing process. An algorithm converts the data into a specific structure, the so-called root classification. The root has 1284 sectors in Input-Output Product Classification (IOPC) [25] and 2214 regions in Statistical Area Level 2 (SA2) classification [26]. Due to the vast amount of data, IELab offers high-performance-computing for IOT compiling and calculations [27]. We apply a supply-use-framework [28].

For this study, we constructed a multi-region input-output (MRIO)-framework with 123 sectors and eight regions that represent the Australian states and territories. The desalination input data determine the structure of the sector classification. In contrast to available input-output tables, this allows for a detailed and accurate analysis that avoids aggregation errors. For our carbon footprint study, we compiled a satellite account of CO_2e emissions of industrial sectors.

We compiled several concordances for this study [24]. The generation of tailor-made IOTs requires concordances from root to study-specific sector classification and from root to study-specific region classification. To compute demand vectors, we compiled concordances from desalination input data structure to study-specific sector classification. Since supply-use-frameworks are twice the size of usual IO-frameworks, the framework includes 2×123 sectors (industry and commodity) in 8 regions. The structure results in a transaction matrix in the size of 1968×1968. We compiled tables for the years 2005 to 2015, whereas the years refer to Australian financial years.

Compiling IOTs requires the application of mathematic optimisation algorithms. The critical challenge is that the number of variables to be determined significantly exceeds the number of constraints. The IELab implemented advanced optimisation approaches like quadratic programming and Konfliktfreies RAS (KRAS) to solve the optimisation problem [29].

The creation of large MRIO tables represents an underdetermined optimisation problem. Raw data for large economic transactions are much more available than raw data of small transactions. Hence, the number of constraints used for the optimisation is much smaller than the number of elements that we determine in the table. Therefore, large transactions are supported by many raw data points, while small transactions are supported only by a few raw data points. Within the optimisation process, this results in MRIOs representing large transactions with high reliability. However, small transactions are often subject to significant adjustments. Monte Carlo techniques can be used to show that the results of impact analyses remain stable [30].

We show this phenomenon in the calculation of the sectors' outputs from the MRIO. We can calculate outputs in input-output tables in two ways. One way is to calculate outputs by row sums, which represents the production of the intermediate demand for other sectors and the production for the final demand. Also, we can determine the output of a sector by the column sum of this sector. The column sum corresponds to the sum of all goods necessary for the production of one sector's goods, and the value added created by this sector.

Both ways should ideally come to the same result. Since the creation of an MRIO is an underdetermined optimisation problem, adjustments are necessary, which results in deviations. Fig. 1 shows, however, that our MRIO represents large transactions with high reliability and small transactions are subject to greater uncertainty. The impact analysis thus provides reliable results.

2.2. Preparation of desalination data

Data on desalination is scarce [31,32]. Wittholz et al. attempted to estimate the cost structures of desalination plants [33]. The Desalination Economic Evaluation Program (DEEP) model of the International Atomic Energy Agency is also a common model to estimate the cost structure of desalination plants [34]. For our analysis, we deployed data from Desaldata, a database with additional functions [35]. Desaldata offers the most detailed database we found. The cost estimator tool for estimating capital expenditure (capex) and operational expenditure (opex) structures as functions of several variables is also a part of the platform.

Desaldata contains data for 349 seawater desalination, brackish water and wastewater plants in Australia with capacities from 30 to 444,000 m^3/d. For our study, we used data for of the largest 20 seawater reverse osmosis desalination plants (SWRO) that cumulate to 95% capacity of all Australian seawater desalination plants with particular plant capacities from 4000 to 444,000 m^3/d (see Appendix 1). RO is the common desalination technology in Australia, and there is only a small number of other technologies like MED or MSF.

Even though Desaldata is the most detailed database we found, it is fragmentary and partially unreliable. Desaldata offers complete data for location, capacity, feedwater type, award date, and online date. Data of Engineering-Procurement-Construction (EPC) price, feedwater conditions, and power consumption were sketchy. We validated years of construction, capacity, capex, opex, and specific energy consumption by additional literature and adjusted the data if necessary (see Appendix 2). Thus, we were able to validate data for the largest eight plants with a cumulated capacity of 95.9% of all 20 analysed plants. For the residual plants with 4.1% of cumulated capacity, we used the raw results of Desaldata's cost estimator and adjusted capex sums by the database's value if available.

Desaldata's cost estimator tool provides a breakdown for opex and capex depending on different attributes such as location, salinity, temperature or energy consumption. If data for EPC prices were available, we used the capex cost estimator only for ratios of the cost structure. If EPC prices were not available, we used the capex cost estimation for the capex sum as well. We estimated seawater temperatures by yearly average temperatures of the nearest city [36]. We estimated electricity prices by the annual volume-weighted spot prices of states and territories in 2009 [37]. We used Western Australia's Short Term Energy Market (STEM) data for both Western Australia and the Northern Territory since data for the Northern Territory is not available [38]. The cost estimator is only capable of calculating costs for plant capacities larger than 8000 m^3/d. Hence, we used values of this plant to extrapolate cost structures of all smaller plants. The smaller plants account for only about 3.5% of the total investigated capacity. An over- or underestimation will therefore not significantly affect the overall outcome of the study. The cost estimator calculates in US$ currency, so we converted AU$ into US$ using exchange rates from International Monetary Fund [39]. We used 2009 as the base year for the initial cost estimation. We assumed a utilisation rate of 95% for all modelled plants. Even if some plants are currently unused because municipalities

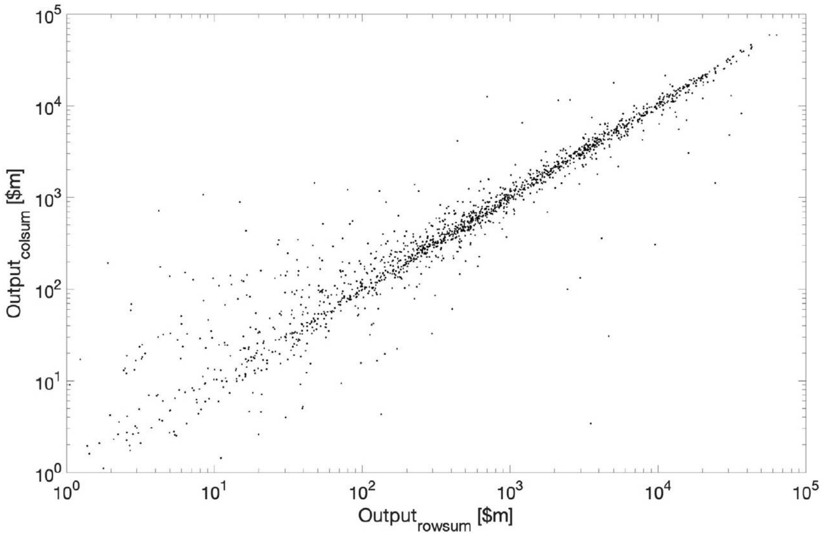

Fig. 1. Rocket plot of outputs calculated via row sum and column sum in 2015.

are currently not in water shortage (like Sydney or Melbourne), we also modelled these plants with a utilisation rate of 95%. Our research objective is not to focus on the reproduction of the most accurate costs of real operations, but rather quantify the carbon footprint of the plants when they produce their capability.

Finally, we estimated data for 20 plants, each of the plant covers twelve data points for capex and four data points for opex demand. The left diagram in Fig. 2 shows the input data for our analysis.

We calculated the final demand vectors as follows:

1. Construction of preliminary demand vectors $\mathbf{y_1}$ for opex and capex.
2. $\mathbf{y_2} = \mathbf{y_1} r^a$ converts the demand vector $\mathbf{y_1}$ from US$ into AU$ with the exchange rate r^a for year a. We applied the exchange rate of the online year for all capex vectors. We converted the opex vectors by the exchange rate of 2015.
3. We distribute capex and opex over the construction period. We prorated capex according to $\mathbf{y}_3^a = \frac{1}{n}\mathbf{y_2}$ for each year a with n as the number of construction years. We assumed only half of the capex investments in the first and the last year of construction works, so we apply $\mathbf{y}_3^a = 0.5\frac{1}{n}\mathbf{y_2}$ for the online and award year respectively. If we assumed a plant that was awarded in 2009 and went online in 2012, then n is 3 as award and online year respectively only gets a half year value. The vector $\mathbf{y_2}$ is distributed among n + 1 vectors $\mathbf{y_3}^\mathbf{a}$. For opex distribution, we applied $\mathbf{y_3}^\mathbf{a} = \mathbf{y_2}$ for each year after the online year. We assumed $\mathbf{y}_3^o = \frac{1}{2}\mathbf{y_2}$ for the online year o.
4. We inflated the demand vectors by $\mathbf{y_4} = \mathbf{y_3}\frac{p_s^a}{p_s^b}$, where $p_s{}^a$ is the producer price index for sector s of year a [40]. $p_s{}^b$ is the producer price index of the base year. The base year of capex vectors is the online year. For opex, we assumed 2015 as the base year.
5. We applied $\mathbf{y_5}^\mathbf{a} = \mathbf{C}\mathbf{y_4}^\mathbf{a}$ to expand the demand vectors of each year from a 1 × 15 to a 1 × 123 demand vector. $\mathbf{C}$ is a 123 × 15 concordance matrix.
6. Since we use an Australian MRIO, we separated the domestic vectors from (rest of the world) import vectors. We aggregated the compiled MRIO tables to the national level to compute the import quota vectors $\mathbf{q}^\mathbf{a}$ for each year a. The vector consists of $q_i{}^a$ for each sector i, defined by $q_i^a = \frac{\sum_{j=1}^{N} \mathbf{I}_{i,j}^a}{\sum_{j=1}^{N} \mathbf{U}_{i,j}^a}$. $\mathrm{I}_{i,\ j}$ is the import intermediate demand matrix and $\mathrm{U}_{i,\ j}$ the total intermediate demand matrix, composed as $\mathbf{U}_{i,\ j} = \mathbf{T}_{i,\ j} + \mathbf{I}_{i,\ j}$. $\mathbf{T}_{i,\ j}$ is the domestic intermediate demand aggregated to the national level. We calculated the domestic desalination demand vectors by $\mathbf{y_6}^\mathbf{a} = \mathbf{y_5}^\mathbf{a} \# \mathbf{q}^\mathbf{a}$, where # denotes elementwise multiplication. The import quota in our model was about 20% in average respective the different years and sectors.
7. As the last point, we expanded the demand vectors $\mathbf{y_6}^\mathbf{a}$ to the size of the MRIO-framework. For the regional allocation, we converted the geographical coordinates of the location of the desalination plants into SA2 classification. We placed the vector $\mathbf{y_6}^\mathbf{a}$ into the rows of the respective region and the columns of the respective year. The constructed opex and capex demand matrices $\mathbf{O_p}$ and $\mathbf{C_p}$ of each plant p have 1968 rows (MRIO size) and 11 columns (one column for each year). We aggregated all matrices to one final demand matrix $\mathbf{Y} = \Sigma_{p=1}{}^{20}\mathbf{O_p} + \Sigma_{p=1}{}^{20}\mathbf{C_p}$.

2.3. Calculation of the carbon footprint

Researchers widely use environmentally extended IOA for carbon footprints of individual products, processes, economic agents like companies or final consumers [41]. Pomponi and Lenzen demonstrate the superiority of using IOTs in a hybrid LCA approach over of using only bottom-up process-based data for LCA [23].

IOTs catch the industrial intermediate dependencies by linear functions. The linear approach causes basic assumptions: Industries have fixed input structures (linear production function), constant economies of scale and commodity prices are constant. Hence, we can interpret the cost structure as average variable costs rather than marginal costs. Furthermore, IOA is an ex-post analysis. Miller and Blair provide a well-detailed overview on IOA [42].

In IOA, we use Leontief's inverse to calculate the total impact of a demand on the output of an economy. We derive the inverse from the basic relationship between supply and demand. Suppose $\mathbf{x}$ as the M × 1 total output vector, $\mathbf{T}$ as the M × M intermediate demand matrix and $\mathbf{Y}$ as the M × N final demand matrix, then

$$\mathbf{x} = \sum_{j=1}^{M} \mathbf{T}_{i,j} + \sum_{j=1}^{N} \mathbf{Y}_{i,j}. \tag{1}$$

As the production recipe of the sectors, we can express the technical coefficient matrix $\mathbf{A}$ as

$$\mathbf{A} = \mathbf{T}\hat{\mathbf{x}}^{-1} \tag{2}$$

It follows from the preceding that

$$\mathbf{T} = \mathbf{A}\hat{\mathbf{x}}. \tag{3}$$

We can insert the preceding equation in Eq. (1) and rearrange to

$$\mathbf{x} = (\mathbf{I} - \mathbf{A})^{-1}\mathbf{Y} \tag{4}$$

as the basic formulation of Leontief, while

$$\mathbf{L} = (\mathbf{I} - \mathbf{A})^{-1} \tag{5}$$

is the Leontief inverse that captures all direct and indirect effects of demand $\mathbf{Y}$ on the output $\mathbf{x}$. The matrix $\mathbf{I}$ is the identity matrix. We extend the economic Leontief model by a satellite account of industrial carbon dioxide equivalent emissions $\mathbf{e}$ and calculate the direct emission intensities

$$\mathbf{q} = \mathbf{e}\hat{\mathbf{x}}^{-1}. \tag{6}$$

Furthermore, we obtain the direct and indirect effects captured in a matrix representing the multipliers for each sector-to-sector relationship from

$$\mathbf{m} = \hat{\mathbf{q}}\mathbf{L}. \tag{7}$$

The total carbon emissions of desalination throughout the entire value chain are finally captured by

$$\mathbf{E} = \hat{\mathbf{q}}\mathbf{L}\hat{\mathbf{y}}. \tag{8}$$

Row sums $\mathbf{r}$ of the matrix $\mathbf{E}$ result in carbon emissions referring to sectors and regions where they physically occur. Hence, row sums reflect the emitting sectors or regions, depending if we aggregate to sectors or regions. Column sums $\mathbf{c}$ will refer to desalination inputs and regions where emissions are accounted regarding consumption responsibility of the analysed desalination plant. We calculate row sums or the column sums by multiplying the Matrix E by sum vector i, which is a column vector with the number of rows according to matrix $\mathbf{E}$ with every element equal to 1.

$$\mathbf{r} = \mathbf{E}\,\mathbf{i}, \tag{9}$$

or

$$\mathbf{c} = \mathbf{i}'\,\mathbf{E}. \tag{10}$$

We aggregate the vectors by multiplying them with aggregators, so-called concordances $\mathbf{C}$.[1] The concordances are tailored to each aggregation and sum up the 1968 sectors to sectors or regions of research interest (e.g. classification of Australian states or desalination input commodities). For example, if the desalination plants emit 100 kt CO_2e, row sums of matrix $\mathbf{E}$ assign emissions to the region where the desalination plant is located respectively the input products, which the desalination plant directly demanded. Column sums assign the same 100 kt CO_2e emissions to the regions where the emissions effectively occur respectively to the sectors which physically emitted the

[1] For more information on using concordances, see supporting information in [24].

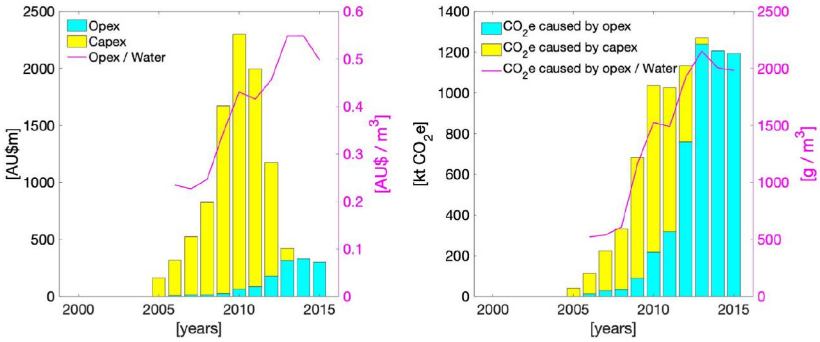

Fig. 2. Overview of costs and CO_2e emissions.

Table 1
Carbon emissions due to opex and capex of desalination in Australia.

Year	CO_2e effects caused by capex				CO_2e effects caused by opex			
	Direct effect	Indirect effect	Total effect	Multiplier	Direct effect	Indirect effect	Total effect	Multiplier
	[kt CO_2e]	[kt CO_2e]	[kt CO_2e]	[kt CO_2e/kt CO_2e]	[kt CO_2e]	[kt CO_2e]	[kt CO_2e]	[kt CO_2e/kt CO_2e]
2005	21	20	41	2.0	0	0	0	–
2006	50	48	99	2.0	8	5	13	1.7
2007	100	95	195	1.9	17	12	28	1.7
2008	158	141	299	1.9	19	13	32	1.7
2009	286	309	595	2.1	58	30	89	1.5
2010	375	445	820	2.2	155	62	217	1.4
2011	311	397	708	2.3	229	88	317	1.4
2012	159	216	375	2.4	544	215	759	1.4
2013	16	15	31	1.9	882	356	1239	1.4
2014	0	0	0	–	854	353	1207	1.4
2015	0	0	0	–	845	349	1193	1.4

greenhouse gases.

We get the final vectors as

$$\mathbf{v} = \mathbf{C}\,\mathbf{r}, \tag{11}$$

respectively

$$\mathbf{v} = \mathbf{c}\,\mathbf{C}. \tag{12}$$

For the production layer decomposition, we formulate the Leontief inverse as

$$\mathbf{L} = \mathbf{I} + \mathbf{A} + \mathbf{A}^2 + \mathbf{A}^3 + ...+\mathbf{A}^n. \tag{13}$$

We disaggregate the total carbon emission into several layers. $\mathbf{E_1} = \hat{\mathbf{q}}\mathbf{A}\hat{\mathbf{y}}$ results in emission for the first layer, defined as direct effects. $\mathbf{E_2} = \hat{\mathbf{q}}\mathbf{A}^3\hat{\mathbf{y}}$ gives emission for the second layer and so on. Each layer represents one supplier-stage of production. The first layer consists of carbon emissions from direct suppliers. The second layer shows carbon emissions of the supplier-suppliers.

3. Results and discussion

Desalination is an energy- and thus carbon-intensive technology for gaining fresh water. IOA methodology enables to uncover not only direct carbon emissions of desalination but also indirect effects along the entire value chain. The following section will present detailed insights into the carbon footprint of desalination in Australia over the years 2005 to 2015.

3.1. Cost and CO_2e emissions overview

Within the last 15 years, Australia has faced an extreme drought, mainly from 2003 to 2012. One consequence of this drought has been a political discussion about Australian's freshwater strategy. Desalination was used already before in a much smaller scale. However, facing this severe drought, several Australian cities, states, and firms have started huge investments in desalination plants.

The left axis curve of the left diagram in Fig. 2 shows domestic capex and opex expenditures from 2005 to 2015 in current year prices. The total expenditures reach their maximum in 2010 by AU$2.3 bn. Capex was the predominantly driver of the expenditures.

Average opex per produced water (right axis) increased within the 11 years from about AU$0.2 per cubic meter to AU$0.5 per cubic meter. Increasing energy costs mainly determine the growth of opex. The construction of different sized desalination plants within the analysed period also affects the growth of opex.

The bar graph (left axis) in the right figure shows the total carbon emissions (direct and indirect effects) due to operational and capital expenditures. We can see that CO_2e due to capex is predominant until 2011. After the main investment period, opex becomes predominant. In 2013, desalination emitted 1269 kt CO_2e mainly driven by opex. The right axis figure shows the total carbon emission per cubic meter of produced water, only determined by opex. We observed increasing opex per cubic meter up to 2000 g/m^3 at the end of the investigated period.

Table 1 shows the direct, indirect and total carbon emissions for the years 2005 to 2015 due to opex and capex. Construction activities determine capex while the operation of existing plants results in opex. In 2005, only capex was responsible for CO_2e emissions. As of 2012, opex was the driving force. During the construction phase, CO_2e emissions due to capex played a significant role with a peak of 820 kt CO_2e. These high carbon emissions focus on just a few years. The annual CO_2e emissions due to opex exceed the emissions of capex already in 2012 with 759 kt CO_2e. Due to the runtime of the plants over several decades, opex makes a significant contribution to the carbon footprint over its lifecycle. The last column shows the carbon multiplier c, that is defined

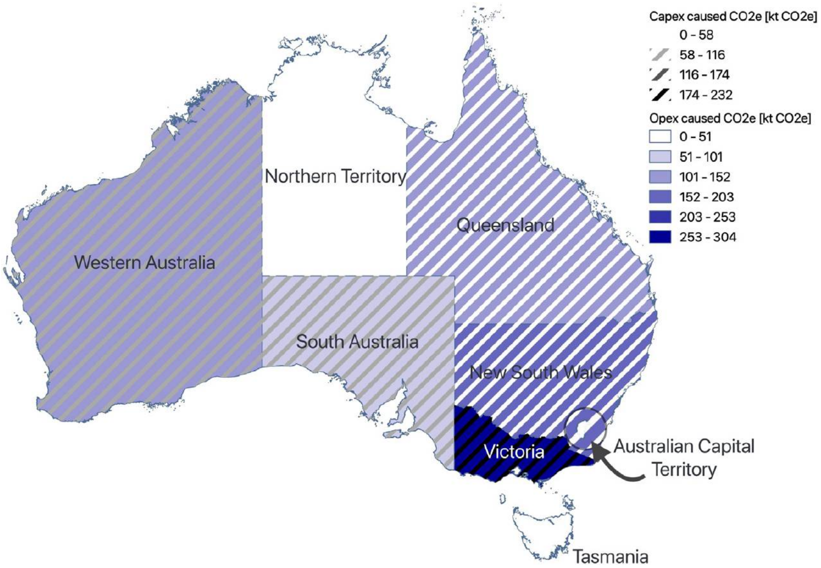

Fig. 3. CO_2e emissions by states and territories caused by capex and opex in 2012.

by $c = \frac{Q_{tot}^{a}}{Q_{dir}^{a}}$, with the total carbon emission $Q_{tot}{}^{a}$ and the direct carbon emission $Q_{dir}{}^{a}$ for the year a. Due to the larger multiplier of capex, we see that its supply chain has a more significant impact on CO_2e emissions than the supply chain of opex. Over the years, the multiplier of capex increases (except in 2013), while the multiplier of opex decreases. The higher the multiplier, the higher is the contribution of the upstream value chain to the overall effects. In conclusion, the value chain of the construction of desalination plants becomes more unsustainable over time, while the value chain of operations becomes more sustainable.

IOA with MRIOs is well suitable to uncover the spatial distribution of observed effects. In our study, we show the spatial distribution of carbon emissions. We can assign carbon emissions either to desalination inputs and locations of the plants or to emitting industries and emitting locations. Fig. 3 shows carbon emissions in 2012 due to capex and opex assigned to locations of the desalination plants. We created tables with eight regions representing the eight states and territories in Australia. In 2012, we can still observe a high level of construction activities, but also high expenses for operations. Australian Capital Territory and Tasmania do not operate desalination plants, so there is no carbon emission assigned. Northern Territory's desalination activity induces negligible emissions due to opex in 2012. In Queensland and New South Wales, we only find emissions due to opex. Western Australia and South Australia have emissions due to opex and capex on a medium scale. Victoria built the Victorian Desalination Plant from 2009 to 2012. Hence, the state is the leader in emission due to opex and capex in 2012.

Fig. 4 shows the total carbon emissions for 2005–2015. The four individual diagrams break down the emissions according to different systematics. We see that the emissions increase over time, dominated by capex in 2010. As of 2012, opex contributes significantly to carbon emissions.

In the left-hand diagrams, we assigned carbon emissions to emission-causing desalination inputs and locations of the plants. The diagrams on the right side show emitting industries and emitting locations. We compiled individual demand vectors for capex and opex so that we can illustrate the effects of opex and capex separately.

The diagram on the top left shows the carbon emissions assigned according to desalination inputs, each for capex and opex. The peak of capex caused emissions marks the boom in construction activities around 2010. Construction of inlets and outlets cause the main emissions. The second most considerable emission-causing input is the construction process of pipes. Both mainly require steel, which explains the high-level emissions. Opex-caused emissions mainly occur due to the demand for electricity as a direct input. At the end of the period, electricity causes almost all carbon dioxide. We aggregated all other inputs such as parts, chemicals and membranes for the sake of convenience. Since desalination plants usually operate for several decades up to 20 to 40 years, opex especially the energy source is the crucial point regarding environmental sustainability of desalination in the long run.

In the upper right chart, we can see which industry sectors emitted CO_2e due to the production of inputs, also divided into emissions caused by capex and opex. It is noticeable that even for capex demand the electricity sector emits a significant amount of CO_2e. The manufacturing sector is another key sector for carbon emissions during the construction phase, followed by the construction sector as the third largest emitter. As we have already discovered that the primary input of opex is electricity, it is not surprising that the electricity sector has the highest emissions. It indicates that the value chain of conventional energy plays a minor role in carbon emissions.

The graph at the bottom left shows the carbon emissions assigned to the desalination plant's locations, separated by capex and opex. Around the year 2010 Victoria caused the most substantial emissions due to capex, followed by South Australia. In the years around 2008, construction activities in New South Wales were a significant driver. In the following years after 2011, when the construction activities decline, opex becomes dominant for carbon emissions. Victoria has by far the most significant emissions of CO_2e, followed by Western Australia and New South Wales.

The diagram to the right shows in which states and territories CO_2e was emitted. At high trading volume, the graphs differ because consumption and production happen on different locations. Here we see that the diagrams are almost identical. Already in the diagrams above, we found for capex and opex that the electricity, gas, water and waste service sector dominates the carbon emissions. Even if Australia has a national electricity market, electricity trade between different states is at a low level. Western Australia and the Northern Territory are not even connected to the National Electricity Market [43].

Finally, we compiled a production layer decomposition (PLD)

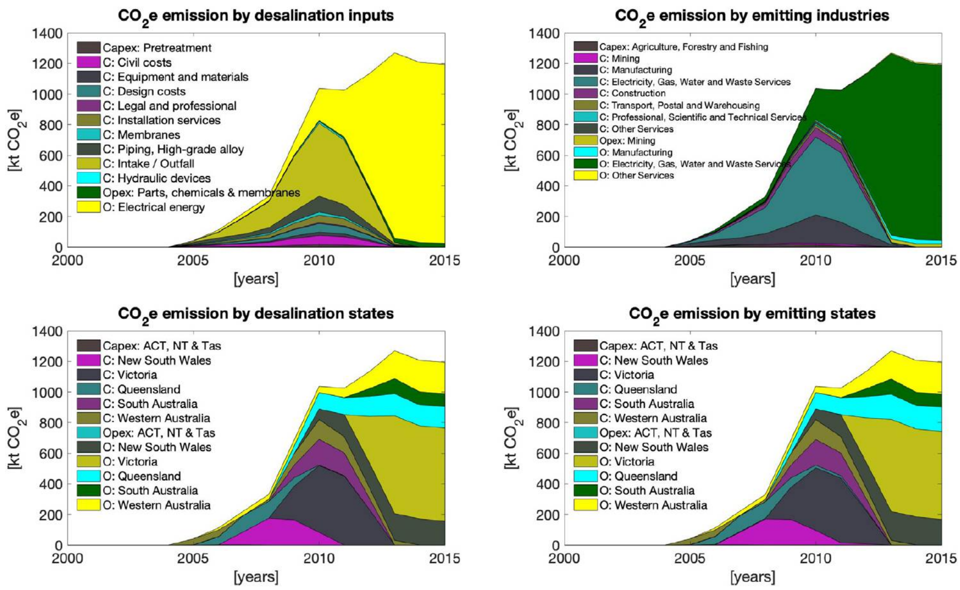

Fig. 4. CO_2e emission by desalination inputs and emitting industries.

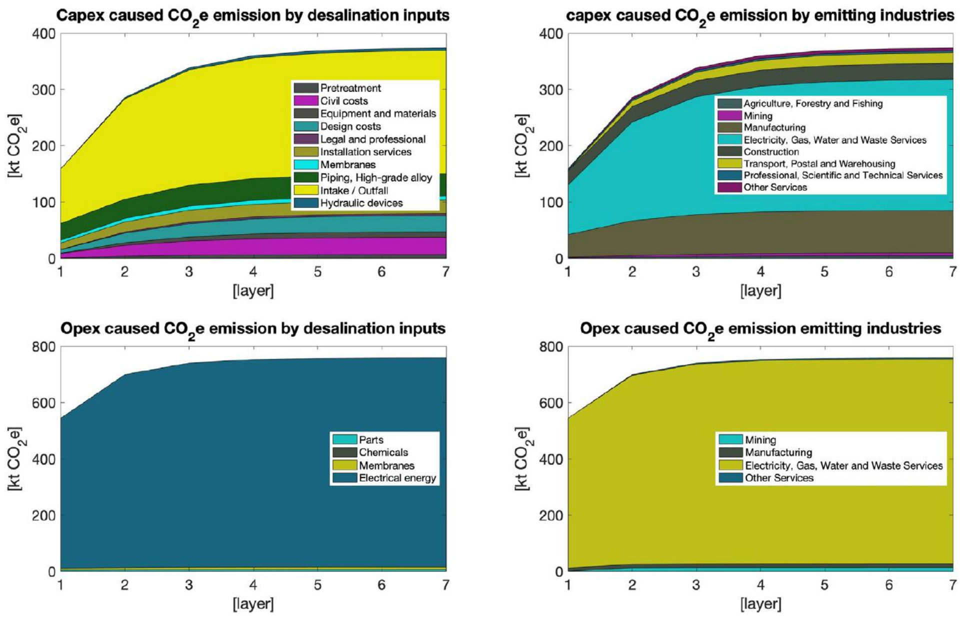

Fig. 5. Production layer decomposition for desalination inputs and emitting industries in 2012.

analysis for 2012. This approach determines the emissions for each production layer individually. Production layers are the several tiers within a value chain. We define the first layer as the direct effect. The direct effect accounts for carbon dioxide emitted by the direct supplier. Thus, the direct effect is the emission directly assigned to the desalination industry itself. The second layer is the supplier of the first supplier and so on. The Leontief inverse captures the whole supply chain with an infinite number of suppliers. Fig. 5 illustrates the results of the PLD Analysis for 2012 for desalination inputs and (left diagrams) and emitting industries (right diagrams). We see that a higher proportion of capex's emissions (compared to opex) occur in upstream stages of the value chain (lower diagrams). For opex, this means that the direct supplier already contributes a higher share to the total CO_2e emissions. The value chain is less critical for total emissions at opex than at capex. Generally, carbon emission mainly occurs within the first three to five layers. The following layers contribute with decreasing significance.

On the upper left diagram, we see that about two-thirds of capex carbon emission occurs due to the construction of intake and outfall. For intake and outfall, we note that the supply chain makes a higher contribution to total emissions than we can note e.g. for piping and high-grade alloy. On the upper right chart, we see how the supply chains of emitting sectors contribute to total emissions. The electricity sector mainly contributes in later layers, because the manufacturing industry sectors mainly use electricity as an input.

The situation is different at opex in the lower diagrams. In the left diagram, we can see the inputs of operating desalination plants. Electricity is the input factor, that is responsible for a significant share of total emissions. As a result, the electricity sector contributes a high proportion of its total emissions already in earlier stages, as we see on the right chart. The share that the sector emits as a supplier is higher than at capex.

4. Conclusion

Desalination is an energy-intensive technology. When powered by fossil fuel, high carbon emissions ensue. For our study, we have assumed that all seawater desalination plants are operated by conventional energy, even if Australia operates some plants with renewable energy. Economic requirements and population growth are the drivers of desalination and carbon emission in the first place. Carbon emissions from desalination occur first notably at the economic hot spots, especially in Victoria as the location of Australia's largest desalination plant. We want to point out that the results relate to CO_2e emissions in Australia. Our model does not cover the value chains of imports. According to the estimated import quotas of about 80% on average, we estimate that capex has covered about 80% of the emissions. Supplying countries emit additional greenhouse gases.

We show that policy must consider the entire supply chains to make desalination environmentally sustainable. Construction of intake and outfall is highly carbon-intensive within the construction period. In the construction phase, the electricity industry is the economic sector with the highest carbon emissions. The electricity sector becomes even more crucial for carbon emissions within the operation phase. The sector is not only the crucial point for carbon emissions due to direct demand, but the sector is also a key factor regarding intermediate demands throughout the entire value chain. This is made clear once again, as Australia's energy sector accounts for 35% of greenhouse gas emissions in 2012–2013 [44].

The electricity sector significantly outperforms its contribution to carbon emissions within the life cycle of desalination, compared to its national contribution of 35%. During the construction phase in 2010 (with simultaneous operation), the electricity sector accounts for 69% of all greenhouse gas emissions attributable to seawater desalination. In the pure operating phase in 2015, the share of carbon emissions of the electricity sector even accounts for 96% of the total emissions.

Substitution of fossil energies by renewable energies can thus be the game changer for the sustainability of desalination. Especially dry regions are affected by climate change. These regions are strongly dependent on seawater desalination. The use of desalination is only sustainable if it does not substantially emit more greenhouse gases. Policy must act and focus on the energy sector. The key is the transformation of the electricity sector and the change in the current energy mix with a drastic increase in the share of renewable energies.

In our following studies, we will analyse carbon effects if we substitute electrical energies by renewable sources. We will further study the social and economic effects of desalination.

Acknowledgements

This research was supported by Integrated Sustainability Analysis in the School of Physics at the University of Sydney. The Authors acknowledge financial support by the Department of Energy Engineering at Technical University of Berlin, the National eResearch Collaboration Tools and Resources project (NeCTAR) through its Industrial Ecology Virtual Laboratory. NeCTAR is an Australian Government project conducted as part of the Super Science initiative and financed by the Education Investment Fund. We finally acknowledge the Friedrich Naumann Foundation for Freedom. The authors appreciate the anonymous reviewers for their helpful comments and suggestions on the paper.

Appendix 1. Adjustment of the costs of seawater desalination plants

Desalination plant	Capacity [m^3/d]	Location	Award year	Online year
Victorian Desalination Plant	444,000	Victoria	2009	2012
Port Stanvac	274,000	South Australia	2009	2012
Sydney Desalination Plant (Kurnell)	250,000	New South Wales	2007	2010
Kwinana	143,700	Western Australia	2005	2006
Southern Seawater desalination plant	140,000	Western Australia	2009	2011
Sino Iron Ore Project, Cape Preston	140,000	Western Australia	2008	2012
Southern Seawater Desalination Plant (expansion)	140,000	Western Australia	2011	2013
Tugun (Gold Coast)	133,000	Queensland	2006	2009
Browse downstream engineering processes	10,560	Western Australia	2011	2012
Agnes Water Integrated Water Project	7500	Queensland	2008	2011
Bechtel Wheatstone construction	7500	Western Australia	2012	2012
Onslow	7500	Western Australia	2013	2013
Gorgon	7000	Western Australia	2010	2012
Curtis LNG Project	5000	Queensland	2010	2011
Jabiru	5000	Northern Territory	2006	2007
Bechtel Wheatstone compaction 2	4500	Western Australia	2011	2012
Onslow2	4500	Western Australia	2013	2013
Onesteel Whyalla Plant	4100	South Australia	2010	2011
Penrice	4050	South Australia	2005	2006
Fortescue Metals Group Port Headland	4000	Western Australia	2011	2012

Appendix 2. Adjustment of the costs of seawater desalination plants

#	Plant	Adjustment	Used sources
1	Victoria Desalination Plant (Melbourne)	Capacity and construction years not adjusted • Not adjusted Capex: • $1.8 bn (desaldata)	Capacity: https://www.aquasure.com.au/uploads/files/DesalinationProcessFactSheet-1482449673.pdf Capex: https://www.copyschool.com/wp-content/uploads/2014/09/Olex-Cables-Case-Studies.pdf

		• A$3.5 bn (2009) • Adjusted to US$3.908 bn (2012) Opex: • Net present value $2.602 bn, 27 years, intern 7.3%, assumption progression factor 3%, result: A$167 m (2009), US$162 m (2015), subtracted labour cost according to share of cost estimator, final result: US$128 m (2015) Electricity: • 4.8 kWh/m^3	https://www.dtf.vic.gov.au/sites/default/files/2018-01/Project-Summary-for-Victorian-Desalination-Project.pdf https://en.wikipedia.org/wiki/Victorian_Desalination_Plant#Cost https://www.water.vic.gov.au/_data/assets/pdf_file/0013/54202/Fact-sheet-project-costs-March-2015.pdf https://www.water.vic.gov.au/_data/assets/pdf_file/0013/54202/Fact-sheet-project-costs-March-2015.pdf Opex: https://en.wikipedia.org/wiki/Victorian_Desalination_Plant https://www.dtf.vic.gov.au/sites/default/files/2018-01/Project-Summary-for-Victorian-Desalination-Project.pdf Electricity: Email from operator watersure
2	Port Stanvac (Adelaide)	Capacity and construction years not adjusted Capex: • US$ 1.374 bn (desaldata) • Source AU$1.824 bn • Adjusted to AU$1.883 bn (2012) Opex: • Source AU$130 m (2010) • Adjusted to US$123 m (2015) Electricity: • 3.6 kWh/m^3	Capex: https://www.water-technology.net/projects/adelaide-plant/ http://www.acciona.com.au/projects/water/desalination-plants/adelaide-desalination-plant/ https://www.mcconnelldowell.com/markets/water-waste-water/42-adelaide-desalination-plant-project https://www.environment.sa.gov.au/topics/water/resources/desalination https://en.wikipedia.org/wiki/Adelaide_Desalination_Plant Opex: http://www.abc.net.au/news/2017-10-28/adelaide-desal-plant-too-big-and-too-expensive/9096046 http://www.abc.net.au/news/2010-12-01/130m-annual-cost-to-run-desal-plant/2358158 Electricity: http://www.awa.asn.au/AWA_MBRR/Publications/Water_e-Journal/SEAWATER_DESALINATION_A_SUSTAINABLE_SOLUTION_TO_WORLD_WATER_SHORTAGE_.aspx
3	Sydney Desalination Plant	Capacity and construction years not adjusted Capex: • US$865 m (desaldata) • Source AU$1.803 m (2010) • US$1.591 m (2010) Opex: • Own calculations of average from 2012 to 2017 cost at full production: AU$85.5 m (2012) • US$76 m (2015) Electricity: • Own calculations 3.6 kWh/m^3	Official reports: https://www.ipart.nsw.gov.au/Home/Publications Capex: https://ac.els-cdn.com/S0011916409004822/1-s2.0-S0011916409004822-main.pdf?_tid=772d2a54-cf01-4a98-a874-d046d29407f1&acdnat=1537779245_70eb5b6abda146143e7804e2640c58cb http://www.awa.asn.au/AWA_MBRR/Publications/Fact_Sheets/Desalination_Fact_Sheet.aspx https://link.springer.com/content/pdf/10.1007%2Fs11269-014-0901-y.pdf http://www.onlineopinion.com.au/view.asp?article=19874 Opex: https://www.ipart.nsw.gov.au/files/sharedassets/website/shared-files/pricing-reviews-water-services-metro-water-legislative-requirements-investigation-into-pricing-for-sydney-desalination-plant-pty-ltd-from-1-july-2017/final-report-sydney-desalination-plant-pty-ltd-review-of-prices-from-1-july-2017-to-30-june-2022.pdf https://www.ipart.nsw.gov.au/files/sharedassets/website/trimholdingbay/consultant_report_-_review_of_operating_and_capital_expenditure_by_sydney_desalination_plant_pty_ltd_-_halcrow_-_october_2011-_website_document.pdf Electricity: https://www.ipart.nsw.gov.au/files/sharedassets/website/shared-files/pricing-reviews-water-services-metro-water-legislative-requirements-investigation-into-pricing-for-sydney-desalination-plant-pty-ltd-from-1-july-2017/consultant-report-by-atkins-sydney-desalination-plant-expenditure-review-february-2017.pdf
4	Perth Seawater Desalination Plant	Capacity and construction years not adjusted Capex: • AU$347 m (desaldata) • Source AU$387 m (2007) • US$304 m (2006) Opex • Source AU$22.5(2006) • Adjusted to US$ 24 m (2015) Electricity: • 4.2 kWh/m^3	Capex: https://www.water-technology.net/projects/perth/ https://ac.els-cdn.com/S0011916409004822/1-s2.0-S0011916409004822-main.pdf?_tid=7f58ad1e-7572-4dbb-8969-98a20db72204&acdnat=1537799019_c48bd7caca98a56c8fb033b96743b013 https://www.watercorporation.com.au/about-us/news/media-statements/media-release/desalination-plant-per-kilolitre-cost-based-on-comprehensive-analysis Opex: https://www.water-technology.net/projects/perth/ https://www.watercorporation.com.au/about-us/news/media-statements/media-release/desalination-plant-per-kilolitre-cost-based-on-comprehensive-analysis http://pacinst.org/wp-content/uploads/2013/02/financing_final_report3.pdf http://www.ecosmagazine.com/?act=view_file&file_id=EC124p23.pdf Electricity: https://www.water-technology.net/projects/perth/ http://www.degremont.com.au/media/general/Perth_Seawater_

			Desalination_Plant_1.pdf https://ac.els-cdn.com/S0011916409004822/1-s2.0-S0011916409004822-main.pdf?_tid=7f58ad1e-7572-4dbb-8969-98a20db72204&acdnat=1537799019_c48bd7caca98a56c8fb033b96743b013 https://www.researchgate.net/publication/228491362_Low_energy_consumption_in_the_Perth_seawater_desalination_plant Construction: http://www.degremont.com.au/projects/perth-seawater-desalination-plant/ Electricity: https://en.wikipedia.org/wiki/Perth_Seawater_Desalination_Plant
5 & 7	Southern Seawater Desalination Plant (Perth)	Capacity not adjusted Online year of expansion adjusted to 2014 Capex: • desaldata: US$592 m first stage and US$471 m expansion • AU$955 m (first stage in 2011) • US$ 944 m (2011) • AU$450 m (expansion in 2013) • US$463 m (2013) Opex: • No data, we used cost estimator sum Electricity: • 4.0 kWh/m^3	Capex: https://www.water-technology.net/projects/southern-seawater-desalination-plant/ http://www.abc.net.au/news/2009-06-24/final-approval-for-sw-desalination-plant/1330958?site=news https://www.bunburymail.com.au/story/1253516/first-seawater-flows-into-binningup-desalination-plant/ https://www.water-technology.net/projects/southern-seawater-desalination-plant/ http://www.ancr.com.au/southern_seawater_desalination.pdf Construction: https://www.bunburymail.com.au/story/1253516/first-seawater-flows-into-binningup-desalination-plant/ https://www.water-technology.net/projects/southern-seawater-desalination-plant/ https://www.watercorporation.com.au/about-us/news/media-statements/media-release/southern-seawater-desalination-plant—expansion-project-update Electricity: http://www.epa.wa.gov.au/sites/default/files/EPA_Report/2797_Rep1302Desal_61008.pdf http://www.epa.wa.gov.au/sites/default/files/EPA_Report/2797_Rep1302Desal_61008.pdf
6	Sino Iron Project	Capacity and construction years not adjusted No further data found, we used data from desaldata without adjustments	Capacity: https://www.ide-tech.com/en/our-projects/cape-preston-desalination-plant/?data=item_1 Construction: https://www.ide-tech.com/en/our-projects/cape-preston-desalination-plant/?data=item_1
7	Gold Coast Desalination Plant	Capacity and construction years not adjusted Capex: • Desaldata: US$838 m (2009) • AU$1.12 bn (2009) • Desaldata is correct, no adjustment needed Opex: • Desaldata: • AU$1021 per megalitre (2012) at full capacity • Own calculations: AU$47 m (2012), US$42 m (2015) Electricity: • 3.6 kWh/m^3	Capex: https://www.advisian.com/en-gb/global-perspectives/the-cost-of-desalination https://en.wikipedia.org/wiki/Gold_Coast_Desalination_Plant https://www.water-technology.net/projects/gold-coast-plant/ Opex: https://www.advisian.com/en-gb/global-perspectives/the-cost-of-desalination http://www.qca.org.au/getattachment/8da7c759-06cf-462c-96df-de7bcbe29514/Seqwater-submission-Appendix-C.aspx http://www.parliament.qld.gov.au/Documents/TableOffice/TabledPapers/2015/5515T1824.pdf Electricity: https://www.water-technology.net/projects/gold-coast-plant/ https://www.water-technology.net/projects/gold-coast-plant/

References

[1] M.M. Mekonnen, A.Y. Hoekstra, Four billion people facing severe water scarcity, Sci. Adv. 2 (2016) 1–6, https://doi.org/10.1126/sciadv.1500323.

[2] WHO, UNICEF, Progress on drinking water and sanitation: 2012 update, http://www.wssinfo.org/fileadmin/user_upload/resources/JMP-report-2012-en.pdf, (2012).

[3] S. Lattemann, T. Höpner, Environmental impact and impact assessment of seawater desalination, Desalination 220 (2008) 1–15, https://doi.org/10.1016/j.desal.2007.03.009.

[4] United Nations Development Programme, Water Governance in the Arab Region: Managing Scarcity and Securing the Future, New York (2013).

[5] C.A. Scott, S.A. Pierce, M.J. Pasqualetti, A.L. Jones, B.E. Montz, J.H. Hoover, Policy and institutional dimensions of the water-energy nexus, Energy Policy 39 (2011) 6622–6630, https://doi.org/10.1016/j.enpol.2011.08.013.

[6] V.G. Gude, Desalination and sustainability - an appraisal and current perspective, Water Res. 89 (2016) 87–106, https://doi.org/10.1016/j.watres.2015.11.012.

[7] B.M. Haddad, A case for an ecological-economic research program for desalination, Desalination 324 (2013) 72–78, https://doi.org/10.1016/j.desal.2013.06.003.

[8] The World Bank, Renewable Energy Desalination. An Emerging Solution to Close the Water Gap in the Middle East and North Africa, (2012), https://doi.org/10.1596/978-0-8213-8838-9.

[9] R. Einav, K. Harussi, D. Perry, The footprint of the desalination processes on the environment, Desalination 152 (2003) 141–154, https://doi.org/10.1016/S0011-9164(02)01057-3.

[10] I. Muñoz, A.R. Fernández-Alba, Reducing the environmental impacts of reverse osmosis desalination by using brackish groundwater resources, Water Res. 42 (2008) 801–811, https://doi.org/10.1016/j.watres.2007.08.021.

[11] J. Liu, S. Chen, H. Wang, X. Chen, Calculation of carbon footprints for water diversion and desalination projects, Energy Procedia 75 (2015) 2483–2494, https://doi.org/10.1016/j.egypro.2015.07.239.

[12] A.A. Setiawan, Y. Zhao, C.V. Nayar, Design, economic analysis and environmental considerations of mini-grid hybrid power system with reverse osmosis desalination plant for remote areas, Renew. Energy 34 (2009) 374–383, https://doi.org/10.1016/j.renene.2008.05.014.

[13] F. Vince, F. Marechal, E. Aoustin, P. Bréant, Multi-objective optimization of RO desalination plants, Desalination 222 (2008) 96–118, https://doi.org/10.1016/j.desal.2007.02.064.

[14] J.J. Sadhwani, J.M. Veza, C. Santana, Case studies on environmental impact of seawater desalination, Desalination 185 (2005) 1–8, https://doi.org/10.1016/j.desal.2005.02.072.

[15] M.F.A. Goosen, H. Mahmoudi, N. Ghaffour, Today's and future challenges in applications of renewable energy technologies for desalination, Crit. Rev. Environ. Sci.

Technol. 44 (2014) 929–999, https://doi.org/10.1080/10643389.2012.741313.
[16] G. Raluy, L. Serra, J. Uche, Life cycle assessment of MSF, MED and RO desalination technologies, Energy 31 (2006) 2361–2372, https://doi.org/10.1016/j.energy.2006.02.005.
[17] Q. Zou, X. Liu, Economic effects analysis of seawater desalination in China with input–output technology, Desalination 380 (2016) 18–28, https://doi.org/10.1016/j.desal.2015.11.010.
[18] J. Stokes, A. Horvath, Life cycle energy assessment of alternative water supply systems, Int. J. Life Cycle Assess. 11 (2006) 335–343, https://doi.org/10.1065/lca2005.06.214.
[19] M.P. Shahabi, A. McHugh, M. Anda, G. Ho, Environmental life cycle assessment of seawater reverse osmosis desalination plant powered by renewable energy, Renew. Energy 67 (2014) 53–58, https://doi.org/10.1016/j.renene.2013.11.050.
[20] W.W. Leontief, Input-Output Economics, 1st ed., Oxford University Press, New York, 1966.
[21] S. Nagashima, Y. Uchiyama, K. Okajima, Hybrid input–output table method for socioeconomic and environmental assessment of a wind power generation system, Appl. Energy 185 (2017) 1067–1075, https://doi.org/10.1016/j.apenergy.2016.01.018.
[22] B. Corona, C. de la Rúa, G. San Miguel, Socio-economic and environmental effects of concentrated solar power in Spain: a multiregional input output analysis, Sol. Energy Mater. Sol. Cells 156 (2016) 112–121, https://doi.org/10.1016/j.solmat.2016.03.014.
[23] F. Pomponi, M. Lenzen, Hybrid life cycle assessment (LCA) will likely yield more accurate results than process-based LCA, J. Clean. Prod. 176 (2018) 210–215, https://doi.org/10.1016/j.jclepro.2017.12.119.
[24] M. Lenzen, A. Geschke, T. Wiedmann, J. Lane, N. Anderson, T. Baynes, J. Boland, P. Daniels, C. Dey, J. Fry, M. Hadjikakou, S. Kenway, A. Malik, D. Moran, J. Murray, S. Nettleton, L. Poruschi, C. Reynolds, H. Rowley, J. Ugon, D. Webb, J. West, Compiling and using input–output frameworks through collaborative virtual laboratories, Sci. Total Environ. 485–486 (2014) 241–251, https://doi.org/10.1016/J.SCITOTENV.2014.03.062.
[25] Australian Bureau of Statistics, Input Output Product Classification, ABS Catalogue No. 5215.0.55.001, Canberra, (2012).
[26] Australian Bureau of Statistics, Australian Statistical Geography Standard: Design of the Statistical Areas Level 2, ABS Catalogue No. 1216.0.55.003, Canberra, (2010).
[27] M. Lenzen, A. Geschke, A. Malik, J. Fry, J. Lane, T. Wiedmann, S. Kenway, K. Hoang, A. Cadogan-Cowper, New multi-regional input–output databases for Australia – enabling timely and flexible regional analysis, Econ. Syst. Res. 29 (2017) 275–295, https://doi.org/10.1080/09535314.2017.1315331.
[28] M. Lenzen, J.M. Rueda-Cantuche, A note on the use of supply-use tables in impact analyses, Stat. Oper. Res. Trans. 36 (2012) 139–152.
[29] M. Lenzen, B. Gallego, R. Wood, Matrix balancing under conflicting information, Econ. Syst. Res. 21 (2009) 23–44, https://doi.org/10.1080/09535310802688661.
[30] M. Lenzen, K. Kanemoto, D. Moran, A. Geschke, Mapping the structure of the world economy, Environ. Sci. Technol. 46 (2012) 8374–8381, https://doi.org/10.1021/es300171x.
[31] P. Glueckstern, History of desalination cost estimations, Proc. Int. Conf. Desalin. Costing, 2004.
[32] J.R. Ziolkowska, R. Reyes, Impact of socio-economic growth on desalination in the US, J. Environ. Manag. 167 (2016) 15–22, https://doi.org/10.1016/j.jenvman.2015.11.013.
[33] M.K. Wittholz, B.K. O'Neill, C.B. Colby, D. Lewis, Estimating the cost of desalination plants using a cost database, Desalination 229 (2008) 10–20, https://doi.org/10.1016/j.desal.2007.07.023.
[34] K.C. Kavvadias, I. Khamis, The IAEA DEEP desalination economic model: a critical review, Desalination 257 (2010) 150–157, https://doi.org/10.1016/j.desal.2010.02.032.
[35] Global Water Intelligence, Desaldata, Database, http://www.desaldata.com, (2016) , Accessed date: 1 February 2018.
[36] World Sea Temperature, World sea temperature, Database, https://www.seatemperature.org, (2018) , Accessed date: 20 January 2018.
[37] Australian Energy Regulator, Annual volume weighted average spot prices, https://www.aer.gov.au/wholesale-markets/wholesale-statistics/annual-volume-weighted-average-spot-prices, (2009) , Accessed date: 29 January 2018.
[38] Australian Energy Market Operator, Short term energy market data, http://data.wa.aemo.com.au/#stem-summary, (2009) , Accessed date: 1 February 2018.
[39] International Monetary Fund, Australian dollar exchange rates, https://www.imf.org/external/np/fin/ert/GUI/Pages/CountryDataBase.aspx, (2018) (accessed February 2, 2018).
[40] [dataset], Australian Bureau of Statistics, Producer Price Indexes, ABS Catalogue No. 6427.0, Canberra, (2017).
[41] T. Wiedmann, Editorial: carbon footprint and input-output analysis - an introduction, Econ. Syst. Res. 21 (2009) 175–186, https://doi.org/10.1080/09535310903541256.
[42] R.E. Miller, P.D. Blair, Input-Output Analysis: Foundations and Extensions, 2nd ed., Cambridge University Press, New York, 2009.
[43] Australian Energy Regulator, State of the energy market, Melbourne, https://www.aer.gov.au/publications/state-of-the-energy-market-reports/state-of-the-energy-market-may-2017, (2017).
[44] P. Wolfram, T. Wiedmann, M. Diesendorf, Carbon footprint scenarios for renewable electricity in Australia, J. Clean. Prod. 124 (2016) 236–245, https://doi.org/10.1016/j.jclepro.2016.02.080.

Glossary

capex: capital expenditure
CO_2e: carbon dioxide equivalents
DEEP: Desalination Economic Evaluation Program
EPC: Engineering-Procurement-Construction
IELab: Industrial Ecology Lab
IO: input-output
IOA: input-output analysis
IOPC: Input-Output Product Classification
IOT: input-output table
IAEA: International Atomic Energy Agency
LCA: life cycle assessment
KRAS: Konfliktfreies RAS
MED: multiple-effect distillation
MRIO: multi region input-output
opex: operational expenditure
PLD: production layer decomposition
RO: Reverse Osmosis
SA2: Statistical Area Level 2
STEM: Short Term Energy Market
WIOD: World Input Output Database

Environmental Research Letters

LETTER • OPEN ACCESS

Renewable-powered desalination as an optimisation pathway for renewable energy systems: the case of Australia's Murray–Darling Basin

To cite this article: Michael Heihsel *et al* 2019 *Environ. Res. Lett.* **14** 124054

IOP Publishing Environ. Res. Lett. 14 (2019) 124054 https://doi.org/10.1088/1748-9326/ab57ab

Environmental Research Letters

CrossMark

OPEN ACCESS

RECEIVED
1 August 2019

REVISED
7 October 2019

ACCEPTED FOR PUBLICATION
14 November 2019

PUBLISHED
11 December 2019

LETTER

Renewable-powered desalination as an optimisation pathway for renewable energy systems: the case of Australia's Murray–Darling Basin

Michael Heihsel[1,4], **Syed Muhammad Hassan Ali**[2], **Julian Kirchherr**[3] **and Manfred Lenzen**[2]

[1] Department of Energy Engineering, Technical University of Berlin, Berlin, Germany
[2] ISA, School of Physics, The University of Sydney, Sydney, New South Wales 2006, Australia
[3] Copernicus Institute of Sustainable Development, Utrecht University, Utrecht, The Netherlands
[4] Author to whom any any correspondence should be addressed.

E-mail: michael.heihsel@campus.tu-berlin.de

Keywords: renewable energy, desalination, climate change, load-shifting, water management

Supplementary material for this article is available online

Abstract

The ecology in the Murray–Darling Basin in Australia is threatened by water scarcity due to climate change and the over-extraction and over-use of natural water resources. Ensuring environmental flows and sustainable water resources management is urgently needed. Seawater desalination offers high potential to deliver water in virtually unlimited quantity. However, this technology is energy-intensive. In order to prevent desalination becoming a driver of greenhouse gases, the operation of seawater desalination with renewables is increasingly being considered. Our study examines the optimisation of the operation of a 100% renewable energy grid by integrating seawater desalination plants and pipelines as a variable load. We use a GIS-based renewable energy load-shifting model and show how both technologies create synergy effects. First, we analyse what quantity of water is missing in the basin in the long run. We determine locations for seawater desalination plants and pipelines to distribute the water into existing storages in the Murray–Darling Basin. Second, we design a pipeline system and calculate the electricity needed to pump the water from the plants to the storages. Third, we use the combined renewable energy load-shifting model. We minimise the total cost of the energy system by shifting energy demand for water production to periods of high renewable energy availability. Our calculations show that in such a system, the unused spilt electricity can be reduced by at least 27 TWh. The electricity system's installed capacity and levelised cost of electricity can be reduced by up to 29%, and 43% respectively. This approach can provide an annual net economic benefit of $22.5 bn. The results illustrate that the expansion of seawater desalination capacity for load-shifting is economically beneficial.

Abbreviations

GIS	Geographic information system
LCOE	Levelised cost of electricity
MDB	Murray–Darling Basin
MDBA	Murray–Darling Basin Authority
RE	Renewable energies
RO	Reverse osmosis
SDL	Surface-water diversion limit
SWRO	Seawater reverse osmosis

1. Introduction

The Murray–Darling Basin (MDB) is Australia's largest river catchment. The MDB includes about

30 000 wetlands and the multinational Ramsar Convention on Wetlands protects 16 of these wetlands (Forghani *et al* 2011). Between 1997 and 2009, Australia and especially the MDB suffered heavily from drought (Leblanc *et al* 2012). The MDB supplies about 20 million people with food (Forghani *et al* 2011), and Agricultural production in the MDB amounts to $24 bn (Murray–Darling Basin Authority 2019a). The natural habitat of many animal and plant species, and the agricultural economy are in danger (Crimp *et al* 2010) (Kirby *et al* 2014) (Kirby *et al* 2012) (Wittwer and Griffith 2011). Extreme and changeable climate conditions have intensified recently. Following the hottest December since records began, January 2019 marked the hottest month ever measured (Bureau of Meteorology 2019).

To fight the drought in the MDB, the Australian government passed the Water Act 2007 (The Parliament of Australia 2007). Based on this, the Murray–Darling Basin Authority (MDBA) published the Guide to the Proposed Basin Plan in 2010 (Murray–Darling Basin Authority 2010). In it, the MDBA stated that it plans to shorten the existing water allocation rights and thereby to increase natural flows (Connell and Grafton 2011). In a recently published study, Williams and Grafton (2019) have shown that the government's actions worth $3.5 bn to increase water flows in the MDB are failing.

Desalination has a high technical potential to provide large amounts of additional water. Since the millennium drought, every major city in Australia operates a seawater desalination plant (El Saliby *et al* 2009). Porter *et al* (2015) have shown that desalination can be a strategy for the economic development of arid coastal regions. Reverse osmosis (RO) is the leading desalination technology worldwide. With 3–5 kWh m^{-3}, RO is more energy-efficient than other thermal desalination technologies, which results in lower specific costs of less than $0.75 per m^3 (Bennett 2011) (Alhaj and Al-Ghamdi 2019a). Nevertheless, RO is an energy-, and therefore carbon-intensive technology when operated with conventional energy. When operated within the Australian grid, electricity causes over 90% of carbon emissions during operation (Heihsel *et al* 2019). Renewable energy (RE) thus solves a fundamental issue with desalination, rendering the process sustainable (The World Bank 2012) (Baten and Stummeyer 2013) (Ghaffour *et al* 2014). Despite its high ecological potential, only 1% of desalination water worldwide is produced using RE (Shahzad *et al* 2017). Market barriers for widespread use are high capital costs and uncertainty over optimal system integration strategies (Alhaj and Al-Ghamdi 2019b). A high proportion of RE in the electricity grid requires a completely different operational management (Olatomiwa *et al* 2016). Australia has a high potential for generating electricity from renewable resources. However, without corresponding operational management, the generation capacity is about three times larger than the current capacity in an almost exclusively conventional energy system (Lenzen *et al* 2016). Seawater desalination can buffer the volatility in renewable electricity production, which in turn is followed by economic benefits due to the reduction in generation capacity.

Some researchers and operators believe that RO should be operated in a steady state. However, membrane technology has evolved significantly in recent years. As a result, more flexible operation in a partial load range is possible without damaging membranes (Ghobeity and Mitsos 2010). Although the durability of the membranes will be reduced by intermittent operation, operating with antiscalant and rinsing reduces this effect significantly (Freire-Gormaly and Bilton 2018). Anyway, with 32%, electricity contributes significantly to the total cost of water production, while membranes account for just 4% of the total costs and they are becoming continually cheaper (the other cost components are 38% capital costs, 13% labour costs, 9% chemicals, and 4% other parts) (Ziolkowska 2015). To realise a flexible operation, desalination plants can be provided by a positive displacement pump with a variable frequency drive (Ghobeity and Mitsos 2010). Numerous studies show the feasibility of RO's direct operation with intermittent energies such as wind and sun (Li *et al* 2019) (Richards *et al* 2014) (Bognar *et al* 2013) (Richards *et al* 2011) (Park *et al* 2012) (Park *et al* 2011). Besides, practical examples show the feasibility of direct coupling of RO and RE and the associated variability of electricity (Desalination.biz 2017) (Augsten 2007).

For the first time, our study examines the economic benefits of coupling a large seawater desalination and pipeline system with a 100% RE grid within a Geographic Information System (GIS) based load-shifting model. At the same time, we introduce an entirely new approach to the water management of a large basin like the MDB. In doing so, we address a crucial problem of arid regions in the critical area of the water-energy-food nexus (Leck *et al* 2015) (Scanlon *et al* 2013) (Grubert and Webber 2015). This study is particularly relevant for water management and energy practitioners, such as government agencies and engineers. Furthermore, our study shows the potential for additional benefit from the coupling of both technologies. Policymakers can benefit from this knowledge regarding the implementation of regulatory frameworks.

2. Methods and data

2.1. A 100% renewable energy model[5]

We used a GIS-based electricity dispatch model with a geographic resolution of 90 × 110 grid boxes by Lenzen *et al* (2016). Within this model, we simulated a

[5] Please see supplementary material S1 for more details.

IOP Publishing Environ. Res. Lett. 14 (2019) 124054 Letters

sequential competitive bidding process that proceeds hourly over one year. In our dispatch optimisation model of the RE system, we simulated a spot market with competitive bidding. We optimised the cost of power generation sequentially and iteratively for every hour and every location. The algorithm proceeds by the following steps:

1. The generators supply the demand for every hour and every location grid box of the optimisation period. We rank all generators according to the lowest total cost for each hour and location separately. The total cost results from variable cost and fixed cost per MWh. Variable costs and fuel costs are data-based. We estimate fixed capital, maintenance and transmission costs for the first run.
2. After a run, the model recalculates the pre-run estimated fixed costs with the endogenously determined capacity factor. Based on these post-run costs, the algorithm calculates the total cost for each generator.
3. The algorithm adjusts the transmission network according to the new generator capacity and location.
4. We rank all generators based on cost efficiency over the entire optimisation period. We subsequently exclude inefficient generators.
5. The algorithm repeats the exclusion of inefficient generators while the reliability standard of 0.002% of the total demand complies.

Lenzen *et al* (2016) have provided a more detailed formal description of the optimisation approach.

2.2. The load-shifting algorithm

Our load-shifting algorithm is based on the work of Ali *et al* (2018), Ali *et al* (2019), and Keck *et al* (2019). Our concept of using the demand of seawater desalination for load-shifting has the following additional key benefits:

- Seawater reverse osmosis plants (SWRO) have a high electricity consumption which is available for load-shifting.
- The plants are utility-scale; in other words, they are centrally and simply controllable. They do not depend directly on a specific user behaviour. Thus, network operators can directly control them.
- Unlike electricity, water can easily and economically be stored in large reservoirs.

We integrated the load-shifting algorithm into the clean grid optimisation model from Lenzen *et al* (2016). We considered the electricity load of Australia as a non-shiftable load. We use the additional load of desalination and pipelines for the load-shifting procedure. The algorithm applies the locally and hourly optimised electricity system from Lenzen's clean grid as a starting point. The algorithm shifts demand from expensive generators to cheaper ones to utilise spilt energy. Spilt energy is the generated electricity which cannot be utilised due to missing demand at a specific time. It runs according to the following procedure:

1. We set a load-shifting period that determines a time range that the algorithm considers for the shifting. For our study, we considered shifting periods of 10 d, 30 d, and 90 d, respectively. The length of the periods is derived from the ability to store water in more extended periods. The computational requirement increases exponentially with the extension of the shifting period.
2. The variables of generated and spilt electricity are ranked separately.
3. The programme consequently shifts the demand within the load-shifting period from the generators with the highest cost to those with the lowest cost that produce spilt electricity. We determine the load-shifting potential **P** by

$$\mathbf{P} = \min[\mathbf{G}_{\text{inefficient}}(\mathbf{t} + \Delta t_s), \mathbf{S}_{\text{efficient}}(\mathbf{t}), \mathbf{D}(\mathbf{t} + \Delta t_s)], \quad (1)$$

where $\mathbf{G}_{\text{inefficient}}$ is the generation of the expensive generator, which we reduce. $\mathbf{S}_{\text{efficient}}$ is the spilt energy of the cost-efficient generator. **D** is the electricity demand of the SWROs that is available for shifting. The variable **t** determines each hour of the optimisation period. The period Δt_s is the shifting period. The algorithm considers every single hour within the shifting period.

4. The next step is to update the variables of the power generation to

$$\mathbf{G}^{\text{update}}_{\text{efficient}}(\mathbf{t}) = \mathbf{G}_{\text{efficient}}(\mathbf{t}) + \mathbf{P} \quad (2)$$

and

$$\mathbf{G}^{\text{update}}_{\text{inefficient}}(\mathbf{t} + \Delta t_s) = \mathbf{G}_{\text{inefficient}}(\mathbf{t} + \Delta t_s) - \mathbf{P}. \quad (3)$$

$\mathbf{G}_{\text{efficient}}$ is the electricity produced by the cost-efficient generators. $\mathbf{G}_{\text{inefficient}}$ is the electricity produced by reduced inefficient generators. The index update marks the adjusted variables.

5. As with the variables of electricity generation, we update the spilt energy variables resulting in

$$\mathbf{S}^{\text{update}}_{\text{efficient}}(\mathbf{t}) = \mathbf{S}_{\text{efficient}}(\mathbf{t}) - \mathbf{P} \quad (4)$$

and

$$\mathbf{S}^{\text{update}}_{\text{inefficient}}(\mathbf{t} + \Delta t_s) = \mathbf{S}_{\text{inefficient}}(\mathbf{t} + \Delta t_s) + \mathbf{P}. \quad (5)$$

Here, $\mathbf{S}_{\text{efficient}}$ is the spilt energy of the efficient generator, which is utilised by the shifted demand. $\mathbf{S}_{\text{inefficient}}$ is the spilt energy of the inefficient

IOP Publishing Environ. Res. Lett. 14 (2019) 124054 Letters

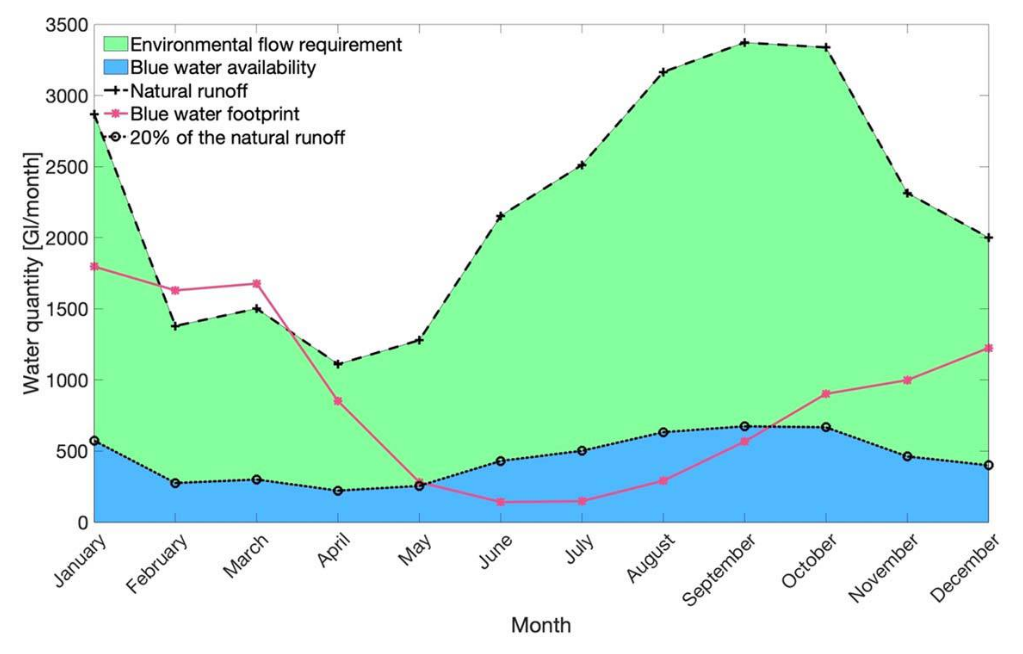

Figure 1. The water availability in the MDB according to (Hoekstra *et al* 2012); own depiction.

generator, which is increased by the shifting. The algorithm aims to supply the demand throughout the optimisation period by efficient generators alone. Consequently, we eliminate inefficient generators from the system.

6. Finally, we update the electricity demand **D** by the shifted reduction potential. We reduce electricity production by the reduction potential at time $(\mathbf{t} + \Delta t)$ and shift it to **t**, which is represented by

$$\mathbf{D}^{\text{update}}(\mathbf{t} + \Delta t_s) = \mathbf{D}(\mathbf{t} + \Delta t_s) - \mathbf{P} \tag{6}$$

and

$$\mathbf{D}^{\text{update}}(\mathbf{t}) = \mathbf{D}(\mathbf{t}) + \mathbf{P}. \tag{7}$$

We repeat from step 3 onwards for every hour and every demand location. The shifting ends when either the available demand **D** is completely shifted or when no more spilt energy is available. After the load-shifting programme has optimised all hours and locations, all inefficient generators that are no longer needed are removed from the system. Subsequently, we adjust the transmission system and the total demand.

2.3. Modelling the desalination energy demand

2.3.1. Total desalination water demand

The government's Guide to the Proposed Basin Plan (Murray–Darling Basin Authority 2010) demanded a total of between 3000 and 7600 Gl per year of recovered water in order to achieve the objectives of the Water Act 2007 (The Parliament of Australia 2007). For economic reasons, the MDBA recommended that no more than 4000 Gl should be recovered. In the end, the government agreed on only 2750 Gl (Murray–Darling Basin Authority (2012)).

Hoekstra *et al* (2012) have calculated the total runoff and the blue water footprint for the MDB, including the resulting available water according to the presumptive environmental standard (see figure 1) (Richter *et al* 2012) (Hoekstra *et al* 2011). During the months where demand exceeds supply, water should be added from outside the system. The water shortage is the difference between blue water availability and the blue water footprint. We calculated the difference for each month and added up all negative water budgets, which results in 6200 Gl. However, it is conceivable that from May to September when the budget is positive, water is stored to compensate for negative budgets in other months. In this way, the water shortage would amount to 5100 Gl. We calculated a weighted average of both values, with a slightly higher weighting of the lower limit (60%) which results in 5500 Gl.

2.3.2. Local water distribution

We estimated locations and capacities of desalination plants that pump the produced water into existing storages via a modelled pipeline system. Therefore, we used 31 MDBA government storages and data concerning their capacity and extended this with coordinates, altitudes and direct distances to the sea (Murray–Darling Basin Authority 2019b). We locally distributed the 5500 Gl of water in the MDB according to the relative demand of the areas. For this purpose, we followed the area delineation according to Murray–Darling Basin Authority (2018) and used the water demand data for the 29 areas. Pipelines supplied the desalinated water to storages in or near the area. Each storage was supplied by one or more pipelines. Each pipeline, in turn, supplied one or more storages. We have planned 29 sites for pipelines and desalination plants. We considered 35 pipelines, which were determined endogenously. The number of desalination plants has not been determined because only location and capacity are critical for the modelling.

Distributing the water to the pipeline locations required the following steps:

1. In a GIS analysis, we linked all storages to the areas in which they are located. If there was no storage in an area, we allocated the closest storage.
2. The pipelines temporarily supplied the storages with water. From the storages, the water was distributed to the areas. We created a $i \times j$ concordance **C**, which describes the supply links between the pipelines and the areas. The rows represent area i; the columns represent pipeline j. The concordance consists of ones and zeros. If pipeline j supplies water to area i, then $c_{ij} = 1$, otherwise $c_{ij} = 0$.
3. We determined the distribution of the water among the areas. For this, we used the data from the surface water diversion limit (SDL) Trial Water Take Account (Murray–Darling Basin Authority 2018). We calculated the average demand **d** of area i of the annual Take Account for the years 2012–13–2016–17. With these data, we calculated the percentage distribution **r** of the demand in area i by
$$\mathbf{r} = \frac{\mathbf{d}}{\sum_{i=1}^{29} \mathbf{d}}, \tag{8}$$
4. We calculated the capacity fraction **p** of the pipelines j,
$$\mathbf{p} = \frac{\mathbf{c}}{\sum_{j=1}^{29} \mathbf{c}}, \tag{9}$$
where the vector **c** is the capacity of the pipelines j resulting from the capacity of the supplied storages.
Each area i is supplied by one or more pipelines. The sum **s** of the capacity fractions for each area i results in
$$\mathbf{s} = \mathbf{C} * \mathbf{p}, \tag{10}$$
where the column vector **s** is the sum of the capacity fractions of the pipelines supplying each area i. In the next step, we modified the concordance **C** by placing the capacity fraction **p** of the pipeline j where $c_{ij} = 1$. Therefore
$$\tilde{\mathbf{C}} = \mathbf{C} * \hat{\mathbf{p}}, \tag{11}$$
where $\tilde{\mathbf{C}}$ is the modified concordance, and $\hat{}$ denotes the diagonalisation. For each $\tilde{c}_{ij}$, the capacity fraction of pipeline j that supplies area i was divided by the sum of the capacity fractions of all pipelines supplying area i, resulting in
$$\dot{\mathbf{C}} = \hat{\mathbf{s}}^{-1} * \tilde{\mathbf{C}}. \tag{12}$$

For each i, $\sum_{j=1}^{29} \dot{c}_{ij} = 1$ applies. So far, the concordance **C** merely indicated that an area receives water from a given pipeline. The normalised concordance $\dot{\mathbf{C}}$ indicates the percentage of water for each area i delivered by pipeline j.

5. We calculated the amount of water **w** supplied by pipeline j by multiplying the transposed normalised concordance $\dot{\mathbf{C}}'$ by the vector **r**, resulting in
$$\mathbf{q} = \dot{\mathbf{C}}' * \mathbf{r}. \tag{13}$$

The vector **q** indicates the percentage distribution of the water on the pipelines j. To distribute the total amount of water l to the pipelines, we calculated
$$\mathbf{w} = l * \mathbf{q}, \tag{14}$$
where **w** is the vector for the amount of water that each pipeline j supplies, and l is the total quantity of 5500 Gl of water. Figure 2 shows the MDB with the locations of the storages, the pipelines, the desalination plants, and the areas overlaid.

2.3.3. The electricity demand of the pipeline and desalination locations

We have iteratively optimised the pipelines' diameters based on their hydraulic head loss h_f. The iteration procedure is explained in more detail in the supplementary material S2, which is available online at stacks.iop.org/ERL/14/124054/mmedia. We limited the maximum diameter to 3.1 m[6]. If the diameter exceeded this limit, we added another pipeline to this location and split up the flow. The specific energy consumption e for each pipeline results in
$$e = \frac{\rho\, g\, (b + h_f)}{\eta_{\mathrm{tot}} * 3.6 * 10^6}, \tag{15}$$
where ρ represents the density of water, g the gravitational acceleration, b the altitude and η_{tot} the total efficiency of the motor and pump, with an assumed $\eta_{\mathrm{tot}} = 0.873$.

2.3.4. Electricity demand profiles

For the desalination plants, we assumed a specific electricity consumption of $e_{\mathrm{desal}} = 3.5\frac{\mathrm{kWh}}{\mathrm{m}^3}$, which corresponds to the average value for large SWROs (Heihsel *et al* 2019). Thus, we used the vector $\boldsymbol{e}$ with the specific electricity consumption for all pipelines to calculate the specific electricity demand $\mathbf{e}_{\mathbf{spec}}$ for each desalination/pipeline location by

[6] For comparison: the diameter of the Victorian desalination plant pipeline is 1.93 m (Aquasure 2015).

IOP Publishing Environ. Res. Lett. 14 (2019) 124054 Letters

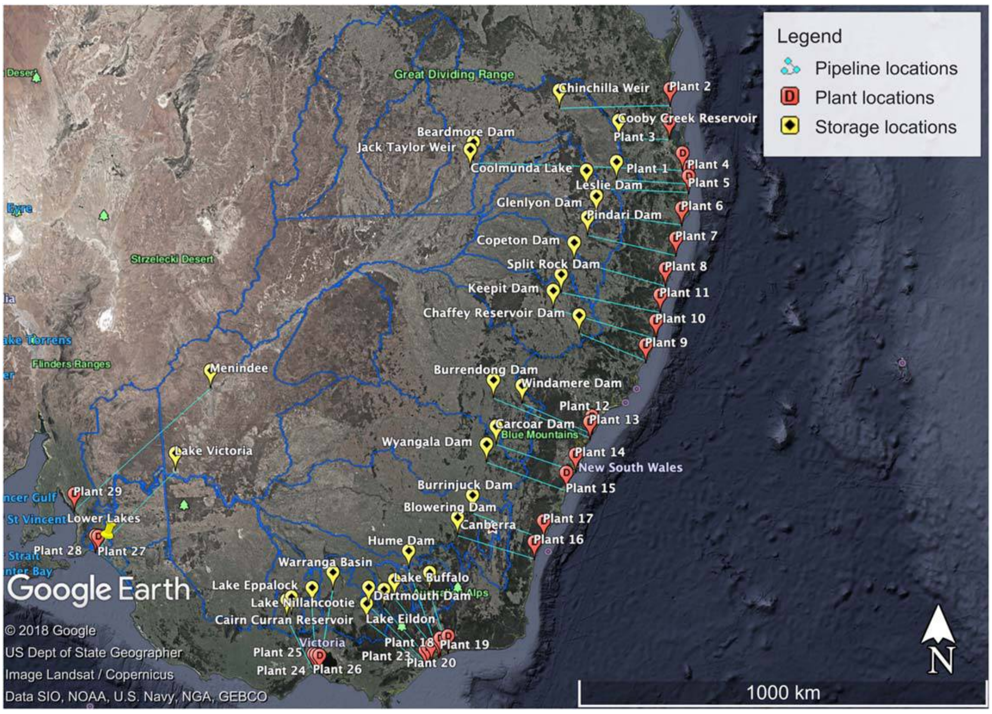

Figure 2. Locations of the storages, the desalination plants, the pipelines and the MDB areas.

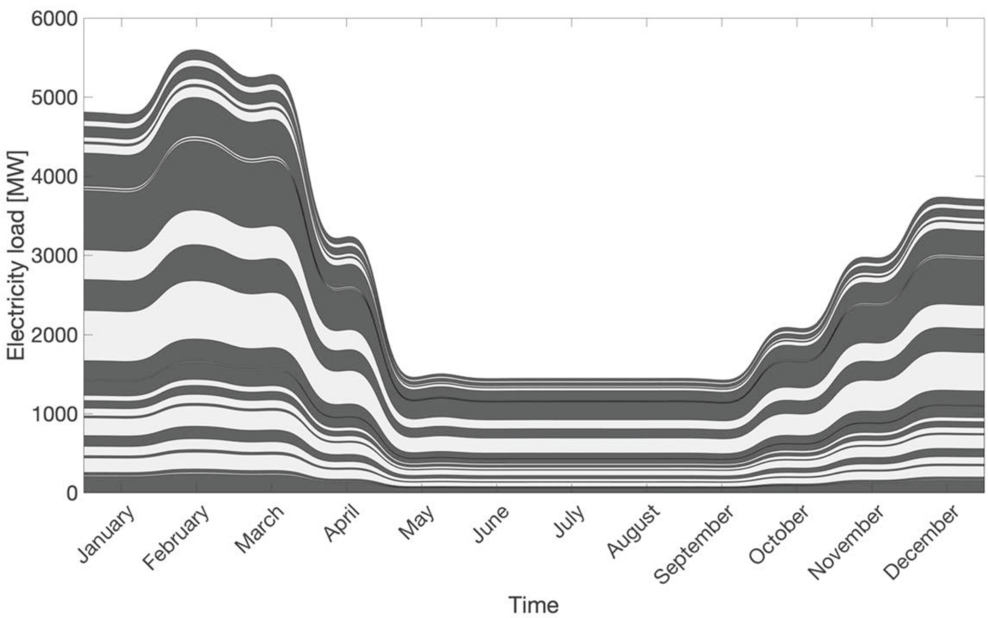

Figure 3. Monthly distributed electricity demand of the 29 combined pipeline and desalination locations.

$$\mathbf{e}_{\text{spec}} = e_{\text{desal}} + \mathbf{e}. \tag{16}$$

We get the vector with the total electricity demand $\mathbf{e}_{\text{tot}}$ for all locations by

$$\mathbf{e}_{\text{tot}} = \mathbf{e}_{\text{spec}} \# \mathbf{w} * 10^{-3}, \tag{17}$$

where $\mathbf{w}$ is the vector with the water demand of all pipelines from equation (14), and # denotes the elementwise multiplication. From monthly profiles of missing water in the MDB (Hoekstra *et al* 2012), we

IOP Publishing Environ. Res. Lett. 14 (2019) 124054 Letters

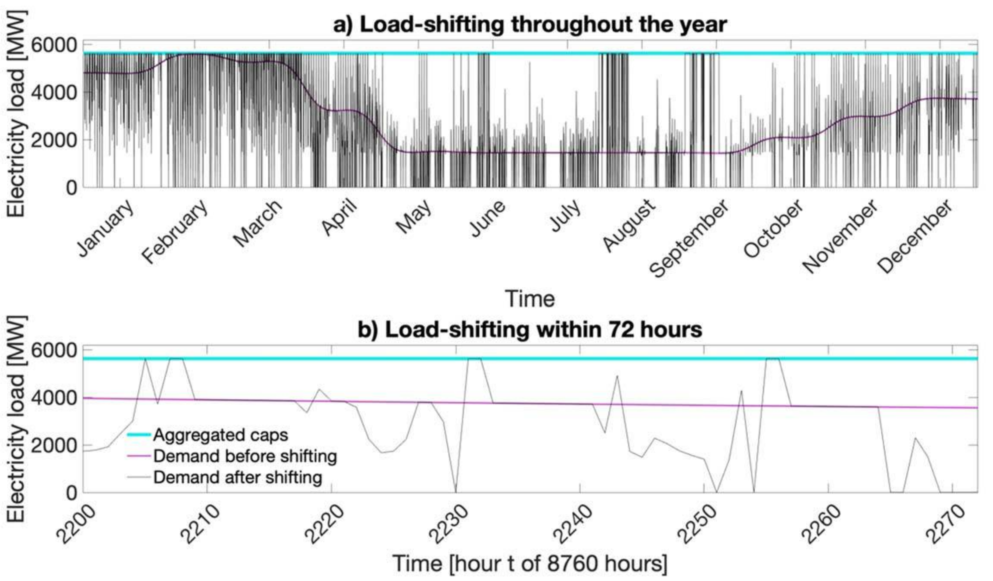

Figure 4. Aggregated electricity demand before and after the load-shifting process for the 10 d load-shifting period. Subplot (a) shows the entire observation period of one year. Subplot (b) shows a period of 72 h.

derived a monthly percentage distribution profile. In order to avoid huge production differences between individual months, we equally distributed a share of the total electricity demand over the year. We distributed 50% of the electricity demand (from equation (17)) as a constant baseload throughout the year, and the remaining 50% was distributed using the monthly percentage distribution profiles. Figure 3 shows the compiled and curve fitted load profiles. Finally, we used the 29 hourly resolved electricity demand profiles for the load-shifting analysis.

3. Results and discussion

3.1. Electricity demand-side implications

Subplot (a) of figure 4 shows the electricity demand of the ten-day load-shifting period scenario.[7] In the load-shifting program, we set demand caps (according to the oversize factor of 1.5) that specify the largest possible electricity demand for the desalination and pipeline spots (blue line). We note that the load-shifting algorithm exploits the maximum values especially in the Australian summer months (October—April). At the same time, the demand available for shifting is exploited to zero more extensively in the winter months.

We also recognise that the months around the Australian summer from October to April ('high-season months') dominate in demand before shifting. As a result of the load-shifting, the 'low-season months' from May to September were used more intensively for desalination. The considerable shifting period is possible in particular due to the large storage capacities in the MDB. The shift in water production from summer to winter thus allows more cost-effective production of water, as we can reduce the capacity of the power generation system.

Subplot (b) shows a typical load variation within 72 h for the 10 d load-shifting period. In our calculation, we did not limit the variability of ramp-ups and shut-downs. We analysed the variability of demand for load-shifting on a daily basis. For the load-shifting with a shifting period of 10 d, the median of the coefficient of variation of all days is 0.33. The largest value is 1.53, the smallest 1×10^{-16}. Although this shows a significant variability in the resulting demand, the variability is realistic for the real operation of seawater desalination plants (Freire-Gormaly and Bilton 2018) (Richards *et al* 2014) (Park *et al* 2012).

In figure 5, we see the monthly average shift by time of day. Positive values show the amount of electricity that was shifted to the specific hour of a month so that desalination plants utilise additional electricity at these points. A negative value shows that demand was reduced in this hour of the month. We recognise the shift in demand from summer to winter, which has already been discussed above, causing a seasonal balance of demand. The axis of hours shows a significant shift to the morning hours until early noon. This effect is strong around April and at the end of the year. Around 5 a.m. and 7 p.m., a systematic reduction of the resulting demand can be observed throughout the year. We explain this effect by the combination of high residual demand and low electricity supply, in particular from solar power. The negative peaks of the

[7] Please see supplementary material S3 for the results of the 30 and 90 d load-shifting periods.

IOP Publishing Environ. Res. Lett. 14 (2019) 124054 Letters

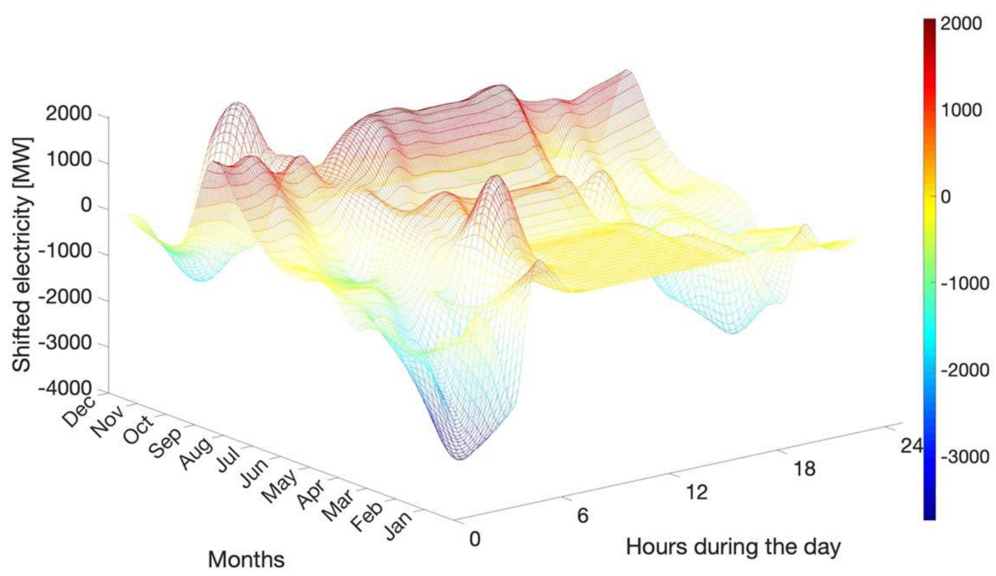

Figure 5. Average shifted load by month and daytime for the 10 d load-shifting period.

Table 1. Optimised electricity supply system after load-shifting with a 10 d period.

Fuel type	Capacity (GW)	Capacity share	Generation (TWh)	Generation share	Spillage (TWh)	Capacity factor
Hydro	3.7	2.7%	23.0	7.1%	0	71.1%
Biofuels	1.6	1.2%	5.0	1.5%	0	35.4%
Wind	42.7	31.7%	135.0	41.8%	13.4	39.7%
Utility PV	70.1	52.0%	119.1	36.9%	49.5	27.5%
CSP	12.3	9.1%	26.9	8.3%	9.5	33.8%
Ocean	0.21	0.2%	1.5	0.5%	0	83.6%
Geothermal	0.1	0.1%	0.7	0.2%	0	80.3%
Rooftop PV	4	3.0%	11.7	3.6%	0	33.5%
Total	135	100%	**322.9**	100%	**72.3**	**33.5%**

shifting are higher than the positive peaks. This effect stems from the limitation of maximum demand by caps. At the same time, this shows that the use of higher permissible demand could have a positive effect on the electricity system. In conclusion, we find that the ability to move demand both seasonally and across the hours of the day is useful for optimising the energy system.

3.2. Electricity supply-side and cost-implications

Table 1 provides an overview of the electricity supply resulting from load-shifting with a period of 10 d. Here, the total electricity generation capacity is 135 GW. We see that utility PV holds the highest share with 70.1 GW of generation capacity, which equates to 52% of the total capacity. The energy generated by utility PV (and utilised by the demand i.e. which is not spilt) is 119.1 TWh, which is only 36.9%. Wind energy has the largest share here, with 135.0 TWh and a share of 41.8%—the higher value for generated energy results from the fact that wind energy is the most continuous, compared to other volatile energy carriers. Therefore, wind energy can also achieve the relatively high capacity factor of 39.7%. Although energy sources with continuous availability such as ocean power have a very high capacity factor of up to 83.6%, they have minimal expansion potential.

Furthermore, wind energy, which contributes the largest share to the amount of electricity generated, has a relatively small amount of spilt energy itself. Only 13.4 TWh of the produced wind energy is lost. By way of comparison, utility PV generates 49.5 TWh of spilt energy. Thus, not even 9% of electricity produced by wind is spilt energy, whereas utility PV reaches 29%; The high value of the spilt PV energy, which is still prevalent even after the load-shifting, illustrates the range of PV electricity availability. High electricity supply with low demand prevails in many periods. Wind energy, on the other hand, is much more congruent with demand. If a load-shifting is performed, the spilt energy can thus be reduced by at least 27 TWh. If we increase the load-shifting period to 30 d and 90 d, the necessary generation capacity decreases to 122.5 GW and 114.5 GW respectively. Overall, desalination load-

IOP Publishing Environ. Res. Lett. 14 (2019) 124054 Letters

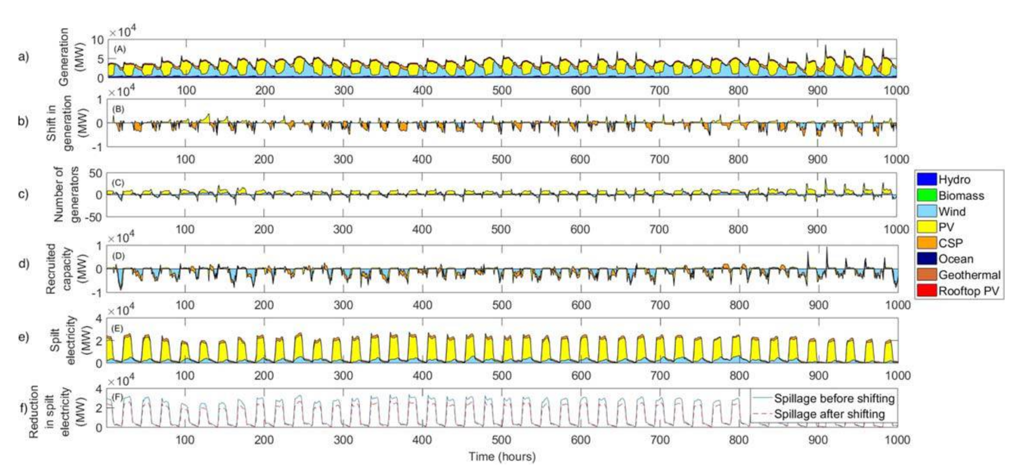

Figure 6. Electricity supply after the load-shifting process for a 10 d load-shifting period. With (a) generation, (b) shifted electricity, (c) number of shifted generators, (d) change in recruited capacity, (e) spilt electricity, (f) reduction in spilt electricity.

shifting can reduce the installed capacity and levelised cost of electricity (LCOE) by up to 29%, and 43%, respectively (see supplementary material S3 and S4 for further details).

Figure 6 presents the change in the electricity supply after load-shifting for a range of 1000 h. Subfigure (a) shows the structure of electricity generation. Utility PV is dominant among the generators. During the nights, wind power produces electricity, whereas during the days, utility PV dominates electricity production. Subfigure (b) shows the shifted generation. Positive values mean that electricity demand is shifted to the respective hour. Negative values indicate hours where electricity is no longer utilised. We can see that the load-shifting program has systematically replaced CSP and partially replaced wind with cheaper utility PV.

Subfigure (c) shows the change in the number of generators dispatched for electricity production after the load-shifting process. Subfigure (d) illustrates the recruited capacity of these generators. A negative recruited capacity means that the capacity utilised before the load-shifting is no longer needed at this hour. The program shifted the respective loads from more expensive to less expensive generators. At the end of an optimisation run, unused expensive generators are removed from the network.

Subfigures (e) and (f) visualise the spilt electricity. Figure (e) shows that a significant proportion of the spilt electricity comes from utility PV. Wind power, on the other hand, has a much smaller amount of spilt electricity. Now it becomes clear that on the one hand, the load-shifting program replaces wind power with PV; on the other hand, it shifts the demand so as to utilise more PV to reduce the total cost of the system. Figure (f) shows how the load-shifting optimises the generation structure. Hence, the peaks of spilt energy were reduced significantly. The results show that wind and solar complement each other under Australian conditions. The peaks of PV occur during the day, while the peaks of wind occur mostly at night. The use of CSP can further flatten the supply by the use of heat storages. Therefore, we recommend a mixed application of these technologies when combining with desalination.

3.3. Estimation of additional costs and benefits[8]

In the following, we estimated the benefits and costs directly related to the load-shifting. When load-shifting is applied, less power generation capacity is needed compared to the situation where no load-shifting would be applied. Hence, we define the additional benefit as saving in the total cost of electricity generation. We define the direct costs related to the load-shifting by the necessary increase in the desalination capacity. Our approach is a simple static analysis. Hence, we do not consider dynamic price changes or indirect effects, such as social effects. We provide further details on the assumptions and the calculation in the supplementary material S5. With applied load-shifting, the LCOE of power generation was 11.3–13.5 ct kW^{-1} h^{-1}. Without load-shifting, LCOE was 20 ct kW^{-1} h^{-1}. With the LCOEs and the respective total electricity quantities, we calculated the total costs of electricity generation for both the load-shifting scenarios and the basic scenario without load-shifting. The difference between the total costs of electricity results in an average gross economic benefit of $24.6 bn per year. This cost saving is made possible by not operating desalination plants continuously but providing their demand flexibly for load-shifting purposes. In our study, we applied an oversize factor of 1.5; in other words, the desalination and pipeline capacity were 50% higher than in a baseload scenario

[8] Explanations of the methodology and assumptions can be found in the supplementary material at S5.

for continuous operation throughout the year. To calculate the additional costs of the desalination plants and the pipelines, we used specific capital costs from IAEA (2013) and Bluefield Research (2018), respectively. Oversizing desalination plants results in an additional annuity of \$1.27 bn. The expansion of pipeline capacity leads to an additional annuity of \$809 m. In conclusion, considering desalination demand for load-shifting under the given assumptions promises high net economic benefits of \$22.5 bn, which is 35% of the total cost of electricity in the no-shifting scenario.

3.4. Challenges and global prospects

Recently, we see a growing awareness of climate change worldwide. Movements, such as the protests movement of 'Fridays for Future', are pushing governments to take more determined action. The electricity sector plays a key role for a climate-neutral economy (Wolfram *et al* 2016), but a high proportion of RE in the electricity sector requires a fundamentally different network operation (Olatomiwa *et al* 2016). The slow implementation of RE technologies in Australia, although with very high meteorological potential, is a major obstacle to implementing these strategies. The slow adaptation, as well as the historically high dependence on coal, currently lead to a carbon lock-in of the Australian economy (Unruh 2000).

When implementing seawater desalination on this scale, other environmental effects must be considered. The impacts of brine discharge on the marine environment continue to be the subject of controversial research discussions (Darwish *et al* 2013) (Zhou *et al* 2014) (Mannan *et al* 2019) (Saeed *et al* 2019). However, in a recent large-scale ecological impact study, Clark *et al* (2018) have demonstrated that the effects of brine in seawater desalination are significantly smaller than previously thought. Furthermore, Seawater desalination is still costly, but the cost of technology has decreased significantly in recent decades. New research in the field of graphene for desalination shows that the energy efficiency of seawater desalination could once again decrease by a factor of more than 10 (Aghigh *et al* 2015). Through international agreements such as the Paris Agreement, countries worldwide will increasingly implement climate policy measures, whereby RE will become competitive by pricing CO_2.

In our study, we demonstrated the advantages of the combination of desalination plants, pipelines and RE. The calculated 35 pipelines with an average diameter of 2.1 m are an enormous challenge to build. Twenty-four locations can be supplied with just one pipeline each, two locations require two pipelines each, and one location requires three pipelines. An adaptation of the operational management, e.g. by pursuing a more continuous operation, would provide opportunities to reduce the number of pipelines at individual sites. We are aware of the magnitude of the idea of building seawater desalination plants with a capacity of 5500 Gl per year for the MDB. Cutting edge practice and research worldwide show that projects on this scale are a realistic option in the battle against drought: The Israeli government plans to save the drought-threatened Sea of Galilee with seawater desalination (The Economist 2018). To do this, they want to increase their desalination capacity and pump water from the Mediterranean Sea to the Sea of Galilee. At the World Water Conference 2019, the idea of a 'climate correction project' was presented (Stiftung Forschung für Leben 2019). The idea applies seawater desalination with RE to keep the rising sea level constant in the context of climate change. At the same time, according to this idea, water should be pumped into dry regions to increase vegetation and simultaneously to counteract climate change.

4. Conclusion

Our study focusses on two global challenges: First, global areas of arid regions are growing due to climate change. Second, the majority of the world community has agreed on ambitious CO_2 reductions for the coming decades, which should limit global temperature increases to 1.5 °C. This study proposes a combined solution of seawater desalination with RE. For this, we modelled a desalination and pipeline system to provide water for the MDB. RE contribute to making desalination plants sustainable. At the same time, desalination serves as a variable load, which reduces the generation capacity of RE plants and therefore, the cost of the system. With our approach, the generation capacity of the electricity system can be reduced by more than 29%. We achieve net annual cost savings of more than \$22.5 bn, which equates to 35% of the total cost of electricity in the no-shifting scenario. Desalination is particularly suitable for load-shifting, because storing water for a longer period is affordable and technically feasible.

Our study showed how available flexible loads in a 100% RE system can significantly reduce the installed capacity. We demonstrated how sun and wind energy complement each other when coupling with desalination. Instead of operating with only one energy source, a mix of both is preferable. Furthermore, loads are advantageous, which can be shifted both, within a day and between seasons. However, the policy needs to create regulatory frameworks that price the external costs of carbon emissions and water extraction and distribute the benefits of load-shifting to the shiftable loads, i.e. desalination and pipeline operators, creating incentives to provide the necessary variable loads. Given the continuing aridity, the MDBA should limit the water extraction in the short term (in the 5500 Gl range) to increase environmental flows. In the medium term, water prices for extracted water should be increased (e.g. through taxes) in order to ensure sustainable water use. In the long term, the collected taxes can be used to expand RE, desalination plants and pipelines.

Nonetheless, our study is limited to investigating the immediate interaction of RE and desalination plants. Our study does not analyse environmental, economic and social factors or compile a comprehensive cost-benefit analysis. We also do not compare with alternative water supply options, such as wastewater reuse or reducing water consumption. Even though these options are essential for the entire Australian water supply, we show a solution that is able to provide large volumes of water in dry coastal regions. We will investigate social, environmental and economic factors in detail in further research.

Acknowledgments

We thank Professor Dr Frank Behrendt from the Department of Energy Engineering of the Technical University of Berlin for his continuous support. This work was financially supported the Friedrich Naumann Foundation for Freedom. We acknowledge support by the German Research Foundation and the Open Access Publication Fund of TU Berlin. Finally, we also thank the anonymous reviewers for the valuable comments, which have improved this study.

Data availability statement

The data that support the findings of this study are available from the corresponding author upon reasonable request.

References

Aghigh A, Alizadeh V, Wong H Y, Islam M S, Amin N and Zaman M 2015 Recent advances in utilization of graphene for filtration and desalination of water: a review *Desalination* **365** 389–97

Alhaj M and Al-Ghamdi S G 2019a Integrating concentrated solar power with seawater desalination technologies: a multi-regional environmental assessment *Environ. Res. Lett.* **14** 74014

Alhaj M and Al-Ghamdi S G 2019b Why is powering thermal desalination with concentrated solar power expensive? assessing economic feasibility and market commercialization barriers *Sol. Energy* **189** 480–90

Ali S M H, Lenzen M and Huang J 2018 Shifting air-conditioner load in residential buildings: benefits for low-carbon integrated power grids *IET Renew. Power Gener.* **12** 1314–23

Ali S M H, Lenzen M and Tyedmers E 2019 Optimizing 100%-renewable grids through shifting residential water-heater load *Int. J. Energy Res.* **43** 1479–93

Aquasure 2015 *Victorian Desalination Project Fact Sheet—Pipeline and Power Supply* (https://aquasure.com.au/pipeline-powerline)

Augsten E 2007 Desalination by means of wind and sun *Sun Wind Energy* (https://sunwindenergy.com/system/files/swe_0702_032-037_desalination.pdf)

Baten R and Stummeyer K 2013 How sustainable can desalination be? *Desalination Water Treat.* **51** 44–52

Bennett A 2011 Cost effective desalination: innovation continues to lower desalination costs *Filtr. Sep.* **48** 24–7

Bluefield Research 2018 *Relative Piping Costs* (Boston, MA) (https://wateronline.com/doc/water-and-wastewater-pipeline-infrastructure-opportunities-0001)

Bognar K, Pohl R and Behrendt F 2013 Seawater reverse osmosis (SWRO) as deferrable load in micro grids *Desalination Water Treat.* **51** 1190–9

Bureau of Meteorology 2019 Monthly Weather Review (http://bom.gov.au/climate/mwr/)

Clark G F, Knott N A, Miller B M, Kelaher B P, Coleman M A, Ushiama S and Johnston E L 2018 First large-scale ecological impact study of desalination outfall reveals trade-offs in effects of hypersalinity and hydrodynamics *Water Res.* **145** 757–68

Connell D and Grafton R Q 2011 Water reform in the Murray–Darling basin *Water Resour. Res.* **47** W00G03

Crimp S J, Stokes C J, Howden S M, Moore A D, Jacobs B, Brown P R, Ash A J, Kokic P and Leith P 2010 Managing Murray–Darling basin livestock systems in a variable and changing climate: challenges and opportunities *Rangel. J.* **32** 293–304

Darwish M, Hassabou A H and Shomar B 2013 Using seawater reverse osmosis (SWRO) desalting system for less environmental impacts in Qatar *Desalination* **309** 113–24

Desalination.biz 2017 Chile project envisions multiple mining clients for solar-powered SWRO *Desalination.biz* (https://desalination.biz/news/3/Chile-project-envisions-multiple-mining-clients-for-solar-powered-SWRO/8761/)

El Saliby I, Okour Y, Shon H K, Kandasamy J and Kim I S 2009 Desalination plants in Australia, review and facts *Desalination* **247** 1–14

Forghani A, Alexandra J and Donaldson J 2011 *Spatially Enabled MDBA* (Canberra) (http://csdila.unimelb.edu.au/BeyondSpatialEnablement/pdf/Forghani.pdf)

Freire-Gormaly M and Bilton A M 2018 Experimental quantification of the effect of intermittent operation on membrane performance of solar powered reverse osmosis desalination systems *Desalination* **435** 188–97

Ghaffour N, Lattemann S, Missimer T, Ng K C, Sinha S and Amy G 2014 Renewable energy-driven innovative energy-efficient desalination technologies *Appl. Energy* **136** 1155–65

Ghobeity A and Mitsos A 2010 Optimal time-dependent operation of seawater reverse osmosis *Desalination* **263** 76–88

Grubert E A and Webber M E 2015 Energy for water and water for energy on Maui Island, Hawaii *Environ. Res. Lett.* **10** 64009

Heihsel M, Lenzen M, Malik A and Geschke A 2019 The carbon footprint of desalination: an input–output analysis of seawater reverse osmosis desalination in Australia for 2005–2015 *Desalination* **454** 71–81

Hoekstra A Y, Chapagain A K, Aldaya M M and Mekonnen M M 2011 *The water footprint assessment manual—setting up the global standard* (London) (https://waterfootprint.org/media/downloads/TheWaterFootprintAssessmentManual_2.pdf)

Hoekstra A Y, Mekonnen M M, Chapagain A K, Mathews R E and Richter B D 2012 Global monthly water scarcity: blue water footprints versus blue water availability *PLoS One* **7** e32688

IAEA 2013 Desalination Economic Evaluation Program 5.1 (https://pub.iaea.org/MTCD/Publications/PDF/CMS-19_web.pdf)

Keck F, Lenzen M, Vassallo A and Li M 2019 The impact of battery energy storage for renewable energy power grids in Australia *Energy* **173** 647–57

Kirby M, Bark R, Connor J, Qureshi M E and Keyworth S 2014 Sustainable irrigation: How did irrigated agriculture in Australia's Murray–Darling basin adapt in the millennium drought? *Agric. Water Manag.* **145** 154–62

Kirby M, Connor J, Bark R, Qureshi E and Keyworth S 2012 The economic impact of water reductions during the Millennium Drought in the Murray-Darling Basin *56th AARES Annu. Conf. Fremantle, West. Aust. Febr. 56th AARES Annu. Conf.*

Fremantle (West. Aust., 7–10 February) (https://doi.org/10.22004/ag.econ.124490)

Leblanc M, Tweed S, Van Dijk A and Timbal B 2012 A review of historic and future hydrological changes in the Murray–Darling Basin *Glob. Planet. Change* **80–81** 226–46

Leck H, Conway D, Bradshaw M and Rees J 2015 Tracing the water-energy-food nexus: description *Theory Practice Geogr. Compass* **9** 445–60

Lenzen M, McBain B, Trainer T, Jütte S, Rey-Lescure O and Huang J 2016 Simulating low-carbon electricity supply for Australia *Appl. Energy* **179** 553–64

Li S, Cai Y-H, Schäfer A I and Richards B S 2019 Renewable energy powered membrane technology: a review of the reliability of photovoltaic-powered membrane system components for brackish water desalination *Appl. Energy* **253** 113524

Mannan M, Alhaj M, Mabrouk A N and Al-Ghamdi S G 2019 Examining the life-cycle environmental impacts of desalination: a case study in the State of Qatar *Desalination* **452** 238–46

Murray–Darling Basin Authority 2010 *Guide to the proposed Basin Plan: Technical background* (Canberra) (https://mdba.gov.au/sites/default/files/archived/guide_pbp/Guide-to-proposed-BP-vol2-0-12.pdf)

Murray–Darling Basin Authority 2018 Transition Period Water Take Report *2016–17. Report on Cap compliance and transitional SDL accounting* (https://mdba.gov.au/sites/default/files/pubs/transition-period-water-take-report-2016-17.pdf)

Murray–Darling Basin Authority 2019a Discover the Basin (https://mdba.gov.au/discover-basin)

Murray–Darling Basin Authority 2019b Murray–Darling Basin Government Storages (https://mdba.gov.au/managing-water/water-storage)

Murray–Darling Basin Authority 2012 *Basin Plan 2012* (Canberra: Australian Government) (https://www.legislation.gov.au/Details/F2017C00078)

Olatomiwa L, Mekhilef S, Ismail M S and Moghavvemi M 2016 Energy management strategies in hybrid renewable energy systems: a review *Renew. Sustain. Energy Rev.* **62** 821–35

Park G L, Schäfer A I and Richards B S 2011 Renewable energy powered membrane technology: the effect of wind speed fluctuations on the performance of a wind-powered membrane system for brackish water desalination *J. Membr. Sci.* **370** 34–44

Park G L, Schäfer A I and Richards B S 2012 The effect of intermittent operation on a wind-powered membrane system for brackish water desalination *Water Sci. Technol.* **65** 867–74

Porter M G, Downie D, Scarborough H, Sahin O and Stewart R A 2015 Drought and desalination: Melbourne water supply and development choices in the twenty-first century *Desalination Water Treat.* **55** 2278–95

Richards B S, Park G L, Pietzsch T and Schäfer A I 2014 Renewable energy powered membrane technology: Brackish water desalination system operated using real wind fluctuations and energy buffering *J. Membr. Sci.* **468** 224–32

Richards L A, Richards B S and Schäfer A I 2011 Renewable energy powered membrane technology: salt and inorganic contaminant removal by nanofiltration/reverse osmosis *J. Membr. Sci.* **369** 188–95

Richter B D, Davis M M, Apse C and Konrad C 2012 A presumptive standard for environmental flow protection *River Res. Appl.* **28** 1312–21

Saeed M O, Ershath M M and Al-Tisan I A 2019 Perspective on desalination discharges and coastal environments of the Arabian Peninsula *Mar. Environ. Res.* **145** 1–10

Scanlon B R, Duncan I and Reedy R C 2013 Drought and the water-energy nexus in texas *Environ. Res. Lett.* **8** 45033

Shahzad M W, Burhan M, Ang L and Ng K C 2017 Energy-water-environment nexus underpinning future desalination sustainability *Desalination* **413** 52–64

Stiftung Forschung für Leben 2019 Climate Correction Project (http://climate-correction-project.com)

The Economist 2018 Can the Sea of Galilee be saved? *Econ* (https://economist.com/middle-east-and-africa/2018/12/01/can-the-sea-of-galilee-be-saved)

The Parliament of Australia 2007 *Water Act 2007* (Canberra: The Parliament of Australia) (https://www.legislation.gov.au/Details/C2017C00151)

The World Bank 2012 *Renewable energy desalination. An emerging solution to close the water gap in the Middle East and North Africa* (Washington, DC: World Bank) (http://documents.worldbank.org/curated/en/443161468275091537/Renewable-energy-desalination-an-emerging-solution-to-close-the-water-gap-in-the-Middle-East-and-North-Africa)

Unruh G C 2000 Understanding carbon lock-in *Energy Policy* **28** 817–30

Williams J and Grafton R Q 2019 Missing in action: possible effects of water recovery on stream and river flows in the Murray–Darling Basin, Australia *Australas. J. Water Resour.* (https://doi.org/10.1080/13241583.2019.1579965)

Wittwer G and Griffith M 2011 Modelling drought and recovery in the southern Murray–Darling basin *Aust. J. Agric. Resour. Econ.* **55** 342–59

Wolfram P, Wiedmann T and Diesendorf M 2016 Carbon footprint scenarios for renewable electricity in Australia *J. Clean. Prod.* **124** 236–45

Zhou J, Chang V W C and Fane A G 2014 Life cycle assessment for desalination: a review on methodology feasibility and reliability *Water Res.* **61** 210–23

Ziolkowska J R 2015 Is desalination affordable? regional cost and price analysis *Water Resour. Manag.* **29** 1385–97

ENVIRONMENTAL RESEARCH
LETTERS

LETTER • OPEN ACCESS

Desalination and sustainability: a triple bottom line study of Australia

To cite this article: Michael Heihsel *et al* 2020 *Environ. Res. Lett.* **15** 114044

IOP Publishing Environ. Res. Lett. 15 (2020) 114044 https://doi.org/10.1088/1748-9326/abbd63

Environmental Research Letters

CrossMark

OPEN ACCESS

RECEIVED
11 July 2020

REVISED
3 September 2020

ACCEPTED FOR PUBLICATION
1 October 2020

PUBLISHED
18 November 2020

LETTER

Desalination and sustainability: a triple bottom line study of Australia

Michael Heihsel[1], Manfred Lenzen[2] and Frank Behrendt[1]

[1] EVUR, Department of Energy Engineering, Technical University of Berlin, Berlin, Germany
[2] ISA, School of Physics, The University of Sydney, Sydney, New South Wales 2006, Australia

E-mail: michael.heihsel@campus.tu-berlin.de

Keywords: LCA, desalination, renewable energy, sustainability, input-output analysis

Supplementary material for this article is available online

Abstract

For many arid countries, desalination is considered as the final possible option to ensure water availability. Although seawater desalination offers the utilisation of almost infinite water resources, the technology is associated with high costs, high energy consumption and thus high carbon emissions when using electricity from fossil sources. In our study, we compare different electricity mixes for seawater desalination in terms of some economic, social and environmental attributes. For this purpose, we developed a comprehensive multi-regional input-output model that we apply in a hybrid life-cycle assessment spanning a period of 29 yr. In our case study, we model desalination plants destined to close the water gap in the Murray-Darling basin, Australia's major agricultural area. We find that under a 100%-renewable electricity system, desalination consumes 20% less water, emits 90% less greenhouse gases, and generates 14% more employment. However, the positive impacts go hand in hand with 17% higher land use, and a 10% decrease in gross value added, excluding external effects.

Abbreviations

FTE	Full-time equivalents
GHG	Greenhouse gas
GVA	Gross value added
ha	Hectare
hLCA	Hybrid life-cycle assessment
IELab	Industrial Ecology Virtual Laboratory
IO	Input-output
IOT	Input-output table
kha	Kilo hectare
LCA	Life-cycle assessment
MDB	Murray-Darling basin
Mha	Million hectares
MRIO	Multi-regional input-output
RE	Renewable electricity
RO	Reverse osmosis
TBL	Triple bottom line

1. Introduction

Water scarcity affects an increasing proportion of the world's population (Greve *et al* 2018). In Australia, water shortages have intensified over the past two decades (Aijm *et al* 2013). In the 'granary of Australia', the MDB, little precipitation and water over-use has led to environmental issues like high salinity of rivers and fish death (Potter *et al* 2010, Wedderburn *et al* 2012). Over the past few years, Australia faced heat records and intense bushfires (Borchers Arriagada *et al* 2020). The latter put the country in a state of emergency for weeks in early 2020 (Komesaroff and Kerridge 2020).

If using natural resources, improving water management, and measures like wastewater reuse are not sufficient to meet water demand, desalination offers great potential, especially for regions with access to the sea (Crisp 2012, Bell *et al* 2018). However, the technology has some severe drawbacks. The production cost of desalinated water is about twice or three times higher than water from conventional sources (Ziolkowska 2015). Furthermore, effects on the marine ecosystem, high energy consumption and the associated GHG emissions are the primary ecological challenges (Sadhwani *et al* 2005, Stokes and Horvath 2006, Lattemann and Höpner 2008, Shehabi *et al* 2012, Shahabi *et al* 2014, Liu *et al* 2015, Zarzo and Prats 2018, Clark *et al* 2018, Gude and Fthenakis 2020). The use of RE could make a major contribution to environmental sustainability in particular (Jijakli et al 2012, Baten and Stummeyer 2013, Cherif et al 2016, Alhaj and Al-Ghamdi 2019). However, studies that assess total sustainability by measuring environmental, social and economic indicators are missing (Haddad 2013, Gude 2016).

The motivation of this study is to quantify the three dimensions of sustainability of desalination depending on the used electricity source. Therefore, we apply an LCA approach (Malik et al 2016, Hadjikakou et al 2019) to measure supply chain effects. We applied an IO-based hLCA for this study (Joshi 1999). The IO analysis goes back to the research work of Wassily Leontief, who received the Nobel Prize for this in 1973 (Leontief 1966). We applied the Australian IELab to compile tailor-made input-output MRIO tables (Lenzen et al 2014).

In this study, we simulated fictive desalination plants at 29 sites around the MDB in southeast Australia. The desalination plants were designed to provide the missing water supply in the MDB of 5500 GL in total. The plants were not designed for continuous operation, but take into account an oversize factor of 1.5, allowing load-shifting of the electricity demand. Like all large plants in Australia, the plants are designed as RO systems. For the power supply, we considered five scenarios, with 0, 25, 50, 75 and 100% RE. In the 0% RE scenario, the electricity sector corresponds to the generation mix of the corresponding year in Australia, as shown in the IO data. The electricity mix, as well as the locations of the generators in the 100% RE scenario, were the results of a GIS-based dispatch optimisation model of a previous study (Heihsel et al 2019a). The transitional scenarios apply pro-rata combinations of both electricity mixes. The capacities of the technologies wind, biomass, hydro and PV are shown in the table in supplementary material S1, which can be found online (available online at https://stacks.iop.org/ERL/15/114044/mmedia).

To the best of our knowledge, this study is the first comprehensive MRIO TBL study comparing desalination plants in RE and fossil-fuelled electricity scenarios. Thus, we contribute to the research gap in the area of holistic studies on socio-economic and environmental impacts of desalination. The study is structured as follows: In the next chapter, we describe the methodology and the data used. After that, we present our results and end with a conclusion. Further technical details on the methods used can be found in the supplementary material.

2. Methods and data

Two methods are applicable for carrying out LCAs: the bottom-up approach (a process-based LCA) and the top-down approach (based on IOTs) (Finnveden et al 2009). The bottom-up approach employs physical process data, allowing very accurate modelling of immediate upstream stages of the value chain. Since the processes are explicitly modelled, the value chain is only reflected to a limited extent due to data availability, and subordinate levels are not considered. Therefore, a truncation error occurs. The top-down approach, on the other hand, uses statistical data on economic sectors, which allows infinite value chains to be modelled. A truncation error, therefore, does not occur, but an aggregation error arises from the aggregation of different processes in industrial sectors. The combination of top-down and bottom-up data in a hybrid approach minimises both errors, which is the advantage of this method (Pomponi and Lenzen 2018).

Hybrid LCAs are used for carbon footprint studies of products, companies or sectors by extending IO tables with physical environmental satellites (Liu et al 2012, Norwood and Kammen 2012, Rodríguez-Alloza et al 2019, Heihsel et al 2019b). Numerous sustainability studies expand the focus on further economic and social indicators, the so-called TBL (Elkington 1998, Foran et al 2005, Onat et al 2014, Malik et al 2016, Hadjikakou et al 2019). The present framework builds on previous research from Heihsel et al (2019b).

We extended an existing IO model as follows: In addition to the GHG satellite, we implemented additional indicators, namely water use, land use, employment, and GVA. Furthermore, we extended the regional resolution up to 46 regions. The highly detailed regional resolution enables to aggregate the results according to different regional classifications (Australian states and territories, water catchment and rainfall areas). We increased the time series to the years 1990–2018. Since the existing IO data do not contain RE sectors, we augmented the tables with additional process data. By using hybridised process-data from Yu and Wiedmann (2018), we modelled RE sectors for wind, solar, hydro and biomass technologies. Hereby, we analysed the TBL impacts of the construction and operation period of desalination plants. In this study, we followed the IO-based hLCA approach by Malik et al (2014) and Suh and Huppes (2005). A projection of the IO data and the process data into the future would be possible in principle but would be subject to considerable uncertainty when analysing investments spanning decades.

2.1. Input-output and renewable electricity data

To complement the IO data with RE specific data, we used process data from AusLCI. (2020) and Ecoinvent (2014), which Yu and Wiedmann (2018) have hybridised. Yu uses an integrated hLCA framework that includes monetary and physical data. Yu's hLCA framework contains 4463 processes (physical data) and 1284 monetary IO sectors, both in matrix form. For our study, we extracted data from the process-coefficient matrix (the primary life-cycle inventories (LCI) of the processes). Moreover, we utilised the cut-off matrix, which supplements the pure process-based data with IO data. Both matrices describe the production recipe of the technology. While the process-coefficient matrix shows upstream physical pre-processes as inputs to produce a functional unit of the process, the cut-off matrix primarily contains upstream services. Each process is represented by an individual column in the matrices. S2 in the supplementary material shows the structure of the integrated hLCA framework by Yu. The processes extracted for this study are shown in S3. In our hLCA framework, we augmented four RE technologies, namely wind, biomass, hydro and photovoltaic.

Furthermore, adding new sectors to the IO-framework requires physical data for the satellite accounts. Therefore, we collected data for the environmental indicators GHG, water use and land use as well as for the social indicator employment. The electricity generation processes in Yu's LCI have a functional unit of 1 MJ. Hence, we normalised the satellite intensities accordingly. Table 1 summarises the direct intensities of the considered RE technologies. The RE vectors represent the intermediate consumption of the electricity generated and thus take into account both operation and maintenance as well as construction, the latter weighted according to expected lifetime. The construction of RE plants is thus reflected in the indirect effects on an annual basis. The direct intensities of RE thus only refer to direct electricity generation. In the supplementary material S1, we show the LCI data preparation process before augmenting the IO-tables.

2.2. Input-output data

We used the Australian IELab to compile tailor-made IO-tables for our study (Lenzen *et al* 2014). The IELab offers a unique disaggregation level of 1284 IOPC sectors and 2214 SA2 regions. For our study, we created a framework of 64 IO-sectors, including the four augmented RE sectors. Our framework consists of 46 Australian regions. The framework contains both industries and commodities, which means that the intermediate demand framework has a size of $2 \times 64 \times 46 = 5888$ rows and columns. The IELab uses statistical data from ABS (2015f), ABS (2015c), ABS (2015b), ABS (2015d), ABS (2015e) for the IO data and AGEIS (2015), ABS (2015g), ABS (2015a), ABS (2015h) for the social and environmental data, respectively. We created time series IOTs for the years 1990–2018.

2.3. Sector augmentation and re-balancing

Australian IOTs do not include separate RE sectors. Therefore, we post-augmented the IOTs with process data. Columns in IOTs show the input of the production of a particular industry; in other words, it is the recipe of the manufactured commodities. The rows describe the intermediate sales structure of commodities to other industries. While we supplemented columns with the LCI data, we adopted the rows (*i.e.* sales structure) from the structure of the existing electricity sectors. The location of the generators resulted from Heihsel *et al* (2019a).

We compiled separate IOTs for each of the five scenarios with 0, 25, 50, 75 and 100% RE generation. The RE sectors were scaled accordingly. The conventional electricity sectors were scaled according to the complementary value. A schematic diagram of the augmented IOT-framework can be found in the supplementary material S4.

Due to the augmentation of the IOTs, they were no longer balanced, which means that input and output were no longer equal. We used a RAS-type biproportional numerical algorithm to post-balance the IOTs (Lahr and de Mesnard 2004, Malik *et al* 2014).

2.4. Desalination process-data

Heihsel *et al* (2019b) analysed Australia's largest 20 desalination plants, which correspond to 95% of the Australian seawater desalination capacity. For their study, they used process-data from the desaldata database (Global Water Intelligence 2016). We used these data as a weighted-average proxy for the 29 desalination plants. We applied results from Heihsel *et al* (2019a) to specify the capacity and the locations of the plants. We assumed the construction period between 1990 and 1992. We allocated 25% of the capital expenditures (capex) each to the first and the last year. Thus 50% of the capital costs were taken into account for the second year. The operation and maintenance period runs continuously from 1993. Since the desalination plants were used for load shifting scenario in this study, we considered an oversize factor of 1.5.

2.5. Calculation of the triple bottom line impacts

The TBL framework describes an accounting concept in which all three fields of sustainability are examined. The term was first introduced by Elkington (1998). In our analysis, we assessed water use, land use and GHG emissions as environmental indicators. The social indicator is employment and the economic indicator GVA. To measure the supply chain impacts of the choice of electricity source on the sustainability of seawater desalination, we used the standard IO methodology, which goes back to Leontief (1966). In the following section, we present the basic principles of the methodology.

Let Q be the matrix of the physical satellite accounts containing the social and environmental indicators. The same calculations were applied accordingly to GVA as an economic indicator. Each row within the matrix represents another indicator. For each indicator row i, we got the vector of the intensities by dividing by outputs with

$$\mathbf{q}_i = \mathbf{Q}_\mathbf{i}\hat{\mathbf{x}}^{-1}, \qquad (1)$$

where $\hat{\mathbf{x}}$ represents the diagonal matrix of the output.

Table 1. Direct intensities of renewable electricity generation.

		Wind	Biomass	Hydro	Photovoltaic
Water use	$(\mathrm{L\,MJ^{-1}})$	0.00	1.41	7.22	1.05E-03
Land use	$(\mathrm{sqm\,MJ^{-1}})$	3.28E221204	1.75E-05	2.16E-03	1.08E-04
Greenhouse gases	$(\mathrm{g\,CO_{2,e}\,MJ^{-1}})$	0.00	2.10	1.60	0.00
Employment	$(\mathrm{FTE\,MJ^{-1}})$	4.53E-08	3.15E-07	2.92E-08	3.85E-07

The standard Leontief equation estimates the output $\mathbf{x}$ of the sectors depending on the final demand $\mathbf{y}$ by

$$\mathbf{x} = (\mathbf{I} - \mathbf{A})^{-1}\mathbf{y}, \quad (2)$$

where $\mathbf{I}$ is the identity matrix and $\mathbf{A}$ represents the technical coefficient matrix. The matrix of technical coefficients representing the production recipe of the sectors is defined by $\mathbf{A} = \mathbf{T}\hat{\mathbf{x}}^{-1}$ The Leontief inverse $\mathbf{L} = (\mathbf{I} - \mathbf{A})^{-1}$ contains the supply chain multipliers. We obtained the supply chain impacts $\mathbf{Q}^{\mathrm{d}}{}_{i}$ $(k \times l)$ from (1) and (2) by

$$\mathbf{Q}_i^{\mathrm{d}} = \hat{\mathbf{q}}_i(\mathbf{I} - \mathbf{A})^{-1}\hat{\mathbf{y}}. \quad (3)$$

Each value in row k and column l in $\mathbf{Q}^{\mathrm{d}}{}_{i}$ shows the contribution of industry k or the product l to the total magnitude of indicator i.

The GVA impacts were determined accordingly to (3), using the GVA intensities $\mathbf{v}$ instead of $\mathbf{q}$. The results can be aggregated into two different representations. The formula $1^{Q'}\mathbf{Q}_i^{\mathrm{d}}$ shows the impacts caused by the production of commodities. Summing the rows by $\mathbf{Q}_i^{\mathrm{d}}1^{Q}$ aggregates the impacts by emitting industries. The operator 'transposes the summation vector $\mathbf{1}^{Q}$ $\mathbf{Q}^{\mathrm{d}}{}_{i}$. Electricity is distributed to the conventional electricity sector and to the RE sectors by the electricity penetration ratio $\lambda = 0, 25, 50, 75\,\mathrm{or}\,100\%$. We allocated the total electricity demand e with $e_c = (1-\lambda)\,\mathrm{e}$ to the conventional electricity sector and with $e_t = \lambda \mathrm{e}\frac{g_t}{\sum_{t=1}^{4} g_t}$ to the RE sector in the demand vector $\mathbf{y}$. Here, g is the generation of the RE technology t.

2.6. Uncertainties

Prior LCAs similar to ours (e.g. Malik *et al* 2018) have shown that measurement uncertainty contained in information on the satellite account $\mathbf{Q}$ and the supply-use data $\mathbf{T}$ represent the main origins for uncertainties in aggregate results, such as the TBL scores calculated in this work (Malik *et al* 2019). Because of nonlinearities in Leontief's equation (2), the latter are usually determined using Monte-Carlo simulation (Bullard and Sebald 1977, 1988, Lenzen *et al* 2010). Because of particular features in the propagation of errors in the Leontief system (Heijungs and Lenzen 2014), high errors of individual matrix elements cancel each other out because of their stochastic nature (Quandt 1958, Lenzen 2000), and the uncertainties of aggregate results are usually much smaller than matrix errors. Whilst the latter occupy a wide range between typically a few and a few hundred percent (Bullard and Sebald 1977, 1988, Lenzen *et al* 2010), the former hover between about 5% and 20% (see e.g. Lenzen *et al* 2018 and Lenzen *et al* 2020). Given the high similarity of data sources and mathematical procedures, these uncertainty magnitudes also apply to this study.

3. Results and discussion

3.1. Holistic triple bottom line impacts

In our study, we investigated the TBL impacts of seawater desalination depending on the electrical energy supply on the environmental indicators water use, land use and GHG. We used GVA as an economic indicator and employment as a social indicator.

Table 2 shows the overall results of the TBL footprints from 1990–2018, for the scenarios with only conventional electricity and 100% RE. The first three years represent the construction period of all plants, the years from 1993 onwards represent the operating and maintenance period over 26 yr, which is in the average range of the concession periods of large Australian plants (Global Water Intelligence 2016). The spider plots in figures 1 and *2* show the relative performance of the different scenarios in relation to the 0% RE scenario. The values of the charts are calculated by summing the indicator values of each scenario and relating them to the sum of the indicator values of the 0% RE scenario. The values of the 0% RE scenario are thus always 1, *i.e.* they set the benchmark. In order to show better performance consistently greater than 1, the reciprocal value is formed for indicators for which less is better (for example, GHG, land use, water use). Hence, the normalised index $n_{k,s}$ for key figure k and scenario s (where scenario 0 is the base scenario with 0% RE) in the spider plots result from $n_{k,s} = \frac{\sum_{y=1}^{29} i_{k,s,y}}{\sum_{y=1}^{29} i_{k,0,y}}$ for the key figure employment and GVA (where more is better) and from $n_{k,s} = \frac{\sum_{y=1}^{29} i_{k,0,y}}{\sum_{y=1}^{29} i_{k,s,y}}$ for water use, land use and GHG emissions (where less is better) with y as year of investigation and i as the indicator values. Hence, the spider plots indicate better performances compared to the base scenario outside and weaker performances inside the blue base scenario circle.

We see that RE have a positive impact on water consumption during the entire life cycle. In both scenarios, the construction phase accounts for around

Table 2. Overall results of the TBL footprints of desalination with 0% RE and 100% RE.

		Water use		Land use		Greenhouse gas emission		Employment		Gross value added	
	RE-ratio	0%	100%	0%	100%	0%	100%	0%	100%	0%	100%
	Year	(GL)	(GL)	(kha)	(kha)	(Mt $CO_{2,e}$)	(Mt $CO_{2,e}$)	(10^3 FTE)	(10^3 FTE)	(AU$ bn)	(AU$ bn)
Construction	1990	443	414	5747	5643	50	15	273	272	13	13
	1991	912	852	11 668	11 470	105	31	533	531	26	26
	1992	439	411	5613	5511	51	15	255	253	13	13
	Total	1794	1677	23 029	22 623	206	60	1061	1056	52	52
	Contribution	43%	51%	77%	65%	23%	70%	72%	63%	42%	47%
Operation and maintenance	1993	114	73	582	842	32	1	24	29	2.1	1.7
	1994	109	70	534	785	31	1.4	23	29	2.1	1.6
	1995	105	69	493	752	30	1.3	22	29	2.0	1.6
	1996	103	68	461	723	30	1.3	20	28	2.1	1.7
	1997	101	66	434	663	30	1.2	20	28	2.1	1.7
	1998	97	65	370	625	29	1.2	18	26	2.0	1.7
	1999	88	64	327	592	27	1.1	16	25	1.9	1.6
	2000	89	63	299	552	27	1.1	16	25	2.0	1.6
	2001	85	63	273	563	26	1.1	15	25	1.9	1.7
	2002	94	66	276	620	29	1.1	15	25	2.0	1.7
	2003	87	62	272	576	27	1.0	12	22	2.1	1.8
	2004	85	56	156	378	29	1.0	12	22	2.1	1.8
	2005	64	57	174	377	19	1.1	14	24	2.2	2.1
	2006	63	58	171	339	20	1.1	14	23	2.3	2.2
	2007	59	43	190	237	18	0.9	13	20	2.4	2.2
	2008	60	42	187	234	19	0.9	12	20	2.6	2.4
	2009	62	44	191	237	20	0.9	13	20	2.8	2.6
	2010	56	41	199	246	20	0.8	15	21	3.0	2.6
	2011	67	54	94	241	24	0.9	11	18	3.2	2.7
	2012	103	61	94	273	27	0.8	12	20	3.3	2.8
	2013	115	70	129	269	31	0.7	15	22	4.0	3.0
	2014	113	66	136	280	29	0.7	16	22	4.1	3.1
	2015	96	65	133	287	28	0.7	13	22	4.0	3.1
	2016	90	70	190	473	25	0.7	14	21	3.6	2.9
	2017	108	73	219	499	31	0.7	16	23	3.8	3.0
	2018	121	71	239	494	35	0.8	18	23	4.2	3.2
	Total	2335	1604	6821	12 156	692	26	409	613	70	58
	Contribution	57%	49%	23%	35%	77%	30%	28%	37%	58%	53%

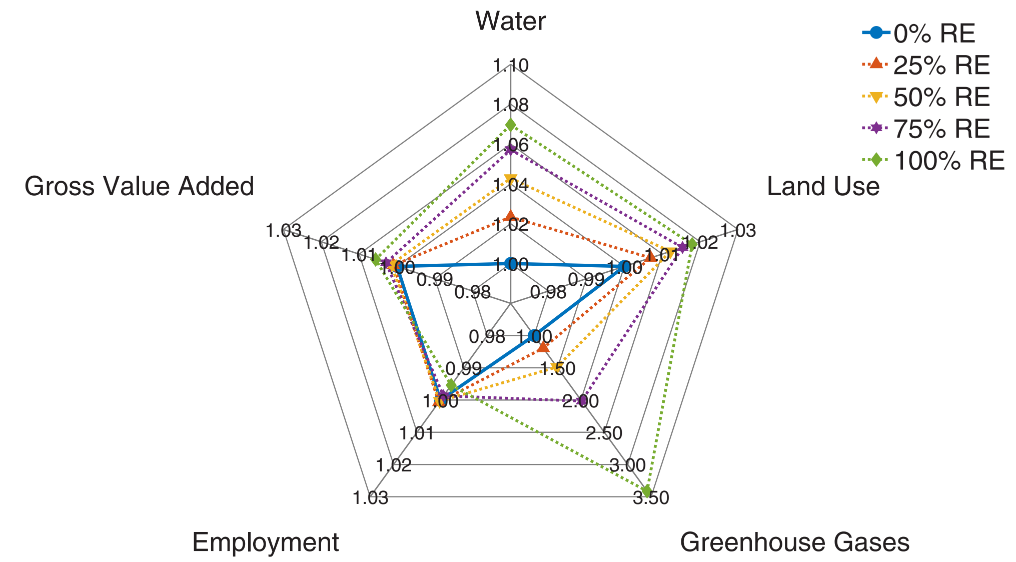

Figure 1. Construction period TBL performances of desalination utilising different electricity mixes.

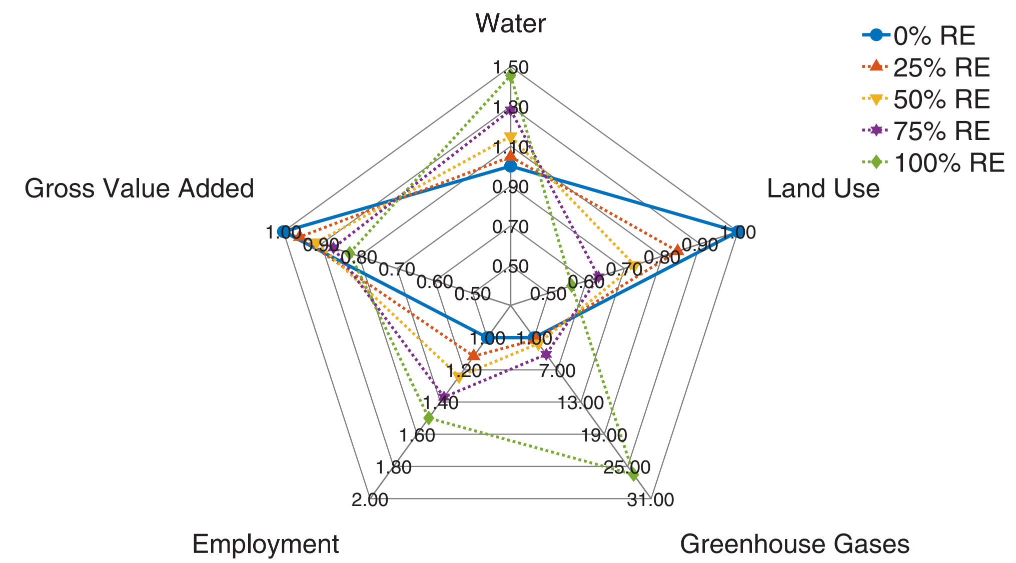

Figure 2. Operation and maintenance period TBL performances of desalination utilising different electricity mixes.

half of the total water consumption. The use of 100% RE would reduce water consumption by 31% in the operating phase and by 7% in the construction phase of desalination plants. Thermal power plants require vast quantities of water due to their technical concept. In particular, the cooling required for the thermodynamic process is highly water-intensive. In coal-fired power plants, the amount of water required to generate electricity can, therefore, account for up to ten times the weight of the coal required (Gleick 1994). Further water is required for the post-treatment of ash and waste disposal. Indirectly, coal mining and recultivation of the landscape are water-intensive. In contrast, the direct water consumption of PV and wind is negligible. Although the water consumption of hydro and geothermal electricity by evaporation and cooling is also substantial, PV and wind dominate the 100% RE system in this case study, which is why water consumption would be significantly reduced.

For the construction, operation and maintenance of the 29 seawater desalination plants, approx. 3300 GL of water would be needed over the entire period of 29 yr when using RE. In contrast, the plants would produce 5500 GL of water per year, *i.e.* over the estimated life cycle of 29 yr, water consumption would amount to 2.3% of the total amount of water produced. With conventional energies, the water consumption share is 2.9%. Over the total period, 21% of water use could be saved by using RE.

Within the construction phase, the land use of desalination would average around 7.5 Mha per year. Moreover, the construction phase is the driver in land use with 77% contribution when using conventional electricity. The use of RE during the construction phase, which would reduce land consumption by 2%, has only a marginal impact. If RE is used in the operational phase, land use would increase significantly by 78%.

RE would have the most significant positive impact on carbon emissions from desalination plants, both during construction and operation. In detail, 206 Mt $CO_{2,e}$ would be generated by the construction using the Australian electricity mix. Only 60 Mt $CO_{2,e}$ would be emitted if Australia had a 100% RE grid. The savings correspond to a reduction of 71%. An even more significant reduction in emissions could be achieved in the operating phase. While 692 Mt $CO_{2,e}$ is emitted in the 0% RE scenario, we see a reduction to 26 Mt with 100% RE. Consequently, carbon emission could be reduced by 96% in the operational period. In the base scenario, the operating phase contributes 77% to carbon emissions. In the RE scenario, the construction phase is the main contributor, with 70% of the total emissions. The results thus show that further measures are needed in other sectors to further reduce emissions during the construction phase.

Regardless of the power source, the average employment during the construction period would be over 350 000 FTE per year. The construction period therefore contributes significantly to total employment, accounting for around 72% of total jobs. While employment in the 100% RE scenario would decrease slightly during the construction phase, employment during the operation phase would increase significantly to 50%. Hence, jobs would increase by 50% from an average of around 16 000 FTE to around 24 000 FTE per year when using 100% RE.

The construction and operating periods have a similarly high contribution to GVA. In both scenarios, the construction of the 29 plants generates GVA of around AU$52 bn (current prices). If 100% RE were used, GVA would be significantly reduced by 17.5% during the operation and maintenance period. Only AU$58 bn instead of AU$70 bn would be generated. Overall, this leads to a reduction of around 10% of GVA over the entire life cycle of 29 yr. This decline can be explained by the fact that Australia is mining a large proportion of its conventional fuels domestically. However, this calculation does not take the external costs of using conventional energy into account.

3.2. Sectoral implications

In the following section, we identified the sectors that have a significant impact on the indicators. Figure 3 shows the percentage contribution of the different sectors to the overall impact. The upper diagram shows the contribution of each industry where the impacts occur. The lower diagram shows the commodities that trigger the impacts through their demand. The bars compare the 0% RE with the 100% RE scenario. The electricity industry is mainly responsible for water consumption in both scenarios. Furthermore, the decrease in water consumption in the 100% RE scenario is mainly caused by the electricity industry and to a lesser extent by the mining industry. In contrast, the water consumption of the agricultural industry increases with the increasing share of RE in the electricity grid, mainly due to the use of biomass. Moreover, electricity is the most relevant commodity determining water consumption. The decrease in water consumption with 100% RE use is also driven by this commodity.

Land use in both scenarios is dominated by the agricultural industry. The same industry causes additional land use when increasing RE share. While the contribution of the commodity electricity to land use is still relatively small when fossil-based electricity is used, it would more than double if RE were used. The main contributing commodities for land use are civil engineering services and installations, the construction of intakes and outfalls and the manufacturing of equipment and materials.

The electricity industry is the driving force for GHG emissions when desalination is operated and built by utilising conventional electricity. This picture changes with a higher share of RE so that the manufacturing industry plays the most considerable role. If we examine the commodities, a similar picture emerges. Electricity as a commodity, but also the construction of intake and outlet play a significant role in GHG emissions. Both commodities reduce their contribution in increasing the share of RE.

The manufacturing industry substantially contributes to employment. A transition to 100% RE would not change the contribution. However, the electricity sector becomes more critical in the 100% RE scenario, making it the second most job-relevant industry. When looking to commodities, the production of equipment and materials is primarily

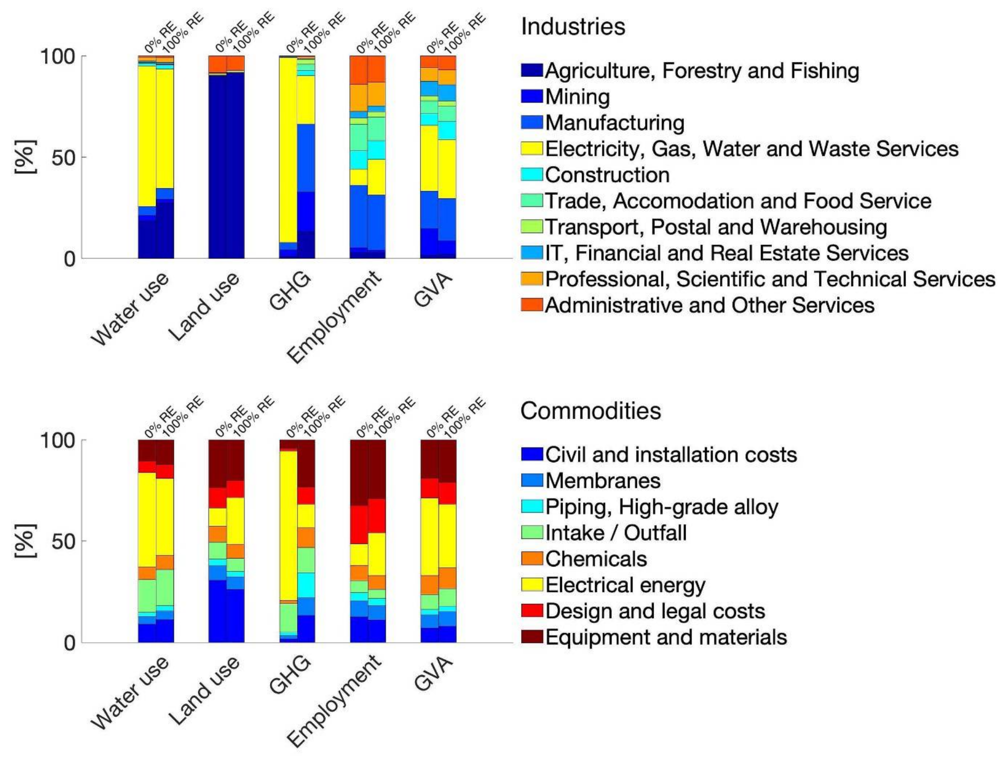

Figure 3. Percentage impact contributions of industries and commodities, comparing the 0% RE and 100% RE scenario.

responsible for job creation. The contribution of the electricity commodity would also increase significantly due to a higher RE-share.

The electricity industry is the largest contributor to GVA, but the contribution decreases as RE increases. With an increasing share of RE, the mining industry would also reduce its contribution to GVA. On the other hand, the construction industry would increase its GVA contribution by increasing the share of RE. In all scenarios, the second most important industry sector in terms of GVA is the manufacturing industry. In both scenarios, the commodity electricity is the main driver of GVA, although the share is reduced by increasing the RE share.

3.3. Regional implications

Figure 4 shows the percentage change in the indicator totals for each of the 46 regions over the entire life cycle when switching from conventional electricity to 100% RE. Red indicates a reduction, green an increase of the indicator. The relative change for each region is given by $p_{k,r} = \frac{\sum_{y=1}^{29} i_{k,RE100,r,y}}{\sum_{y=1}^{29} i_{k,RE0,r,y}}$ where i is the total amount of the indicator of the key figure k, RE100 is the 100% RE scenario and RE0 is the 0% RE scenario. Furthermore, r indicates the region and y the year. It should be noted that especially regions that previously achieved relatively low values and have now experienced a high relative increase may still show low values in absolute terms. The diagram only shows the relative changes to the values in the 0% RE scenario. The key messages of the chart are the relative change in the indicator values in individual regions and, in particular, the shift in the indicator values, but not the absolute level of these values. The maps on the bottom show the classification of the 46 regions, aggregated to Australian states and territories, water catchments (with the MDB) and rainfall areas. The map of the states and territories also shows the locations of the desalination plants.

Throughout the Eastern Region, water consumption would increase, particularly in MDB areas, through greater integration of RE. As the desalination plants in our case study were built to address water scarcity in this area, this is an unsatisfactory result. However, we have seen in section 3.1 that water consumption is only about 2% of total production, so the additional consumption is relatively small. By contrast, water consumption is reduced in the direct coastal areas of the east coast, where most of the economic activity and population is located. Although these regions face higher rainfall than other areas off the coast, these regions are subject to long-term water stress due to high population density and economic activity. Victoria, in particular, would have to cope

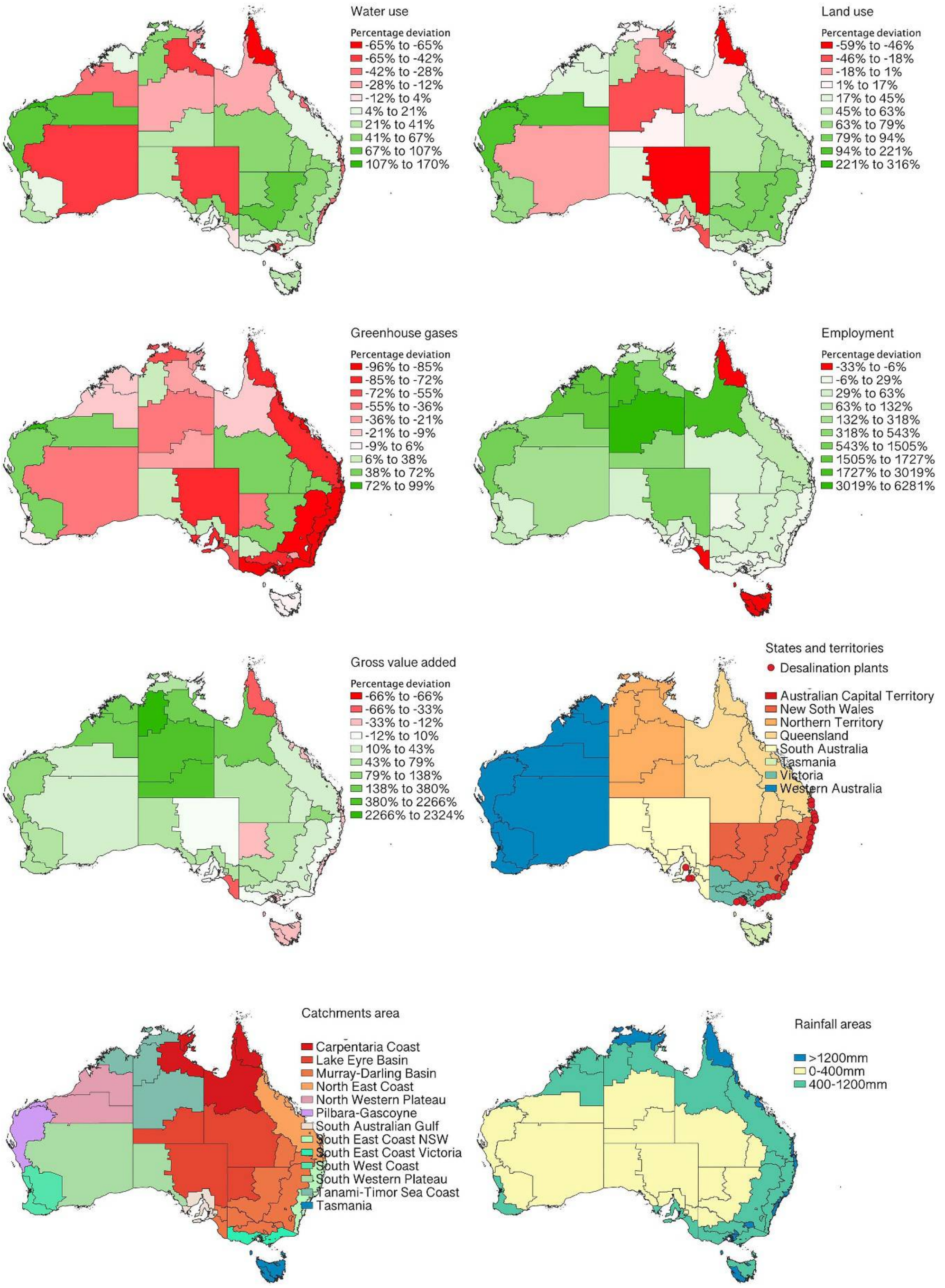

Figure 4. Relative changes of the TBL indicators in the analysed 46 regions.

with a significant increase in water consumption at 100% RE.

The densely populated areas on the east coast would not face any significant change in land use when shifting to RE. In order to provide water in the MDB, demand is generated at the desalination plant sites shown in the states and territories diagram. Compared to centralised power plants, which are mostly located near the coast, the demand for the construction and operation of decentralised RE plants also generates a decentralised demand. Decentralisation is also reflected in land use, which is why areas in eastern Australia and in the MDB in particular are increasingly used in the 100% RE scenario. In central Australia, on the other hand, land use would tend to decrease, while on the west coast, land use would increase significantly.

On the east coast, where economic activities take place, we see an obvious reduction in carbon emissions at 100% RE. The entire east coast with its high population density and economic activity would significantly reduce carbon emissions from desalination by switching to RE. In areas where decentralised RE increase economic activity, emissions would increase, e.g. inland in eastern Australia or on the west coast.

If desalination is built and operated on the basis of RE instead of conventional electricity, fewer jobs would be created in a few regions in the north and south, including Tasmania. On the other hand, employment would increase in the inland areas. All areas in central and western Australia would see an increase in employment, as RE is much more decentralised than conventional power stations. Diversification of employment is beneficial for a country like Australia, where population and economic activity are concentrated in a few areas, while there are large unused areas in the hinterland.

Like employment, GVA would be regionally diversified due to the increasing use of RE. However, GVA would decrease in the economic areas of the east coast, especially in the north, but also in Tasmania. In the Northern Territory, GVA would increase significantly. From an economic point of view, such a development would be beneficial as economic activity diversifies into areas with lower population density and less economic activity.

4. Conclusion

In our IO-based hLCA assessment, we showed the comprehensive TBL sustainability impacts of seawater desalination, depending on the utilised electricity source. Using social, economic ecological indicators, we explained in detail which sectors and regions contribute positively or negatively to the sustainability of desalination through a 100% RE grid.

With higher RE penetration, we measured rising employment but also falling GVA. Even if there is a trade-off between employment and GVA, the assessment shows that a higher RE share would contribute to regional diversification of economic activity. In fact, the spatial diversification of GVA is itself a value, as the local concentration of GVA increases the cost of land use. Therefore, decentralised GVA prevents price increases caused by land scarcity. While desalination with conventional electricity generates higher GVA through domestic fuel mining, this economic benefit is not sustainable in the light of the Paris Agreement.

Furthermore, the environmental performance of desalination with RE is highly beneficial. The application of a 100% RE system reduces the carbon emissions of desalination during construction by 71% and during operation by 96%. The benefit becomes even more evident when we monetise the reduced external costs. Let us assume an external cost of AU$100 per tonne of CO_2 and 25 Mt as an average amount of carbon emissions reduced by RE during an operating year. Then the reduction in external costs through avoided emissions would result in savings of AU$3.75 bn per year. In contrast, the total loss of GVA over the same period is some hundred million dollars. However, our analysis shows that about 30% of the carbon emissions during the construction period of the desalination plants cannot be reduced by 100% RE. Hence, further measures are still needed.

The results clearly show that RE and desalination benefit from synergy effects. Due to the high energy consumption, this applies in particular to desalination, but similar effects can also be expected for other water supply technologies due to the technical similarities. Due to the consequences of climate change, it is to be predicted that Australia's water problems will increase in the future. Policymakers should, therefore, aim for a common strategy for Australia's water and energy supply. The scope of consideration should be as broad as possible and should also include, for example, other related problems such as the discharge of brine with increased desalination use.

Our holistic assessment approach has several strengths for the analysis of infrastructure projects. Since we examined all three areas of sustainability using an hLCA framework, the results are directly comparable. We used the same system boundaries, the same assumptions and framework conditions, and the same economic linkages. Trade-offs, such as GVA and GHG emissions, can be compared directly. The methodology is particularly useful for practitioners to estimate the impact of infrastructure projects in the early planning phase. The political value of the findings is substantial. Our MRIO approach allows detailed regional and sectoral conclusions. The highly disaggregated analysis enables long-term economic policies, e.g. due to changes in regional water use, employment or economic activities.

The sustainability of seawater desalination plants depends in particular on regional factors such as local energy supply or industrial interconnections. In order to make these influences apparent, regional economic data are indispensable. The hLCA approach with the use of the IELab offers an efficient and effective possibility to break down statistical data to create tailor-made IOTs. The achievable granularity depends in particular on local data availability, whose quality is increasing worldwide. In recent years, IELabs for Australia, China, Indonesia, Taiwan, Japan, and the USA have been created that can be used for these assessments (Geschke and Hadjikakou 2017).

Further research is needed on the effects of large quantities of brine intake on marine biology. Furthermore, the development of new membranes promises remarkable increases in desalination efficiency. The associated effects on sustainability also require further research.

Acknowledgments

This work was financially supported by the Friedrich Naumann Foundation for Freedom. We acknowledge support by the German Research Foundation and the Open Access Publication Fund of TU Berlin. The Authors further acknowledge financial support by the National eResearch Collaboration Tools and Resources project (NeCTAR) through its Industrial Ecology Virtual Laboratory. NeCTAR is an Australian Government project conducted as part of the Super Science initiative and financed by the Education Investment Fund. We thank Man Yu for providing the RE process data. We would also like to thank Ka Leung Lam, Syed Muhammad Hassan Ali and Bonnie McBain for their advice on processing the input data. We would like to acknowledge Arunima Malik for her advice on the post-balance procedure. Finally, we also thank the anonymous reviewers for the valuable comments, which have improved this study.

Data availability statement

The data that support the findings of this study are available upon reasonable request from the authors.

ORCID iDs

Michael Heihsel https://orcid.org/0000-0001-9886-0006
Manfred Lenzen https://orcid.org/0000-0002-0828-5288
Frank Behrendt https://orcid.org/0000-0002-7282-8806

References

ABS 2015a Agricultural Commodities, cat. no. 7121 (www.abs.gov.au/ausstats/abs@.nsf/mf/7121.0)

ABS 2015b Australian National Accounts: input-output tables, cat. no. 5209 (www.abs.gov.au/AUSSTATS/abs@.nsf/DetailsPage/5209.0.55.0012014-15?OpenDocument)

ABS 2015c Australian National Accounts: input-output tables (Product Details), cat. no. 5215. (www.abs.gov.au/ausstats/abs@.nsf/mf/5215.0.55.001)

ABS 2015d Australian National Accounts: national Income, cat. no. 5206 (www.abs.gov.au/ausstats/abs@.nsf/mf/5206.0)

ABS 2015e Australian National Accounts: state Accounts, cat. no. 5220 (www.abs.gov.au/AUSSTATS/abs@.nsf/DetailsPage/5220.02017-18?OpenDocument)

ABS 2015f Household Expenditure Survey, cat. no. 6530.0 (www.abs.gov.au/AUSSTATS/abs@.nsf/Lookup/6530.0ExplanatoryNotes12015-16?OpenDocument)

ABS 2015g Manufacturing Industry, cat. no. 8221 (www.abs.gov.au/ausstats/abs@.nsf/mf/8221.0)

ABS 2015h Water Use on Australian Farms, cat. no. 4618 (www.abs.gov.au/ausstats/abs@.nsf/mf/4618.0)

AGEIS 2015 National Greenhouse Gas Inventory (https://ageis.climatechange.gov.au)

Aijm V D, Beck H E, Crosbie R S, Ram D J, Liu Y Y, Podger G M, Timbal B and Viney N R 2013 The Millennium Drought in southeast Australia (2001–2009): natural and human causes and implications for water resources, ecosystems, economy, and society *Water Resour. Res.* **49** 1040–57

Alhaj M and Al-Ghamdi S G 2019 Integrating concentrated solar power with seawater desalination technologies: a multi-regional environmental assessment *Environ. Res. Lett.* **14** 74014

AusLCI. 2020 *The Australian Life Cycle Inventory Database Initiative*. (www.auslci.com.au)

Baten R and Stummeyer K 2013 How sustainable can desalination be? *Desalin. Water Treat.* **51** 44–52

Bell E M, Stokes-Draut J R and Horvath A 2018 Environmental evaluation of high-value agricultural produce with diverse water sources: case study from Southern California *Environ. Res. Lett.* **13** 25007

Borchers Arriagada N, Bowman D M J S, Palmer A J and Johnston F H 2020 Climate change, wildfires, heatwaves and health impacts in Australia *Extreme Weather Events and Human Health* ed R Akhtar (Cham: Springer International Publishing) pp 99–116

Bullard C W and Sebald A V 1977 Effects of parametric uncertainty and technological change on input-output models *Rev. Econ. Stat.* **59** 75–81

Bullard C W and Sebald A V 1988 Monte Carlo sensitivity analysis of input-output models *Rev. Econ. Stat.* **70** 708–12

Cherif H, Champenois G and Belhadj J 2016 Environmental life cycle analysis of a water pumping and desalination process powered by intermittent renewable energy sources *Renew. Sustain. Energy Rev.* **59** 1504–13

Clark G F, Knott N A, Miller B M, Kelaher B P, Coleman M A, Ushiama S and Johnston E L 2018 First large-scale ecological impact study of desalination outfall reveals trade-offs in effects of hypersalinity and hydrodynamics *Water Res.* **145** 757–68

Crisp G J 2012 Desalination and water reuse-sustainably drought proofing Australia *Desalin. Water Treat.* **42** 323–32

Ecoinvent 2014 Ecoinvent Database 2.2 (Zurich, Switzerland)

Elkington J 1998 *Cannibals with Forks: The Triple Bottom Line of 21st Century Business* (Gabriola Island, BC: New Society Publishers)

Finnveden G, Hauschild M Z, Ekvall T, Guinée J, Heijungs R, Hellweg S, Koehler A, Pennington D and Suh S 2009 Recent developments in life cycle assessment *J. Environ. Manage.* **91** 1–21

Foran B, Lenzen M, Dey C and Bilek M 2005 Integrating sustainable chain management with triple bottom line accounting *Ecol. Econ.* **52** 143–57

Geschke A and Hadjikakou M 2017 Virtual laboratories and MRIO analysis—an introduction *Econ. Syst. Res.* **29** 143–57

Gleick P H 1994 Water and Energy *Annu. Rev. Energy Environ.* **19** 267–99

Global Water Intelligence 2016 Desaldata *Database* (www.desaldata.com)

Greve P *et al* 2018 Global assessment of water challenges under uncertainty in water scarcity projections *Nat. Sustain.* **1** 486–94

Gude V G 2016 Desalination and sustainability - an appraisal and current perspective *Water Res.* **89** 87–106

Gude V G and Fthenakis V 2020 Energy efficiency and renewable energy utilization in desalination systems *Prog. Energy* **2**

Haddad B M 2013 A case for an ecological-economic research program for desalination *Desalination* **324** 72–78

Hadjikakou M, Stanford B D, Wiedmann T, Rowley H V, Kobayashi Y, Ishii S, Gaitan J P A, Johns G, Lundie S and Khan S J 2019 A flexible framework for assessing the sustainability of alternative water supply options *Sci. Total Environ.* **671** 1257–68 (https://linkinghub.elsevier.com/retrieve/pii/S004896971931280X)

Heihsel M, Ali S M H, Kirchherr J and Lenzen M 2019a Renewable-powered desalination as an optimisation pathway for renewable energy systems: the case of Australia's Murray-Darling Basin *Environ. Res. Lett.* **14** 124054

Heihsel M, Lenzen M, Malik A and Geschke A 2019b The carbon footprint of desalination: an input-output analysis of seawater reverse osmosis desalination in Australia for 2005–2015 *Desalination* **454** 71–81

Heijungs R and Lenzen M 2014 Error propagation methods for LCA—a comparison *Int. J. Life Cycle Assess.* **19** 1445–61

Jijakli K, Arafat H, Kennedy S, Mande P and Theeyattuparampil V V 2012 How green solar desalination really is? Environmental assessment using life-cycle analysis (LCA) approach *Desalination* **287** 123–31

Joshi S 1999 Product environmental life-cycle assessment using input-output techniques *J. Ind. Ecol.* **3** 95–120

Komesaroff P and Kerridge I 2020 A continent aflame: ethical lessons from the Australian Bushfire Disaster *J. Bioeth. Inq.* **17** 11-14

Lahr M L and de Mesnard L 2004 Biproportional techniques in input-output analysis: table updating and structural analysis *Econ. Syst. Res.* **16** 115–34

Lattemann S and Höpner T 2008 Environmental impact and impact assessment of seawater desalination *Desalination* **220** 1–15

Lenzen M 2000 Errors in conventional and input-output-based life-cycle inventories *J. Ind. Ecol.* **4** 127–48

Lenzen M *et al* 2014 Compiling and using input–output frameworks through collaborative virtual laboratories *Sci. Total Environ.* **485–486** 241–51

Lenzen M *et al* 2020 Global socio-economic losses and environmental gains from the Coronavirus pandemic *PloS One* **15** e0235654

Lenzen M, Sun Y Y, Faturay F, Ting Y P, Geschke A and Malik A 2018 The carbon footprint of global tourism *Nat. Clim. Change* **8** 522–8

Lenzen M, Wood R and Wiedmann T 2010 Uncertainty analysis for multi-region input-output models—a case study of the UK'S carbon footprint *Econ. Syst. Res.* **22** 43–63

Leontief W W 1966 *Input-output Economics* (Oxford : Oxford University Press)

Liu C H, Lenzen M and Murray J 2012 A disaggregated emissions inventory for Taiwan with uses in hybrid input-output life cycle analysis (IO-LCA) *Nat. Resour. Forum* **36** 123–41

Liu J, Chen S, Wang H and Chen X 2015 Calculation of carbon footprints for water diversion and desalination projects *Energy Procedia* **75** 2483–94

Malik A, Lenzen M and Geschke A 2016 Triple bottom line study of a lignocellulosic biofuel industry *GCB Bioenergy* **8** 96–110

Malik A, Lenzen M, Mcalister S and Mcgain F 2018 The carbon footprint of Australian health care *Lancet Planet. Health* **2** e27–35

Malik A, Lenzen M, Rô N E and Dietzenbacher E 2014 Simulating the impact of new industries on the economy: the case of biorefining in Australia *Ecol. Econ.* **107** 84–93

Malik A, Mcbain D, Wiedmann T O, Lenzen M and Murray J 2019 Advancements in input-output models and indicators for consumption-based accounting *J. Ind. Ecol.* **23** 300–12

Norwood Z and Kammen D 2012 Life cycle analysis of distributed concentrating solar combined heat and power: economics, global warming potential and water *Environ. Res. Lett.* **7** 44016

Onat N C, Kucukvar M and Tatari O 2014 Integrating triple bottom line input-output analysis into life cycle sustainability assessment framework: the case for US buildings *Int. J. Life Cycle Assess.* **19** 1488–505

Pomponi F and Lenzen M 2018 Hybrid life cycle assessment (LCA) will likely yield more accurate results than process-based LCA *J. Clean. Prod.* **176** 210–5

Potter N J, Chiew F H S and Frost A J 2010 An assessment of the severity of recent reductions in rainfall and runoff in the Murray-Darling Basin *J. Hydrol.* **381** 52–64

Quandt R E 1958 Probabilistic errors in the leontief system *Nav. Res. Logist. Q.* **5** 155–70

Rodríguez-Alloza A M, Heihsel M, Fry J, Gallego J, Geschke A, Wood R and Lenzen M 2019 Consequences of long-term infrastructure decisions—the case of self-healing roads and their CO_2 emissions *Environ. Res. Lett.* **14** 114040

Sadhwani J J, Veza J M and Santana C 2005 Case studies on environmental impact of seawater desalination *Desalination* **185** 1–8

Shahabi M P, Mchugh A, Anda M and Ho G 2014 Environmental life cycle assessment of seawater reverse osmosis desalination plant powered by renewable energy *Renew. Energy* **67** 53–58

Shehabi A, Stokes J R and Horvath A 2012 Energy and air emission implications of a decentralized wastewater system *Environ. Res. Lett.* **7** 24007

Stokes J and Horvath A 2006 Life cycle energy assessment of alternative water supply systems *Int. J. Life Cycle Assess.* **11** 335–43

Suh S and Huppes G 2005 Methods for life cycle inventory of a product *J. Clean. Prod.* **13** 687–97

Wedderburn S D, Hammer M P and Bice C M 2012 Shifts in small-bodied fish assemblages resulting from drought-induced water level recession in terminating lakes of the Murray-Darling Basin, Australia *Hydrobiologia* **691** 35–46

Yu M and Wiedmann T 2018 Implementing hybrid LCA routines in an input–output virtual laboratory *J. Econ. Struct.* **7** 33

Zarzo D and Prats D 2018 Desalination and energy consumption. What can we expect in the near future? *Desalination* **427** 1–9

Ziolkowska J R 2015 Is desalination affordable? Regional cost and price analysis *Water Resour. Manage.* **29** 1385–97

References

[1] ABS. Australian Statistical Geography Standard: Design of the Statistical Areas Level 2, Catalogue No. 1216.0.55.003. Australian Bureau of Statistics, 2010.

[2] ABS. Agricultural Commodities, Catalogue No. 7121. Australian Bureau of Statistics, Canberra, 2015.

[3] ABS. Australian National Accounts: Input-Output Tables, Catalogue No. 5209. Australian Bureau of Statistics, Canberra, 2015.

[4] ABS. Australian National Accounts: Input-Output Tables (Product Details), Catalogue No. 5215. Australian Bureau of Statistics, Canberra, 2015.

[5] ABS. Australian National Accounts: National Income, Catalogue No. 5206. Australian Bureau of Statistics, Canberra, 2015.

[6] ABS. Australian National Accounts: State Accounts, Catalogue No. 5220. Australian Bureau of Statistics, Canberra, 2015.

[7] ABS. Household Expenditure Survey, Catalogue No. 6530.0. Australian Bureau of Statistics, Canberra, 2015.

[8] ABS. Manufacturing Industry, Catalogue No. 8221. Australian Bureau of Statistics, Canberra, 2015.

[9] ABS. Water Use on Australian Farms, Catalogue no. 4618. Australian Bureua of Statistics, Canberra, 2015.

[10] ABS. Producer price indexes, Catalogue No. 6427.0. Australian Bureau of Statistics, 2017.

[11] AEMO. Short Term Energy Market Data. Australian Energy Market Operator, http://data.wa.aemo.com.au/#stem-summary, 2009.

[12] AEMO. 100 per cent Renewables Study – Modelling Outcomes. Technical report, Australian Energy Market Operator, Canberra, 2013.

[13] AER. Annual Volume Weighted Average Spot Prices. Australian Energy Regulator, https://www.aer.gov.au/wholesale-markets/wholesale-statistics/annual-volume-weighted-average-spot-prices, 2009.

[14] AER. State of the Energy Market, May 2017. Technical report, Australian Energy Regulator, Melbourne, 2017.

[15] AGEIS. National Greenhouse Gas Inventory. Australian Government, Canberra, 2015.

[16] A. Aghigh, V. Alizadeh, H. Y. Wong, M. S. Islam, N. Amin, and M. Zaman. Recent advances in utilization of graphene for filtration and desalination of water: A review. *Desalination*, 365:389–397, 2015.

[17] A. Al-Karaghouli and L. L. Kazmerski. Energy consumption and water production cost of conventional and renewable-energy-powered desalination processes. *Renewable and Sustainable Energy Reviews*, 24:343–356, 2013.

[18] A. Al-Karaghouli, D. Renne, and L. L. Kazmerski. Technical and economic assessment of photovoltaic-driven desalination systems. *Renewable Energy*, 35(2):323–328, 2010.

[19] M. Alhaj and S. G. Al-Ghamdi. Integrating concentrated solar power with seawater desalination technologies: a multi-regional environmental assessment. *Environmental Research Letters*, 14(7):74014, 2019.

[20] M. Alhaj and S. G. Al-Ghamdi. Why is powering thermal desalination with concentrated solar power expensive? assessing economic feasibility and market commercialization barriers. *Solar Energy*, 189:480–490, 2019.

[21] S. M. H. Ali, M. Lenzen, and J. Huang. Shifting air-conditioner load in residential buildings: benefits for low-carbon integrated power grids. *IET Renewable Power Generation*, 12(11):1314–1323, 2018.

[22] S. M. H. Ali, M. Lenzen, and E. Tyedmers. Optimizing 100%-renewable grids through shifting residential water-heater load. *International Journal of Energy Research*, 43(4):1479–1493, 2019.

[23] Aquasure. Victorian Desalination Project Fact Sheet - Pipeline and Power Supply. Technical report, https://www.aquasure.com.au/pipeline-powerline, 2015.

[24] E. Augsten. Desalination by means of wind and sun. Technical report, https://www.sunwindenergy.com/system/files/swe_0702_032-037_desalination.pdf, 2007.

[25] AusLCI. AusLCI Database. Australian Life Cycle Assessment Society, 2020.

[26] R. Baten and K. Stummeyer. How sustainable can desalination be? *Desalination and Water Treatment*, 51(1-3):44–52, 2013.

[27] E. M. Bell, J. R. Stokes-Draut, and A. Horvath. Environmental evaluation of high-value agricultural produce with diverse water sources: Case study from Southern California. *Environmental Research Letters*, 13(2):25007, 2018.

[28] A. Bennett. Cost effective desalination: Innovation continues to lower desalination costs. *Filtration and Separation*, 48(4):24–27, 2011.

[29] Bluefield Research. Relative Piping Costs. https://www.wateronline.com/doc/water-and-wastewater-pipeline-infrastructure-opportunities-0001, 2018.

[30] K. Bognar. *Energy and Water Supply Systems in Remote Regions Considering Renewable Energies and Seawater Desalination*. Dissertation, Technische Universität Berlin, 2013.

[31] BOM. Monthly Weather Review. Bureau of Meteorology, http://www.bom.gov.au/climate/mwr/, 2019.

[32] N. Borchers Arriagada, D. M. J. S. Bowman, A. J. Palmer, and F. H. Johnston. Climate Change, Wildfires, Heatwaves and Health Impacts in Australia. In R. Akhtar, editor, *Extreme Weather Events and Human Health*, pages 99–116. Springer International Publishing, Cham, 2020.

[33] C. W. Bullard and A. V. Sebald. Monte carlo sensitivity analysis of input-output models. *The Review of Economics and Statistics*, 70(4):708–712, 1988.

[34] H. Cherif, G. Champenois, and J. Belhadj. Environmental life cycle analysis of a water pumping and desalination process powered by intermittent renewable energy sources. *Renewable and Sustainable Energy Reviews*, 59:1504–1513, 2016.

[35] G. F. Clark, N. A. Knott, B. M. Miller, B. P. Kelaher, M. A. Coleman, S. Ushiama, and E. L. Johnston. First large-scale ecological impact study of desalination outfall reveals trade-offs in effects of hypersalinity and hydrodynamics. *Water Research*, 145:757–768, 2018.

[36] D. Connell. Water reform and the federal system in the Murray-Darling Basin. *Water Resources Management*, 25(15):3993–4003, 2011.

[37] B. Corona, C. de la Rúa, and G. San Miguel. Socio-economic and environmental effects of concentrated solar power in Spain: A multiregional input output analysis. *Solar Energy Materials and Solar Cells*, 156:112–121, 2016.

[38] D. Crawford, T. Jovanovic, O. O'Connor, A. Herr, J. Raison, and T. Baynes. AEMO 100% Renewable Energy Study: Potential for Electricity Generation in Australia from Biomass in 2010, 2030 and 2050. Technical report, CSIRO Energy Transformed Flagship, Newcastle, 2012.

[39] S. J. Crimp, C. J. Stokes, S. M. Howden, A. D. Moore, B. Jacobs, P. R. Brown, A. J. Ash, P. Kokic, and P. Leith. Managing Murray-Darling Basin livestock systems in a variable and changing climate: Challenges and opportunities. *Rangeland Journal*, 32(3):293–304, 2010.

[40] G. J. Crisp. Desalination and water reuse-sustainably drought proofing Australia. *Desalination and Water Treatment*, 42(1-3):323–332, 2012.

[41] M. Darwish, A. H. Hassabou, and B. Shomar. Using Seawater Reverse Osmosis (SWRO) desalting system for less environmental impacts in Qatar. *Desalination*, 309:113–124, 2013.

[42] Ecoinvent. Ecoinvent Database 2.2. Swiss Centre for Life Cycle Inventories, 2014.

[43] B. Edwards, M. Gray, and B. Hunter. The social and economic impacts of drought. *Australian Journal of Social Issues*, 54(1):22–31, 2019.

[44] R. Einav, K. Harussi, and D. Perry. The footprint of the desalination processes on the environment. *Desalination*, 152(1):141–154, 2003.

[45] I. El Saliby, Y. Okour, H. K. Shon, J. Kandasamy, and I. S. Kim. Desalination plants in Australia, review and facts. *Desalination*, 247(1-3):1–14, 2009.

[46] J. Elkington. *Cannibals with Forks: The Triple Bottom Line of 21st Century Business*. New Society Publishers, Gabriola Island, BC, 1998.

[47] B. Elliston, I. MacGill, and M. Diesendorf. Least cost 100% renewable electricity scenarios in the Australian National Electricity Market. *Energy Policy*, 59:270–282, 2013.

[48] D. R. Farine, D. A. O'Connell, R. J. Raison, B. M. May, M. H. O'Connor, D. F. Crawford, A. Herr, J. A. Taylor, T. Jovanovic, P. K. Campbell, M. I. Dunlop, L. C. Rodriguez, M. L. Poole, A. L. Braid, and D. Kriticos. An assessment of biomass for bioelectricity and biofuel, and for greenhouse gas emission reduction in Australia. *GCB Bioenergy*, 4(2):148–175, 2012.

[49] G. Finnveden, M. Z. Hauschild, T. Ekvall, J. Guinée, R. Heijungs, S. Hellweg, A. Koehler, D. Pennington, and S. Suh. Recent developments in life cycle assessment. *Journal of Environmental Management*, 91(1):1–21, 2009.

[50] B. Foran, M. Lenzen, C. Dey, and M. Bilek. Integrating sustainable chain management with triple bottom line accounting. *Ecological Economics*, 52(2):143–157, 2005.

[51] A. Forghani, J. Alexandra, and J. Donaldson. Spatially Enabled MDBA. Technical report, Murray-Darling Basin Authority, Canberra, http://www.csdila.unimelb.edu.au/BeyondSpatialEnablement/pdf/Forghani.pdf, 2011.

[52] M. Freire-Gormaly and A. M. Bilton. Experimental quantification of the effect of intermittent operation on membrane performance of solar powered reverse osmosis desalination systems. *Desalination*, 435:188–197, 2018.

[53] A. Geschke and M. Hadjikakou. Virtual laboratories and MRIO analysis – an introduction. *Economic Systems Research*, 29(2):143–157, 2017.

[54] N. Ghaffour. The challenge of capacity-building strategies and perspectives for desalination for sustainable water use in MENA. *Desalination and Water Treatment*, 5(1-3):48–53, 2009.

[55] N. Ghaffour, S. Lattemann, T. Missimer, K. C. Ng, S. Sinha, and G. Amy. Renewable energy-driven innovative energy-efficient desalination technologies. *Applied Energy*, 136:1155–1165, 2014.

[56] N. Ghaffour, T. M. Missimer, and G. L. Amy. Technical review and evaluation of the economics of water desalination: Current and future challenges for better water supply sustainability. *Desalination*, 309(2013):197–207, 2013.

[57] A. Ghobeity and A. Mitsos. Optimal time-dependent operation of seawater reverse osmosis. *Desalination*, 263(1-3):76–88, 2010.

[58] D. P. Giurco, A. Turner, S. Fane, and S. B. White. Desalination for urban water: Changing perceptions and future scenarios in Australia. *Chemical Engineering Transactions*, 42:13–18, 2014.

[59] P. H. Gleick. Water and energy. *Annual Review of Energy and the Environment*, 19(1):267–299, 1994.

[60] P. Glueckstern. History of Desalination Cost Estimations. In *Proceedings of the International Conference on Desalination Costing*, Tel-Aviv, 2004.

[61] M. F. A. Goosen, H. Mahmoudi, and N. Ghaffour. Today's and future challenges in applications of renewable energy technologies for desalination. *Critical Reviews in Environmental Science and Technology*, 44(9):929–999, 2014.

[62] P. Greve, T. Kahil, J. Mochizuki, T. Schinko, Y. Satoh, P. Burek, G. Fischer, S. Tramberend, R. Burtscher, S. Langan, and Y. Wada. Global assessment of water challenges under uncertainty in water scarcity projections. *Nature Sustainability*, 1(9):486–494, 2018.

[63] E. A. Grubert and M. E. Webber. Energy for water and water for energy on Maui Island, Hawaii. *Environmental Research Letters*, 10(6):64009, 2015.

[64] V. G. Gude. Desalination and sustainability - An appraisal and current perspective. *Water Research*, 89:87–106, 2016.

[65] V. G. Gude and V. Fthenakis. Energy efficiency and renewable energy utilization in desalination systems. *Progress in Energy*, 2(2):022003, 2020.

[66] GWI. Desaldata. Global Water Intelligence, http://www.desaldata.com, 2016.

[67] GWI. Desalination Markets 2016. Technical report, Global Water Intelligence, Oxford, 2016.

[68] B. M. Haddad. A case for an ecological-economic research program for desalination. *Desalination*, 324:72–78, 2013.

[69] M. Hadjikakou, B. D. Stanford, T. Wiedmann, H. V. Rowley, Y. Kobayashi, S. Ishii, J. P. A. Gaitan, G. Johns, S. Lundie, and S. J. Khan. A flexible framework for assessing the sustainability of alternative water supply options. *Science of the Total Environment*, 671:1257–1268, 2019.

[70] C. Hanshik, H. Jeong, K. W. Jeong, and S. H. Choi. Improved productivity of the MSF (multi-stage flashing) desalination plant by increasing the TBT (top brine temperature). *Energy*, 107:683–692, 2016.

[71] M. Heihsel, S. M. H. Ali, J. Kirchherr, and M. Lenzen. Renewable-powered desalination as an optimisation pathway for renewable energy systems: The case of Australia's Murray-Darling Basin. *Environmental Research Letters*, 14(12):124054, 2019.

[72] M. Heihsel, M. Lenzen, and F. Behrendt. Desalination and sustainability: A triple bottom line study of Australia. *Environmental Research Letters*, 15(11):114044, 2020.

[73] M. Heihsel, M. Lenzen, A. Malik, and A. Geschke. The carbon footprint of desalination: An input-output analysis of seawater reverse osmosis desalination in Australia for 2005–2015. *Desalination*, 454:71–81, 2019.

[74] R. Heijungs and M. Lenzen. Error propagation methods for LCA — a comparison. *The International Journal of Life Cycle Assessment*, 19(7):1445–1461, 2014.

[75] A. Y. Hoekstra, A. K. Chapagain, M. M. Aldaya, and M. M. Mekonnen. The Water Footprint Assessment Manual - Setting the Global Standard. Technical report, Earthscan, London, 2011.

[76] A. Y. Hoekstra, M. M. Mekonnen, A. K. Chapagain, R. E. Mathews, and B. D. Richter. Global monthly water scarcity: Blue water footprints versus blue water availability. *PLoS ONE*, 7(2), 2012.

[77] S. Homaeigohar and M. Elbahri. Graphene membranes for water desalination. *NPG Asia Materials*, 9(e427), 2017.

[78] T. Höpner and J. Windelberg. Elements of environmental impact studies on coastal desalination plants. *Desalination*, 108(1-3):11–18, 1997.

[79] IAEA. Desalination Economic Evaluation Program 5.1 (DEEP - 3.0) User's Manual. Technical report, International Atomic Energy Agency, Vienna, 2013.

[80] Y. Ibrahim, H. A. Arafat, T. Mezher, and F. AlMarzooqi. An integrated framework for sustainability assessment of seawater desalination. *Desalination*, 447:1–17, 2018.

[81] C. W. B. III and A. V. Sebald. Effects of parametric uncertainty and technological change on input-output models. *The Review of Economics and Statistics*, 59(1):75, 1977.

[82] IMF. Australian Dollar Exchange Rates. International Monetary Fund, https://www.imf.org/external/np/fin/ert/GUI/Pages/CountryDataBase.aspx, 2018.

[83] K. Jijakli, H. Arafat, S. Kennedy, P. Mande, and V. V. Theeyattuparampil. How green solar desalination really is? Environmental assessment using life-cycle analysis (LCA) approach. *Desalination*, 287:123–131, 2012.

[84] S. Joshi. Product environmental life-cycle assessment using input-output techniques. *Journal of Industrial Ecology*, 3(2-3):95–120, 1999.

[85] K. C. Kavvadias and I. Khamis. The IAEA DEEP desalination economic model: A critical review. *Desalination*, 257(1-3):150–157, 2010.

[86] F. Keck, M. Lenzen, A. Vassallo, and M. Li. The impact of battery energy storage for renewable energy power grids in Australia. *Energy*, 173:647–657, 2019.

[87] M. Kirby, R. Bark, J. Connor, M. E. Qureshi, and S. Keyworth. Sustainable irrigation: How did irrigated agriculture in Australia's Murray-Darling Basin adapt in the Millennium Drought? *Agricultural Water Management*, 145:154–162, 2014.

[88] M. Kirby, J. Connor, R. Bark, E. Qureshi, and S. Keyworth. The Economic Impact of Water Reductions During the Millennium Drought in the Murray-Darling Basin. In *56th AARES annual conference, Fremantle, Western Australia*, 2012.

[89] P. Komesaroff and I. Kerridge. A continent aflame: Ethical lessons from the Australian bushfire disaster. *Journal of Bioethical Inquiry*, 17(1):11–14, 2020.

[90] M. L. Lahr and L. de Mesnard. Biproportional techniques in input-output analysis: Table updating and structural analysis. *Economic Systems Research*, 16(2):115–134, 2004.

[91] S. Lattemann and T. Höpner. Environmental impact and impact assessment of seawater desalination. *Desalination*, 220(1):1–15, 2008.

[92] M. Leblanc, S. Tweed, A. Van Dijk, and B. Timbal. A review of historic and future hydrological changes in the Murray-Darling Basin. *Global and Planetary Change*, 80-81:226–246, 2012.

[93] H. Leck, D. Conway, M. Bradshaw, and J. Rees. Tracing the water-energy-food nexus: Description, theory and practice. *Geography Compass*, 9(8):445–460, 2015.

[94] Lenntech. Reverse Osmosis Demineralization. https://www.lenntech.com/processes/reverse-osmosis-demineralization.htm, 2020.

[95] M. Lenzen. Errors in conventional and input-output-based life-cycle inventories. *Journal of Industrial Ecology*, 4(4):127–148, 2000.

[96] M. Lenzen, B. Gallego, and R. Wood. Matrix balancing under conflicting information. *Economic Systems Research*, 21(1):23–44, 2009.

[97] M. Lenzen, A. Geschke, A. Malik, J. Fry, J. Lane, T. Wiedmann, S. Kenway, K. Hoang, and A. Cadogan-Cowper. New multi-regional input–output databases for Australia – enabling timely and flexible regional analysis. *Economic Systems Research*, 29(2):275–295, 2017.

[98] M. Lenzen, A. Geschke, T. Wiedmann, J. Lane, N. Anderson, T. Baynes, J. Boland, P. Daniels, C. Dey, J. Fry, M. Hadjikakou, S. Kenway, A. Malik, D. Moran, J. Murray, S. Nettleton, L. Poruschi, C. Reynolds, H. Rowley, J. Ugon, D. Webb, and J. West. Compiling and using input–output frameworks through collaborative virtual laboratories. *Science of The Total Environment*, 485-486:241–251, 2014.

[99] M. Lenzen, K. Kanemoto, D. Moran, and A. Geschke. Mapping the structure of the world economy. *Environmental Science and Technology*, 46(15):8374–8381, 2012.

[100] M. Lenzen, M. Li, A. Malik, F. Pomponi, Y.-Y. Sun, T. Wiedmann, F. Faturay, J. Fry, B. Gallego, A. Geschke, J. Gómez-Paredes, K. Kanemoto, S. Kenway, K. Nansai, M. Prokopenko, T. Wakiyama, Y. Wang, and M. Yousefzadeh. Global socio-economic losses and environmental gains from the Coronavirus pandemic. *PLOS ONE*, 15(7):e0235654, 2020.

[101] M. Lenzen, B. McBain, T. Trainer, S. Jütte, O. Rey-Lescure, and J. Huang. Simulating low-carbon electricity supply for Australia. *Applied Energy*, 179:553–564, 2016.

[102] M. Lenzen and J. M. Rueda-Cantuche. A note on the use of supply-use tables in impact analyses. *Statistics and Operations Research Transactions*, 36(2):139–152, 2012.

[103] M. Lenzen, Y. Y. Sun, F. Faturay, Y. P. Ting, A. Geschke, and A. Malik. The carbon footprint of global tourism. *Nature Climate Change*, 8(6):522–528, 2018.

[104] M. Lenzen, R. Wood, and T. Wiedmann. Uncertainty analysis for multi-region input-output models - a case study of the UK'S carbon footprint. *Economic Systems Research*, 22(1):43–63, 2010.

[105] W. W. Leontief. *Input-Output Economics*. Oxford University Press, New York, 1st edition, 1966.

[106] S. Li, Y.-H. Cai, A. I. Schäfer, and B. S. Richards. Renewable energy powered membrane technology: A review of the reliability of photovoltaic-powered membrane system components for brackish water desalination. *Applied Energy*, 253:113524, 2019.

[107] C. H. Liu, M. Lenzen, and J. Murray. A disaggregated emissions inventory for Taiwan with uses in hybrid input-output life cycle analysis (IO-LCA). *Natural Resources Forum*, 36(2):123–141, 2012.

[108] J. Liu, S. Chen, H. Wang, and X. Chen. Calculation of carbon footprints for water diversion and desalination projects. *Energy Procedia*, 75:2483–2494, 2015.

[109] T. Luo, R. Young, and P. Reig. Aqueduct Projected Water Stress Country Rankings. Technical report, World Resources Institute, Washington D.C., 2015.

[110] A. Malik, M. Lenzen, R. N. Ely, and E. Dietzenbacher. Simulating the impact of new industries on the economy: The case of biorefining in Australia. *Ecological Economics*, 107:84–93, 2014.

[111] A. Malik, M. Lenzen, and A. Geschke. Triple bottom line study of a lignocellulosic biofuel industry. *GCB Bioenergy*, 8(1):96–110, 2016.

[112] A. Malik, M. Lenzen, S. Mcalister, and F. Mcgain. The carbon footprint of Australian health care. *The Lancet Planetary Health*, 2(1):e27–e35, 2018.

[113] A. Malik, D. McBain, T. O. Wiedmann, M. Lenzen, and J. Murray. Advancements in input-output models and indicators for consumption-based accounting. *Journal of Industrial Ecology*, 23(2):300–312, 2019.

[114] M. Mannan, M. Alhaj, A. N. Mabrouk, and S. G. Al-Ghamdi. Examining the life-cycle environmental impacts of desalination: A case study in the State of Qatar. *Desalination*, 452:238–246, 2019.

[115] MDBA. Guide to the Proposed Basin Plan: Technical Background. Technical report, Murray-Darling Basin Authority, Canberra, 2010.

[116] MDBA. Basin Plan 2012. Murray-Darling Basin Authority, made under subparagraph 44(3)(b)(i) of the Water A, https://www.legislation.gov.au/Details/F2017C00078, 2012.

[117] MDBA. Transition Period Water Take Report 2016–17. Report on Cap Compliance and Transitional SDL Accounting. Technical report, Murray-Darling Basin Authority, Canberra, 2018.

[118] MDBA. Discover the Basin. Murray-Darling Basin Authority, https://www.mdba.gov.au/discover-basin, 2019.

[119] MDBA. Murray-Darling Basin Government Storages. Murray-Darling Basin Authority, https://www.mdba.gov.au/managing-water/water-storage, 2019.

[120] G. L. Meerganz von Medeazza. "Direct" and socially-induced environmental impacts of desalination. *Desalination*, 185(1-3):57–70, 2005.

[121] M. M. Mekonnen and A. Y. Hoekstra. Four billion people facing severe water scarcity. *Science Advances*, 2(2):1–6, 2016.

[122] R. E. Miller and P. D. Blair. *Input-Output Analysis: Foundations and Extensions*. Cambridge University Press, New York, 2nd edition, 2009.

[123] M. Molinos-Senante and D. González. Evaluation of the economics of desalination by integrating greenhouse gas emission costs: An empirical application for Chile. *Renewable Energy*, 133:1327–1337, 2019.

[124] I. Muñoz and A. R. Fernández-Alba. Reducing the environmental impacts of reverse osmosis desalination by using brackish groundwater resources. *Water Research*, 42(3):801–811, 2008.

[125] S. Nagashima, Y. Uchiyama, and K. Okajima. Hybrid input–output table method for socioeconomic and environmental assessment of a wind power generation system. *Applied Energy*, 185:1067–1075, 2017.

[126] Z. Norwood and D. Kammen. Life cycle analysis of distributed concentrating solar combined heat and power: Economics, global warming potential and water. *Environmental Research Letters*, 7(4):44016, 2012.

[127] L. Olatomiwa, S. Mekhilef, M. S. Ismail, and M. Moghavvemi. Energy management strategies in hybrid renewable energy systems: A review. *Renewable and Sustainable Energy Reviews*, 62:821–835, 2016.

[128] N. C. Onat, M. Kucukvar, and O. Tatari. Integrating triple bottom line input-output analysis into life cycle sustainability assessment framework: The case for US buildings. *International Journal of Life Cycle Assessment*, 19(8):1488–1505, 2014.

[129] G. L. Park, A. I. Schäfer, and B. S. Richards. Renewable energy powered membrane technology: The effect of wind speed fluctuations on the performance of a wind-powered membrane system for brackish water desalination. *Journal of Membrane Science*, 370(1-2):34–44, 2011.

[130] G. L. Park, A. I. Schäfer, and B. S. Richards. The effect of intermittent operation on a wind-powered membrane system for brackish water desalination. *Water Science and Technology*, 65(5):867–874, 2012.

[131] F. Pomponi and M. Lenzen. Hybrid life cycle assessment (LCA) will likely yield more accurate results than process-based LCA. *Journal of Cleaner Production*, 176:210–215, 2018.

[132] M. G. Porter, D. Downie, H. Scarborough, O. Sahin, and R. A. Stewart. Drought and desalination: Melbourne water supply and development choices in the twenty-first century. *Desalination and Water Treatment*, 55(9):2278–2295, 2015.

[133] N. J. Potter, F. H. Chiew, and A. J. Frost. An assessment of the severity of recent reductions in rainfall and runoff in the Murray-Darling Basin. *Journal of Hydrology*, 381(1-2):52–64, 2010.

[134] R. E. Quandt. Probabilistic errors in the leontief system. *Naval Research Logistics Quarterly*, 5(2):155–170, 1958.

[135] G. Raluy, L. Serra, and J. Uche. Life cycle assessment of MSF, MED and RO desalination technologies. *Energy*, 31(13):2361–2372, 2006.

[136] B. S. Richards, G. L. Park, T. Pietzsch, and A. I. Schäfer. Renewable energy powered membrane technology: Brackish water desalination system operated using real wind fluctuations and energy buffering. *Journal of Membrane Science*, 468:224–232, 2014.

[137] L. A. Richards, B. S. Richards, and A. I. Schäfer. Renewable energy powered membrane technology: Salt and inorganic contaminant removal by nanofiltration/reverse osmosis. *Journal of Membrane Science*, 369(1-2):188–195, 2011.

[138] B. D. Richter, M. M. Davis, C. Apse, and C. Konrad. A presumptive standard for environmental flow protection. *River Research and Applications*, 28(8):1312–1321, 2012.

[139] A. M. Rodríguez-Alloza, M. Heihsel, J. Fry, J. Gallego, A. Geschke, R. Wood, and M. Lenzen. Consequences of long-term infrastructure decisions — the case of self-healing roads and their CO2 emissions. *Environmental Research Letters*, 14(11):114040, 2019.

[140] Ruhrpumpen. Desalination - Reverse Osmosis, Multi-Stage Flash and Multi-Effect Distillation. Technical report, Ruhrpumpen, Witten, https://www.ruhrpumpen.com/en/downloads/resources/markets/51-desalination-market-en/file, 2011.

[141] J. J. Sadhwani, J. M. Veza, and C. Santana. Case studies on environmental impact of seawater desalination. *Desalination*, 185(1-3):1–8, 2005.

[142] M. O. Saeed, M. M. Ershath, and I. A. Al-Tisan. Perspective on desalination discharges and coastal environments of the Arabian Peninsula. *Marine Environmental Research*, 145:1–10, 2019.

[143] Y. Saif and A. Almansoori. Design and operation of water desalination supply chain using mathematical modelling approach. *Desalination*, 351:184–201, 2014.

[144] M. A. Sanz. Dynamic Growth for Desalination and Water Reuse in 2019. In *Advanced Water Treatment*, pages 14–15, Topsfield, 2019. International Desalination Association.

[145] B. R. Scanlon, I. Duncan, and R. C. Reedy. Drought and the water–energy nexus in Texas. *Environmental Research Letters*, 8(4):45033, 2013.

[146] H. Scarborough, O. Sahin, M. Porter, and R. Stewart. Long-term water supply planning in an Australian coastal city: Dams or desalination? *Desalination*, 358:61–68, 2015.

[147] M. Schiffler. Perspectives and challenges for desalination in the 21st century. *Desalination*, 165:1–9, 2004.

[148] C. A. Scott, S. A. Pierce, M. J. Pasqualetti, A. L. Jones, B. E. Montz, and J. H. Hoover. Policy and institutional dimensions of the water-energy nexus. *Energy Policy*, 39(10):6622–6630, 2011.

[149] A. A. Setiawan, Y. Zhao, and C. V. Nayar. Design, economic analysis and environmental considerations of mini-grid hybrid power system with reverse osmosis desalination plant for remote areas. *Renewable Energy*, 34(2):374–383, 2009.

[150] M. P. Shahabi, A. McHugh, M. Anda, and G. Ho. Environmental life cycle assessment of seawater reverse osmosis desalination plant powered by renewable energy. *Renewable Energy*, 67:53–58, 2014.

[151] M. W. Shahzad, M. Burhan, L. Ang, and K. C. Ng. Energy-water-environment nexus underpinning future desalination sustainability. *Desalination*, 413:52–64, 2017.

[152] A. Shehabi, J. R. Stokes, and A. Horvath. Energy and air emission implications of a decentralized wastewater system. *Environmental Research Letters*, 7(2):24007, 2012.

[153] W. Short, P. Sullivan, T. Mai, M. Mowers, C. Uriarte, N. Blair, D. Heimiller, and A. Martinez. Regional Energy Deployment System (ReEDS). Technical report, National Renewable Energy Laboratory, Colorado, https://www.nrel.gov/docs/fy12osti/46534.pdf, 2011.

[154] R. A. Stewart. Verifying the End Use Potable Water Savings from Contemporary Residential Water Supply Schemes. Technical Report 61, Waterlines Report Series No 61, National Water Commission, Canberra, http://www.nwc.gov.au/publications/waterlines/verifying-the-end-use-of-potable-water-savings-from-contemporary-residential-water-supply-schemes, 2011.

[155] Stiftung Forschung für Leben. Climate Correction Project. http://climate-correction-project.com, 2019.

[156] J. Stokes and A. Horvath. Life cycle energy assessment of alternative water supply systems. *International Journal of Life Cycle Assessment*, 11(5):335–343, 2006.

[157] S. Suh and G. Huppes. Methods for life cycle inventory of a product. *Journal of Cleaner Production*, 13(7):687–697, 2005.

[158] S. P. Surwade, S. N. Smirnov, I. V. Vlassiouk, R. R. Unocic, G. M. Veith, S. Dai, and S. M. Mahurin. Water desalination using nanoporous single-layer graphene. *Nature Nanotechnology*, 10(5):459–464, 2015.

[159] The Economist. Can the Sea of Galilee Be Saved? https://www.economist.com/middle-east-and-africa/2018/12/01/can-the-sea-of-galilee-be-saved, 2018.

[160] The Parliament of Australia. Water Act 2007. No. 137, 2007, https://www.legislation.gov.au/Details/C2017C00151, 2007.

[161] The World Bank. Renewable Energy Desalination. An Emerging Solution to Close the Water Gap in the Middle East and North Africa. Technical report, https://openknowledge.worldbank.org/handle/10986/11963, 2012.

[162] R. Tidball, J. Bluestein, N. Rodriguez, and S. Knocke. Cost and Performance Assumptions for Modeling Electricity Generation Technologies. Technical report, National Renewable Energy Laboratory, Colorado, 2010.

[163] UNDP. Water Governance in the Arab Region: Managing Scarcity and Securing the Future. Technical report, United Nations Development Programme, New York, 2013.

[164] G. C. Unruh. Understanding carbon lock-in. *Energy Policy*, 28(12):817–830, 2000.

[165] A. I. J. M. van Dijk, H. E. Beck, R. S. Crosbie, R. A. M. de Jeu, Y. Y. Liu, G. M. Podger, B. Timbal, and N. R. Viney. The Millennium Drought in south-east Australia (2001–2009): Natural and human causes and implications for water resources, ecosystems, economy, and society. *Water Resources Research*, 49(2):1040–1057, 2013.

[166] F. Vince, F. Marechal, E. Aoustin, and P. Bréant. Multi-objective optimization of RO desalination plants. *Desalination*, 222(1-3):96–118, 2008.

[167] D. M. Warsinger, E. W. Tow, K. G. Nayar, L. A. Maswadeh, and J. H. Lienhard V. Energy efficiency of batch and semi-batch (CCRO) reverse osmosis desalination. *Water Research*, 106:272–282, 2016.

[168] Water. desalination + reuse. Chile Project Envisions Multiple Mining Clients for Solar-Powered SWRO. https://www.desalination.biz/news/3/Chile-project-envisions-multiple-mining-clients-for-solar-powered-SWRO/8761/, 2017.

[169] S. D. Wedderburn, M. P. Hammer, and C. M. Bice. Shifts in small-bodied fish assemblages resulting from drought-induced water level recession in terminating lakes of the Murray-Darling Basin, Australia. *Hydrobiologia*, 691(1):35–46, 2012.

[170] J. Wellmann. *Conceptual Design of a Concentrating Solar Power Plant for a Combined Electricity and Water Supply of the City El Gouna*. PhD thesis, Technische Universität Berlin, Berlin, 2015.

[171] WHO and UNICEF. Progress on Drinking Water and Sanitation: 2012 Update. Technical report, Unicef and World Health Organization, New York, 2012.

[172] T. Wiedmann. Editorial: Carbon footprint and input-output analysis - an introduction. *Economic Systems Research*, 21(3):175–186, 2009.

[173] T. Wiedmann, M. Lenzen, L. T. Keyßer, and J. K. Steinberger. Scientists' warning on affluence. *Nature Communications*, 11(1):3107, 2020.

[174] J. Williams and R. Q. Grafton. Missing in action: possible effects of water recovery on stream and river flows in the Murray–Darling Basin, Australia. *Australian Journal of Water Resources*, pages 1–10, 2019.

[175] M. K. Wittholz, B. K. O'Neill, C. B. Colby, and D. Lewis. Estimating the cost of desalination plants using a cost database. *Desalination*, 229(1-3):10–20, 2008.

[176] G. Wittwer and M. Griffith. Modelling drought and recovery in the southern Murray-Darling basin. *Australian Journal of Agricultural and Resource Economics*, 55(3):342–359, 2011.

[177] P. Wolfram, T. Wiedmann, and M. Diesendorf. Carbon footprint scenarios for renewable electricity in Australia. *Journal of Cleaner Production*, 124:236–245, 2016.

[178] World Sea Temperature. World sea temperature. https://www.seatemperature.org, 2018.

[179] WSAA. Reducing Leakage in Australia. Technical report, Water Services Association of Australia, Melbourne, https://www.wsaa.asn.au/publication/reducing-leakage-australia, 2019.

[180] M. Yu and T. Wiedmann. Implementing hybrid LCA routines in an input–output virtual laboratory. *Journal of Economic Structures*, 7(1):33, 2018.

[181] D. Zarzo and D. Prats. Desalination and energy consumption. What can we expect in the near future? *Desalination*, 427:1–9, 2018.

[182] J. Zhou, V. W. C. Chang, and A. G. Fane. Life Cycle Assessment for desalination: A review on methodology feasibility and reliability. *Water Research*, 61:210–223, 2014.

[183] J. R. Ziolkowska. Is Desalination Affordable? Regional Cost and Price Analysis. *Water Resources Management*, 29(5):1385–1397, 2015.

[184] J. R. Ziolkowska and R. Reyes. Impact of socio-economic growth on desalination in the US. *Journal of Environmental Management*, 167:15–22, 2016.

[185] Q. Zou and X. Liu. Economic effects analysis of seawater desalination in China with input–output technology. *Desalination*, 380:18–28, 2016.